

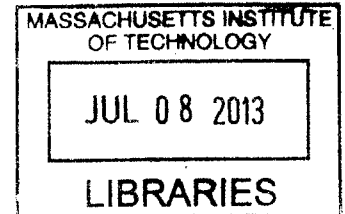
Uganda Manafwa River Early Flood Warning System Development
Hydrologic Watershed Modeling Using HEC-HMS, HEC-RAS, ArcGIS

By

Yan Ma

B.Eng. Environmental Engineering
National University of Singapore 2012

ARCHIVES



Submitted to the Department of Civil and Environmental Engineering in Partial fulfillment of the requirement for the degree of Master of Engineering in Civil and Environmental Engineering

At the

Massachusetts Institute of Technology

June 2013

© 2013 Yan Ma. All rights reserved.

The author hereby grants to MIT permission to reproduce and to distribute publicly paper and electronic copies of this thesis document in whole or in part in any medium now known or hereafter created.

Signature of Author: _____

Department of Civil and Environmental Engineering
May 22nd, 2013

Certified by: _____

Richard Schuhmann, Ph.D.
Senior Lecturer of Civil and Environmental Engineering
Thesis Supervisor

Accepted by: _____

Heidi M. Nepf
Chair, Departmental Committee for Graduate Students

Uganda Manafwa River Early Flood Warning System Development Hydrologic Watershed Modeling Using HEC-HMS, HEC-RAS, ArcGIS

By
Yan Ma

Submitted to the Department of Civil and Environmental Engineering on May 22nd 2013
in Partial fulfillment of the requirement for the degree of Master of Engineering in Civil
and Environmental Engineering

Abstract

The Manafwa River basin spans several districts in Eastern Uganda. Over the years, frequent floods have constantly posed a great threat to the local communities in these districts. The Uganda Red Cross Society (URCS) intends to design a precipitation based flood forecasting system for the Manafwa River Basin. Towards this end, the URCS initiated collaboration with MIT's Department of Civil and Environmental Engineering in January 2013, in an attempt to establish a hydrologic modeling system that relates upstream precipitation with downstream stream discharge using ArcGIS, HEC-HMS and HEC-RAS. This work is dedicated to present the progress in the modeling endeavor, provide technical guidance to the extent possible, and facilitate hydrologic modeling efforts of similar nature. The main focus is on the loss methods used in HEC-HMS: the Curve Number loss method and the Initial and Constant loss method. It is found out that the neither the Curve Number nor Initial and Constant loss method is perfectly suitable to modeling both short-term and long term simulations. The Curve Number method is able to better model the precipitation-runoff processes in short term simulations. The Initial and Constant loss method tends to underestimate water volume runoff in short term simulations from what is observed. The Curve Number loss method produced results that are on average closer to observed values in short term simulations; however, the resulting curve number values from calibration are considerably lower than the estimated values.

Thesis Supervisor: Richard Schuhmann, Ph.D.

Title: Senior Lecturer of Civil and Environmental Engineering

Acknowledgements

Special thanks to Senior Lecturer, Dr. Richard Schuhmann for his meticulous instructions. Dr. Schuhmann led us throughout the project, including the field work in Uganda, and he has been very supportive, very inspiring and attentive to detail.

My gratitude also goes to MEng Program Director Dr. Eric Adams for his valuable inputs as well as impeccable coordination from the very onset of the project, and American Red Cross delegate Ms. Julie Arrighi, for her warm reception in Uganda and devoted cooperation.

I am deeply indebted to Associate Professor Kenneth Marc Strzepek and his PhD student Yohannes Gebretsadik, and Charles Fant. We are honored to have them share their expertise that is indispensable for the progress we were able to make. Yohannes has been extraordinary in helping us overcome many specific modeling challenges.

I am also grateful to senior lecturer Dr. Peter Shanahan, senior lecturer Dr. David Langseth, Dr. John Germaine, librarian Ms. Anne Graham, GIS specialists Daniel Sheehan and Administrative Assistant Ms. Lauren McLean. There are many more who lent their support, including the volunteers and villagers in Uganda.

Last but not least, I thank my classmates Francesca Cecinati and Fidele Bingwa. I admire their diligence and appreciate their support. There are no better teammates for me to expect.

Without the concerted effort of these devoted individuals, this work would not have been possible. I learned a lot from them and I could not thank them enough.

Table of Contents

Abstract	3
Acknowledgements	5
Table of Contents	7
List of Figures	9
List of Tables	13
Glossary	14
1. INTRODUCTION	15
2. METHODOLOGY & DATA.....	17
2.1 Overview	17
2.2 HEC-HMS.....	18
2.3 HEC-RAS	25
2.4 HEC-GeoRAS	27
3. MODEL DEVELOPMENT	29
3.1 HEC-HMS Analysis	29
3.1.1 Watershed delineation & Geometry file Creation	29
3.1.2 Precipitation Data Acquisition.....	29
3.1.3 Observed Flow Acquisition.....	31
3.1.4 Evapotranspiration Estimation	34
3.1.5 SCS CN Number Method.....	35
3.1.6 Estimating Sub basin Lag Time.....	40
3.1.7 Estimating Reach Routing Parameters	43
3.1.8 Initial and Constant Loss method parameters	45
3.1.9 Simulation.....	46
3.1.10 Calibration.....	47
3.2 HEC-RAS Analysis.....	51
3.2.1 Creating Geometry File in ArcGIS using HEC-GeoRAS toolbox	51
3.2.2 Importing geometric data to HEC-RAS.....	63
3.2.3 Manning n values.....	63
3.2.4 Filtering cross-section data points.....	64

3.2.5	Flow data	65
3.2.6	Other simulation assumptions	65
4	RESULTS AND DISCUSSION	66
4.1	Overview	66
4.2	Long term simulation - Run 0	67
4.2.1	Run CN0	67
4.2.2	Run IC0	72
4.3	Short term simulation - Run 1	77
4.3.1	Run CN1	77
4.3.2	Run IC1	83
4.4	Short term simulation - Run2	88
4.4.1	Run CN2	88
4.4.2	Run IC2	93
4.5	Short term simulation Run3	98
4.5.1	Run CN3	98
4.5.2	Run IC3	103
4.6	Short term simulation - Run4	108
4.6.1	Run CN4	108
4.6.2	Run IC4	113
4.7	Short term simulation - Run5	118
4.7.1	Run CN5	118
4.7.2	Run IC5	124
4.9	Performance Evaluation	129
5.	CONCLUSIONS AND RECOMMENDATIONS	133
	REFERENCES	135
	APPENDIX	137
	Appendix A- Weighted Average Rainfall during the Year 2006 in Each Sub-basin	137
	Appendix B - Basin “n” overbank reference roughness values for developed and undeveloped channelization	147

List of Figures

Figure 1 – The Manafwa River Watershed (Cecinati, 2013)	15
Figure 2 - Schematic illustration of software collaboration (Patel, 2009).....	17
Figure 3 - HEC-HMS user interface	19
Figure 4 - Process flow diagram for using HEC-GeoRAS (US Army Corp of Engineers, 2009).....	28
Figure 5 - The sub-basins identified with TRMM cells (Cecinati, 2013)	30
Figure 6 - River gauge position inside the Manafwa River watershed (Cecinati, 2013)	31
Figure 7 - River gauge used by the Water Resources Department	31
Figure 8 - Water level of the Manafwa River in Busiu, as recorded in elevation above the gauge by the Water Resources Department from March 1997 – March 2008.....	32
Figure 9 - River cross sections position (Cecinati, 2013)	33
Figure 10 - Plot of river cross sections	33
Figure 11 - Components of storm event (National Resources Conservation Service, 2004)	35
Figure 12 - Manafwa watershed Sub basins (Bingwa, 2013).....	37
Figure 13 - Manafwa Watershed Land Use Map, Africover 2009 (Bingwa, 2013).....	38
Figure 14 - Soil data - percent clay content, from HWSD database (Bingwa, 2013)	39
Figure 15 - Manafwa watershed CN Map (Bingwa, 2013).....	39
Figure 16 - Screen Shot of ArcMap: Determination of lag equation parameters.....	42
Figure 17 - Screen shot of HEC-HMS: Tabulated observed flow values	48
Figure 18 - Screen shot of HEC-HMS: Calibration point and actual position of observed flow	49
Figure 19 - Screen shot of HEC-HMS: Time series data of observed flow is chosen for W150 (J15)	50
Figure 20 - Screen shot of HEC-HMS: Optimization trial window	50
Figure 21 - Screen Shot of ArcMap: the segment of river network studied in HEC-RAS	52
Figure 22 - Screen Shot of ArcMap: DEM of watershed and shape file of river network.....	53
Figure 23 - Screen Shot of ArcMap: Cropping DEM	54
Figure 24 - Screen Shot of ArcMap: Resample toolset	55
Figure 25 - Screen Shot of ArcMap: Copying Shape file feature to Stream Centerline layer.....	56
Figure 26 - Screen Shot of ArcMap: Populating depth for river feature before converting it to raster	57
Figure 27 - Screen Shot of ArcMap: Converting river feature to raster with a cellsize of 10m.....	57
Figure 28 - Screen Shot of ArcMap: Combining river raster with DEM using Raster Calculator.....	58
Figure 29 - Screen shot of ArcMap: Environments specification in tools	58
Figure 30 - Screen Shot of ArcMap: Smoothing of river cross section using focal statistics tool	59
Figure 31 - Screen Shot of ArcMap: Banks and Flowpaths	60
Figure 32 - Screen Shot of ArcMap: Stream centerline, Banks, Flowpaths and XS Cutlines.....	61
Figure 33 - Screen Shot of ArcMap: RAS Layer Setup.....	61
Figure 34 - Screen Shot of ArcMap: Assign line type attributes	62
Figure 35 - Screen Shot of ArcMap: Data export from ArcMap.....	62
Figure 36 - Screen Shot of HEC-RAS: Geometric data imported as GIS format.....	63
Figure 37 - Screen Shot of HEC-RAS: Manning n table	64
Figure 38 - Screen Shot of HEC-RAS: Cross section data points filter	65
Figure 39 - Screen Shot of HEC-HMS: Flow graph of w150 for Run CNO before calibration.....	67

Figure 40 - Screen Shot of HEC-HMS: Summary table of w150 for Run CNO before calibration	68
Figure 41 - Screen Shot of HEC-HMS: Precipitation loss of w150 for Run CNO before calibration	68
Figure 42 - Screen Shot of HEC-HMS: Soil infiltration of w150 for Run CNO.....	69
Figure 43 - Screen Shot of HEC-HMS: Evapotranspiration of w150 for Run CNO	69
Figure 44 - Screen Shot of HEC-HMS: Optimized parameters of w150 for Run CNO	70
Figure 45 - Screen Shot of HEC-HMS: Optimization objective function of w150 for Run CNO	70
Figure 46 - Screen Shot of HEC-HMS: Flow graph of w150 for Run CNO after calibration	71
Figure 47 - Screen Shot of HEC-HMS: Flow residual of w150 for Run CNO after calibration	71
Figure 48 - Screen Shot of HEC-HMS: Flow graph of w150 for Run IC0 before calibration	72
Figure 49 - Screen Shot of HEC-HMS: Summary table of w150 for Run IC0 before calibration.....	73
Figure 50 - Screen Shot of HEC-HMS: Evapotranspiration of w150 for Run IC0 before calibration	73
Figure 51 - Screen Shot of HEC-HMS: Soil infiltration of w150 for Run IC0 before calibration	74
Figure 52 - Screen Shot of HEC-HMS: Cumulative precipitation loss of w150 for Run IC0 before calibration	74
Figure 53 - Screen Shot of HEC-HMS: Optimization objective function of w150 for Run IC0.....	75
Figure 54 - Screen Shot of HEC-HMS: Optimized parameters of w150 for Run IC0	75
Figure 55 - Screen Shot of HEC-HMS: Flow graph of w150 for Run IC0 after calibration	76
Figure 56 - Screen Shot of HEC-HMS: Flow graph of w150 for Run CN1 before calibration.....	77
Figure 57 - Screen Shot of HEC-HMS: Summary table of w150 for Run CN1 before calibration	78
Figure 58 - Screen Shot of HEC-HMS: Calibrated flow graph of w150 for Run CN1	79
Figure 59 - Screen Shot of HEC-HMS: Calibration objective function of w150 for Run CN1	79
Figure 60 - Screen Shot of HEC-HMS: Optimized parameters of w150 for Run CN1	80
Figure 61 - Screen Shot of HEC-HMS: Potential evapotranspiration of w150 for Run CN1 after calibration	81
Figure 62 - Screen Shot of HEC-HMS: Soil infiltration of w150 for Run CN1 after calibration	81
Figure 63 - Screen Shot of HEC-HMS: Excess precipitation of w150 for Run CN1 after calibration	82
Figure 64 - Screen Shot of HEC-HMS: flow residual of w150 for Run CN1 after calibration.....	82
Figure 65 - Screen Shot of HEC-HMS: Flow graph of w150 for Run IC1 before calibration	83
Figure 66 - Screen Shot of HEC-HMS: Summary table of w150 for Run IC1 before calibration.....	83
Figure 67 - Screen Shot of HEC-HMS: Flow graph of w150 for Run IC1 after calibration	84
Figure 68 - Screen Shot of HEC-HMS: Summary table of w150 for Run IC1 after calibration	85
Figure 69 - Screen Shot of HEC-HMS: Optimization objective function of w150 for Run IC1.....	85
Figure 70 - Screen Shot of HEC-HMS: optimized parameters of w150 for Run IC1	86
Figure 71 - Screen Shot of HEC-HMS: Flow residual of w150 for Run IC1 after calibration.....	86
Figure 72 - Screen Shot of HEC-HMS: Soil infiltration of w150 for Run IC1 after calibration	87
Figure 73 - Screen Shot of HEC-HMS: Excess precipitation of w150 for Run IC1 after calibration	88
Figure 74 - Screen Shot of HEC-HMS: Flow graph of w150 for RunCN2 before calibration.....	88
Figure 75 - Screen Shot of HEC-HMS: Summary table of w150 for RunCN2 before calibration	89
Figure 76 - Screen Shot of HEC-HMS: Flow graph of w150 for RunCN2 after calibration	90
Figure 77 - Screen Shot of HEC-HMS: Summary table of w150 for RunCN2 after calibration.....	90
Figure 78 - Screen Shot of HEC-HMS: Optimization objective function of w150 for RunCN2	91
Figure 79 - Screen Shot of HEC-HMS: Optimized parameters of w150 for RunCN2.....	91
Figure 80 - Screen Shot of HEC-HMS: Excess precipitation of w150 for RunCN2 after calibration.....	92
Figure 81 - Screen Shot of HEC-HMS: Soil infiltration of w150 for RunCN2 after calibration.....	92

Figure 82 - Screen Shot of HEC-HMS: Flow residual of w150 for RunCN2 after calibration	93
Figure 83 - Screen Shot of HEC-HMS: Flow graph of w150 for RunIC2 before calibration	94
Figure 84 - Screen Shot of HEC-HMS: Summary table of w150 for RunIC2 before calibration.....	94
Figure 85 - Screen Shot of HEC-HMS: Flow graph of w150 for RunIC2 after calibration	95
Figure 86 - Screen Shot of HEC-HMS: Summary table of w150 for RunIC2 after calibration	95
Figure 87 - Screen Shot of HEC-HMS: Optimization objective function of w150 for Run IC2.....	96
Figure 88 - Screen Shot of HEC-HMS: Optimized parameters of w150 for Run IC2	96
Figure 89 - Screen Shot of HEC-HMS: Excess precipitation of w150 for Run IC2 after calibration	97
Figure 90 - Screen Shot of HEC-HMS: Flow residuals of w150 for Run IC2 after calibration	97
Figure 91 - Screen Shot of HEC-HMS: Soil infiltration of w150 for Run IC2 after calibration	98
Figure 92 - Screen Shot of HEC-HMS: Flow graph of w150 for Run CN3 before calibration.....	99
Figure 93 - Screen Shot of HEC-HMS: Summary table of w150 for Run CN3 before calibration	99
Figure 94 - Screen Shot of HEC-HMS: Flow graph of w150 for Run CN3 after calibration	100
Figure 95 - Screen Shot of HEC-HMS: Optimized parameter of w150 for Run CN3	100
Figure 96 - Screen Shot of HEC-HMS: Summary table of w150 for Run CN3 after calibration.....	101
Figure 97 - Screen Shot of HEC-HMS: Optimization objective function of w150 for Run CN3	101
Figure 98 - Screen Shot of HEC-HMS: Flow residual of w150 for Run CN3 after calibration	102
Figure 99 - Screen Shot of HEC-HMS: Soil infiltration of w150 for Run CN3 after calibration.....	102
Figure 100 - Screen Shot of HEC-HMS: Excess precipitation of w150 for Run CN3 after calibration.....	103
Figure 101 - Screen Shot of HEC-HMS: Flow graph of w150 for Run IC3 before calibration	103
Figure 102 - Screen Shot of HEC-HMS: Summary table of w150 for Run IC3 before calibration.....	104
Figure 103 - Screen Shot of HEC-HMS: Flow graph of w150 for Run IC3 after calibration	105
Figure 104 - Screen Shot of HEC-HMS: Summary table of w150 for Run IC3 after calibration.....	105
Figure 105 - Screen Shot of HEC-HMS: Screen Shot of HEC-HMS: Optimized parameters of w150 for Run IC3	106
Figure 106 - Screen Shot of HEC-HMS: Optimization objective function of w150 for Run IC3 after calibration	106
Figure 107 - Screen Shot of HEC-HMS: Soil infiltration of w150 for Run IC3 after calibration	107
Figure 108 - Screen Shot of HEC-HMS: Excess precipitation of w150 for Run IC3 after calibration	107
Figure 109 - Screen Shot of HEC-HMS: Flow residual of w150 for Run IC3 after calibration.....	108
Figure 110 - Screen Shot of HEC-HMS: Flow graph of w150 for Run CN4 before calibration.....	108
Figure 111 - Screen Shot of HEC-HMS: Summary table of w150 for Run CN4 before calibration	109
Figure 112 - Screen Shot of HEC-HMS: Flow graph of w150 for Run CN4 after calibration	110
Figure 113 - Screen Shot of HEC-HMS: Summary table of w150 for Run CN4 after calibration	110
Figure 114 - Screen Shot of HEC-HMS: Objective function of w150 for Run CN4 after calibration.....	111
Figure 115 - Screen Shot of HEC-HMS: Optimized parameters of w150 for Run CN4.....	111
Figure 116 - Screen Shot of HEC-HMS: Soil infiltration of w150 for Run CN4 after calibration.....	112
Figure 117 - Screen Shot of HEC-HMS: Excess precipitation of w150 for RunCN4 after calibration.....	112
Figure 118 - Screen Shot of HEC-HMS: Flow residual of w150 for Run CN4 after calibration	113
Figure 119 - Screen Shot of HEC-HMS: Flow graph of w150 for Run IC4 before calibration	114
Figure 120 - Screen Shot of HEC-HMS: Summary table of w150 for Run IC4 before calibration.....	114
Figure 121 - Screen Shot of HEC-HMS: Flow graph of w150 for Run IC4 after calibration	115
Figure 122 - Screen Shot of HEC-HMS: Summary table of w150 for Run IC3 after calibration.....	115

Figure 123 - Screen Shot of HEC-HMS: Objective function of w150 for Run IC3 after calibration	116
Figure 124 - Screen Shot of HEC-HMS: Optimized parameters of w150 for Run IC4	116
Figure 125 - Screen Shot of HEC-HMS: Excess precipitation of w150 for Run IC3 after calibration	117
Figure 126 - Screen Shot of HEC-HMS: Soil infiltration of w150 for Run IC3 after calibration	117
Figure 127 - Screen Shot of HEC-HMS: Flow residual of w150 for Run IC4 after calibration.....	118
Figure 128 - Screen Shot of HEC-HMS: Flow graph of w150 for Run CN5 before calibration.....	119
Figure 129 - Screen Shot of HEC-HMS: Summary table of w150 for Run CN5 before calibration	119
Figure 130 - Screen Shot of HEC-HMS: Flow graph of w150 for Run CN5 after calibration	120
Figure 131 - Screen Shot of HEC-HMS: Summary table of w150 for Run CN5 after calibration	121
Figure 132 - Screen Shot of HEC-HMS: Objective function of w150 for Run CN5 after calibration	121
Figure 133 - Screen Shot of HEC-HMS: Optimized parameters of w150 for Run CN5	122
Figure 134 - Screen Shot of HEC-HMS: Soil infiltration of w150 for Run CN5 after calibration.....	122
Figure 135 - Screen Shot of HEC-HMS: Excess precipitation of w150 for Run CN5 after calibration	123
Figure 136 - Screen Shot of HEC-HMS: Flow residual of w150 for Run CN5after calibration	123
Figure 137 - Screen Shot of HEC-HMS: Flow graph of w150 for Run IC5 before calibration	124
Figure 138 - Screen Shot of HEC-HMS: Summary table of w150 for Run IC5 before calibration.....	124
Figure 139 - Screen Shot of HEC-HMS: Flow graph of w150 for Run IC5 after calibration	125
Figure 140 - Screen Shot of HEC-HMS: Summary table of w150 for Run IC5 after calibration.....	125
Figure 141 - Screen Shot of HEC-HMS: Objective function of w150 for Run IC5 after calibration	126
Figure 142 - Screen Shot of HEC-HMS: Optimized parameters of w150 for Run IC5	126
Figure 143 - Screen Shot of HEC-HMS: Flow residual of w150 for Run IC5 after calibration.....	127
Figure 144 - Screen Shot of HEC-HMS: Soil infiltration of w150 for Run IC5 after calibration	127
Figure 145 - Screen Shot of HEC-HMS: Excess precipitation of w150 for Run IC5 after calibration	128
Figure 146 - Summary values histogram for performance evaluation.....	130
Figure 147 - Root-mean-square values histogram for long term and short term simulations	132

List of Tables

Table 1 - The average of the TRMM cells contained in every sub-basin, weighted on the areas (Cecinati, 2013)	30
Table 2 - Average monthly evapotranspiration value for an average year	34
Table 3 - Recommended value for initial abstraction (HEC-1 & HEC-HMS, 1999)	36
Table 4 - Recommended Impervious Percentage values (HEC-1 & HEC-HMS, 1999)	37
Table 5 - CN values for respective sub-basins (Bingwa, 2013)	40
Table 6 - Parameter values for lag time estimation using Basin “n” method	43
Table 7 - Velocity profile measured at one location in the Manafwa River	44
Table 8 - Muskingum parameter estimation (R15 represents an artificial reach with length 100m)	45
Table 9 - SCS Soil groups and infiltration loss rates (Hydrologic Engineering Center, 2000).....	46
Table 10 - Other simulation specifications and assumptions for HEC-HMS	47
Table 11 - Periods selected for various simulation runs	66
Table 12 - Summary of optimized parameter values for Curve Number loss method	128
Table 13 - Summary of optimized parameter values for Initial and Constant loss method.....	129
Table 14 - Summary values of objective function	130
Table 15 - Root-mean-square values for long term and short term simulations.....	131

Glossary

cms - cubic meter per second

DEM - Digital Elevation Model

DTM - Digital Terrain Model

TIN - Triangulated Irregular Network

1. INTRODUCTION

The Manafwa River basin mainly spans several districts in Eastern Uganda, namely Bududa, Manafwa, Mbale and Butaleja. Over the years, frequent floods have posed a great threat to the local communities. With climate change and anthropogenic perturbations believed to have increased the flooding frequency, as many as 45,000 people are affected each year. While Bududa is more affected by landslides caused by excessive precipitation in rainy seasons, Manafwa, Mbale and Butaleja suffer from the runoff produced by the upstream rainfall (Bingwa, 2013).

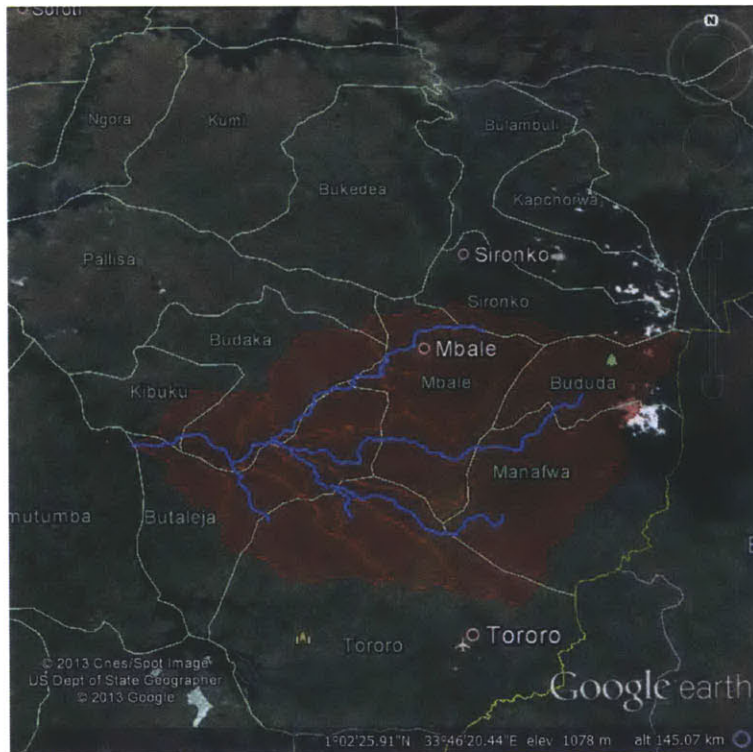


Figure 1 – The Manafwa River Watershed (Cecinati, 2013)

The Uganda Red Cross Society (URCS) intends to design a precipitation based flood forecasting system for the Manafwa River Basin (Figure 1). The long term goal is to have an early flood warning system working by 2015, which would be used to assess the probability of flood events and alert the local community in cases necessary. Towards this

end, the URCS initiated collaboration with MIT's Department of Civil and Environmental Engineering MEng team in January 2013, in an attempt to establish a hydrologic modeling system that relates upstream precipitation with downstream discharge. The team, consisting of Senior Lecturer Dr. Richard Schuhmann, and three MIT students, Francesca Cecinati, Fidele Bingwa and Ma Yan, decided to employ ArcGIS, HEC-HMS and HEC-RAS towards this goal.

The objective of this work is thus to discuss the data collection and model development, compare the performance of two loss method candidates in HEC-HMS, i.e. the Curve Number loss method, and the Initial and Constant loss method, and provide future recommendations.

2. METHODOLOGY & DATA

2.1 Overview

The objective of the modeling effort is to build a relationship between upstream precipitation and downstream discharge on the Manafwa River. This is an essential step in the attempt to establish an early flood warning system and to formulate a flood control strategy.

To accomplish the objective, several software programs are chosen. As is shown in Figure 2, HEC-HMS is employed to calculate the discharge hydrograph at the start point of the flood area based on historical precipitation data. HEC-RAS is then utilized to analyze the water surface elevation, given the combination of discharge hydrograph and stream channel geometry, in the region of interest. The stream channel geometry is provided through ArcGIS's geo-processing capabilities, specifically with the help of HEC-GeoRAS toolset. ArcGIS is also potentially helpful in visualizing the result generated by HEC-RAS in 3D view.

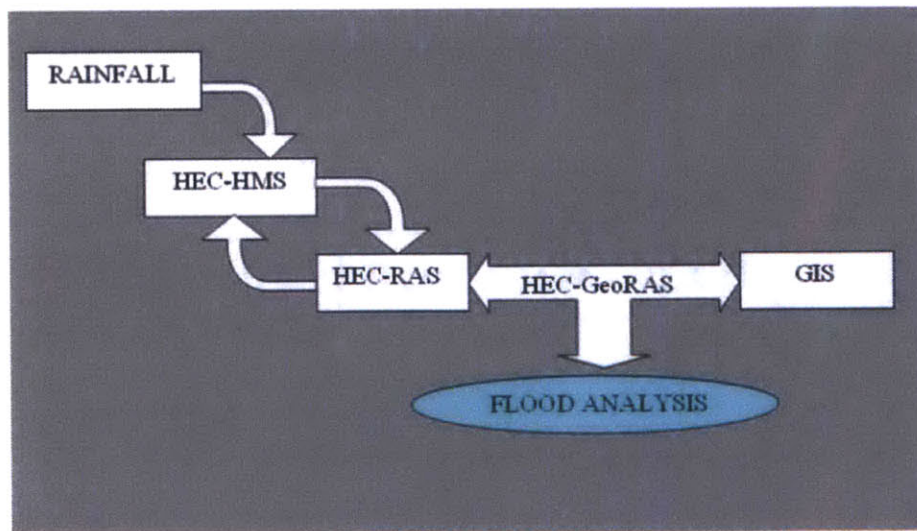


Figure 2 - Schematic illustration of software collaboration (Patel, 2009)

2.2 HEC-HMS

HEC-HMS, or the Hydrologic Engineering Center – Hydrologic Modeling System, is a public-domain software that was developed by US Army Corps of Engineers. It has the capacity of simulating precipitation-runoff processes in dendritic watershed networks (US Army Corp of Engineers). HEC-1, the antecedent version of HEC-HMS, having originated in 1968, was the earliest research and engineering application widely employed by institutions, governments and corporations. It was based on DOS system that took input from a text file. Based on HEC-1, USACE released HEC-HMS in 1998, a version that is suitable to be operated in windows environment featuring a graphical user interface.

While HEC-HMS is versatile in many hydrologic simulations, it has limitations as well. The program is deterministic instead of stochastic, which means parameter values are fixed to be the same for every simulation neglecting probability distributions. It also assumes decoupled relationships between evapotranspiration-infiltration and infiltration-base flow. In addition, it is more suitable for dendritic river systems where diversion of flow is minimal. Looping or braided stream networks should not be simulated with HEC-HMS and its capacity to deal with back water effects is also very limited; a separate hydraulic model should be sought in dealing with these problems. Figure 3 shows a typical HEC-HMS user interface.

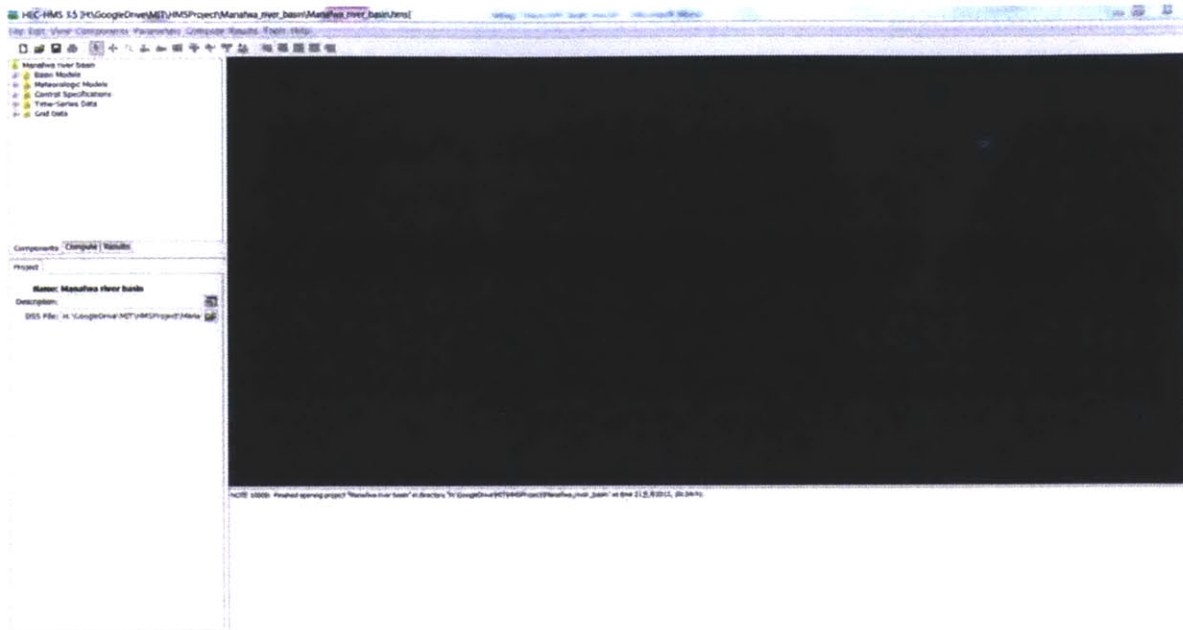


Figure 3 - HEC-HMS user interface

For a HEC-HMS project, there are typically four components. They are,

1. Basin models
2. Meteorological models
3. Control specifications
4. Time series data

Basin model

A basin model incorporates the elements that physically describe the watershed. Hydrologic elements including sub-basins, reaches, junctions, reservoirs, sources and sinks are connected in a dendritic stream network. Based on the characteristic behaviors of these integrated elements, hydrologic computations may be carried out from upstream sequentially (Hydrologic Engineering Center, 2005).

For this analysis, four main categories of methods are available for the user to choose from in the sub-basin editor for water losses from the sub-basin:

1. Loss methods
2. Transform methods
3. Baseflow methods
4. Routing methods

Loss Methods

Nine different loss methods can be utilized by HEC-HMS to calculate water loss volume in the sub basin from infiltration given precipitation and the physical properties of the watershed. If a loss method is not selected then precipitation falling on that sub basin will not infiltrate and is considered to run off. Several of the most commonly used loss methods are described below.

The SCS Curve Number method is a simple and well-established method widely accepted for use in the US and abroad. The FAO (Food and Agriculture Organization of United Nations) soil data are used to determine curve numbers. On site observations are used to estimate average percentage of impervious surface. The curve number varies as function of soil type, land use and treatment, surface condition and antecedent moisture condition (AMC) (Hydrologic Engineering Center, 2000).

In the Green-Ampt loss method, both Darcy's Law in an unsaturated form and mass conservation are combined to describe the transport of infiltration through the soil profile and the infiltration capacity of the soil. It includes an initial abstraction representing surface ponding not otherwise included in the model. Parameters can be estimated for ungauged watersheds from information about the soils present in the watershed. Because the Green-Ampt model is not widely used, it is less mature (Hydrologic Engineering Center, 2000).

The continuous soil-moisture Accounting (SMA) method is a continuous model that simulates both wet and dry weather behaviors. The SMA method relies upon evapotranspiration and precipitation to calculate the behavior of water through the soil profile and into the groundwater. HEC-HMS in conjunction with SMA is able to generate basin surface runoff, groundwater flow, losses due to evapotranspiration and deep percolation over the entire basin (Hydrologic Engineering Center, 2000).

SMA is a mature model that has been used successfully in hundreds of studies throughout the US. As a parsimonious model, it includes only a few parameters necessary to explain the variation of runoff volume. However, it is difficult to apply to ungauged areas because of a lack of direct physical relationship of the parameters with watershed properties. It may be too simple to predict losses within an event, even if it does predict total losses well (Hydrologic Engineering Center, 2000).

The initial constant loss method allows the user to specify the amount of precipitation to be infiltrated and stored within the soil before runoff begins. This water exits the water balance – i.e. it is not available for groundwater recharge or baseflow during periods of no precipitation.

Transform Methods

While loss methods allow the user to specify infiltration water losses, transform methods account for overland flow, storage and energy losses as water flows through a watershed into stream channels. Several transform methods are available for the user to select.

When the SCS Unit Hydrograph (UH) model is selected, the resulting runoff process is linear, so that greater or smaller runoff is just a multiple of the unit runoff hydrograph for

that time period (the multiple determined by the total depth of event precipitation). As a widely used empirical model to describe the relationship between direct runoff and excess precipitation, the model is based upon averages of unit hydrographs extracted from gauged rainfall and runoff for a large number of small agricultural watersheds throughout the US (Hydrologic Engineering Center, 2000).

The Kinematic-wave model is a conceptual watershed model. It represents the watershed as a broad open channel and assumes excess precipitation is the amount of flow that enters this broad open channel. The watershed runoff hydrograph is generated by solving equations that describe unsteady shallow water flow in the open channel (Hydrologic Engineering Center, 2000).

Other models include Snyder's UH model where lag, peak flow, and total time base are the most critical characteristics of the UH. A standard UH is defined and UH parameters are related to measurable watershed characteristics. In Clark's UH model, two main processes, namely translation and attenuation, are explicitly represented in the transformation of excess precipitation to runoff. Another distributed parameter model is the ModClark Model. It accounts explicitly for variations in travel time to the watershed outlet from all regions of a watershed (Hydrologic Engineering Center, 2000).

Baseflow Methods

Baseflow methods are used to represent baseflow contributions to sub-basin outflow. Baseflow values for sub-basins are not auto-calibrated by HEC-HMS. The recession method treats baseflow from a single or multiple sequential events in an exponential decay manner. It has often been used to illustrate drainage from natural storage in watersheds (Hydrologic Engineering Center, 2000). The constant monthly method is the simplest baseflow model and is efficient for continuous simulation. It represents baseflow

as a constant flow, which may vary from month to month. This baseflow is added to direct runoff obtained from precipitation to calculate total discharge in the simulation (Hydrologic Engineering Center, 2000). The linear reservoir method addresses mass conservation by routing infiltrated precipitation to the channel. It is used in conjunction with the continuous soil-moisture (SMA) model and “simulates storage and movement of subsurface flow as storage and movement of water through reservoirs” (Hydrologic Engineering Center, 2000).

Routing Methods

Routing methods are used to simulate flows in open channels. The modified Puls routing method, also called storage routing or level-pool routing, is achieved through both a finite difference approximation of the continuity equation and an empirical description of momentum conservation (Hydrologic Engineering Center, 2000). Like the modified Puls model, the Muskingum routing method utilizes a simple finite difference approximation of the continuity equation. Reach storage is represented by the sum of prism storage and wedge storage (Hydrologic Engineering Center, 2000). Also based on a simple finite difference approximation of the continuity equation and simplification of the momentum equation, the Kinematic-wave model represents a watershed as two angled plane surfaces. The water flows over each surface until it reaches the channel at the intersection of the planes. Looking at a cross section, the shape of the watershed appears like an open book. Stream channels would follow the book’s center binding. Although the Kinematic-wave model is mainly used to represent overland flow on the plane surfaces, it is also instrumental in simulating channel flow (Hydrologic Engineering Center, 2000). The simplest routing model in HEC-HMS is the Lag Model. The outflow hydrograph is identical to the inflow hydrograph except that the latter leads by a specific duration. In the Lag Model, the flows are not attenuated, which means no shape change is present in the hydrographs. The Lag Model is in essence a special form of other models; therefore, its

results could be duplicated with other models by carefully choosing parameter values (Hydrologic Engineering Center, 2000).

Meteorological Model

The second major component of HEC-HMS is the meteorological sub-model. The meteorological sub-model is where time series data and storm rainfall depths are assigned to sub-basins in the watershed in the Basin Model for various storms. HEC-HMS treats the hydrologic response of any watershed as driven by rainfall and evaporation over the watershed.

Precipitation could be any of the following kind: (1) observed rainfall from historic event; (2) frequency-based hypothetical rainfall event; (3) maximum possible precipitation event at a given location. Historical rainfall data are helpful in calibration and verification of model parameters. Hypothetical or design storms are used if the accuracy of the model must be checked, when modeling extreme precipitation events, or if a risk of flooding must be assessed. Similarly, both observed historical data and hypothetical data can be used for evapotranspiration.

The Meteorological model includes four different methods for historical precipitation analysis (Hydrologic Engineering Center, 2005):

1. Precipitation data analyzed outside the program are represented by the user-specified hyetograph method.
2. Both recording and non-recording gauge data are represented by the gage weights method.
3. Dynamic data problems are addressed by the inverse distance method.
4. Radar rainfall data are utilized with the gridded precipitation method.

Four additional methods are available in HEC-HMS to generate synthetic precipitation.

The frequency storm method produces balanced storms given specific exceedance probability using statistical data. Regulations for precipitation are implemented to estimate standard project flood in the standard storm method. The SCS hypothetical storm method is based on Natural Resources Conservation Service criteria and implements primary precipitation distributions for design analysis.

Control Specifications

The Control Specifications component enables the user to specify the simulation start time, end time, and the time interval. Multiple control specifications can be created and connected to simulation runs so that when any time control specification is changed, the correspondent simulation period will change accordingly.

Time Series Data

The Time Series Data component integrates input data related to time into the simulation. These data include precipitation, and observed flow. In the model, the precipitation data are in the form of a DSS file, whereas observed flows are manually tabulated.

2.3 HEC-RAS

HEC-RAS, or Hydrologic Engineering Center – River Analysis System, is an integrated system designed to perform one-dimensional hydraulic calculations for networks with natural and constructed channels (US Army Corp of Engineers, 2008).

HEC-RAS is comprised of four major constituents for one-dimensional river analysis.

1. Steady flow water surface profile calculations.
2. Unsteady flow simulations.
3. Movable boundary sediment transport simulations.
4. Water quality analysis.

The four components share a common geometric data representation and common geometric and hydraulic simulation routines (US Army Corp of Engineers, 2008).

Steady flow means that at any point, depth and velocity remains constant with respect to time, such as a constant head discharge in a long straight canal. The steady flow water surface profiles calculations are useful in determining water surface profiles with steady as well as gradually changed flow. In this context, the system is capable of dealing with not only a single river reach, but also dendritic systems and a full network of stream channels. Flow regimes including subcritical, supercritical as well as mixed are all within the capacity of the system. The computational procedures comply with the fundamental energy equations in one-dimensional form. In the case that the water surface profile is dramatically changed, the momentum equation is employed. This includes hydraulic jumps, bridges and stream junctions. Energy losses are addressed by the Manning's equation (friction), and contraction/expansion. The computations take into account the effect of various elements of the stream network like bridges, culverts, weirs, and spillways. The steady system is mainly used for flood plain management and flood insurance studies to assess floodway encroachment. The steady system approach is also applied in the evaluation of impacts of channel improvement (US Army Corp of Engineers, 2008).

Unsteady flow means depth and/or velocity changes in magnitude or direction with respect to time; a flood hydrograph or a curve in a channel are examples of unsteady flow. The unsteady simulation component was developed primarily for subcritical flow regime simulations. It enables simulation of one-dimensional unsteady flow in a full network of open channels. It also has the capacity to carry out hydraulic calculations similar to that of the steady flow component for cross-sections, culverts, bridges, etc. In addition, water storage areas and hydraulic connections between them could also be modeled. The two fundamental principles in this context are the principle of mass conservation and the

principle of momentum conservation (US Army Corp of Engineers, 2008). Theories behind these calculations that are embedded in HEC-RAS system are detailed in HEC-RAS Reference Manual (US Army Corp of Engineers, 2008).

The main objective of the HEC-RAS model is to determine water surface elevations at locations of interest. This can be achieved either by the user inputting a set of flow data, for the steady flow scenario, or through hydrograph routing, for the unsteady flow scenario. Data needed to perform the necessary calculations varies among geometric data, steady flow data, or unsteady flow data. The geometric data are needed for any type of analysis (US Army Corp of Engineers, 2008).

2.4 HEC-GeoRAS

HEC-GeoRAS is an ArcGIS extension software program developed collaboratively by HEC (Hydrologic Engineering Center) and ESRI (Environmental Systems Research Institute, Inc.). HEC-RAS continues to be developed and the latest version is version 4. The current version of the software is the result of the effort by HEC and ESRI to transplant the functionality of GeoRAS 3.1 to the ArcGIS platform.

As a set of tools specially designed to handle geospatial data for connection with HEC-RAS, the extension enables users with rudimentary experience with GIS to create HEC-RAS input files from DTMs (Digital Terrain Model) and complementary data sets. It is also useful in viewing and processing exported results from HEC-RAS (US Army Corp of Engineers, 2009).

DTM files of a river system in TIN (triangulated irregular network) or GRID format are used to create the import file for HEC-RAS in HEC-GeoRAS. A series of point, line and polygon layers are created. The RAS layers include Stream Centerline, Flow Path

Centerlines, Main Channel Banks, and Cross Section Cut Lines. Additional geometric data can be extracted by using additional RAS layers including Land Use, Levee Alignments, Ineffective Flow Areas, Blocked Obstructions, Bridges/Culverts, Inline Structures, Lateral Structures and Storage Areas (US Army Corp of Engineers, 2009). The process flow of using HEC-GeoRAS is illustrated in Figure 4 below.

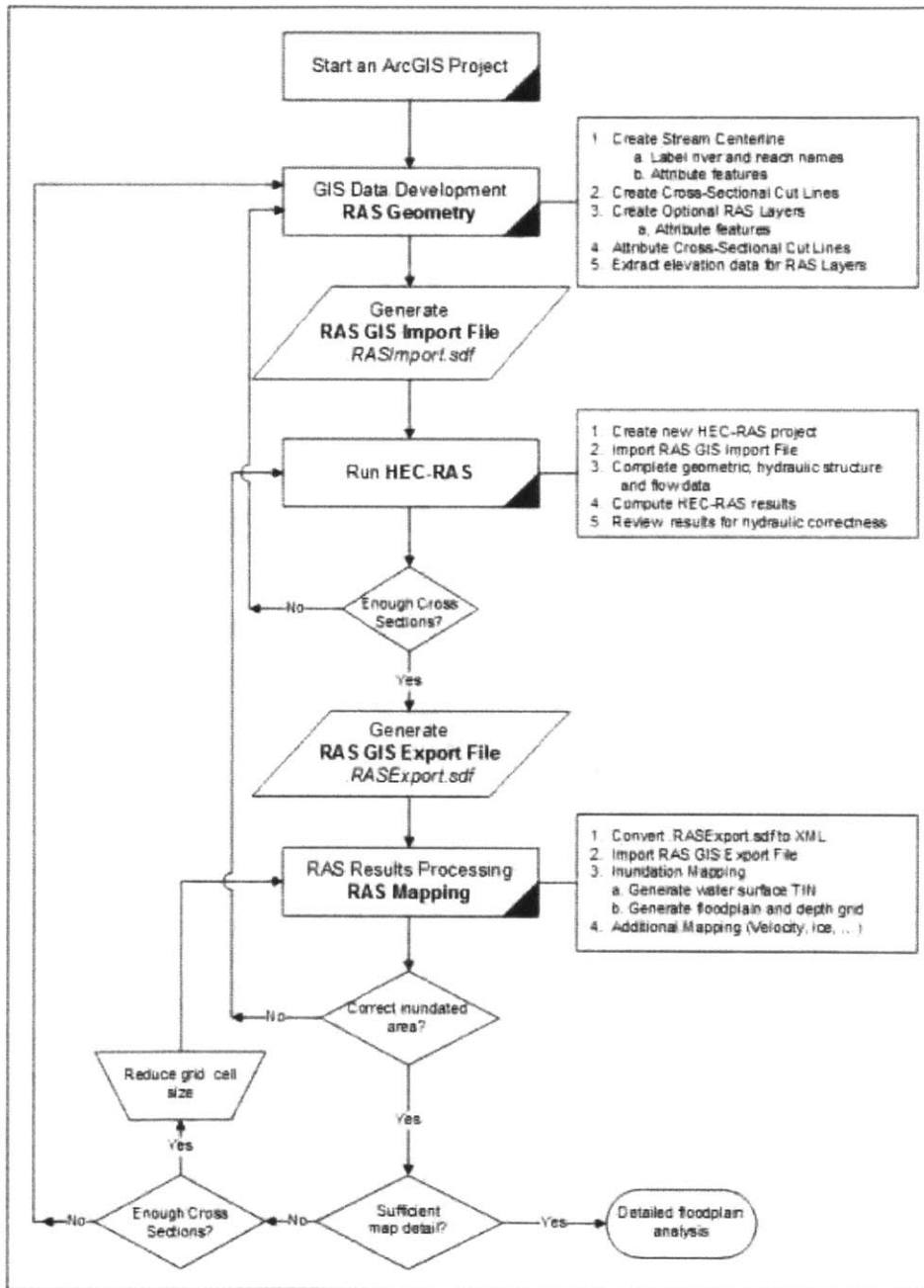


Figure 4 - Process flow diagram for using HEC-GeoRAS (US Army Corp of Engineers, 2009)

3. MODEL DEVELOPMENT

3.1 HEC-HMS Analysis

3.1.1 Watershed delineation & Geometry file Creation

The watershed is delineated in the ArcGIS environment. A *Shape* file is used to generate a basin model that is then directly used by HEC-HMS.

3.1.2 Precipitation Data Acquisition

Rain gauges are usually the best source for historical rainfall data. However, in the study area in Uganda, the availability of rain gauges is limited. Three rain gauges are identified in different regions. While the Bududa and Buginyanya gauges are more recent, the Tororo data spans over the years 1929 to 1986 (Cecinati, 2013).

At the same time, a range of satellite precipitation data was retrieved. Among these data, the TRMM-3B42 performs best in the Mt. Elgon region. Compared with ground rain gauges, the TRMM data appear to be more reliable and consistent than Bududa and Buginyanya gauge data. While Tororo data are also considerably consistent, the time interval of one year is too coarse for the modeling purpose in the short term (Cecinati, 2013).

In order for HEC-HMS to utilize the TRMM rainfall data, weighted averages are taken with respect to the area of each sub basin underlying each data cell. Overlaying the TRMM file onto the watershed shape file, the values of precipitation for every sub-basin were calculated. A map of the sub-basins identified with TRMM cells appears in Figure 5 and Table 1 contains equations used to calculate weightings for each sub-basin based upon area.

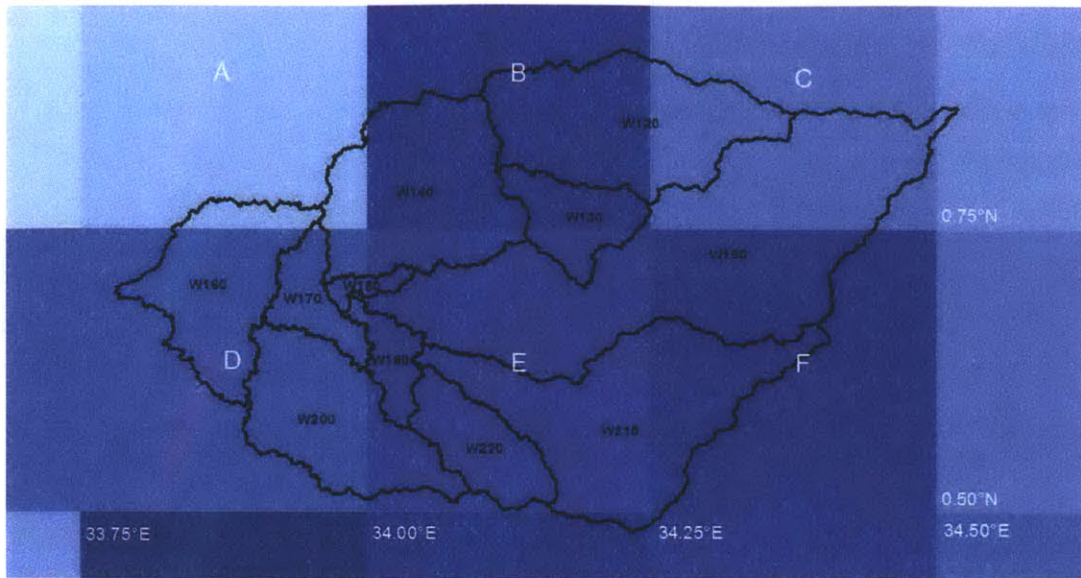


Figure 5 - The sub-basins identified with TRMM cells (Cecinati, 2013)

Sub-basin	Equation
W120	$2/3 B + 1/3 C$
W130	$3/7 E + 4/7 B$
W140	$1/21 D + 2/21 A + 3/21 E + 15/21 B$
W150	$1/3 E + 1/3 F + 1/3 C$
W160	$1/8 A + 7/8 D$
W170	D
W180	$1/2 D + 1/2 E$
W190	$1/15 D + 14/15 E$
W200	$2/3 D + 1/3 E$
W210	$1/2 E + 1/2 F$
W220	E

Table 1 - The average of the TRMM cells contained in every sub-basin, weighted on the areas (Cecinati, 2013)

The mathematical operation is repeated for each sub-basin for each day to give a record of daily rainfall estimates for every sub basin, which is then used in HEC-HMS. The calculated rainfall data is presented in Appendix A. More details can be found in Cecinati's (2013) work.

3.1.3 Observed Flow Acquisition

The Ministry of Water and Environment in Uganda has been managing one river stage gauge in Busiu, which is a community near the center of the watershed (Figure 6). The river gauge is located beside a bridge linking Mbale and Manafwa districts (Figure 7).

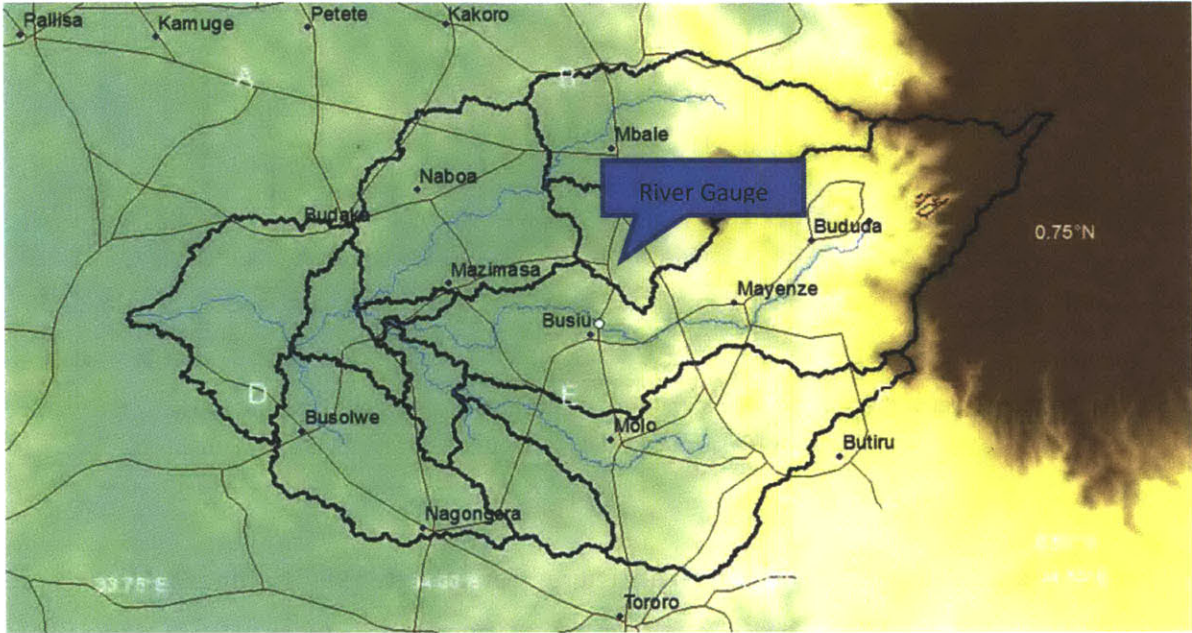


Figure 6 - River gauge position inside the Manafwa River watershed (Cecinati, 2013)



Figure 7 - River gauge used by the Water Resources Department

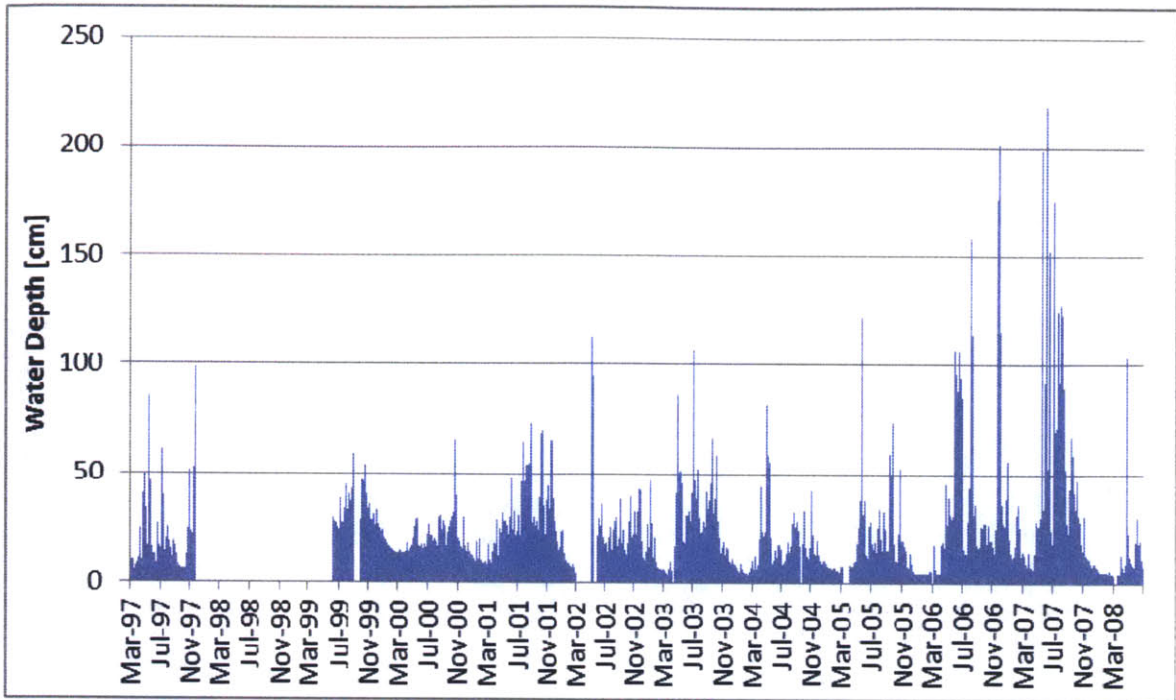


Figure 8 - Water level of the Manafwa River in Busiu, as recorded in elevation above the gauge by the Water Resources Department from March 1997 – March 2008

The river gauge provides river stage data dating from March 1997 to June 2008, except for the period between November 1997 and June 1999 (Figure 8). The missing data are believed to be attributed to a flood in 1997.

To understand the geometric properties of the Manafwa River, and to verify available data, measurements of the river cross section were taken at two different locations during a site visit. One location was selected to be in a bending section of the river, whereas the other was in the straight part, recognizing the difference in the geometry (Figure 9).

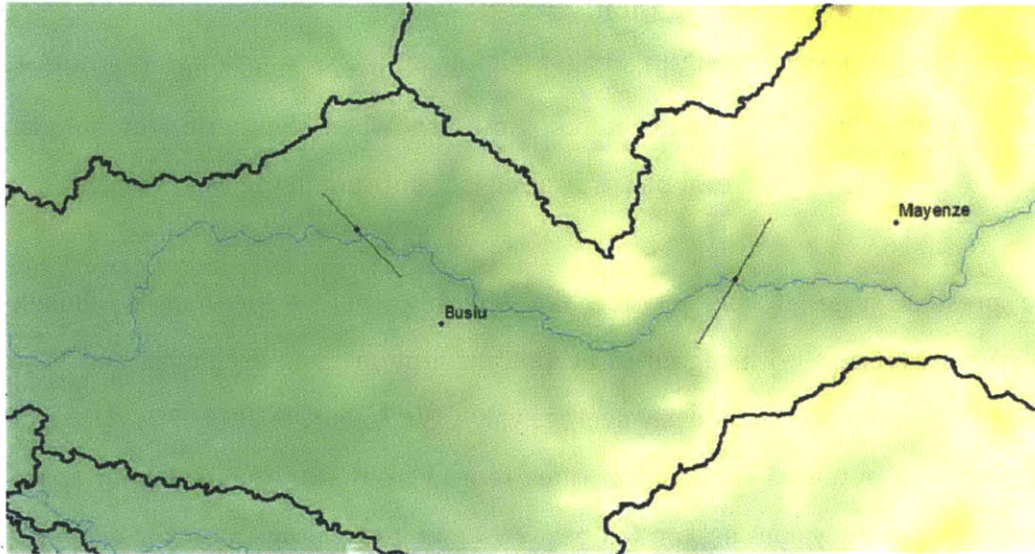


Figure 9 - River cross sections position (Cecinati, 2013)

In Figure 9, the cross section on the left is in a river curve, downstream; the cross section on the right is in a straight section, upstream.

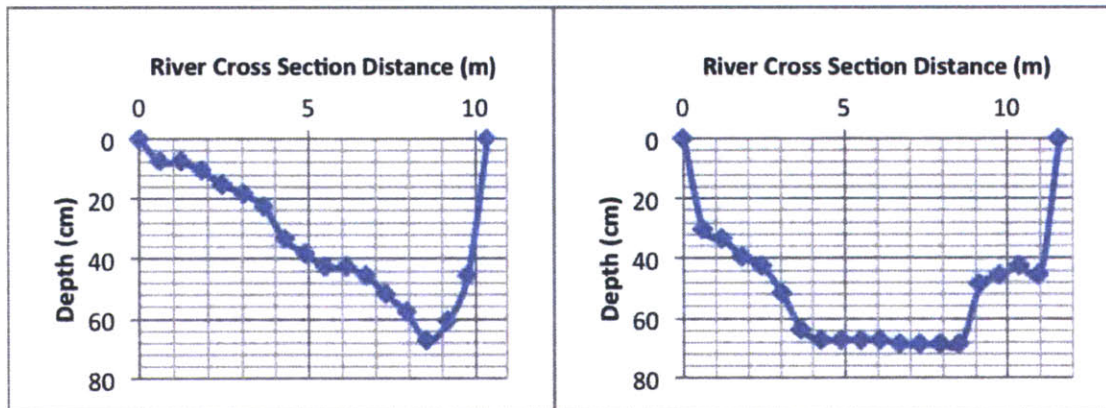


Figure 10 - Plot of river cross sections

In Figure 10, the cross section on the left is in the river curve at a meandering region (river flow into cross section), whereas the cross section on the right is in a straight segment. Based on the comparison between river gauge recording and the cross section measurement, the river stage data appears consistent and reasonable.

3.1.4 Evapotranspiration Estimation

In short term hydrologic modeling, such as flood event modeling, the effect of evapotranspiration can be safely omitted. However, when the period of simulation increases to as long as a year, evapotranspiration is significant in the water budget.

At the present stage of this project, the Monthly Average method is chosen in Meteorological Models. With regard to evapotranspiration rates in Central and Eastern Africa, sources differ on the monthly average value. While Dagg et al (1970) claimed that annual values of potential evaporation rates ranged from 1800 to 2200 mm annually, and average monthly values seldom fell below 90 mm, the average monthly evaporation values over the years are shown to be considerably lower in the map provided by Centre for Ecology & Hydrology, which appear in Table 2. For current long term modeling purpose, the monthly average evaporation values are estimated from the map retrieved online (Centre for Ecology & Hydrology).

Month	Average Monthly Evaporation (mm/month)		
	Low	High	Average
Jan	70	90	80
Feb	70	90	80
Mar	70	100	85
Apr	70	100	85
May	60	90	75
Jun	40	70	55
Jul	40	70	55
Aug	50	70	60
Sep	60	100	80
Oct	50	110	80
Nov	60	100	80
Dec	50	100	75

Table 2 - Average monthly evapotranspiration value for an average year (Centre for Ecology & Hydrology)

In order for HEC-HMS to carry out calculations involving evapotranspiration, the crop

coefficient is also required. Although the watershed is home to a variety of plantations, the coefficient is estimated to be 1.05 as is tabulated for rice and maize in the FAO Corporate Document Repository (Natural Resources Management and Environment Department).

3.1.5 SCS CN Number Method

The Loss Method chosen for HEC-HMS modeling is the SCS Curve Number (CN) method. It is a well-established method with relatively high accessibility. The method incorporates land use, land cover and soil type information into three parameters, namely initial abstraction, CN, and impervious area percentage. Each sub-basin has its own set of parameters specified respectively.

Typically, three mechanisms contribute to the abstraction for a single storm event: (1) rainfall interception, (2) depression storage, and (3) infiltration into the soil (Patel, 2009). These three elements are incorporated into the term Initial Abstraction, which is a threshold value which when exceeded by precipitation results in runoff (HEC-1 & HEC-HMS, 1999). As is illustrated in Figure 11 below, the dark area represents the initial abstraction I_a . It can be considered as the water loss before the runoff begins. In contrast, F stands for the actual retention after runoff begins.

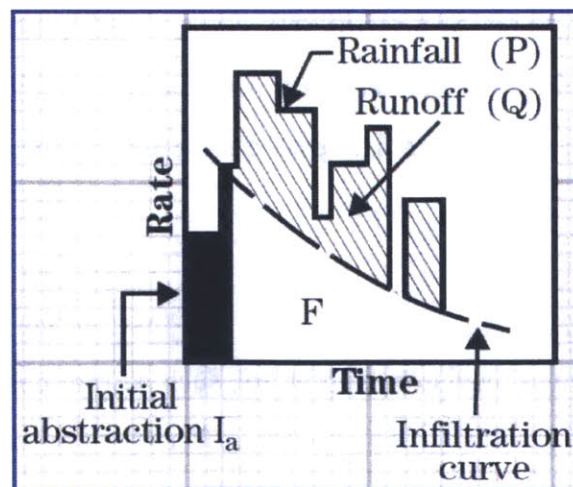


Figure 11 - Components of storm event (National Resources Conservation Service, 2004)

The initial loss, or initial abstraction, is not a mandatory parameter. While it is recommended that the initial abstraction value range from 0 mm to 1 mm, as seen below in Table 3, it is a common practice to relate initial abstraction (i.e. the amount of water infiltrated before runoff begins) to the potential maximum retention (i.e. the maximum amount of water that will be absorbed after runoff begins). The ratio of initial abstraction to potential maximum retention is commonly quoted as 0.2 (The Shodor Education Foundation, Inc., 1998).

Land Use	Recommended Initial Abstraction (mm)
Paved Areas	0
Sloped Roofs	0
Flat Roofs	0
Lawn Grass	0.75
Open Fields with Minimal Vegetation	0.5
Open Fields with Cover Crop	0.75
Wooded Areas	1

Table 3 - Recommended value for initial abstraction (HEC-1 & HEC-HMS, 1999)

For this project, the value of the initial abstraction is set to blank as a start and is changed only for calibration purposes, because the flow result is calibrated against actual flow data where antecedent moisture has been taken into account. Another consideration is that losses to depression storage and canopy are neglected and evapotranspiration data are specified separately.

The impervious area percentage accounts for the fact that certain parts of the modeled area are not a good media for water to infiltrate, such as rooftops, pavements etc. No infiltration losses are incurred from this impervious fraction of the sub basins. In Table 4, recommended values for the impervious area percentage are listed. As the watershed is

most accurately described as open space and is minimally paved, the impervious area parameter value is estimated to be 1% (HEC-1 & HEC-HMS, 1999).

Land Use Type	Impervious Percentage
Highways, Parking Areas	95
Commercial, Industrial, Office	85-95
Apartments, Condominiums	70-80
Single Family Residential (including duplex or split lot housing) 1-10 units/acre	5-60
Parks	5 - 10
Open Space (fields, wooded area)	1 - 5

Table 4 - Recommended Impervious Percentage values (HEC-1 & HEC-HMS, 1999)

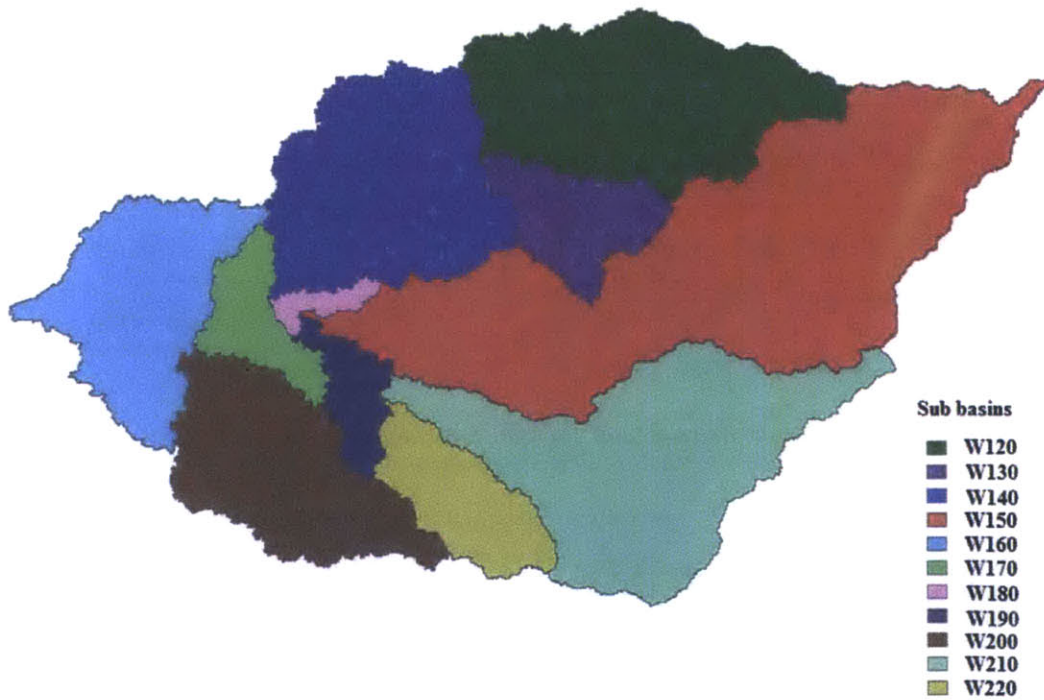


Figure 12 - Manafwa watershed Sub basins (Bingwa, 2013)

Figure 12 shows the different sub-basins with name codes used in HEC-HMS illustrated in different colors. The FAO (Food and Agriculture Organization) developed a map of land use through their AFRICOVER program in 2009, which serves as the main source of information on land use in this project (Figure 13). Soil data were also obtained from FAO's Harmonized World Soil Database (HWSD) represented in different soil clay content as shown in Figure 14.

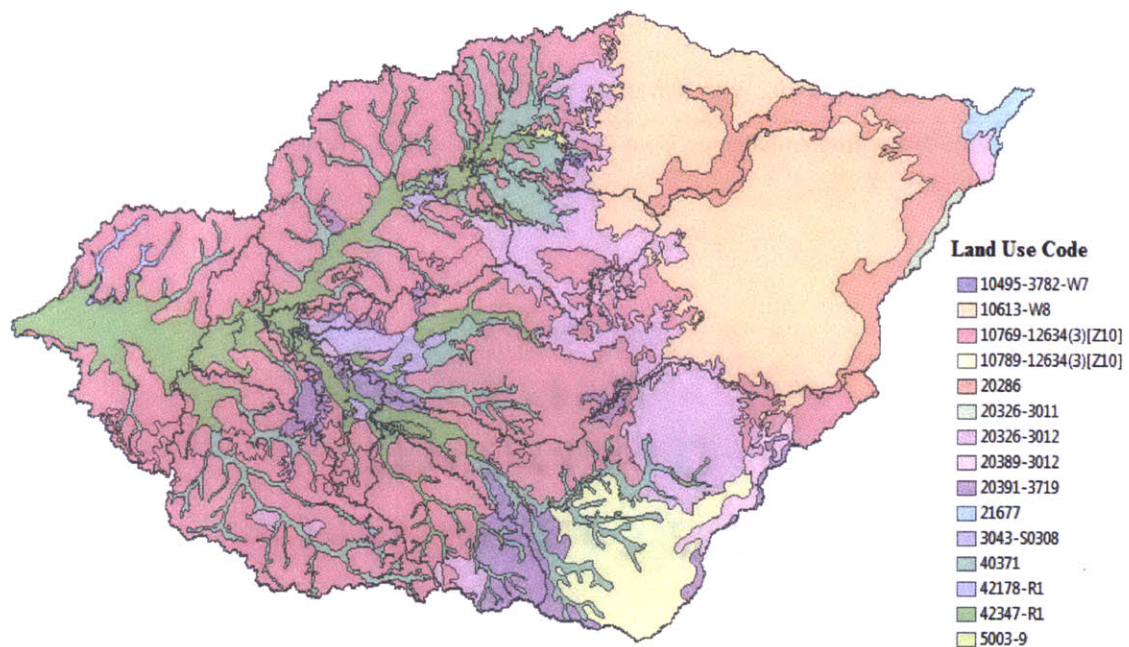


Figure 13 - Manafwa Watershed Land Use Map, Africover 2009 (Bingwa, 2013)

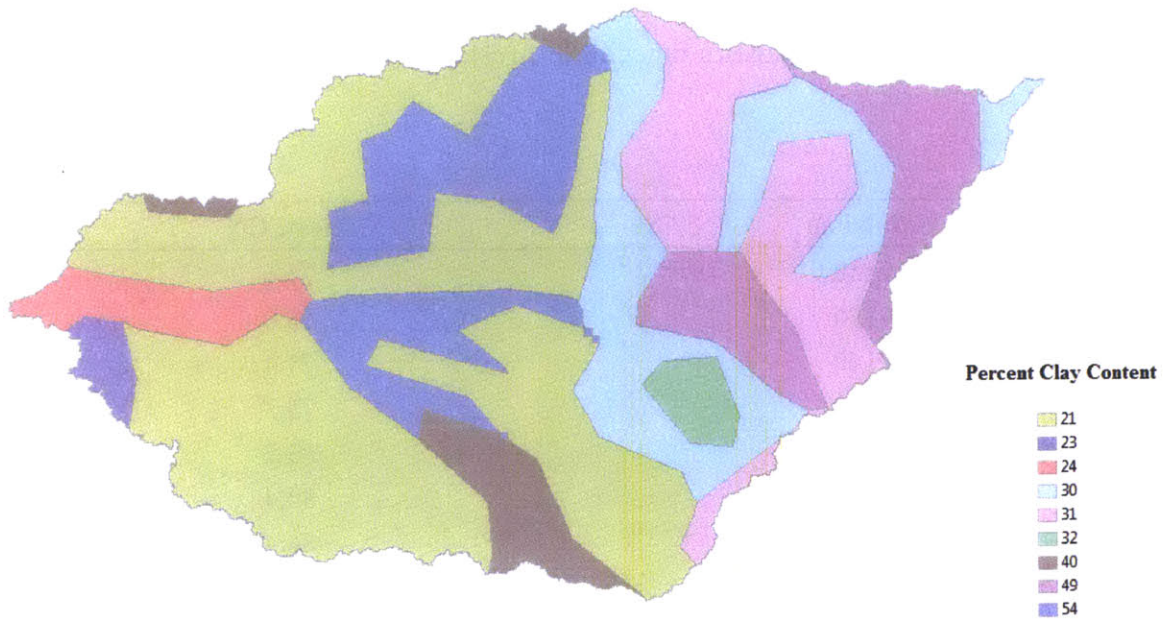


Figure 14 - Soil data - percent clay content, from HWS database (Bingwa, 2013)

Using Matlab, land cover data and soil type data are processed and mapped. The result is a CN map as shown in Figure 15.

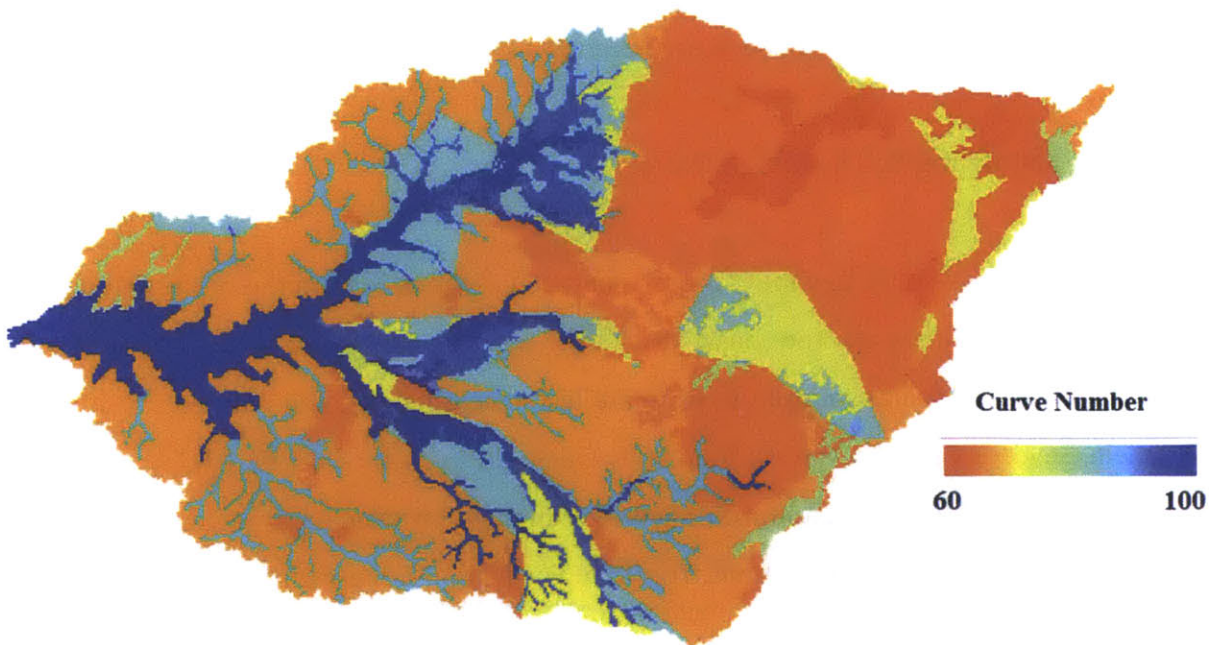


Figure 15 - Manafwa watershed CN Map (Bingwa, 2013)

The CN value in one particular sub basin is obtained by averaging the CN readings within that sub-basin utilizing a statistics function in ArcMap. The result is tabulated below in Table 5.

Sub-basin	Mean CN
W120	75.6
W130	78.0
W140	71.4
W150	75.3
W160	83.2
W170	82.4
W180	86.4
W190	82.2
W200	77.4
W210	77.7
W220	80.2

Table 5 - CN values for respective sub-basins (Bingwa, 2013)

The major disadvantages of the SCS CN method are fixing the initial abstraction ratio, and lack of clear guidance on how to vary Antecedent Moisture Conditions (AMC) (Patel, 2009). More information can be found in Bingwa's (2013) work.

3.1.6 Estimating Sub basin Lag Time

The sub basin-specific lag time is a representation of the time from the center of mass of precipitation excess to the peak discharge (Stantec consulting Inc., 2009). Many equations have been proposed to estimate basin lag time over the last century. Among them, Snyder's equation is most frequently cited (Loukas & Quick, 1996). US Army Corps of Engineers (USACE) customized Snyder's equation, introducing N values relating the effect of development on lag time. The USACE equation appears in the following form (Boucher, 2011).

$$T_{lag} = 24 \times N \times \left(\frac{L \times L_{ca}}{S^{0.5}} \right)^{0.38}$$

T_{lag} is the elapsed time from the beginning of an assumed continuous series of unit effective rainfalls over an area to the instant at which the rate of the resulting runoff at the area concentration point equals 50 percent of the maximum potential rate of the resulting runoff at that point. L is the length of the main drainage path in miles. L_{ca} is the length along the drainage path from a point opposite the centroid of the watershed to the outlet point in miles. S is the overall slope of the main watercourse in feet per mile. N is the dimensionless weighted watershed Manning coefficient (Boucher, 2011).

In the Drainage Manual by the City and County of Sacramento, a similar method called Basin “n” Method is presented, and is easier to implement than USACE’s equation (Boucher, 2011). The Basin “n” lag equation was revised by the USACE and the U.S. Bureau of Reclamation based on Snyder’s equation. It appears in the form below.

$$L_g = C \times n \times \left(\frac{L \times L_c}{S^{0.5}} \right)^{0.33}$$

L_g is the lag time in seconds. C is a constant with value of 174 when lag time is calculated in seconds. n is the tabulated Basin “n” overbank channelization roughness value for developed and undeveloped scenarios. The table of n values is attached in the Appendix B. L is the length of the longest watercourse measured as approximately 90% of the distance from the point of interest to the headwater divide of the basin. It is measured in meters when lag time is in seconds. L_c is the length of the longest watercourse measured upstream from the point of interest to a point close to the centroid of the basin. It is also measured in meters when lag time is in seconds. S is the overall slope of the longest watercourse between the headwaters and concentration point. It is measured in meter per meter when lag time is in seconds (City and County of Sacramento, 1996).

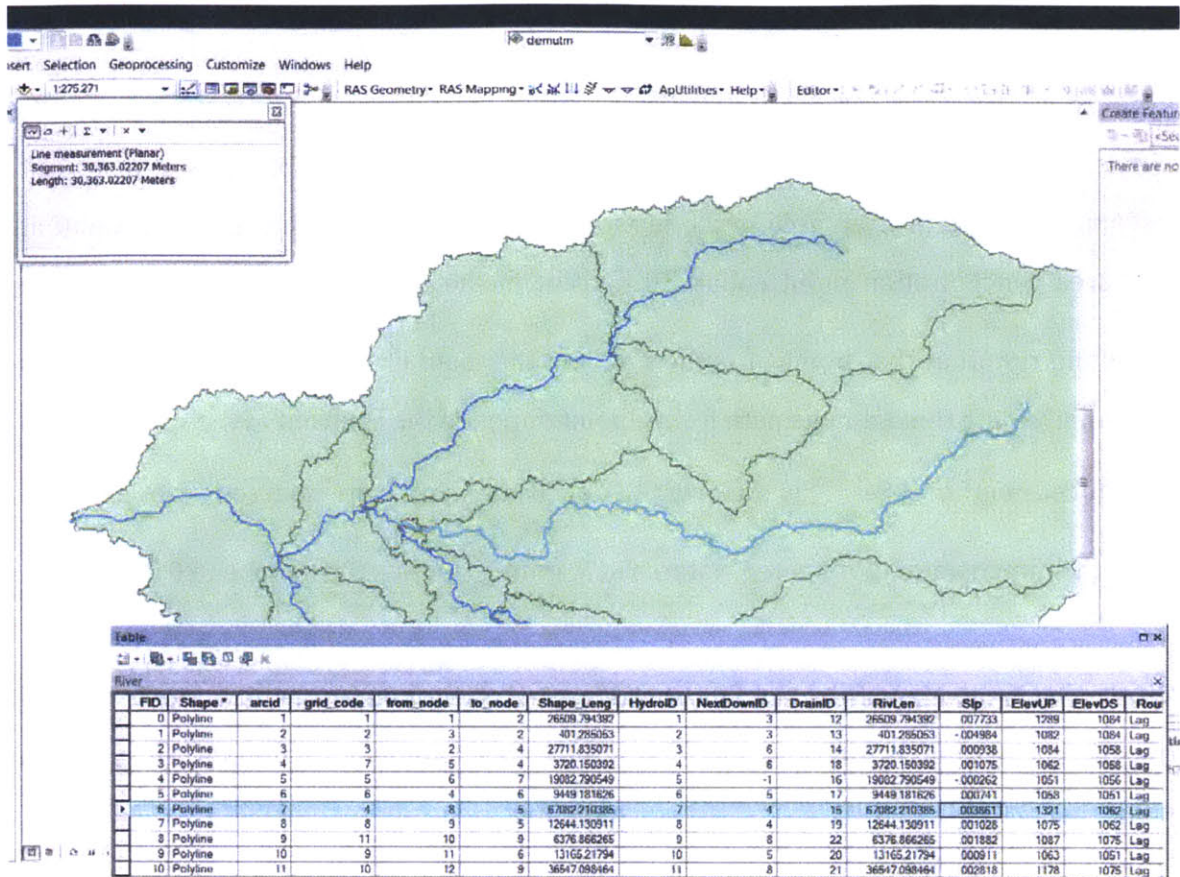


Figure 16 - Screen Shot of ArcMap: Determination of lag equation parameters

As shown in Figure 16 above, ArcGIS is utilized to obtain values for L , L_c , and S in the equation above. L is obtained from the *shape length* column in the *attribute table* in ArcGIS. L_c is measured from the outlet of each sub basin to the centroid of the sub basin. S is obtained from *slope* column in the *attribute table*. The parameters and lag times for this project are determined and presented in Table 6.

Sub-basin	Parameters for lag equation					
	<i>C</i>	<i>n</i>	<i>L</i> (m)	<i>L_c</i> (m)	<i>S</i> (m/m)	<i>L_g</i> (hr)
w120	174	0.12	26509.79	13163	0.007733	8.5
w130	174	0.12	401.2851	8376	0.019	1.6
w140	174	0.12	27711.84	12995	0.000938	12.2
w150	174	0.12	67082.21	30363	0.003861	17.1
w160	174	0.12	19082.79	9723	0.000578	10.6
w170	174	0.12	9449.182	4421	0.000741	6.2
w180	174	0.12	3720.15	3468	0.001075	4.0
w190	174	0.12	12644.13	6985	0.001028	7.6
w200	174	0.12	13165.22	12044	0.000911	9.4
w210	174	0.12	36547.1	21913	0.002818	13.3
w220	174	0.12	6376.866	9787	0.001882	6.1

Table 6 - Parameter values for lag time estimation using Basin “n” method

Another method to calculate Lag Time based on estimation of concentration time can be found in the HEC technical reference manual (Hydrologic Engineering Center, 2000).

3.1.7 Estimating Reach Routing Parameters

Reach routing represents the movement of water through stream channels (Bras, 1990). A discharge hydrograph is generated through routing based on channel properties and the inflow hydrograph. Two routing models are considered in this project.

The simplest routing model in HEC-HMS is the Lag Model. However, it neglects attenuation in the routing processes. As mentioned earlier, the Muskingum routing method utilizes a simple finite difference approximation of continuity equation. It is chosen as it better represents the attenuation of the hydrograph. The method requires two parameters, i.e. *K* and *x*. More details of the method can be found in Bras’s (1990) work. The Muskingum *K* value is essentially the time needed for water to travel through a

certain reach. The lengths of all reaches are obtained using ArcGIS.

Field measurements were taken of flow velocity profiles at the location where cross sections were measured on the Manafwa River; these results appear in Table 7 below.

Depth (ft.)	Velocity (cm/s)
0	54
0.5	50
1	54
1.5	54
2	48
2.2	28

Table 7 - Velocity profile measured at one location in the Manafwa River

The measured surface velocity of the Manafwa River is around 0.5 m/s. Considering the velocity upstream of this point may have equal or higher surface velocities because upstream channels would have steeper slopes and narrower cross sections, the reaches upstream are conservatively assigned an average velocity of 0.5 m/s in estimating the Muskingum K value. The reaches in the middle of the basin are assigned a velocity of 0.4 m/s, whereas the last segment of reach is assigned a velocity of 0.3 m/s. The result is thus presented in Table 8.

Sub-basin	River	Parameters		
		L (m)	Average Velocity (m/s)	Muskingum K (hr)
w120	R12	26509.79	0.5	14.7
w130	R13	401.2851	0.5	0.2
w140	R30	27711.84	0.4	19.2
w150	R15	100	0.5	0.1
w160	R50	19082.79	0.3	17.7
w170	R60	9449.182	0.4	6.6
w180	R40	3720.15	0.4	2.6
w190	R80	12644.13	0.4	8.8
w200	R20	13165.22	0.4	9.1
w210	R21	36547.1	0.5	20.3
w220	R22	6376.866	0.5	3.5

Table 8 - Muskingum parameter estimation (R15 represents an artificial reach with length 100m)

One thing to note here is the length of reach R15; it is set to a small arbitrary value of 100 m. The reason is discussed in the calibration section below.

3.1.8 Initial and Constant Loss method parameters

Three parameters are required in the Initial and Constant loss model: (1) impervious percentage, (2) initial loss, and (3) constant loss rate. As discussed in the curve number method, impervious percentage is assumed to be 1% throughout the watershed. The initial loss represents interception and depression storage and is not unlike the initial abstraction in the curve number method. The value of the initial loss is set to be 0 as simulation results are calibrated against day-to-day observed flow data.

The constant loss rate represents the maximum potential rate of precipitation loss, and is assumed to be constant throughout each event. Recommended values can be found in the technical reference manual (Hydrologic Engineering Center, 2000) and are presented

below in Table 9.

Soil Group	Description	Range of Loss Rates (in/hr)
A	Deep sand, deep loess, aggregated silts	0.30-0.45
B	Shallow loess, sandy loam	0.15-0.3
C	Clay loams, shallow sandy loam, soils low in organic content, and soils usually high in clay	0.05-03.15
D	Soils that swell significantly when wet, heavy plastic clays, and certain saline soils	0.00-0.05

Table 9 - SCS Soil groups and infiltration loss rates (Hydrologic Engineering Center, 2000)

However, as the loss rate is not a measured parameter, it is better determined by calibration (Hydrologic Engineering Center, 2000). Through trials with HEC-HMS, a value of 0.5 mm/hr is found to be a reasonable starting value.

3.1.9 Simulation

Simulations are carried out both in long term and short terms for the CN loss method and initial and constant loss method respectively to compare results. In fact, warning messages from HEC-HMS during long-term simulations suggest that neither of the methods is suitable for simulations longer than 14 days. Other warning messages include that a time interval of 1 day is too large for the Muskingum routing method, and that reaches upstream have no flow. The reason for upstream flow to be 0 is that the runoff of one sub-basin converges at the outlet of that sub-basin before it flows into the next reach downstream. As the upstream reaches have no sub-basins further up, no flow is present.

The analysis with HEC-HMS is based on the parameters discussed above, as well as an array of other assumptions, which appear in Table 10.

Component	Other Specifications and Assumptions
Basin Models	No canopy method considered for sub-basins No surface method considered for sub-basins No baseflow considered for sub-basins Standard graph type used in transformation for sub-basins No loss/gain method considered for each reach
Meteorological Models	Specified Hyetograph used with manually-input satellite data No snowmelt considered Total override with rainfall options No missing replace
Control Specifications	Time interval set to 1 day for long-term simulations and 1 hour for short-term simulations. This is very important in interpreting the graphic results presented below.
Time Series Data	Observed flow depth transformed to observed flow rate assuming river gauge is 1.5m above the river bed.

Table 10 - Other simulation specifications and assumptions for HEC-HMS

For the time series observed flow data at Busiu, several equations are involved in transforming water depth data to flow rate data. Because the actual elevation of the river gauge is unknown, the sensor is assumed to be 1.5 m above the river bed as the flow rate result obtained with this value corresponds well with measured values in Uganda. This value is not indubitable. Close scrutiny of the river gauge elevation data reveals that all elevations are positive even in dry seasons. However, during the site visit in Uganda in the dry season, the river was found to be less than 1.5 m deep. It is implied that the equations and calculations are still subject to further improvement. Details of the transformation can be found in Bingwa's work (Bingwa, 2013).

3.1.10 Calibration

As HEC-HMS refers to calibration also as optimization in the model, the two terms are

used interchangeably in this work. To calibrate the model, the observed flow data is manually input to the time series data component. Figure 17 shows the way observed flow is stored in *Time Series Data* in HEC-HMS.

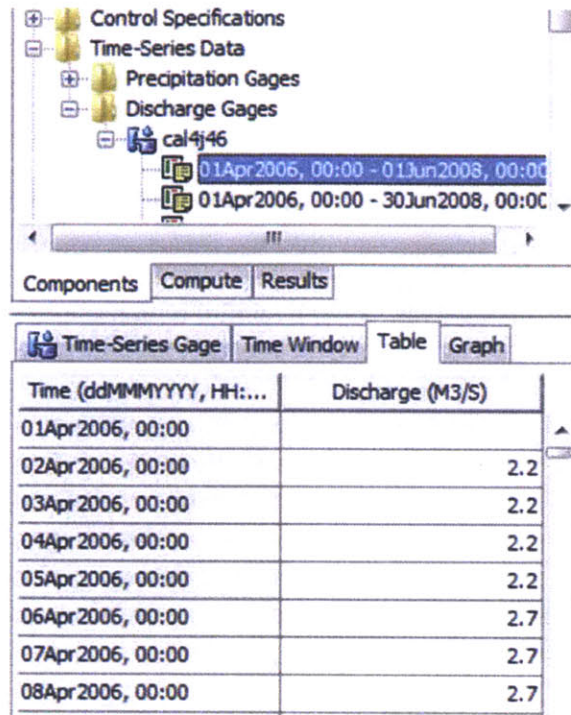


Figure 17 - Screen shot of HEC-HMS: Tabulated observed flow values

As is illustrated in Figure 18, the actual location of the flow observed during the January 2013 site visit is in the middle of the sub-basin w150, where no model result is reported. To obtain an independent value of discharge from sub-basin w150 for calibration purposes, J15 is created as an arbitrary junction downstream to sub-basin w150 and is linked to the original junction through reach R15. This is why the length of R15 is set to 100 arbitrarily to calculate Muskingum K. Screen shots for the calibration scheme appear in Figures 19 and 20.

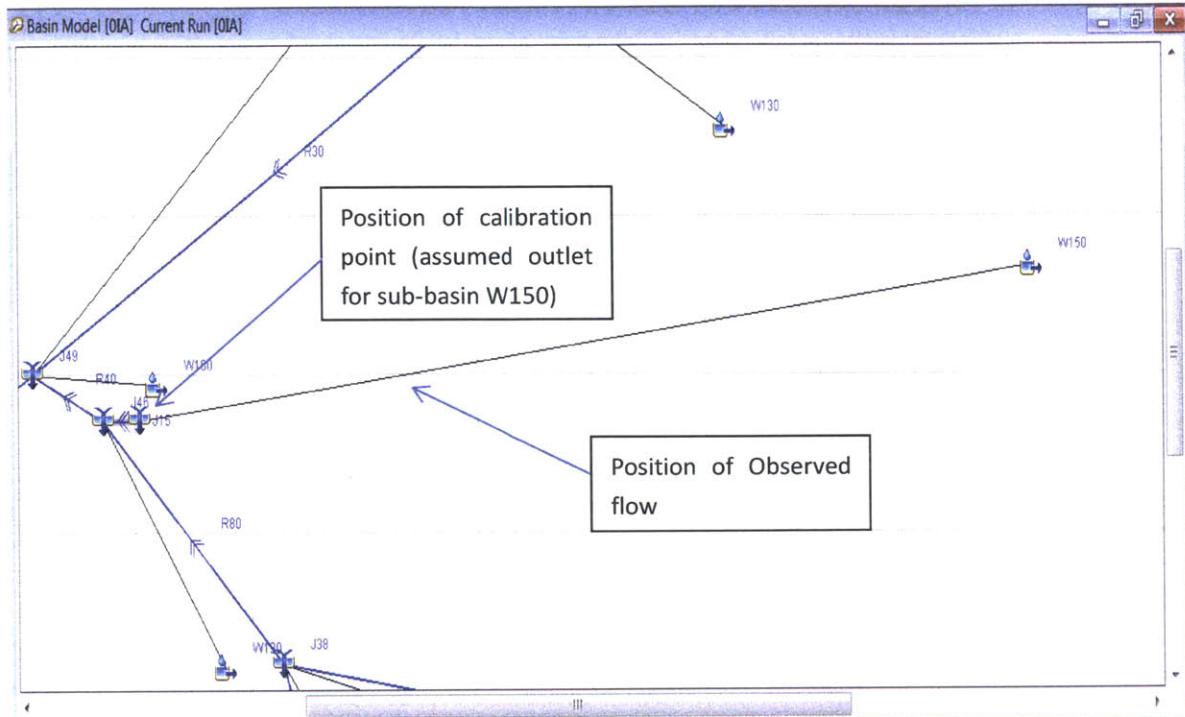


Figure 18 - Screen shot of HEC-HMS: Calibration point and actual position of observed flow

Only parameters for sub-basin W150 are auto-calibrated due to limited measured flow data. Nonetheless, the calibrated values can be used as guidance values for the simulation results obtained for other sub-basins.

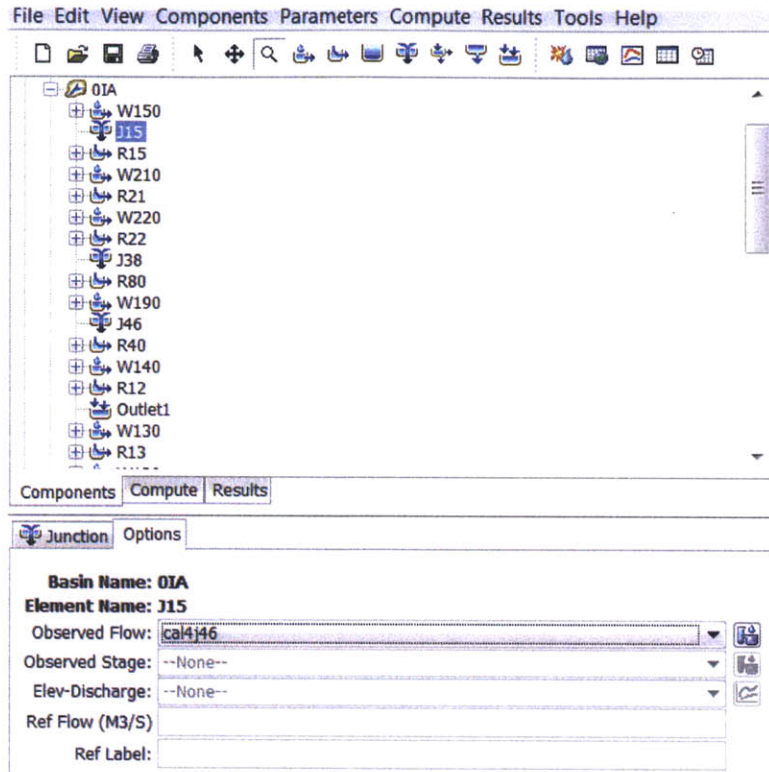


Figure 19 - Screen shot of HEC-HMS: Time series data of observed flow is chosen for W150 (J15)

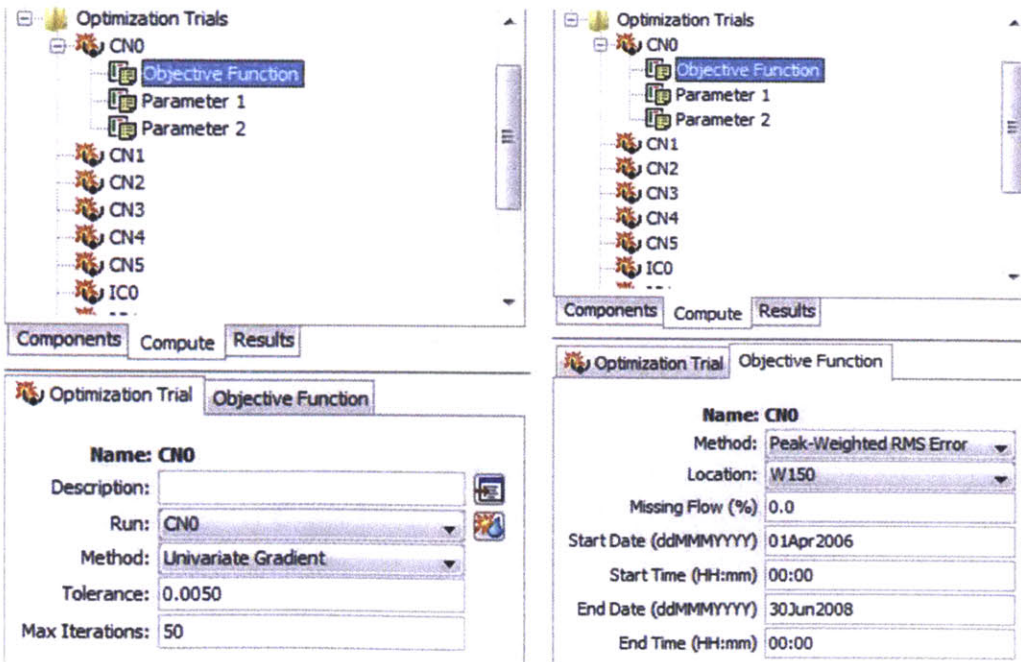


Figure 20 - Screen shot of HEC-HMS: Optimization trial window

The calibration method used in this work is the Peak-Weighted root mean square (RMS) Error method. In the calibration results in HEC-HMS, objective function values are reported. As the calibration is based on an RMS algorithm, the smaller the objective function, the better the simulated results fit the observed flow.

3.2 HEC-RAS Analysis

3.2.1 Creating Geometry File in ArcGIS using HEC-GeoRAS toolbox

The two fundamental data files used for geometry file creation in ArcGIS are the digital elevation model (DEM) of the watershed and the shape file of the river network. With these two datasets, the goal is to generate a raster file that reflects both the river terrain and the potential floodplain in the watershed.

Properties of the river signified in the form of cross sections, bank lines, flow paths, etc. can be abstracted from the DEM data and geo-referenced automatically. The DEM files are retrieved from NASA website (NASA, n.d.). However, the DEM data used have a resolution of 30 m, while the Manafwa River is sometimes less than ~10 m wide. Therefore the river channel is likely to disappear in the DEM map. With this data limitation, the DEM file cannot generate accurate cross section profiles of the river. At this stage of the project, the strategy to generate a preliminary river channel is to neglect the variation in cross sections along the run of the river and assume the river is approximately 10 m wide throughout the entire reach. This is based on the two cross sections measurements taken in Uganda in January 2013. At the same time, based upon observations during the site visit in January 2013, the depth of the river on average is around 1 m from the water surface to the river bottom. Yet this depth reflects only dry season flow and is significantly small compared with the variation in the elevation of terrains in the floodplain. Thus, a somewhat bold assumption is made that the depth of the river channel is 3 m from the top of the banks to the river bottom throughout the

entire reach.

In addition, for the HEC-RAS analysis, the segment of reach between junction J46 and the outlet presented in HEC-HMS is the only segment of interest. This segment represents the area where flooding would most often occur and affect the residing population. See Figure 21 for an image of the shape file of river overlaying DEM map with highlighted reach of interest.

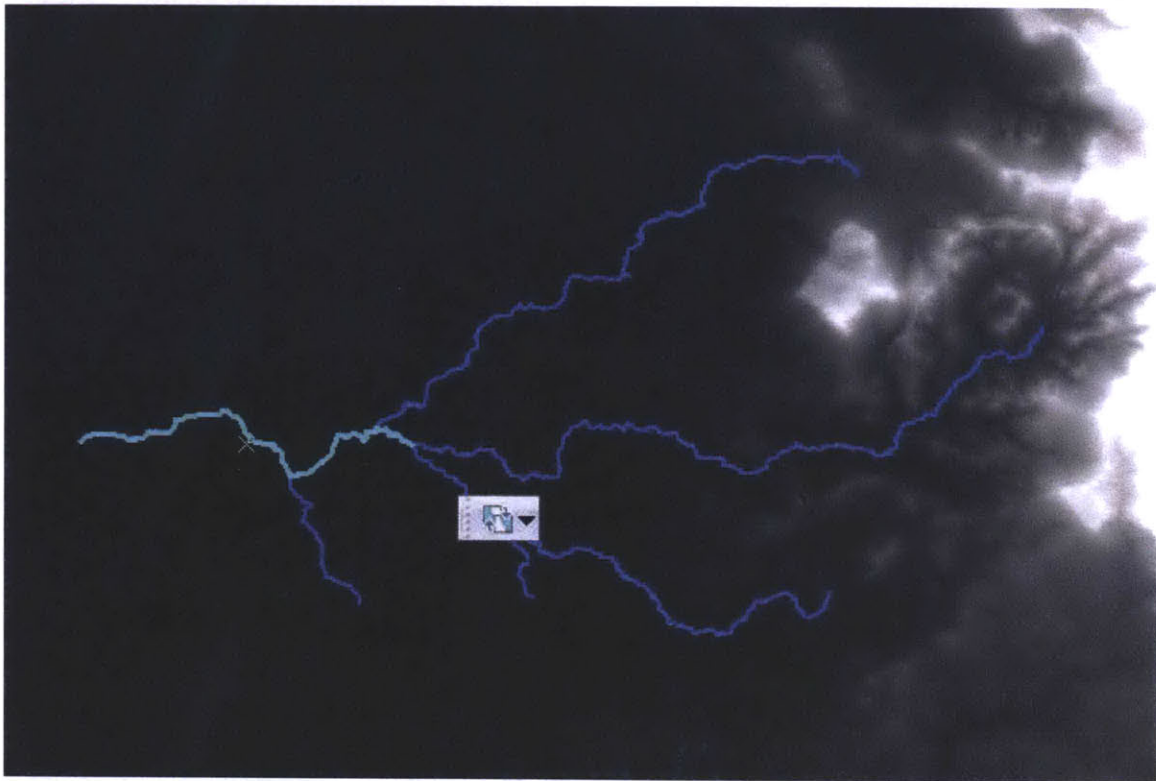


Figure 21 - Screen Shot of ArcMap: the segment of river network studied in HEC-RAS

The DEM data and river network data are processed with the help of built-in ArcMap functions before they are combined into one raster and further geo-referenced with HEC-GeoRAS.

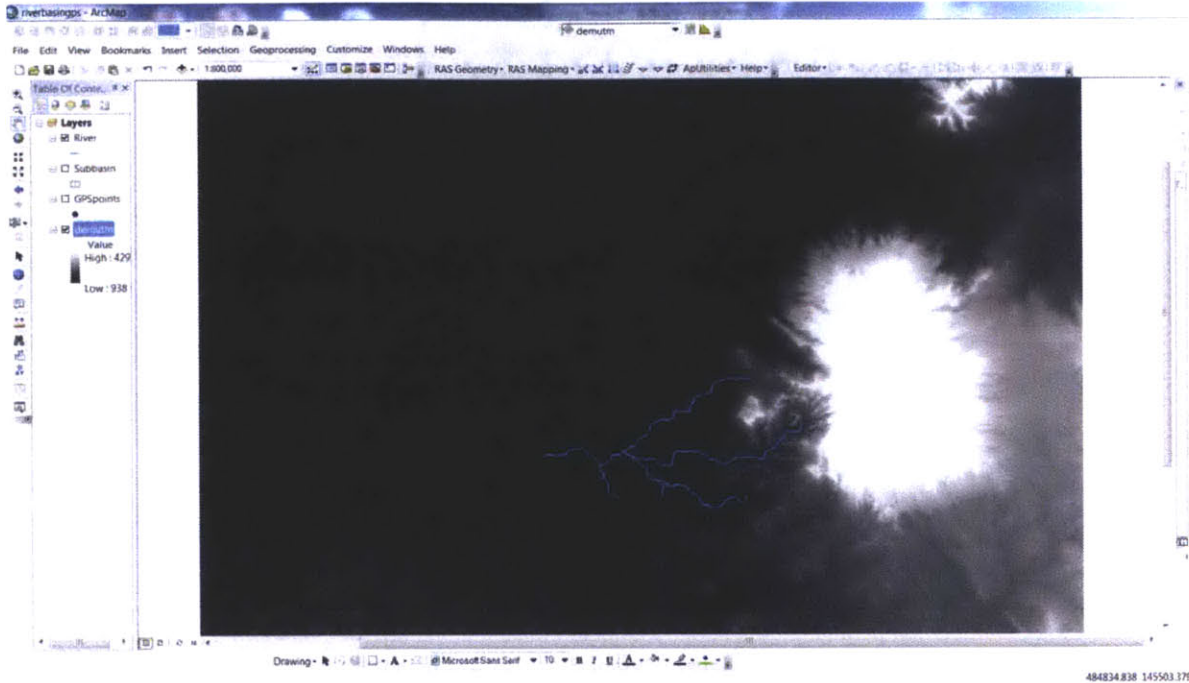


Figure 22 - Screen Shot of ArcMap: DEM of watershed and shape file of river network

After the DEM data is added to ArcMap as shown above in Figure 22, it is cropped to minimize the data size involved in each calculation. This is done through right clicking on the DEM layer, and selecting data export. In the export raster data dialogue box, the extent is set to *Data Frame (current)*, to crop the part of the data currently shown in the window (Figure 23).

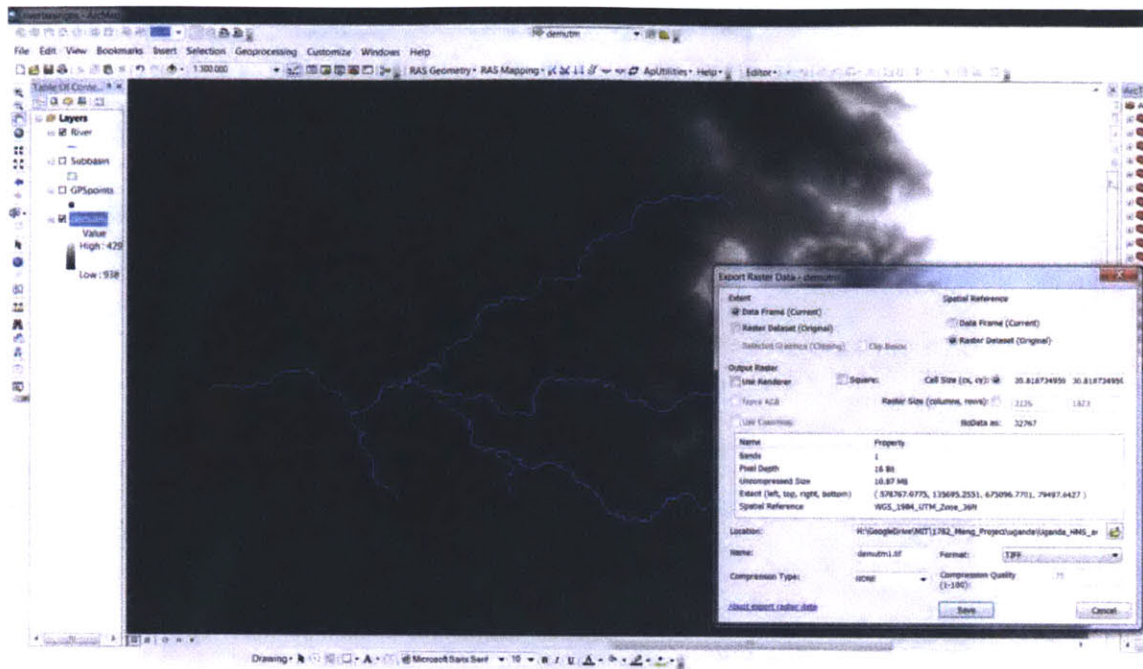


Figure 23 - Screen Shot of ArcMap: Cropping DEM

Then the cropped DEM was smoothed. The original resolution of the DEM used in the project is 30 m. By smoothing it to 4 m, more pixels, or cells, will be shown on the DEM. This apparent increase in resolution is achieved through toolbox functions in ArcMap, without actually improving the quality of the DEM data. The toolset used is *Resample* in *Data Management*. The specifications are shown in Figure 24 below.

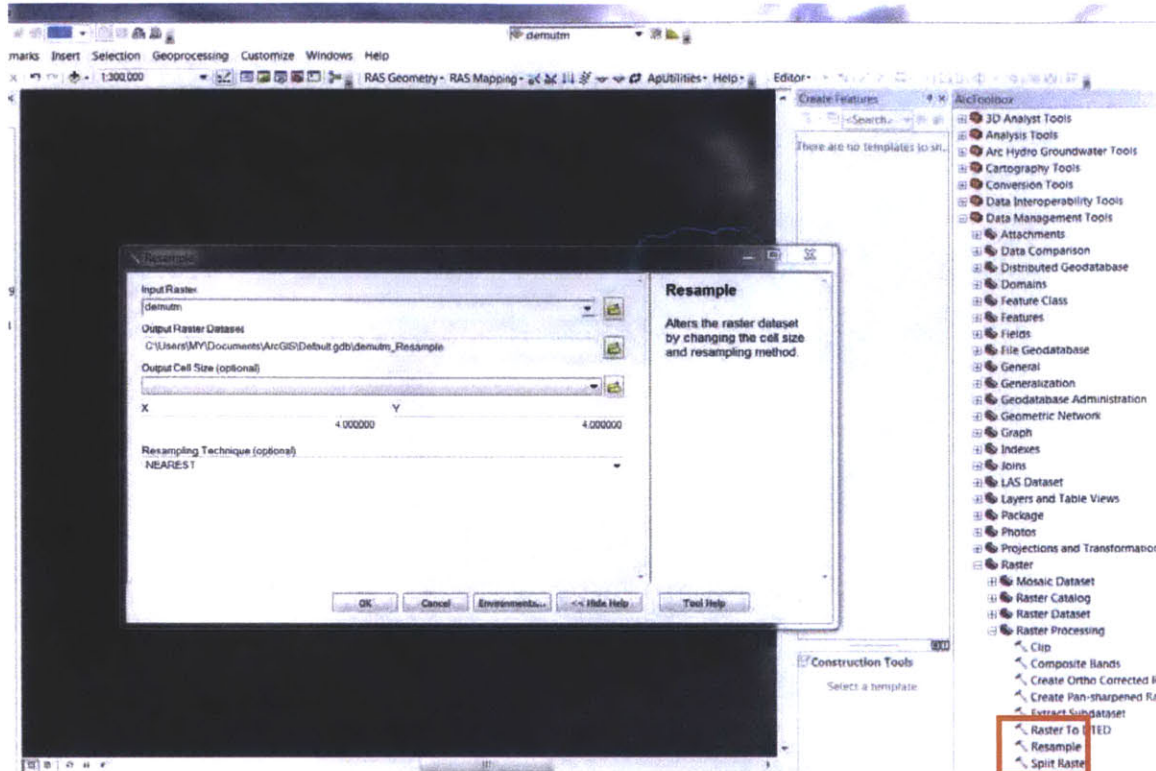


Figure 24 - Screen Shot of ArcMap: Resample toolset

After the shape file of the watershed is added, another River layer is created so that modifications to the river network can be made without making changes to the original shape file. This is accomplished by selecting *RAS Geometry – Create Ras Layers – Stream Centerlines* in the HEC-GeoRAS toolset.

To copy the feature from the shape file, first right click on the layer just created in *Table of Contents* and choose *Edit Features – Start Editing*. Then right click on the shape file layer, choose *Selection – Select All*. Then click in the main menu *Edit – Copy*. Then *Edit – Paste*. Choose the target layer as the one just created. See Figure 25 for a screen shot.

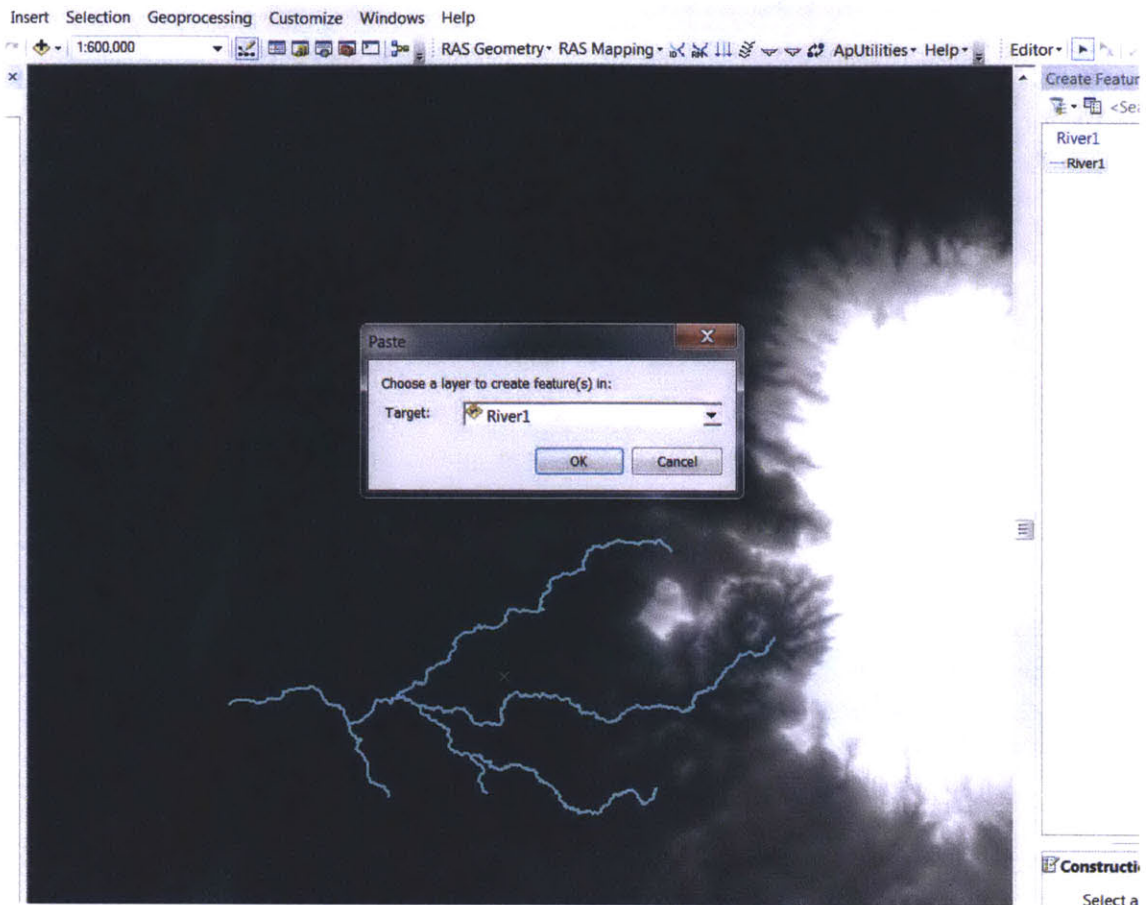


Figure 25 - Screen Shot of ArcMap: Copying Shape file feature to Stream Centerline layer

The reaches that are not of concern in the HEC-RAS analysis are deleted. The contribution of these tributaries to the main stream can be accounted for as lateral inflow in HEC-RAS thus simplifying the model. The remaining reaches are then ready to be converted to raster.

To populate the converted river raster file with depth data, the depth of 3 m is added as a new column in the *Attribute Table* for all remaining reaches before conversion. A new column is added by clicking *Add Field* in *Table Options*. The depths are specified by right clicking the name of the new column, selecting *Field Calculator* and inserting the value “3” (i.e. 3 m). See Figure 26 for a screen shot.

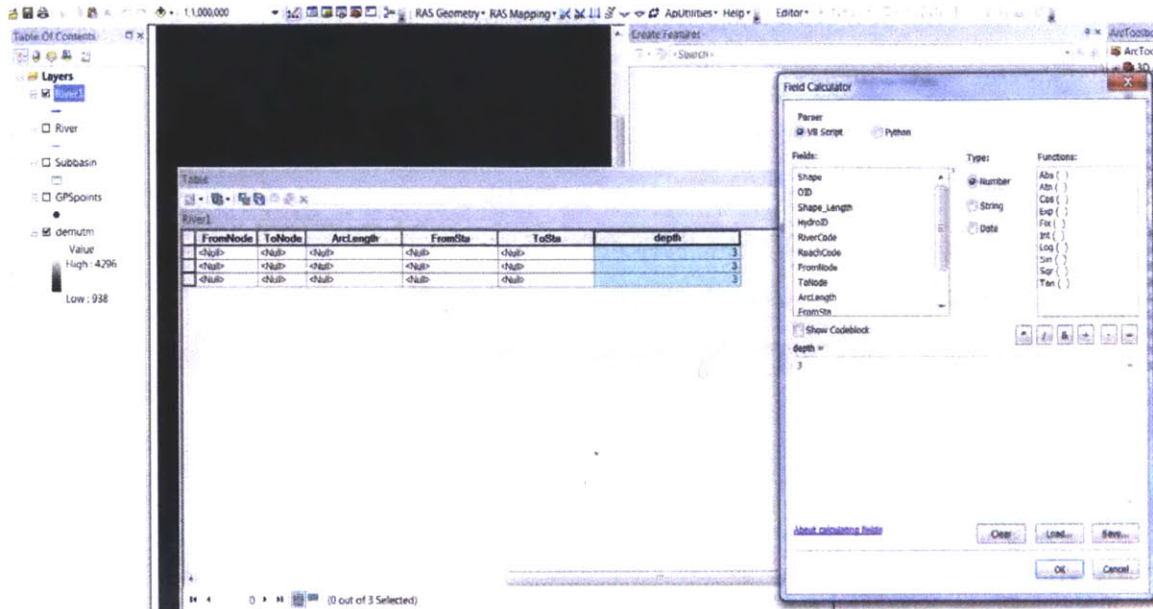


Figure 26 - Screen Shot of ArcMap: Populating depth for river feature before converting it to raster

To convert the river layer to raster, select in the toolbox *Conversion Tools* – *To Raster* – *Polyline to Raster*. In the dialogue box, choose *depth* in the *Value* field. *Cellsize* is set to be 10 m. In this way, the river cross sections are uniformly assigned a rectangular shape with width of 10 m. See Figure 27 for a screen shot.

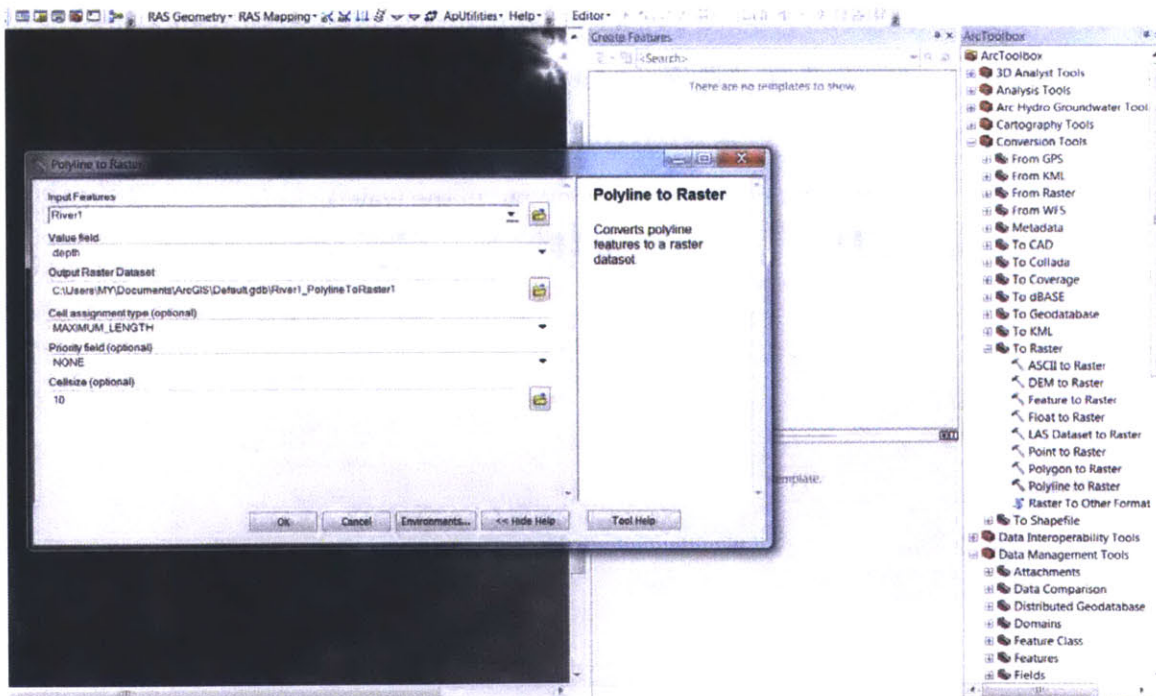


Figure 27 - Screen Shot of ArcMap: Converting river feature to raster with a cellsize of 10m

The DEM data and the river raster are combined by using *Spatial Analyst - Map Algebra - Raster Calculator*. One thing worth noting is that the river raster has no data besides the reach itself where a depth of 3 m is specified. To perform raster calculation, the entire raster layer needs to be populated with data; therefore, a value of 0 needs to be assigned to the rest of the cells. This is realized through the functions `Con()` and `IsNull()` in raster calculator. See Figure 28 for a screen shot.

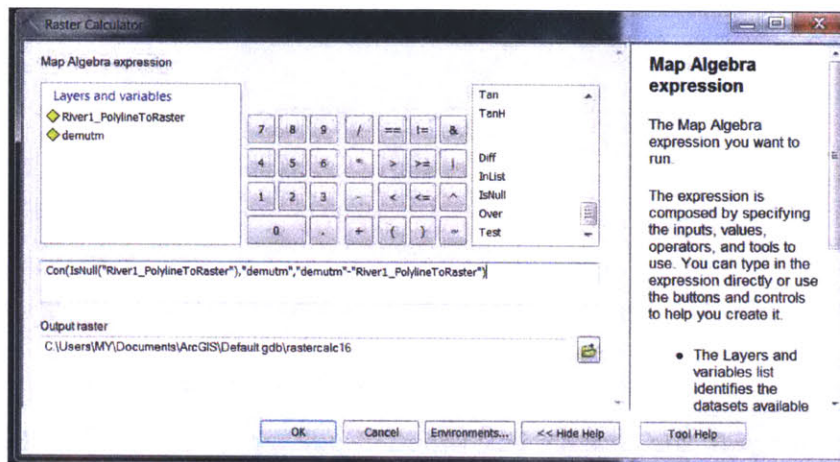


Figure 28 - Screen Shot of ArcMap: Combining river raster with DEM using Raster Calculator

In the *Environments* option (Figure 29), a *cellsize* of 4 m is specified for the output. An array of other parameters is also listed for manipulation in *Environments*. Attention should be paid in particular to the *Processing Extent* and *Raster Analysis* to ensure the conversion and calculation processes are carried out in the way desired.

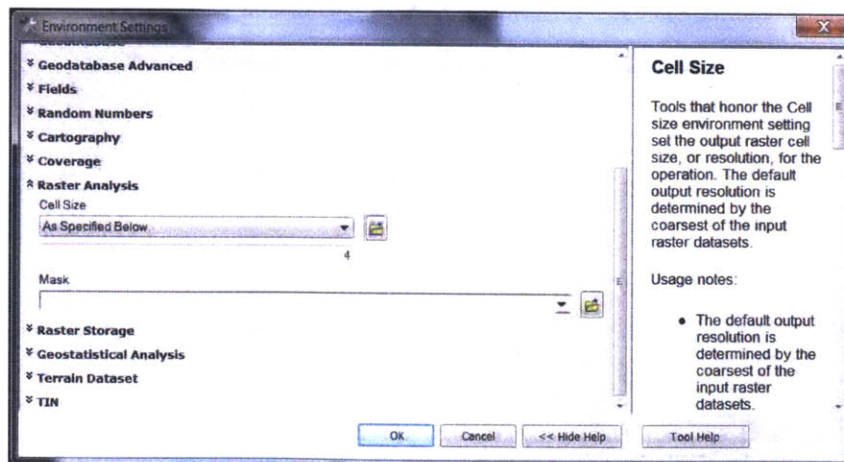


Figure 29 - Screen shot of ArcMap: Environments specification in tools

The next step involves the toolset *Spatial Analyst Tools – Neighborhood – Focal Statistics*. By taking the mean depth value of each cell with the neighboring 2 cells, a smoother and more naturally shaped river cross-section profile is created (Figure 30).

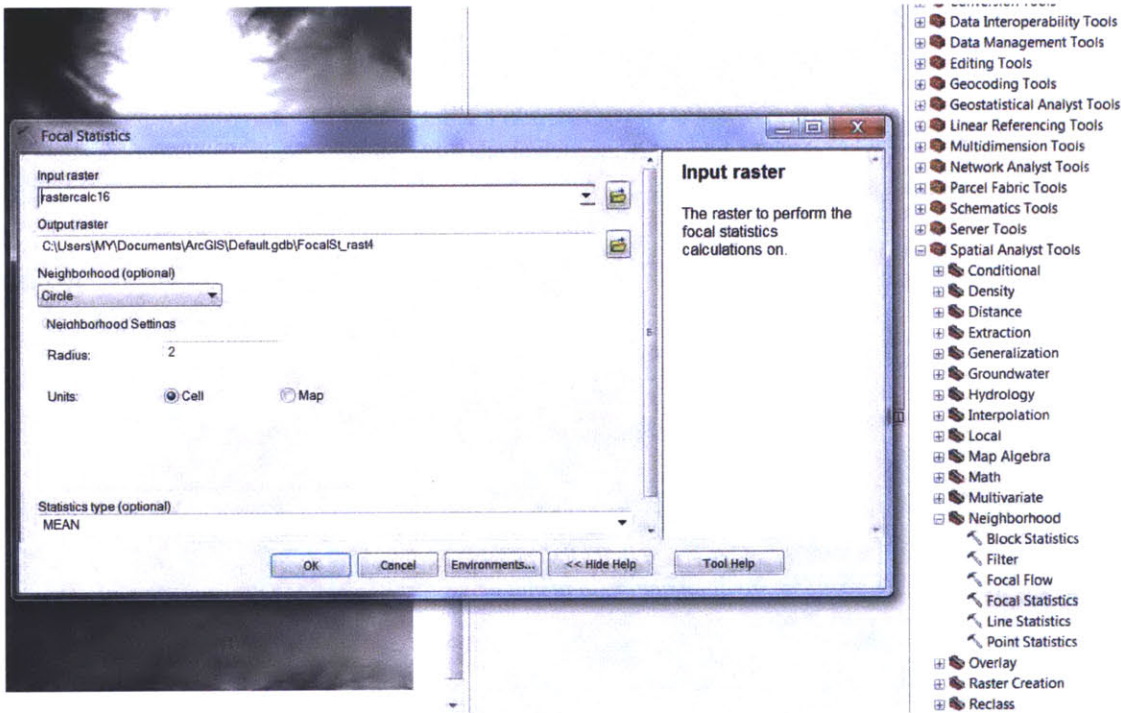


Figure 30 - Screen Shot of ArcMap: Smoothing of river cross section using focal statistics tool

The next step is to geo-reference the dataset obtained with the help of the HEC-GeoRAS toolset. To better visualize the data, the DEM layer's color scheme is changed to color instead of black and white.

Banks and *Flowpaths* are created by clicking *RAS Geometry – Creating Ras Layers*. Because data are not available for these two features, manual construction is required. To add *Banks*, the *Copy Parallel* command from the *Editor Toolbox* is utilized. Distance to *centerline* is set to 10 m for both sides of the banks. This gives a 20 m wide span across the river within which water will preliminarily flow. The *Flowpath*, however, is the region where the flow calculations will be confined. Subjective judgment is used in manually

creating this feature to ensure the flood plain is neither too large nor too small. The *Flowpath* region should consist of the area of relatively low elevation assuming no ineffective flow area is present. Ineffective flow area represents the locations where water is likely to be stored and the longitudinal velocities become minimal (Colorado Water Conservation Board, 2006).

One thing to note in creating *Flowpath* is that the lines are better drawn from upstream to downstream errors do not occur in reach length calculation in HEC-RAS. The result is shown below in Figure 31.

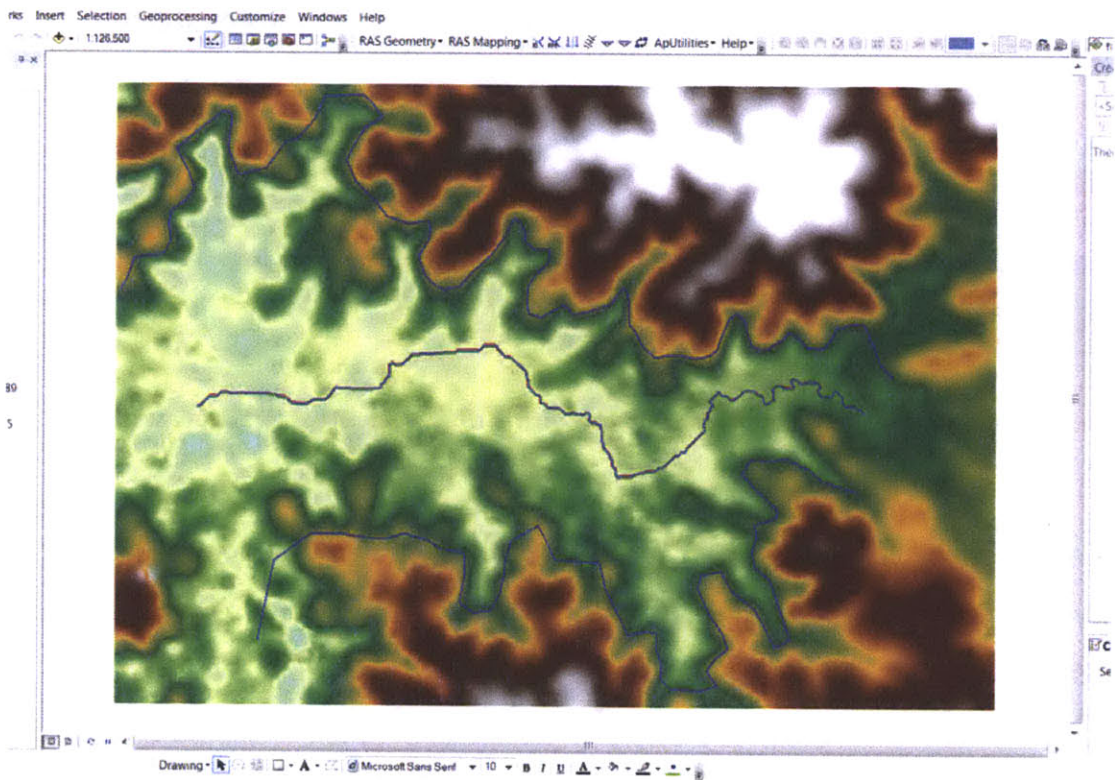


Figure 31 - Screen Shot of ArcMap: Banks and Flowpaths

Then cross section cutlines, or the *XS Cutlines*, are created in the same manual manner because of the irregular shape of the *Flowpath*. The cross section lines must not cross each other. The result is shown in Figure 32.

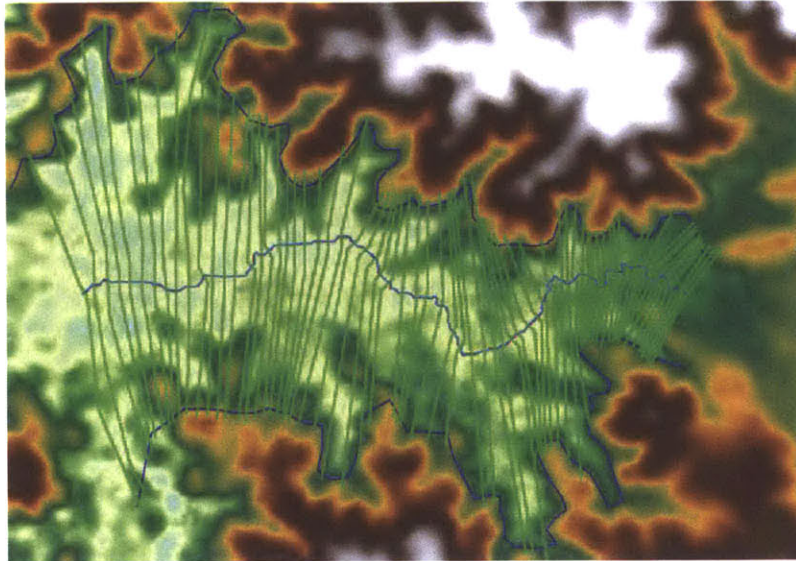


Figure 32 - Screen Shot of ArcMap: Stream centerline, Banks, Flowpaths and XS Cutlines

Then in *Layer Setup* in *RAS-Geometry*, the setup is shown as below in Figure 33.

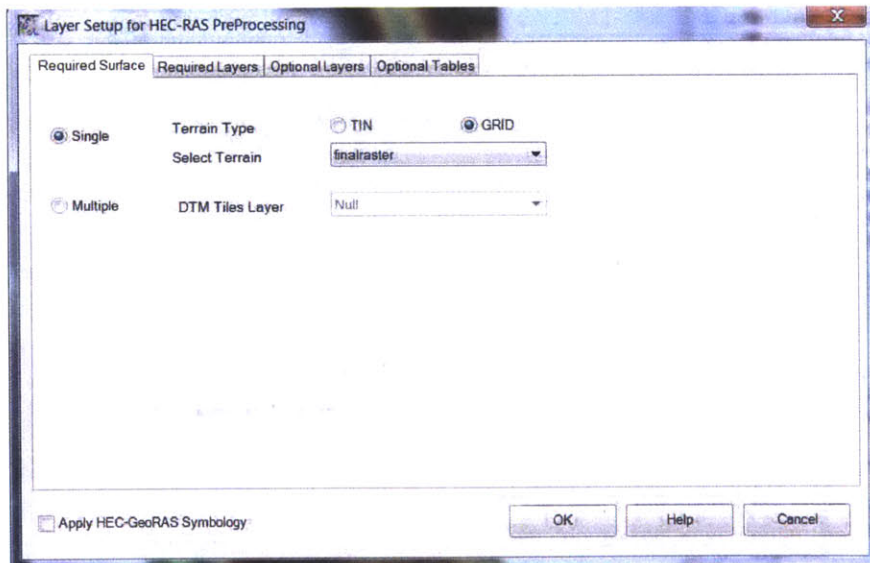


Figure 33 - Screen Shot of ArcMap: RAS Layer Setup

Next, click *All* for both *Stream centerline Attributes* and *XS Cut Line Attributes*, so that attributes are extracted from the calculated raster data. Then use the *Assign Line Type Attributes* to specify left and right *Flowpath*, as well as the channel (Figure 34).

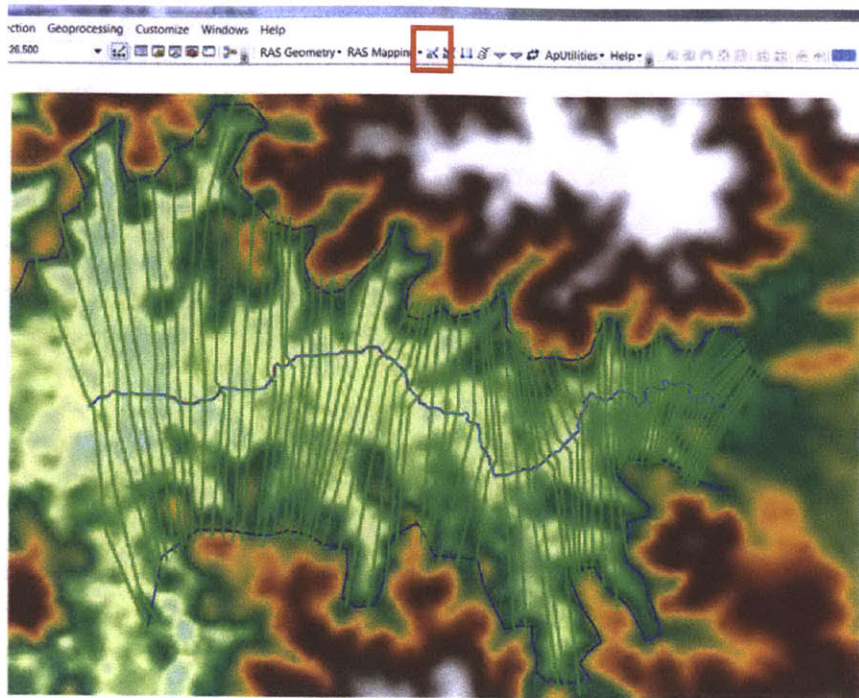


Figure 34 - Screen Shot of ArcMap: Assign line type attributes

The processed dataset is now ready to be exported. To export data, right click on the final raster file and select to export data (Figure 35).

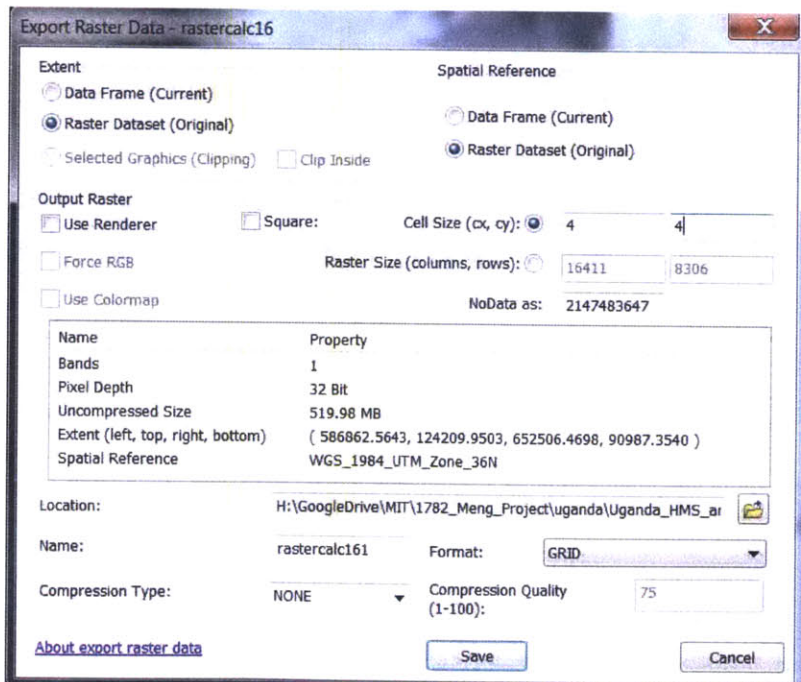


Figure 35 - Screen Shot of ArcMap: Data export from ArcMap

3.2.2 Importing geometric data to HEC-RAS

After the geometric data file is exported, one can import it into HEC-RAS by selecting *GIS Format* in *File – Import Geometry Data* (Figure 36).

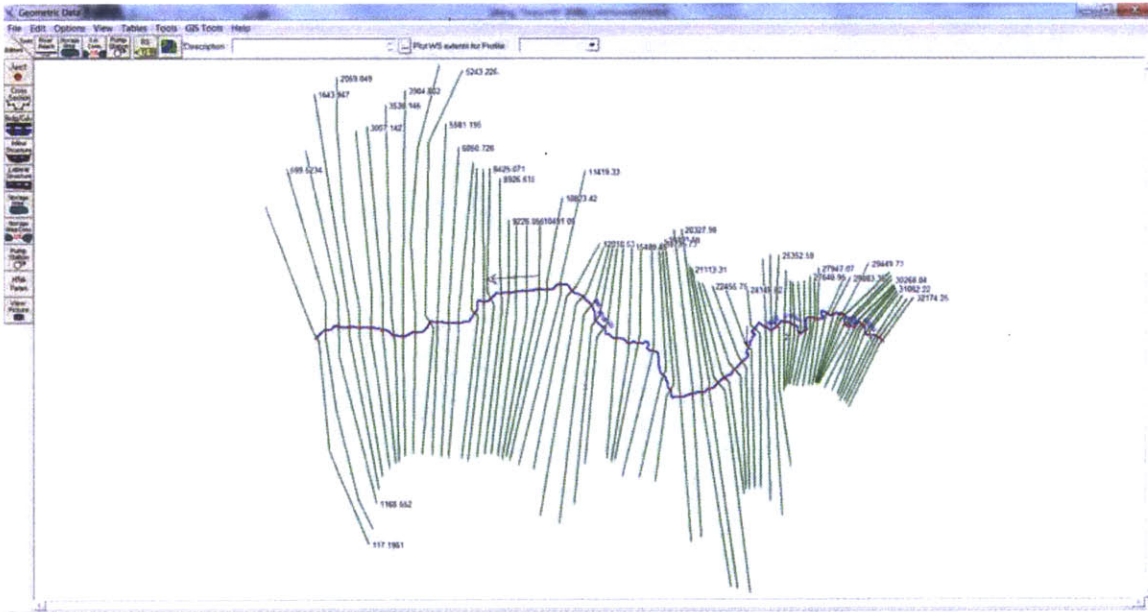


Figure 36 - Screen Shot of HEC-RAS: Geometric data imported as GIS format

In HEC-RAS, the user can edit each cross section manually. This is accomplished using the *Graphic Cross Section Editor* in *Geometric Data*, and allows the river cross section to be shaped to better resemble the actual profile.

3.2.3 Manning n values.

Manning n values used in this project are assumed to be 0.04 for the channel and 0.035 for both banks (Figure 37).

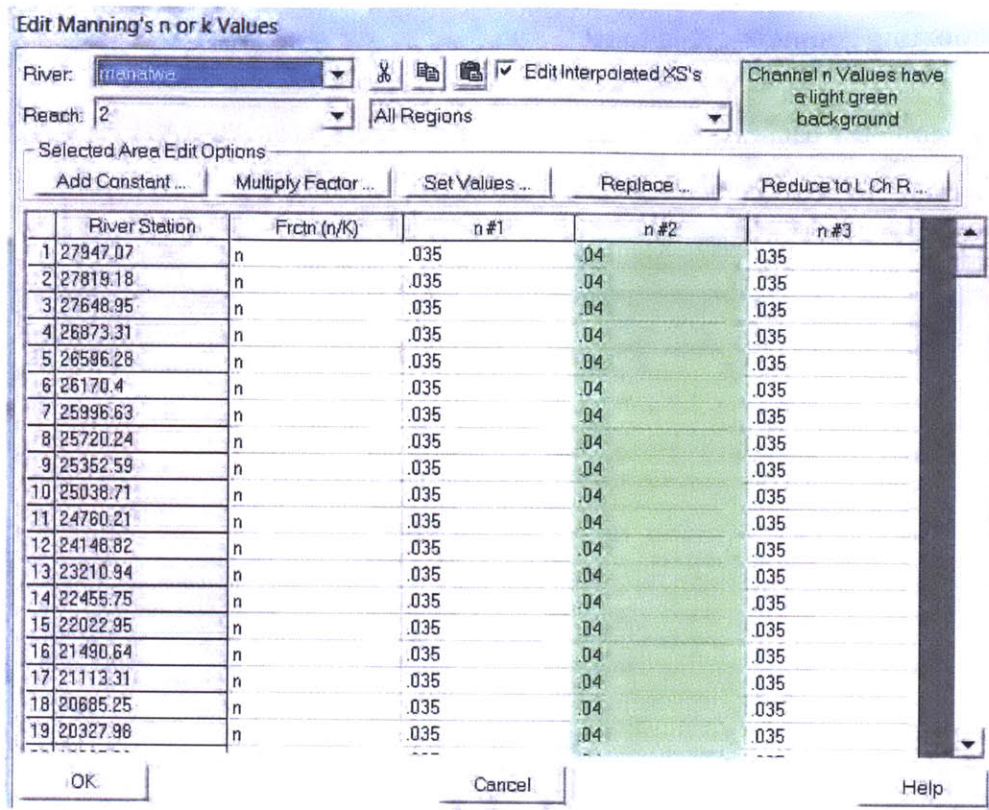


Figure 37 - Screen Shot of HEC-RAS: Manning n table

3.2.4 Filtering cross-section data points.

For the geometric data imported to HEC-RAS, a limit of 500 data points exists with respect to each single cross section. However, as the *flowpath* has a large width and cross section lines are considerably long, the number of data points is on the order of thousands. To manage this issue, in *Geometric Data*, function *Cross Section Points Filter* under *Tools* is utilized to reduce the number of data points at each cross section. The algorithm of the function appears to ensure minimum effect on calculation results. The function is capable of filtering multiple cross sections at one user command. A value of 500 is specified in the number of retained data points (Figure 38).

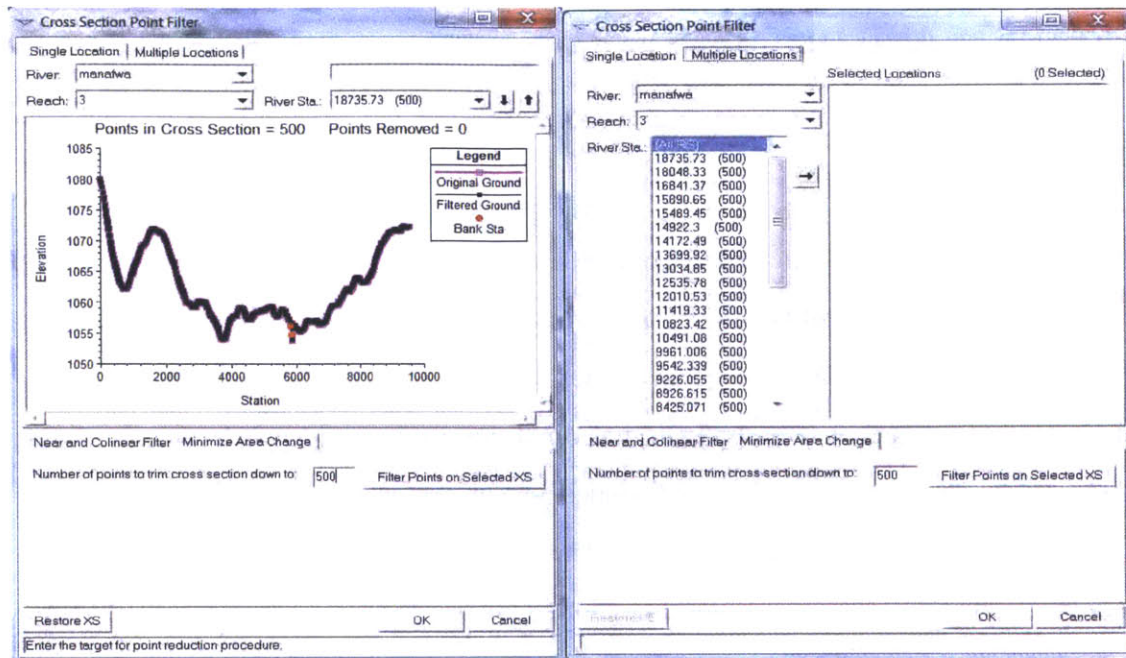


Figure 38 - Screen Shot of HEC-RAS: Cross section data points filter

3.2.5 Flow data

Flow hydrographs can be specified at the start and end point of each segment of river reach. These hydrographs can be input either as DSS files or manually input hydrograph tables. Initial elevation is sometimes also required. To account for the contributions from two different tributaries, *boundary condition location* should be added and *Lateral Inflow Hydro.* be inputted.

3.2.6 Other simulation assumptions

The HEC-RAS analysis is so far based on the assumption that no bridges, culverts, lateral structures or ineffective flow areas exist that affect the simulation result. This is reflected in the absence of these elements in the imported geometric file.

4 RESULTS AND DISCUSSION

4.1 Overview

A number of simulations are carried out independently for the two loss methods: (1) Curve Number Method and (2) Initial and Constant method. Each simulation generates an array of statistics available in either numerical or graphic forms for each and every hydrologic element in the watershed. Discussion of the results in this work focuses on the correlation of resulting and observed values in sub-basin W150 where the river is gauged, followed by calibration, or optimization results. Based on these calibrated parameters, the flow graphs at several key junctions are generated for use in HEC-RAS. Because of a limitation of data availability, simulations are confined to the period between 1 April 2006 and 30 June 2008 and are chosen such that variations in precipitation through each period are relatively conspicuous (i.e. precipitation events are evident and relatively well defined). Performance of the two methods are analyzed in long term simulations that spans the entire period, as well as short term simulations with duration of 14 days. To better compare the two loss methods, this section is presented according to different simulation periods. The simulation periods and name codes appear in Table 11 for convenient reference.

Period	Run #	Run code	
		Curve Number method	Initial and Constant method
01Apr2006-30Jun2008	0	CN0	IC0
25May2007-25Jun2007	1	CN1	IC1
01Aug2006-14Aug2006	2	CN2	IC2
17Nov2006-30Nov2006	3	CN3	IC3
15Apr2008-29Apr2008	4	CN4	IC4
25Jul2007-06Aug2007	5	CN5	IC5

Table 11 - Periods selected for various simulation runs

4.2 Long term simulation

4.2.1 Run CN0

Run CN0 is the simulation run using Curve Number loss method over the period between 01 April 2006 and 30 Jun 2008. The results for Run IC0 appear in Figure 39 and are discussed below.

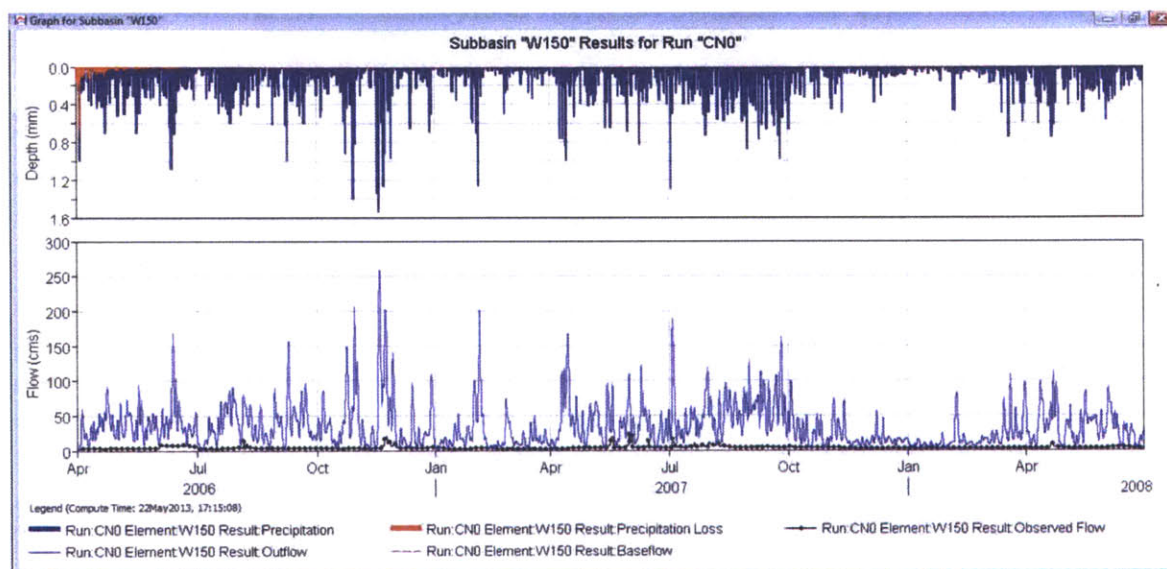


Figure 39 - Screen Shot of HEC-HMS: Flow graph of w150 for Run CN0 before calibration

The dark blue histograms in the upper part of Figure 39 indicate the distribution of precipitation as a function of time. The red histograms indicate precipitation loss. The blue curve shows simulated flow rate. Black dots represent observed flow rates.

It appears that, given the parameters estimated above, the resulting flow rates for the Curve Number method over a long term are unreasonably high when compared with observed flow. It is worth noting that, as shown in Figure 41 and Figure 42, the water loss is much weighted towards the first two months of the simulation period. Not much loss is accounted for in the larger part of the period that follows. This did not change even after setting initial abstraction to 0 mm. It is suspected that the program while giving warning messages indicating the initial abstraction is 0, actually overrides and

accounts for the abstraction anyway. From Figure 40, one can see from the summary that over more than two years' time, precipitation is 3849.64 mm, whereas total water loss is only 80.74 mm. The actual model abstraction ratio is therefore ~ 0.02 .

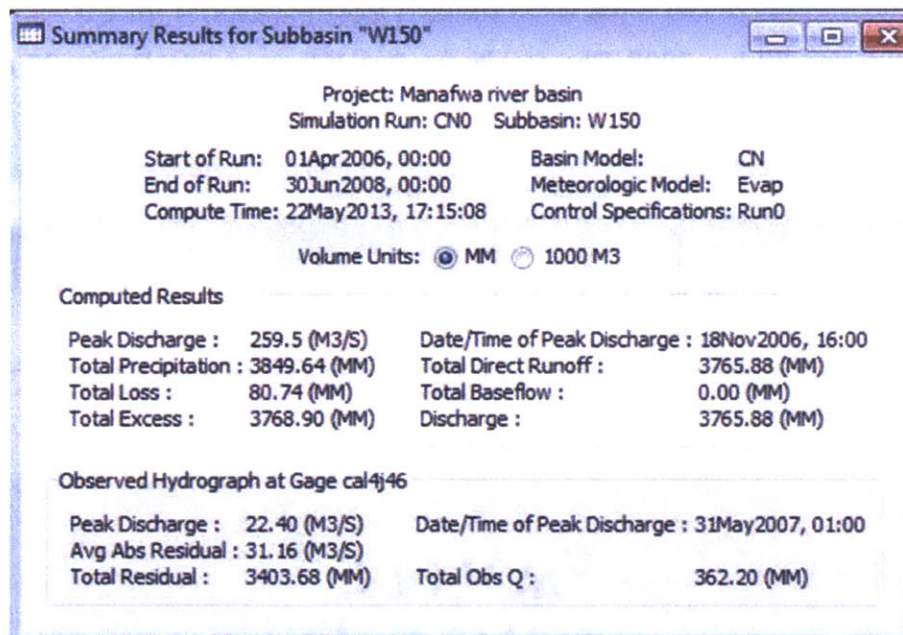


Figure 40 - Screen Shot of HEC-HMS: Summary table of w150 for Run CN0 before calibration

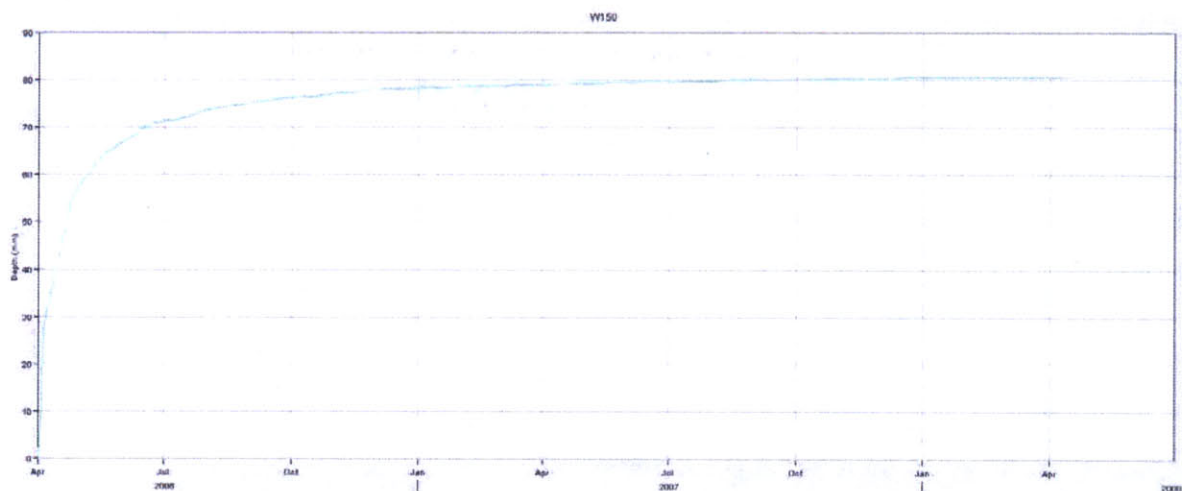


Figure 41 - Screen Shot of HEC-HMS: Precipitation loss of w150 for Run CN0 before calibration

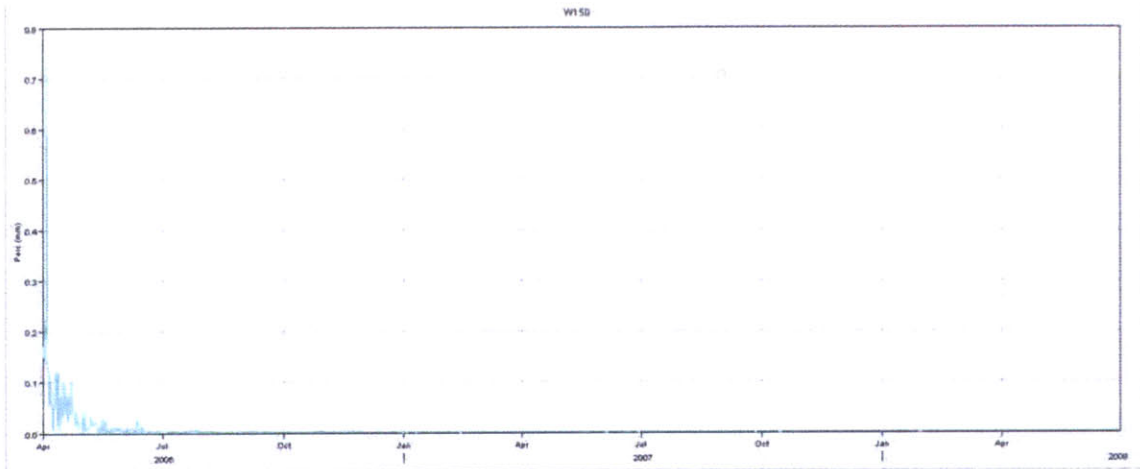


Figure 42 - Screen Shot of HEC-HMS: Soil infiltration of w150 for Run CNO

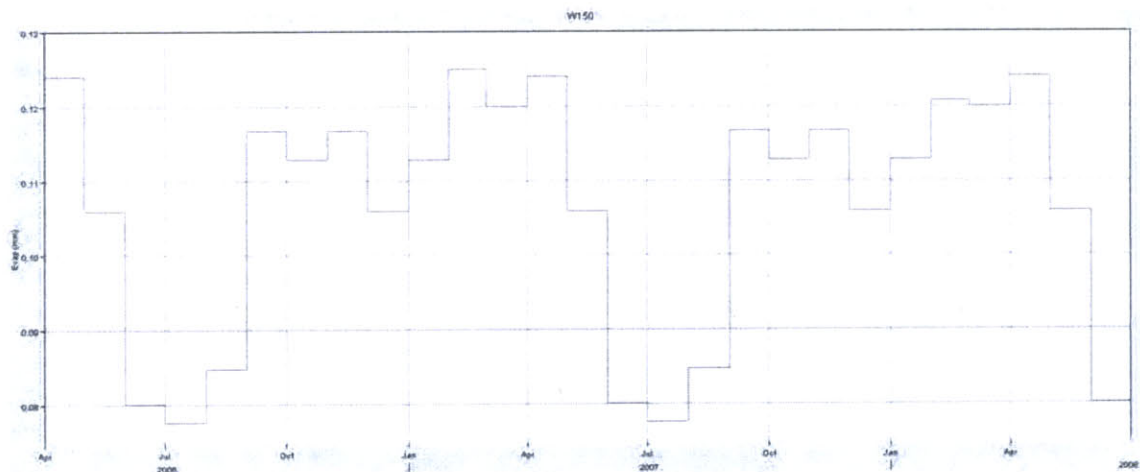


Figure 43 - Screen Shot of HEC-HMS: Evapotranspiration of w150 for Run CNO

As shown in Figure 41, accumulative precipitation loss in the model appears to approach a ceiling value gradually over time. This is in agreement with the trend of the soil infiltration levels illustrated in Figure 42. Evapotranspiration is reported in the output results (Figure 43), but is not reflected in infiltration water loss; it is instead accounted for within the meteorology model which accounts for precipitation, snowmelt, and evapotranspiration. With the specified average monthly precipitation, a potential of almost 1000 mm water loss due to evapotranspiration is expected to be in place

In the optimization run for the long-term simulation, two parameters are optimized, the curve number and the lag time. In sub-basin W150, lag time is calibrated to be 1047.4 min from an initial value of 1027 min (Figure 44). It implies that the method used to estimate lag time is considerably accurate. However, the curve number is calibrated to be 35.864 from an initial value of 75.3. Even with the extremely low calibrated curve number, the modeled flow rates remain unreasonably high, with both volume difference and peak flow difference approaching 1000% (Figure 45).

Element	Parameter	Units	Initial Value	Optim... Value	Objective Fun... Sensitivity
W150	Curve Number		75.3	35.864	0.15
W150	SCS Lag	MIN	1027	1047.4	-0.10

Figure 44 - Screen Shot of HEC-HMS: Optimized parameters of w150 for Run CN0

Measure	Simulated	Observed	Difference	Percent Difference
Volume (MM)	3444.37	362.20	3082.16	850.96
Peak Flow (M3/S)	242.5	22.4	220.1	982.7
Time of Peak	18Nov2006, 16:00	31May2007, 01:00		
Time of Center of Mass	09May2007, 09:31	17Apr2007, 16:48		

Figure 45 - Screen Shot of HEC-HMS: Optimization objective function of w150 for Run CN0

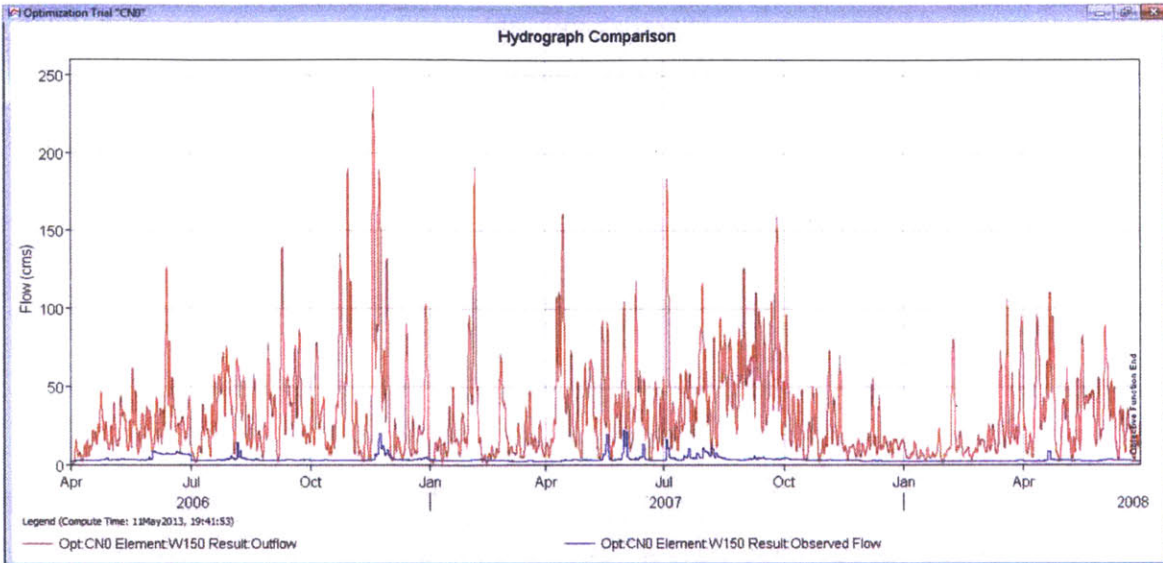


Figure 46 - Screen Shot of HEC-HMS: Flow graph of w150 for Run CN0 after calibration

Figure 46 shows the flow hydrograph after calibration. It is worth noting that, although the model reflects several rainfall events timely, the specificity to capture an arbitrary rainfall event accurately is compromised due to excessive noise.

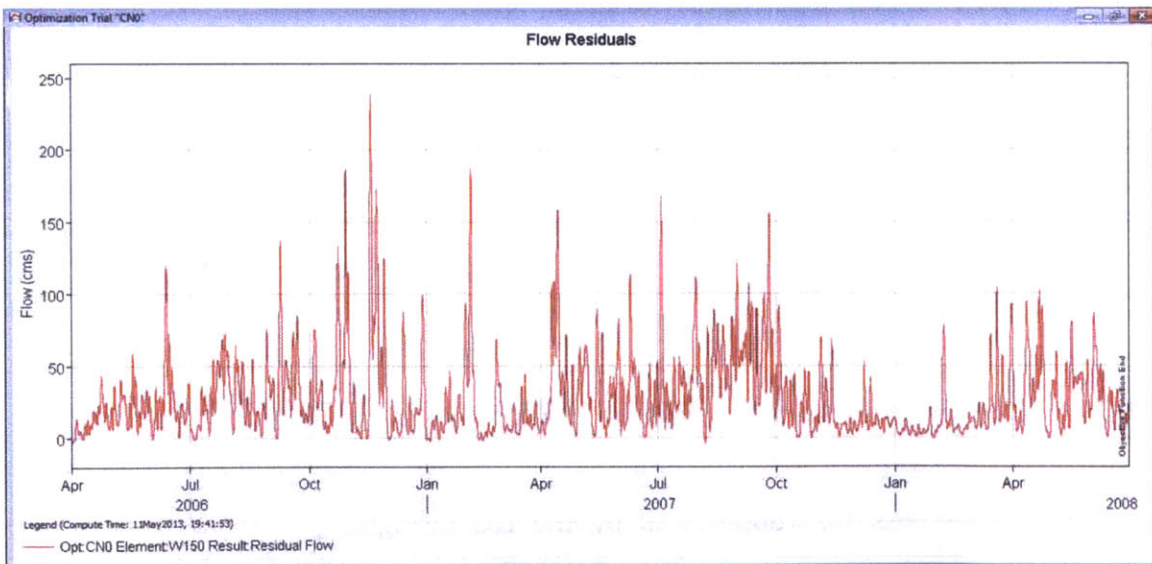


Figure 47 - Screen Shot of HEC-HMS: Flow residual of w150 for Run CN0 after calibration

The flow residual in Figure 47 shows the deviation of resulting flow rates from the

observed values. As the warning messages indicate in the program, the curve number method appears to be problematic in dealing with the long-term water budget, especially water losses through infiltration as well as evapotranspiration.

4.2.2 Run IC0

Run IC0 is the simulation run using initial constant loss method over the period between 01 April 2006 and 30 Jun 2008. The results for Run IC0 are discussed below.

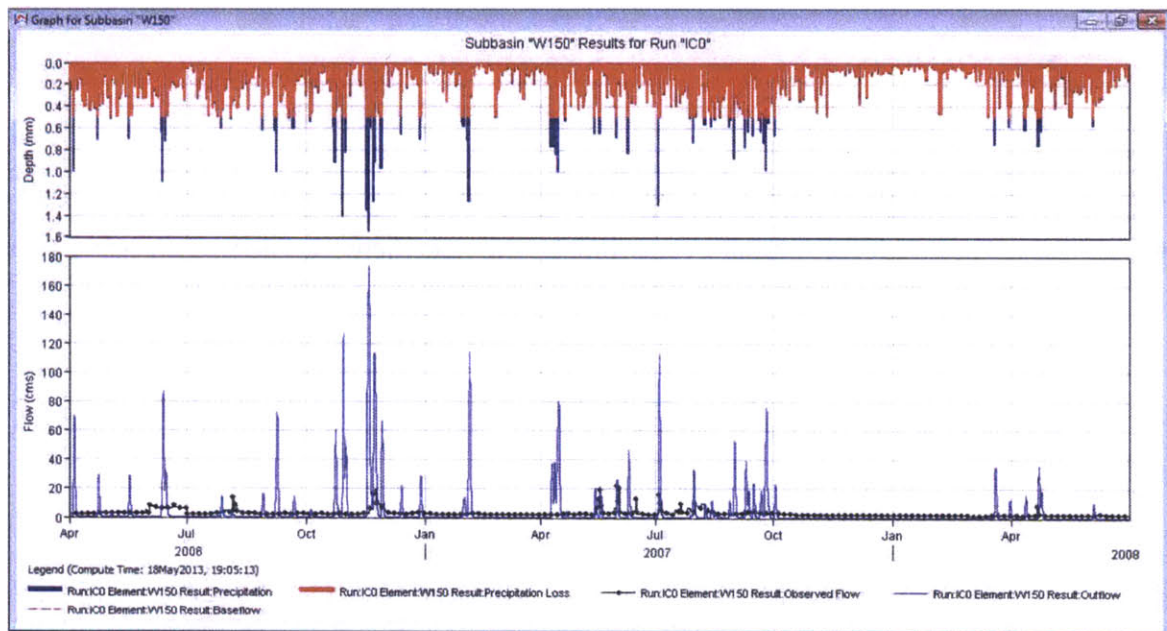


Figure 48 - Screen Shot of HEC-HMS: Flow graph of w150 for Run IC0 before calibration

The feature of the initial and constant loss method is that water loss over the day is almost constant, except for days with minimal precipitation. As shown in Figure 48 above, significant water loss (as represented by the red histogram) is realized over the long-term simulation period. In the summary table shown in Figure 49, one can find the total loss is 3430.83 mm out of a total precipitation of 3849.64 mm.

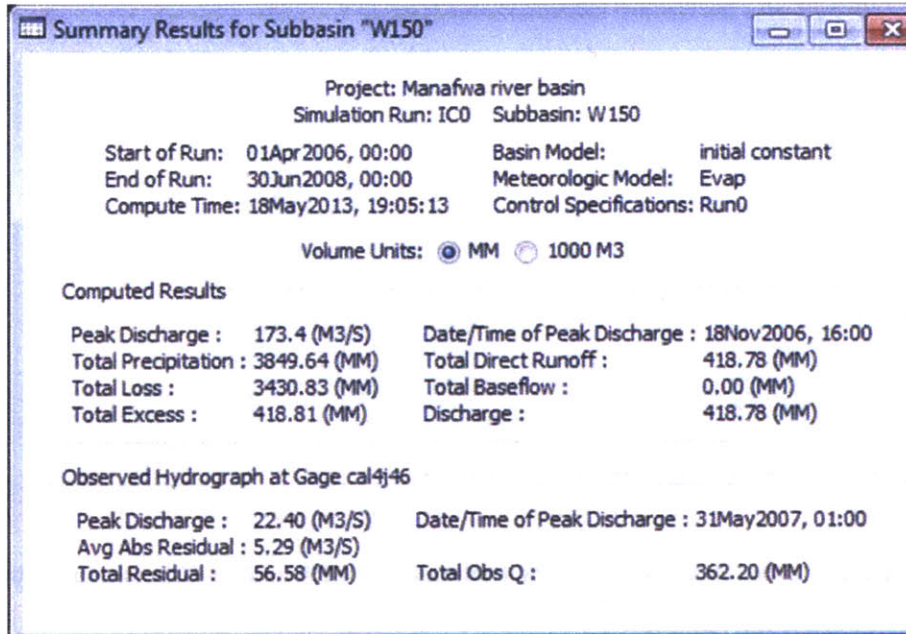


Figure 49 - Screen Shot of HEC-HMS: Summary table of w150 for Run IC0 before calibration

As seen in Figure 50, the modeled evapotranspiration result resembles that of the simulation Run CN0 discussed above.

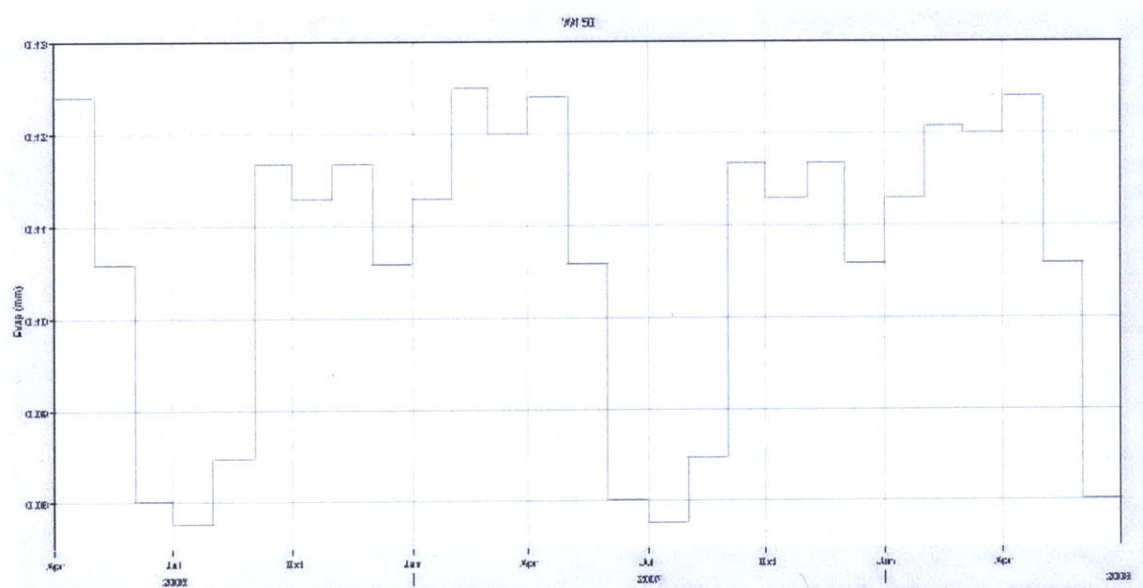


Figure 50 - Screen Shot of HEC-HMS: Evapotranspiration of w150 for Run IC0 before calibration

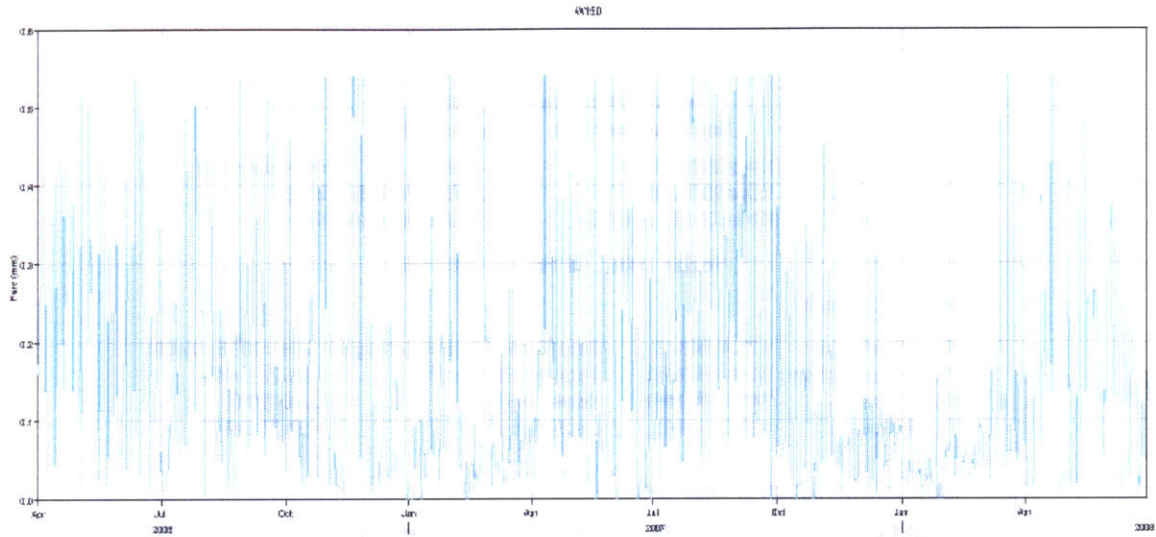


Figure 51 - Screen Shot of HEC-HMS: Soil infiltration of w150 for Run IC0 before calibration

Soil infiltration (Figure 51) fluctuates dramatically with precipitation, and cumulative precipitation loss (Figure 52) is not limited to a ceiling value as it is in the curve number method result.

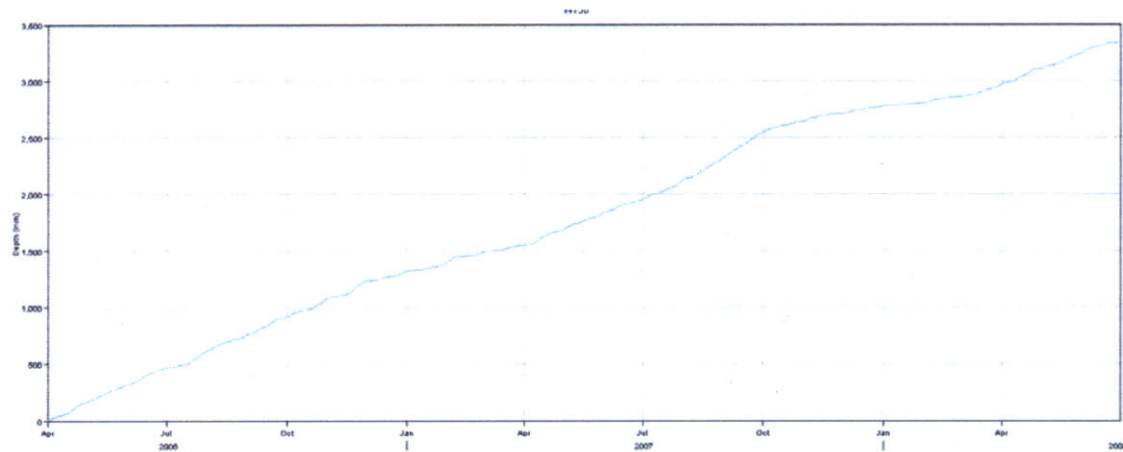


Figure 52 - Screen Shot of HEC-HMS: Cumulative precipitation loss of w150 for Run IC0 before calibration

Calibration is carried out with respect to W150 for both constant loss rate and lag time. The results are as follows.

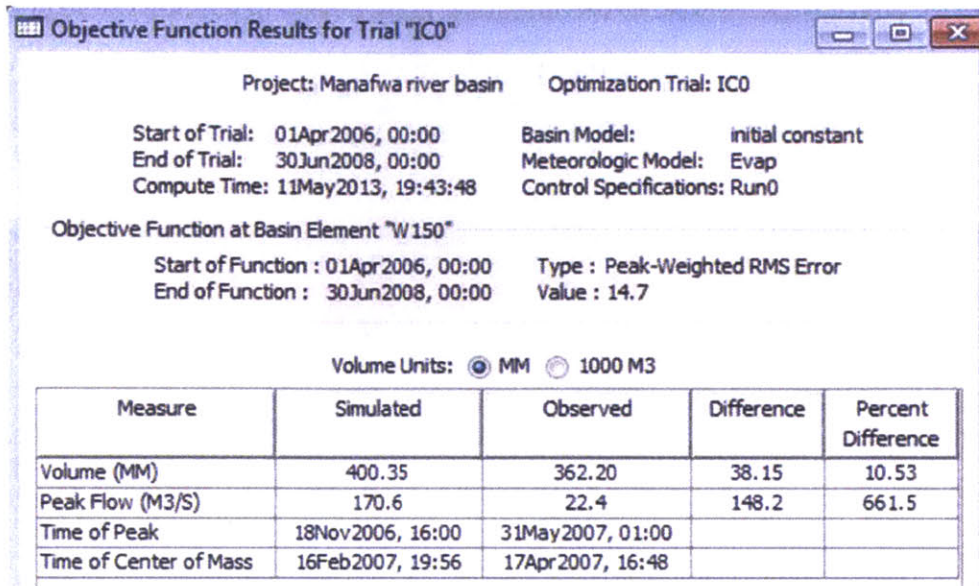


Figure 53 - Screen Shot of HEC-HMS: Optimization objective function of w150 for Run IC0

It can be seen in Figure 53 above that the model calculated a discharge volume that deviates from the observed data by only 10.53%. However, for the peak flow the difference is over 660%. The high peak flow difference reflects the limited capacity of the initial and constant loss method to represent heavy rainfall event in relatively dry period.

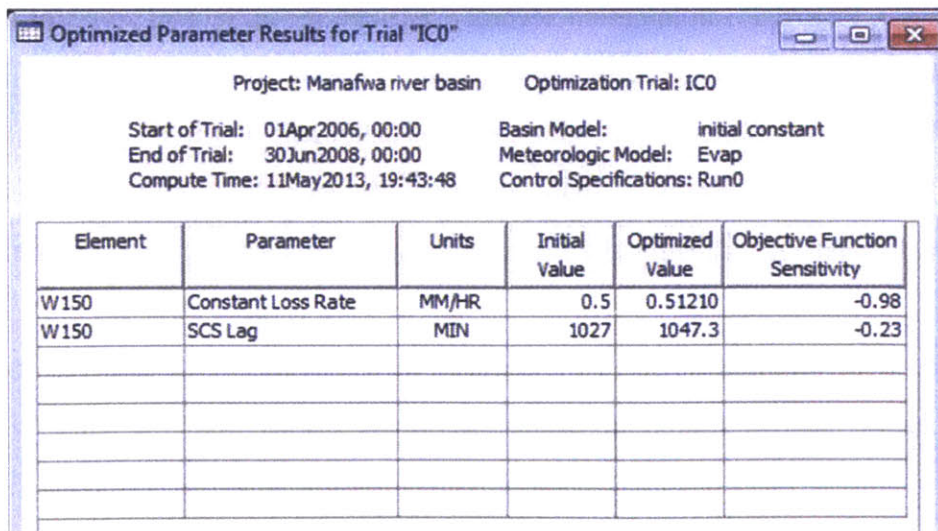


Figure 54 - Screen Shot of HEC-HMS: Optimized parameters of w150 for Run IC0

Calibration suggested an optimized value of 0.51210 mm/hr for the constant loss rate (Figure 54), which is fairly close to the initial estimated value of 0.5 mm/hr. At the same time, similar to what is observed in the curve number method calibration; the lag time is also accurately estimated with a minimal difference from the optimized value.

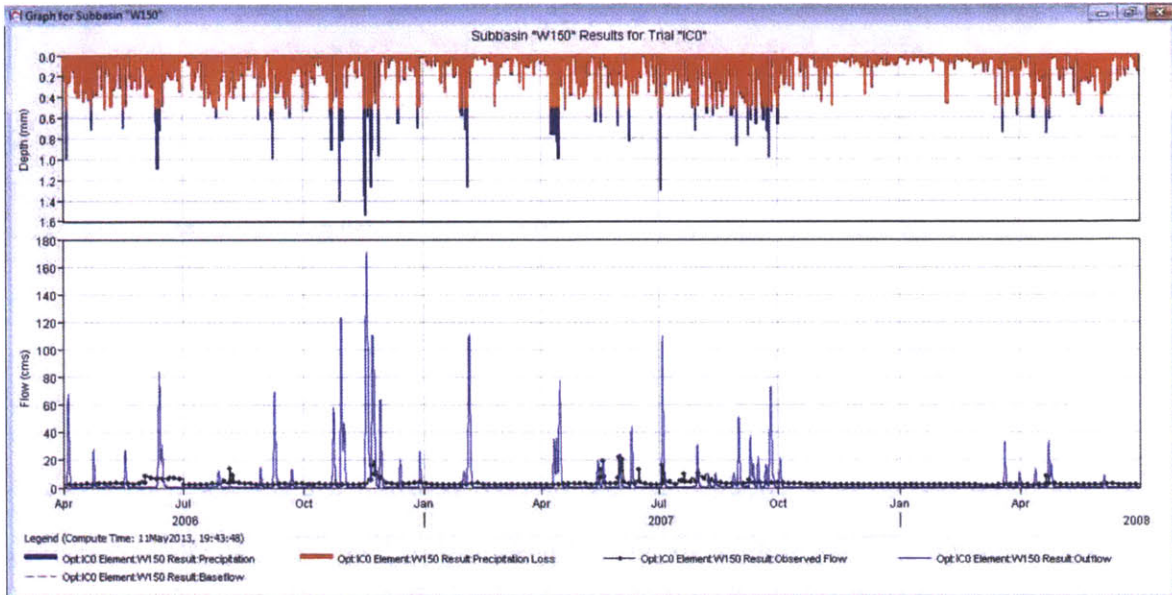


Figure 55 - Screen Shot of HEC-HMS: Flow graph of w150 for Run IC0 after calibration

As is shown in Figure 55, although on several occasions the initial and constant method generated unreasonably high peak flow values over the simulation period, the majority of the modeled results are within the same order of magnitude as the observed flow. The difference between the simulated flow and the observed flow could be reduced by introducing baseflow or validating the observed Manafwa River flow rate calculations.

In addition, with minimal noise in the simulated results, the initial and constant loss method shows more potential in capturing rainfall events than the curve number method in long-term simulations. One possible reason why on occasion the high simulated runoff is not coupled with high observed flow is that perhaps the rainfall took place somewhere else in the satellite rainfall data grid outside sub-basin W150 and did

not affect it. Such rainfall events contribute to the amount of rainfall in the grid that overlaps with part of the sub-basin. But the actual rainfalls are not in the sub-basin so that no water is contributed to the reach studied.

4.3 Short term simulation - Run 1

4.3.1 Run CN1

Run CN1 is the simulation run using the Curve Number loss method over the period between 25 May and 5 Jun 2007. The results for Run CN1 are discussed below.

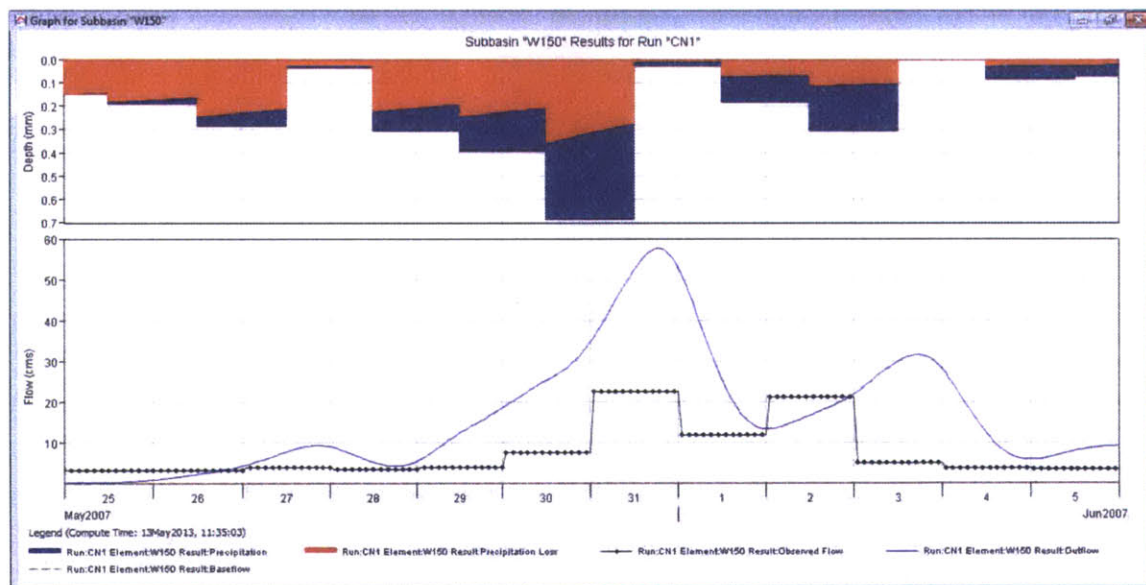


Figure 56 - Screen Shot of HEC-HMS: Flow graph of w150 for Run CN1 before calibration

In Figure 56 above, the smooth curve in blue represents the simulated flow hydrograph, whereas the dotted curve is the observed flow graph. The reason why dotted curve appears in squared wave shape is that the observed flow is on a daily basis and is assumed to be constant. In comparison, the simulated flow hydrograph with a calculation time interval of one hour assumes a much smoother curve.

The Curve Number method abstracts the very first part of precipitation even with the initial abstraction parameter specified to be 0 mm. On the other hand, even though the model does not handle peak flow magnitude very well using the CN method, it generally mimics the variation in the observed flow throughout the period (i.e. it consistently over-represents runoff as compared with observed flow). The only apparent flaw lies in that, the second high flow spike, which closely follows the previous one in the small time window, is not correctly timed by the model. Observed peak flow leads the simulated peak flow by approximately one day. Literature exists that discusses HEC-HMS's controversial capacity to deal with recession limbs in the flow hydrograph. However, the main cause of the delay could be simply attributed to the low frequency of data logging. Observed flow is assumed to be constant through each day, which is actually seldom the case for actual flow. There are chances that peak flow takes place later than what is indicated by the observed flow data and assumes a higher value. A higher-resolution of observed flow data could help determine the actual deviation in the time of peak.

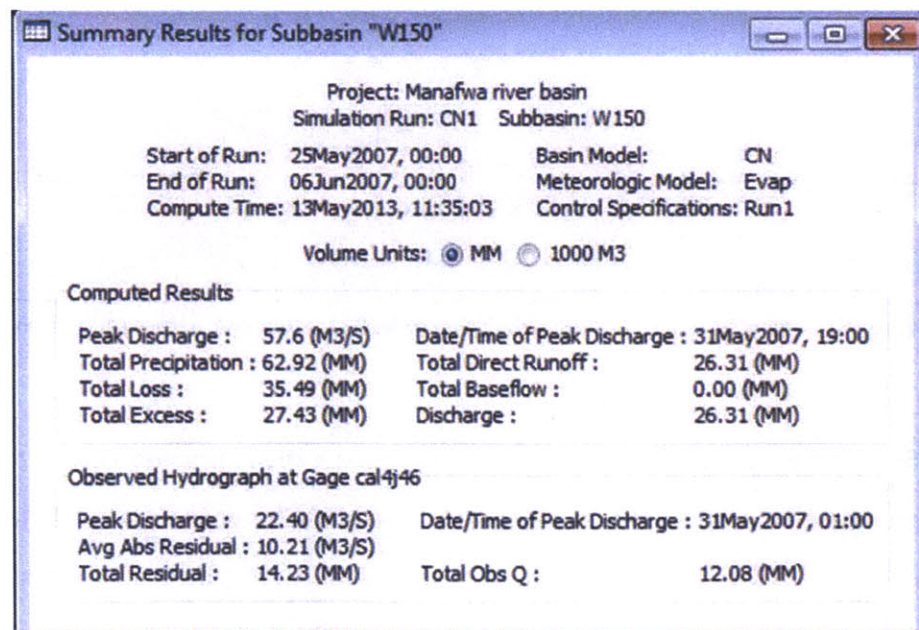


Figure 57 - Screen Shot of HEC-HMS: Summary table of w150 for Run CN1 before calibration

The summary table (Figure 57) shows a peak discharge value of 57.6 cms occurring on 31 May 2007. The peak discharge value is much lower than the calculated value for the same day in Run CN0, which is evidence of the inconsistency of the Curve Number method in accounting for soil infiltration in long term simulations. Calibration is carried out with respect to W150 on curve number and lag time. The results are as follows.

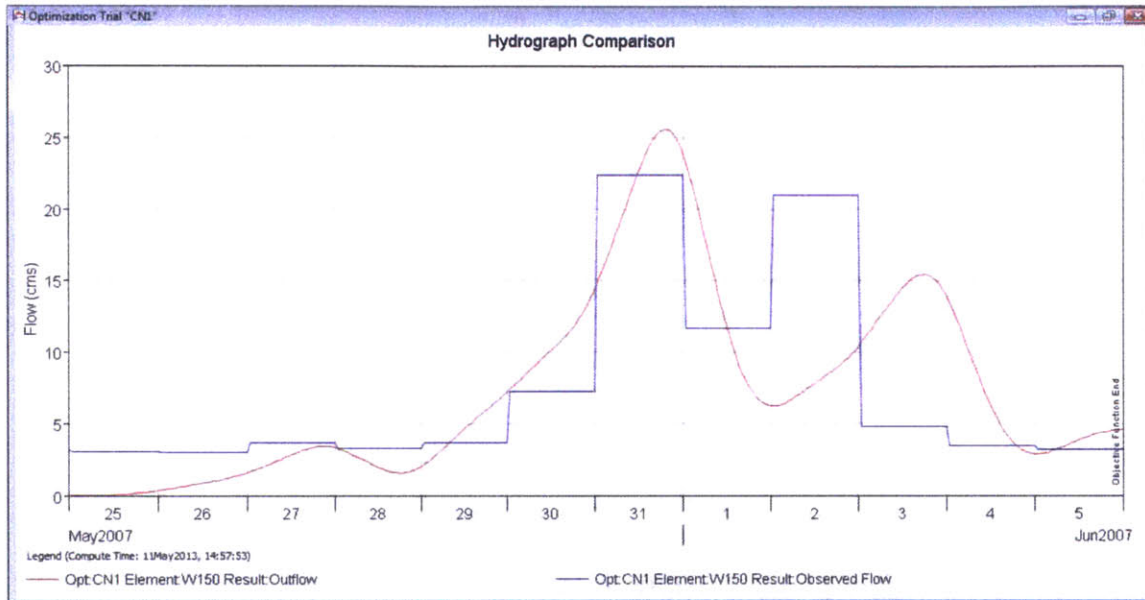


Figure 58 - Screen Shot of HEC-HMS: Calibrated flow graph of w150 for Run CN1

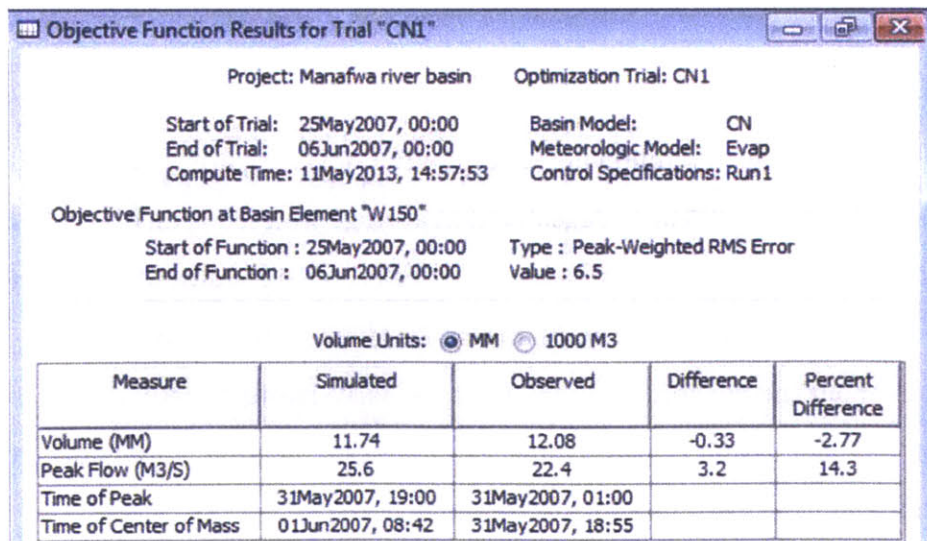


Figure 59 - Screen Shot of HEC-HMS: Calibration objective function of w150 for Run CN1

Element	Parameter	Units	Initial Value	Optimized Value	Objective Function Sensitivity
W150	Curve Number		75.3	48.280	0.09
W150	SCS Lag	MIN	1027	1047.4	0.05

Figure 60 - Screen Shot of HEC-HMS: Optimized parameters of w150 for Run CN1

The accuracy of hydrologic models in calculating peak discharge rates are expected to be $\pm 30\%$ at best for large ungauged watersheds (Fennessey & Hawkins, 2001). From the two figures above (Figure 59 and Figure 60), it is shown that, after reducing the curve number from 75.3 to 48.28 (i.e. $\sim 36\%$), the model is able to bring volume and peak flow values fairly close to the reference values.

In fact, in another study by Fennessey et al, it is found out that in the hypothetical watersheds examined, “traditionally computed” CN values are generally higher than actual values by 10 to 40. They suggested that average watershed inflection angles have a significant impact on the curve number and peak discharge rates of the “minor draws” off the main reach (Fennessey, Hamlett, & Miller, 2001). Nonetheless, expanded discussion about the general applicability of the curve number method is not within the scope of this discussion. The lag time estimated in the runoff transform method is auto-calibrated from 1027 min to 1047.4 min.

Figure 61 shows the estimated potential evapotranspiration curve. The magnitude is presented in the vertical axis on an hourly basis, to be consistent with the simulation time interval.

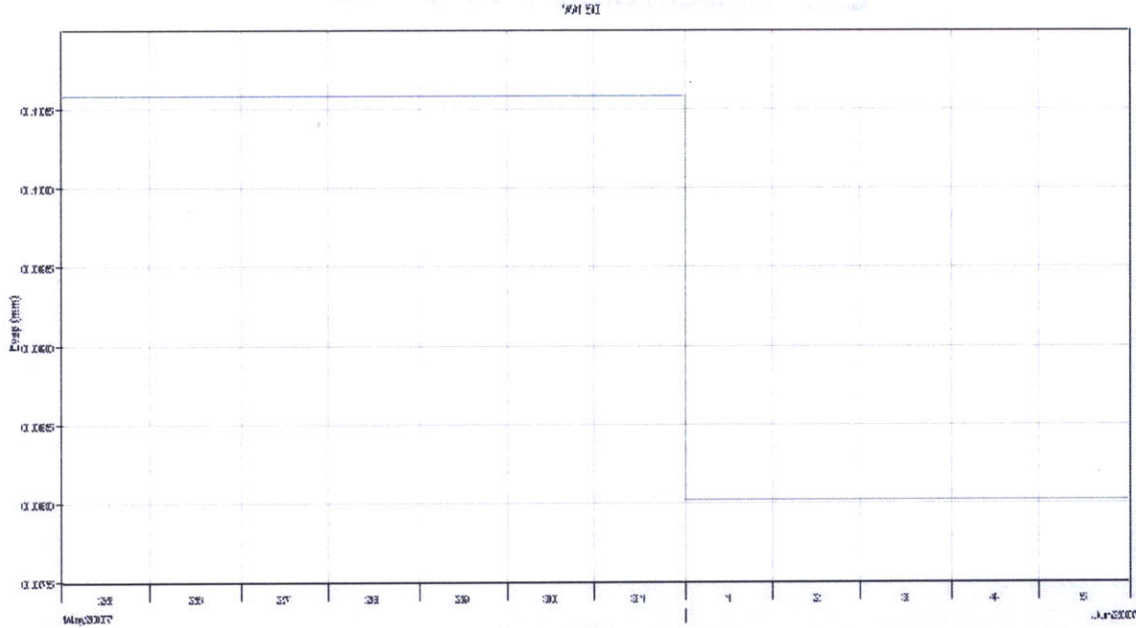


Figure 61 - Screen Shot of HEC-HMS: Potential evapotranspiration of w150 for Run CN1 after calibration

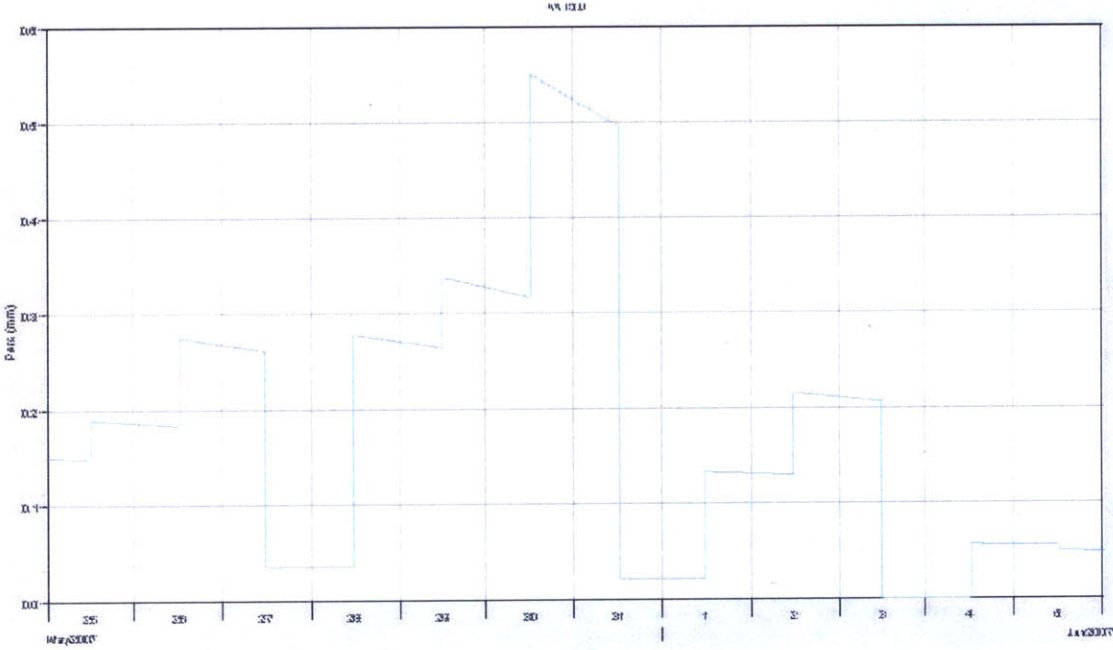


Figure 62 - Screen Shot of HEC-HMS: Soil infiltration of w150 for Run CN1 after calibration

In Run CN1, the soil infiltration did not seem to reach a ceiling value like it did in Run CN0 (Figure 62). This indicates that the model is still accounting for water loss through the soil until the end of the simulation period. Excess precipitation after soil infiltration is illustrated in Figure 63. In Figure 64, the flow residual curve shows the difference between simulated runoff from the observed Manafwa River flow.

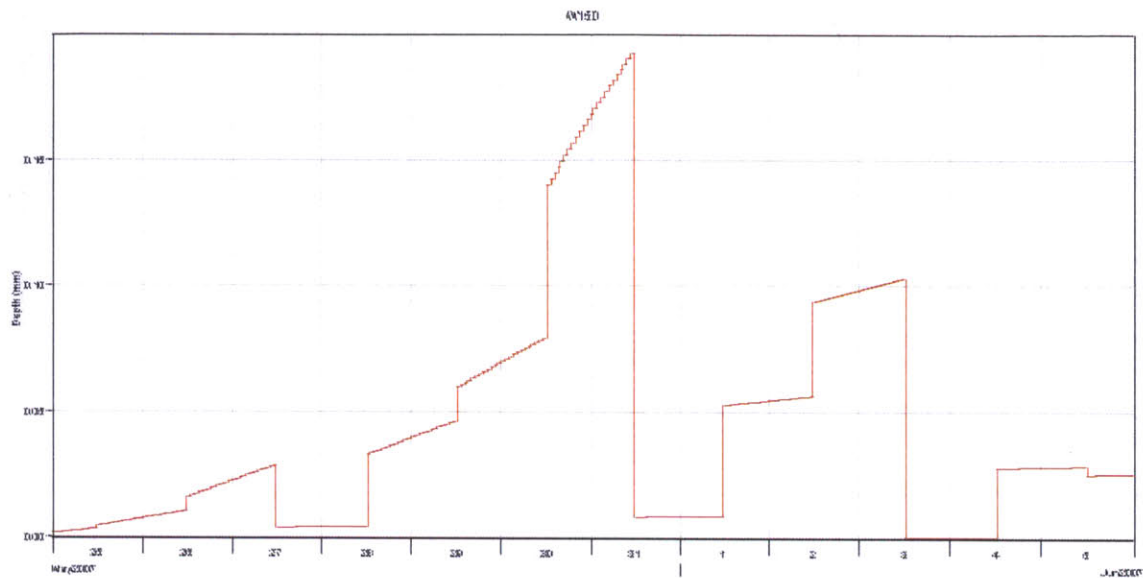


Figure 63 - Screen Shot of HEC-HMS: Excess precipitation of w150 for Run CN1 after calibration

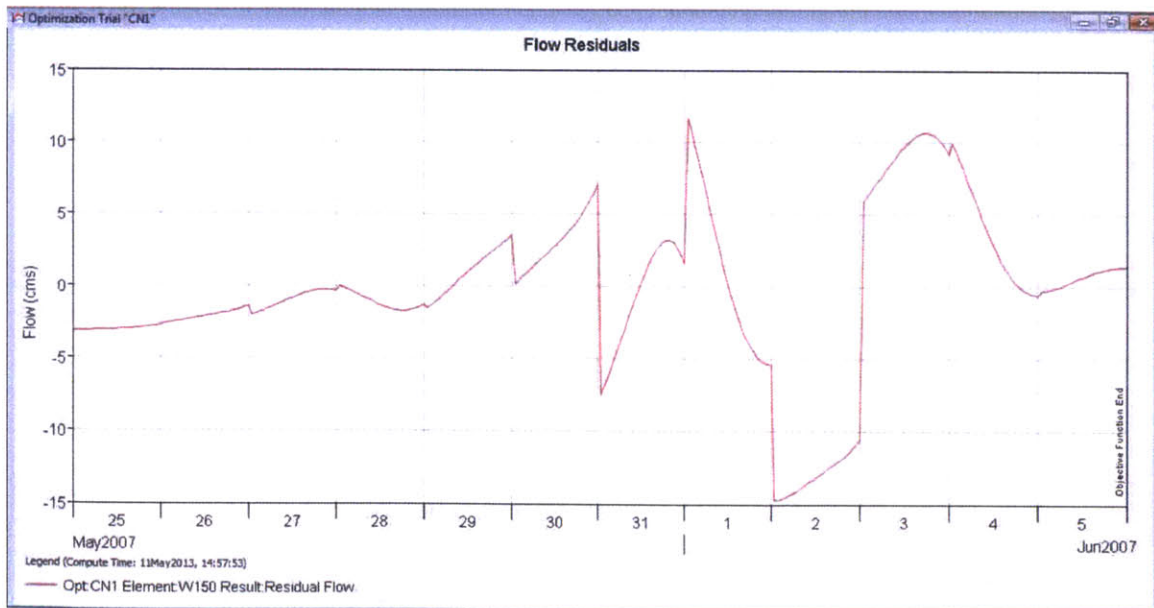


Figure 64 - Screen Shot of HEC-HMS: flow residual of w150 for Run CN1 after calibration

4.3.2 Run IC1

Run IC1 is the simulation run using Initial and Constant loss method over the period between 25 May and 5 June, 2007. The simulated hydrograph for Run IC1 is presented in Figure 65. Much more water loss is observed than that in Run CN1. The value of water loss is shown in Figure 66.

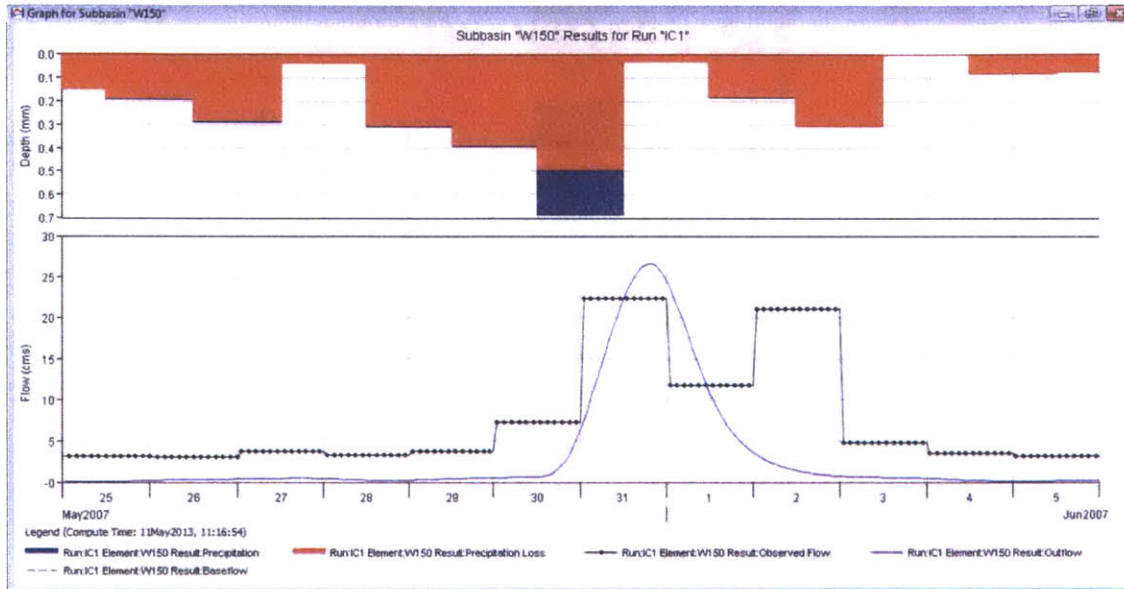


Figure 65 - Screen Shot of HEC-HMS: Flow graph of w150 for Run IC1 before calibration

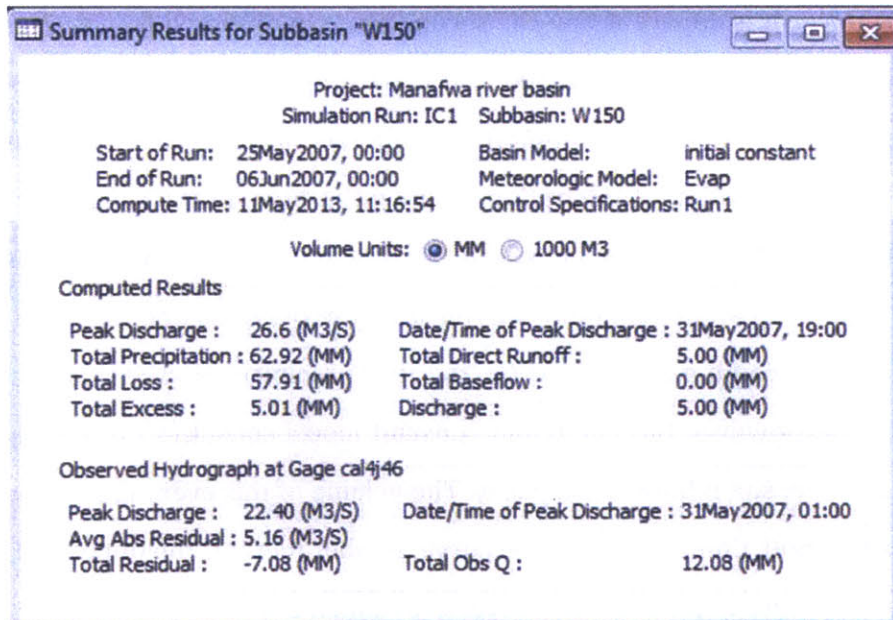


Figure 66 - Screen Shot of HEC-HMS: Summary table of w150 for Run IC1 before calibration

Calibration is carried out with respect to W150 on constant loss rate and lag time. The results are as follows.

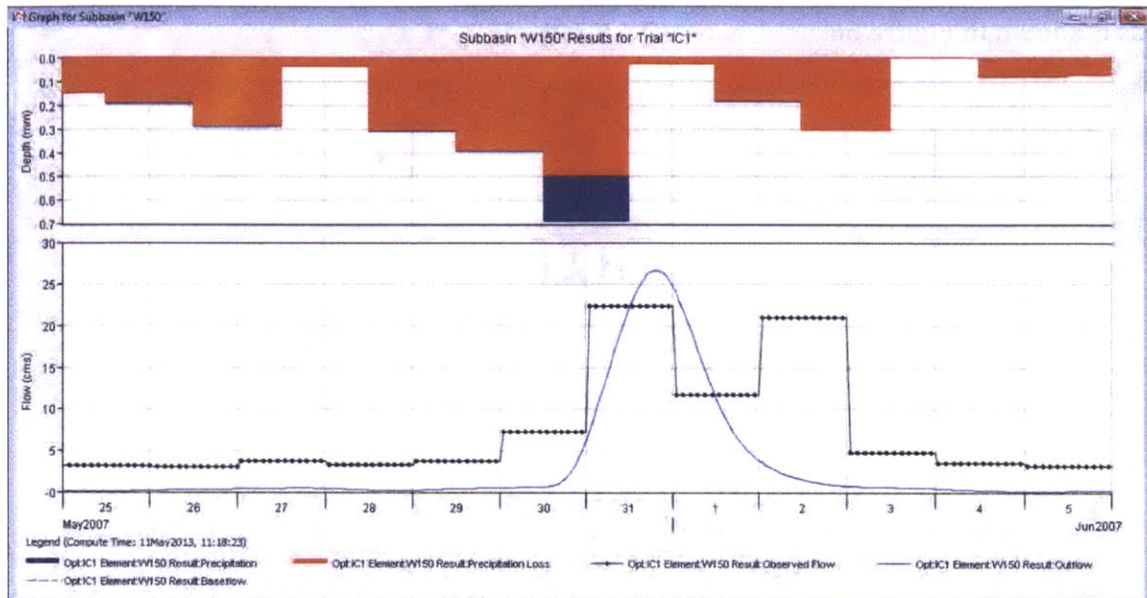


Figure 67 - Screen Shot of HEC-HMS: Flow graph of w150 for Run IC1 after calibration

In Figure 67 above, it is apparent that the second spike in observed flow is not captured using the initial and constant loss method as it was using the CN method. This is because the method assumes a maximum infiltration capacity and antecedent moisture is not considered in the calculation of infiltration at any given time. In the reference flow, it is observed that the second spike of measured flow is considerably high despite the corresponding precipitation being much lower than the previous one. It is most likely a result of the soil becoming saturated after the first precipitation event that causes the first runoff peak. However, the initial and constant model considers the second rainfall and based upon the soil infiltration capacity. The volume of this event is too low to cause any significant runoff. Compared with the curve number method, the initial and constant method is less effective in dealing with successive rainfall events.

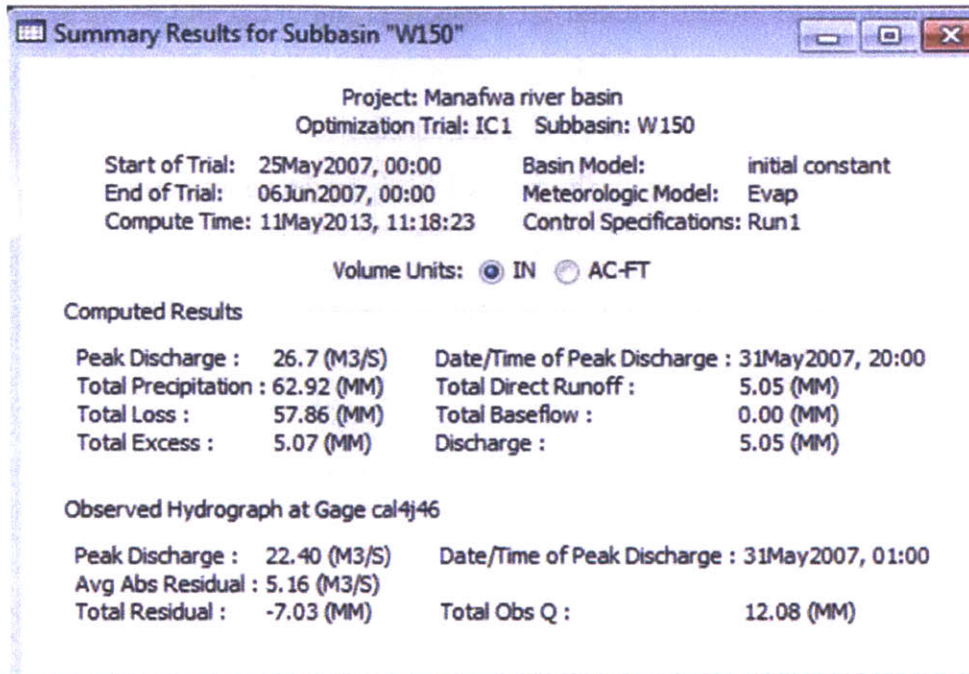


Figure 68 - Screen Shot of HEC-HMS: Summary table of w150 for Run IC1 after calibration

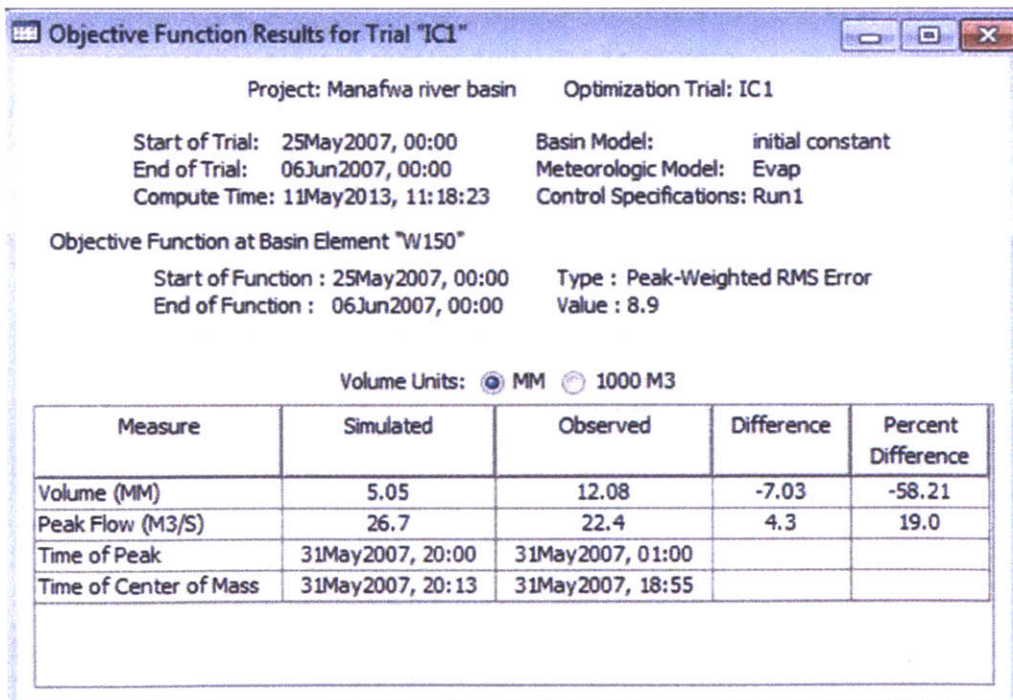


Figure 69 - Screen Shot of HEC-HMS: Optimization objective function of w150 for Run IC1

As is shown above in Figures 68 and 69, because of the initial and constant method's inability to account for antecedent moisture conditions, the initial and constant model fails to generate an accurate runoff volume for successive events. The observed percent difference in total runoff volume for the two events discussed above is ~58%.

Optimized Parameter Results for Trial "IC1"

Project: Manafwa river basin Optimization Trial: IC1

Start of Trial: 25May2007, 00:00 Basin Model: Initial constant
 End of Trial: 06Jun2007, 00:00 Meteorologic Model: Evap
 Compute Time: 11May2013, 11:18:23 Control Specifications: Run1

Element	Parameter	Units	Initial Value	Optimized Value	Objective Function Sensitivity
W150	Constant Loss Rate	MM/HR	0.5	0.49789	0.00
W150	SCS Lag	MIN	1027	1044.5	-0.06

Figure 70 - Screen Shot of HEC-HMS: optimized parameters of w150 for Run IC1

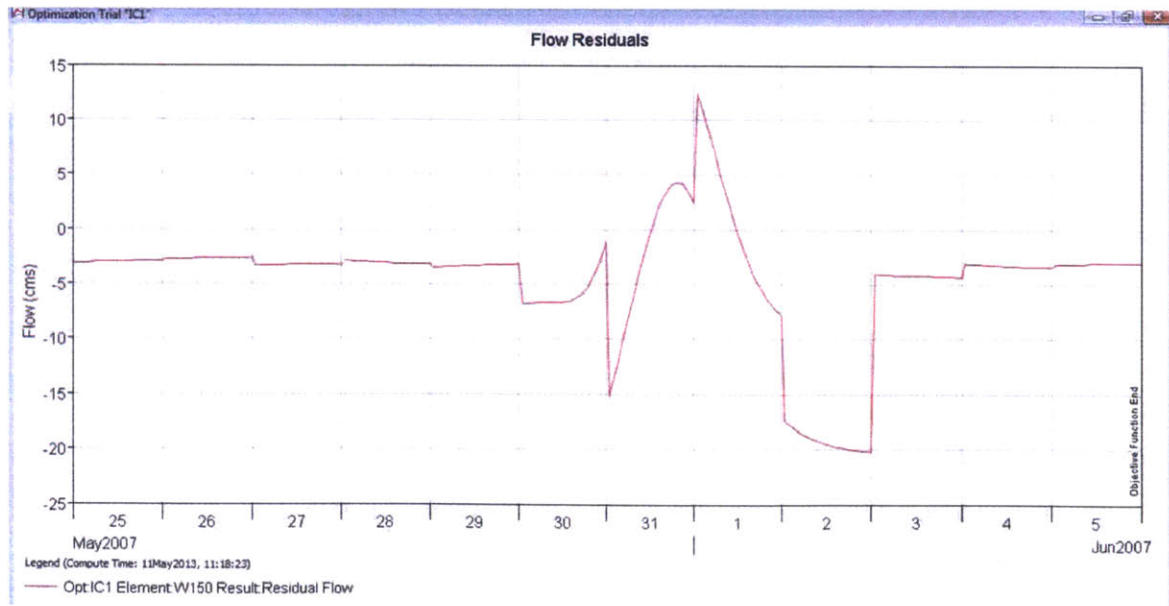


Figure 71 - Screen Shot of HEC-HMS: Flow residual of w150 for Run IC1 after calibration

In Figure 70 above, the deviation of the optimization result from the reference values is shown; the difference is small. Figure 71 shows the residual flow (the computed flow minus the observed flow). It is worth noting that the auto-calibration method used in the software is significantly affected by the peak flow values. The calibrated results render most of the simulation data points lower than the reference values in an attempt to bring peak flow down to the expected order of magnitude. This is not hard to understand considering the algorithm behind the optimization process. As a result, it is common to see a deficit in the simulation result when there is not a considerable amount of rainfall. Advantage could be taken by introducing baseflow to improve the model's accuracy.

Figure 72 and Figure 73 illustrate soil infiltration and excess precipitation levels over the simulation period. Excess precipitation becomes runoff and is essentially the blue part of the histogram in Figure 67.

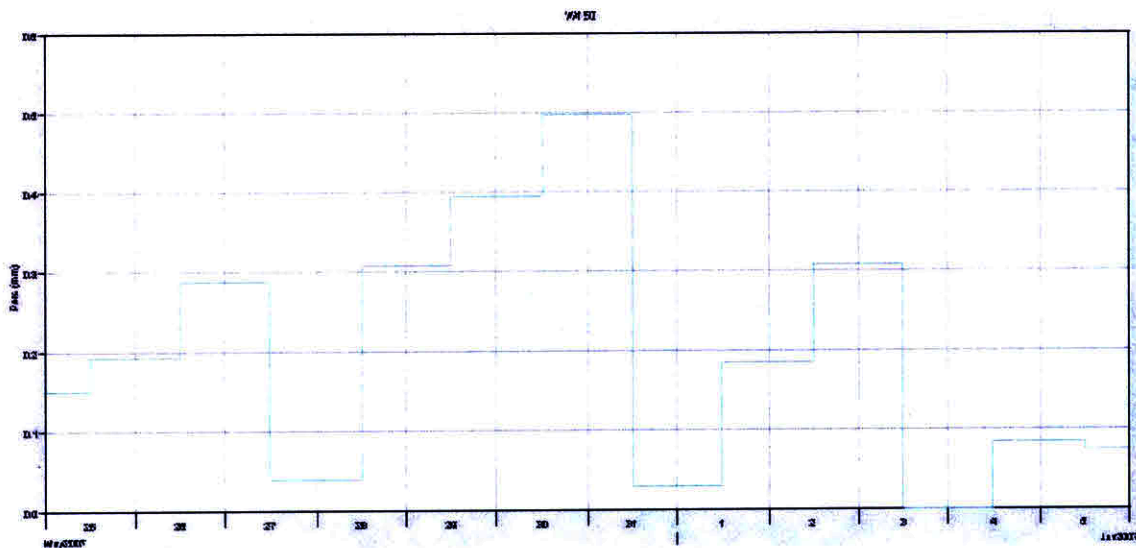


Figure 72 - Screen Shot of HEC-HMS: Soil infiltration of w150 for Run IC1 after calibration

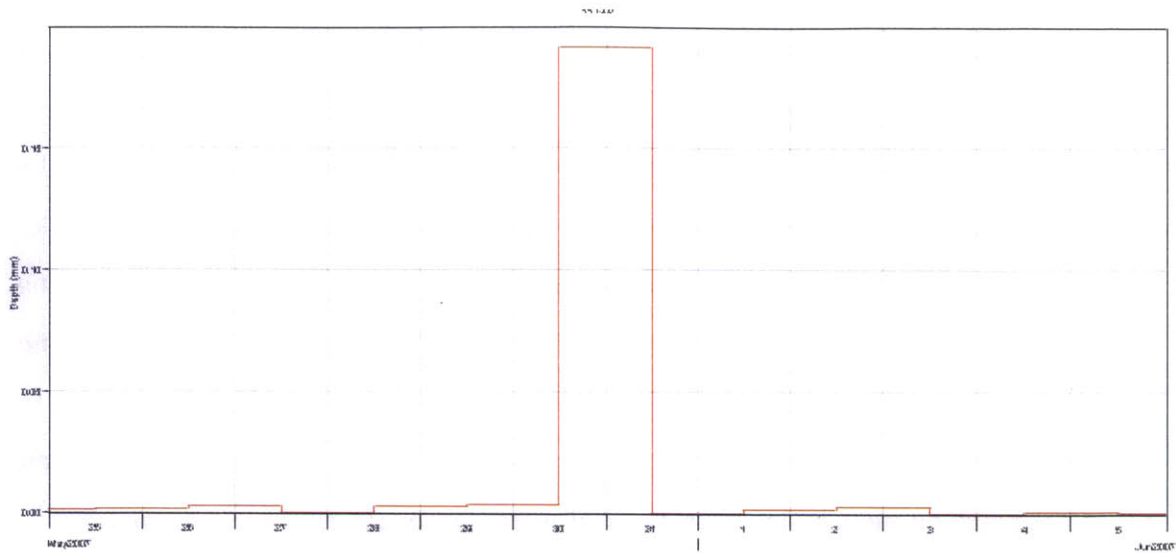


Figure 73 - Screen Shot of HEC-HMS: Excess precipitation of w150 for Run IC1 after calibration

4.4 Short term simulation - Run2

4.4.1 Run CN2

Run CN2 is the simulation run using curve number loss method over the period between 01 Aug 2006 and 15 Aug 2006. The results for Run CN2 are discussed below.

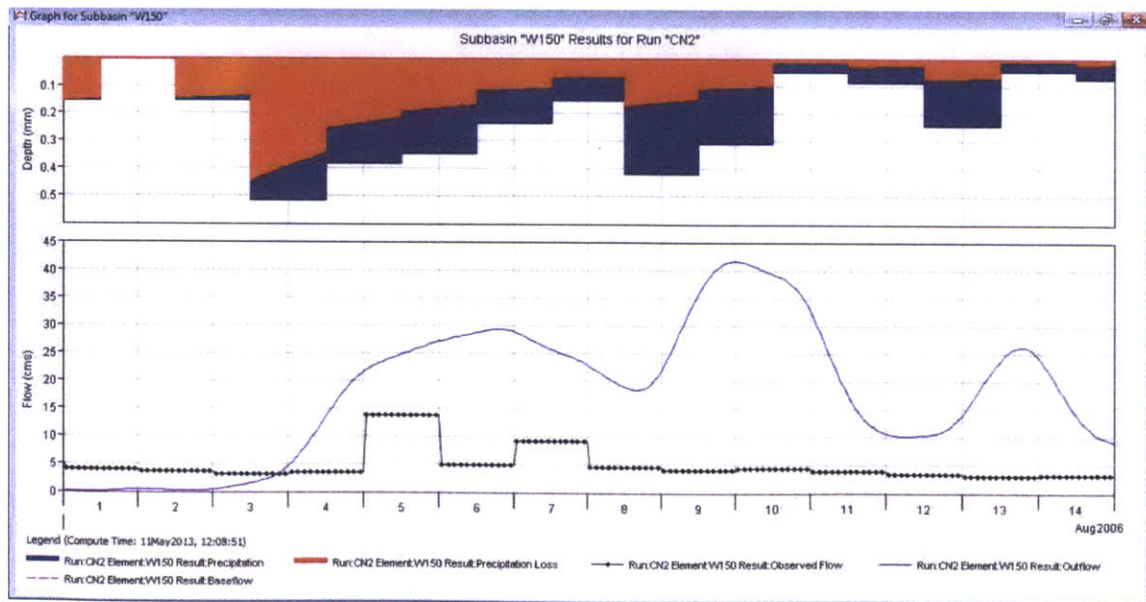


Figure 74 - Screen Shot of HEC-HMS: Flow graph of w150 for RunCN2 before calibration

As shown above in Figure 74, high abstraction is observed in the first three days of the precipitation event. The first prolonged rainfall pulse generated a much higher runoff than is gauged. It is worth noting that, in contrast with the initial and constant loss method, the curve number method result is featured with an angled interface between the blue (precipitation) and red (precipitation loss) components of the precipitation histogram. This indicates that previous rainfall is having an effect on the soil such that less and less subsequent rainfall is infiltrating into the soil. In the summary table in Figure 75, the peak discharge is calculated to be 41.7 cms, whereas the observed peak flow is around 14 cms.

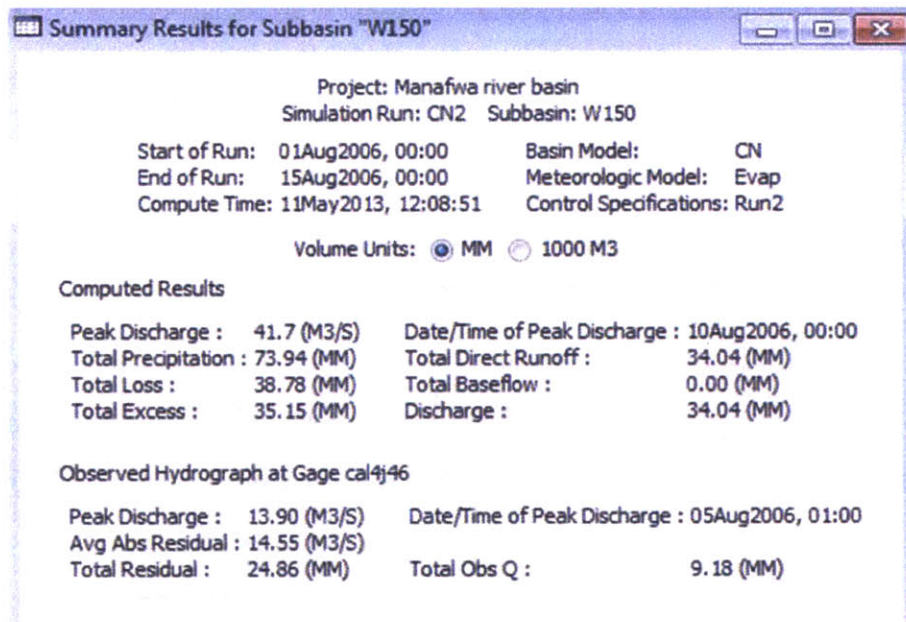


Figure 75 - Screen Shot of HEC-HMS: Summary table of w150 for RunCN2 before calibration

Calibration is carried out with respect to W150 on curve number and lag time. The results are as follows.

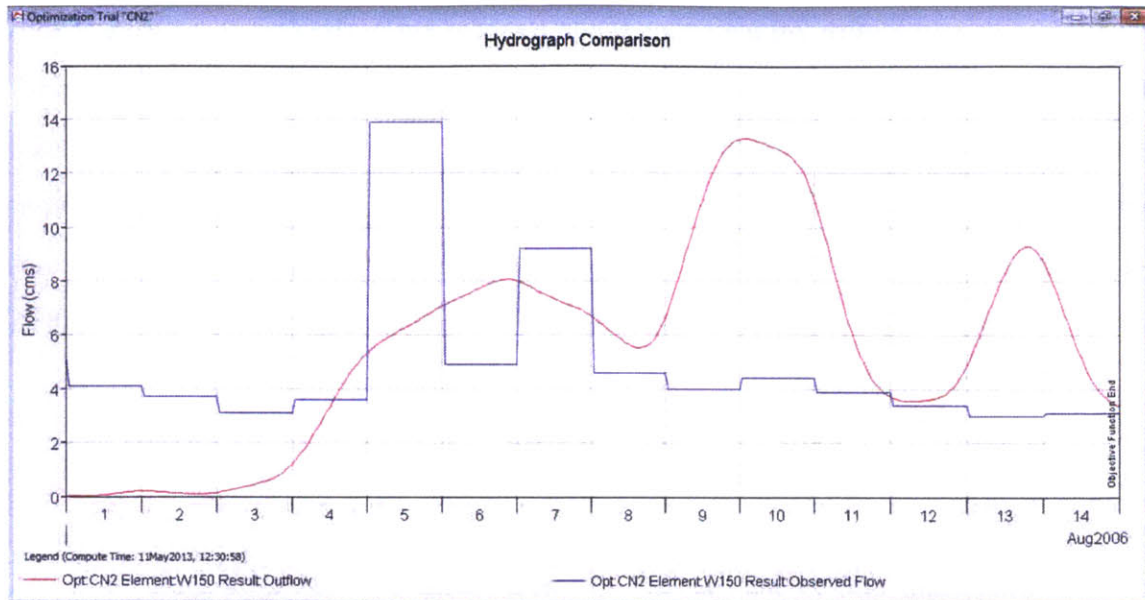


Figure 76 - Screen Shot of HEC-HMS: Flow graph of w150 for RunCN2 after calibration

It is shown in Figure 76 above that as the soil becomes increasingly saturated, more runoff is produced despite the relatively mild second rainfall pulse. One can conclude that the curve number method, in this case, underestimates the actual infiltration capacity of the soil. Were the soil profile to lose the same fraction of precipitation as it does for the first pulse of rainfall, a more accurate simulation might result. The soil in w150 exhibits a high infiltration capacity, which should be noted in future modeling efforts. In the summary table in Figure 77, the peak discharge is reduced from 41.7 cms to 13.3 cms.

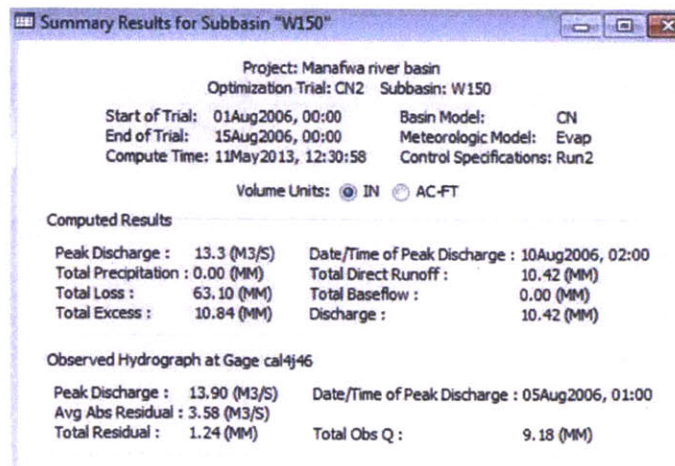


Figure 77 - Screen Shot of HEC-HMS: Summary table of w150 for RunCN2 after calibration

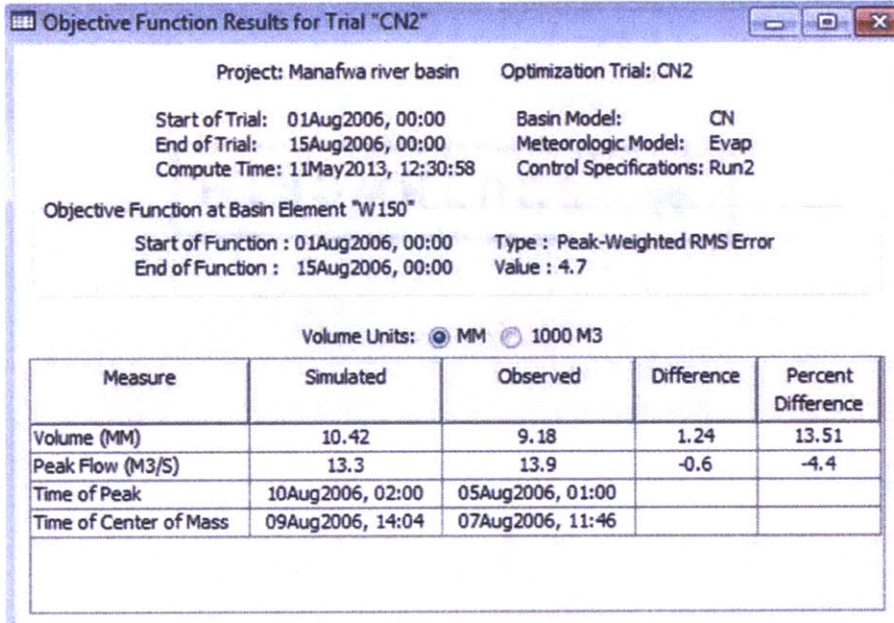


Figure 78 - Screen Shot of HEC-HMS: Optimization objective function of w150 for RunCN2

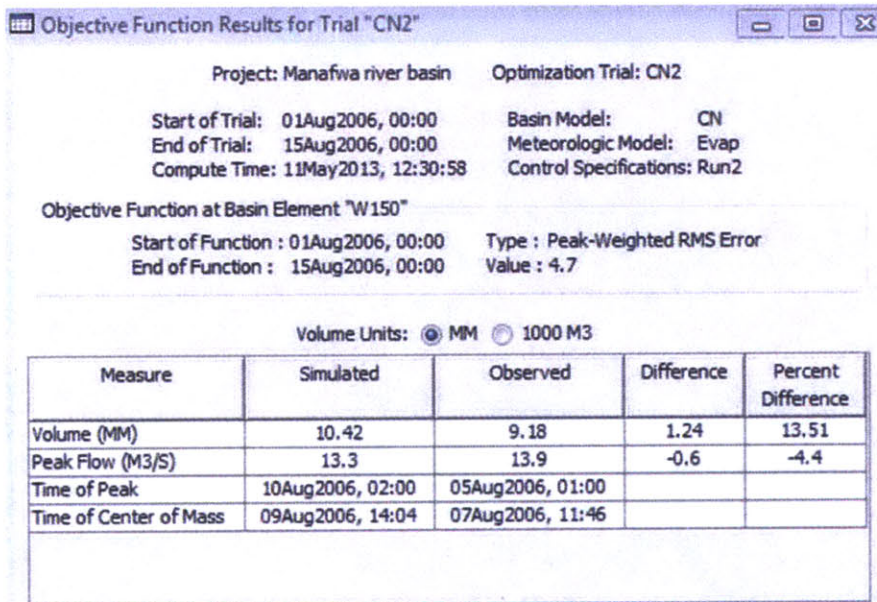


Figure 79 - Screen Shot of HEC-HMS: Optimized parameters of w150 for RunCN2

Figure 78 shows both volume and peak flow can be calibrated close to the reference value; however, the model must modify the curve numbers to very low values in order to do so (Figure 79).

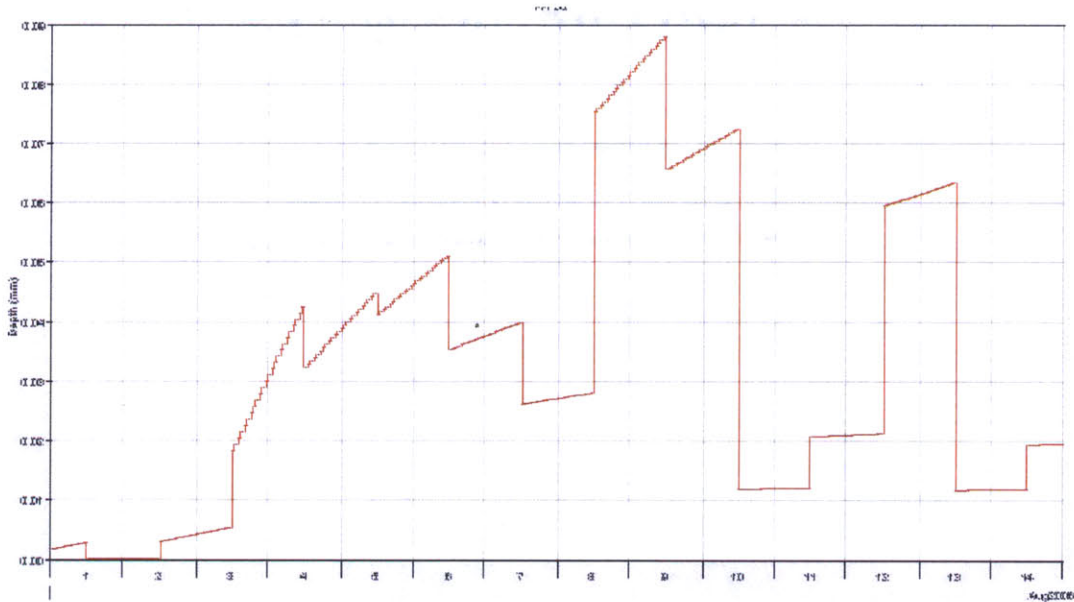


Figure 80 - Screen Shot of HEC-HMS: Excess precipitation of w150 for RunCN2 after calibration

Figure 80 above shows the excess precipitation of the sub-basin studied after calibration in mm.

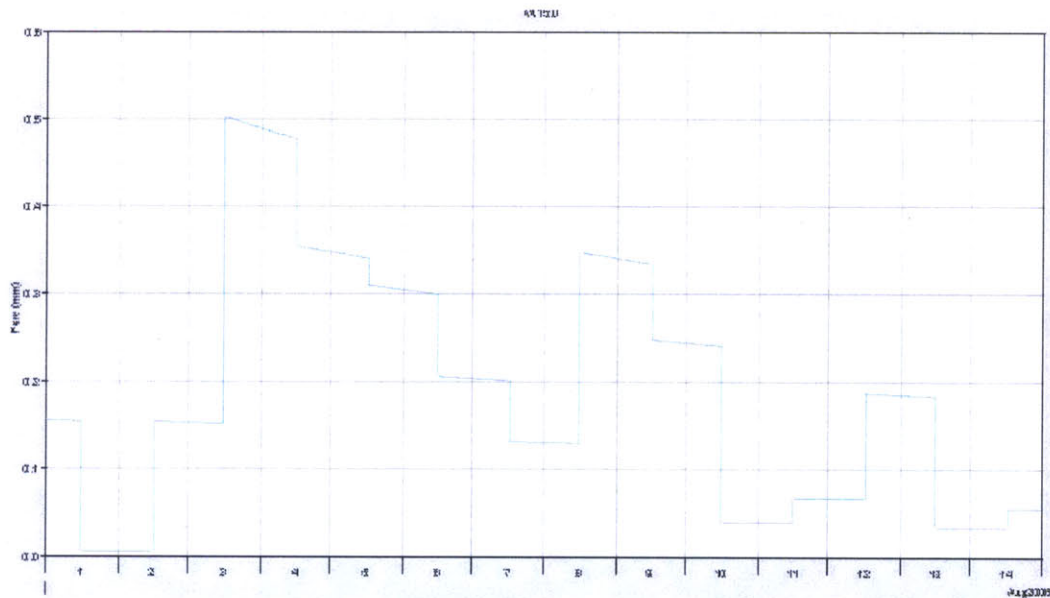


Figure 81 - Screen Shot of HEC-HMS: Soil infiltration of w150 for RunCN2 after calibration

Figure 81 shows soil infiltration of sub-basin w150 after calibration in mm. As the simulation time interval is one hour, soil infiltration is not constant through a single day.

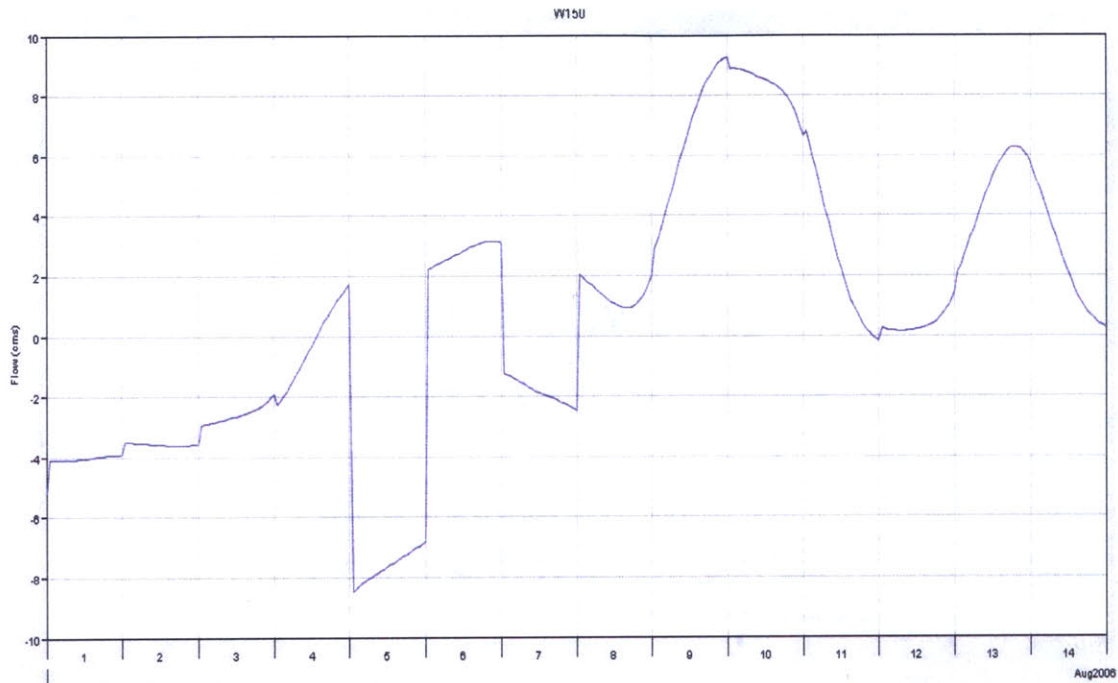


Figure 82 - Screen Shot of HEC-HMS: Flow residual of w150 for RunCN2 after calibration

In Figure 82 the curve represents the difference between calibrated flow hydrograph and the observed flow. As a result of calibration, the flow residual curve fluctuates around the 0 cms.

4.4.2 Run IC2

Run IC2 is the simulation run using initial constant loss method over the period between 01 Aug 2006 and 15 Aug 2006. The flow hydrograph before calibration for Run IC2 is shown in Figure 83. Similar to Run IC1, the second spike of the observed flow on 7 Aug 2006 is not captured.

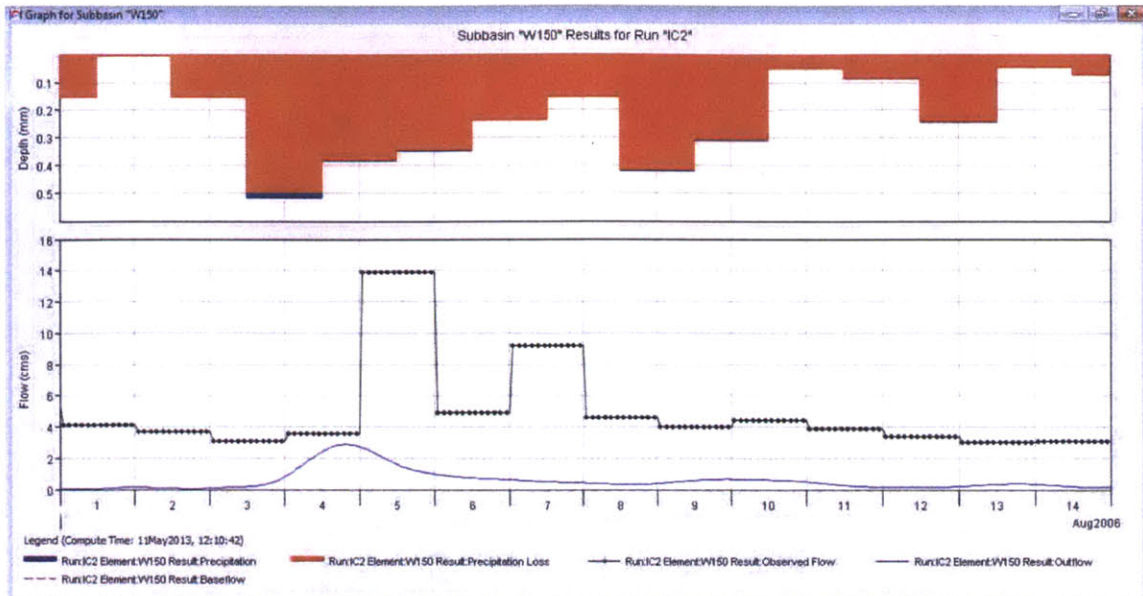


Figure 83 - Screen Shot of HEC-HMS: Flow graph of w150 for RunIC2 before calibration

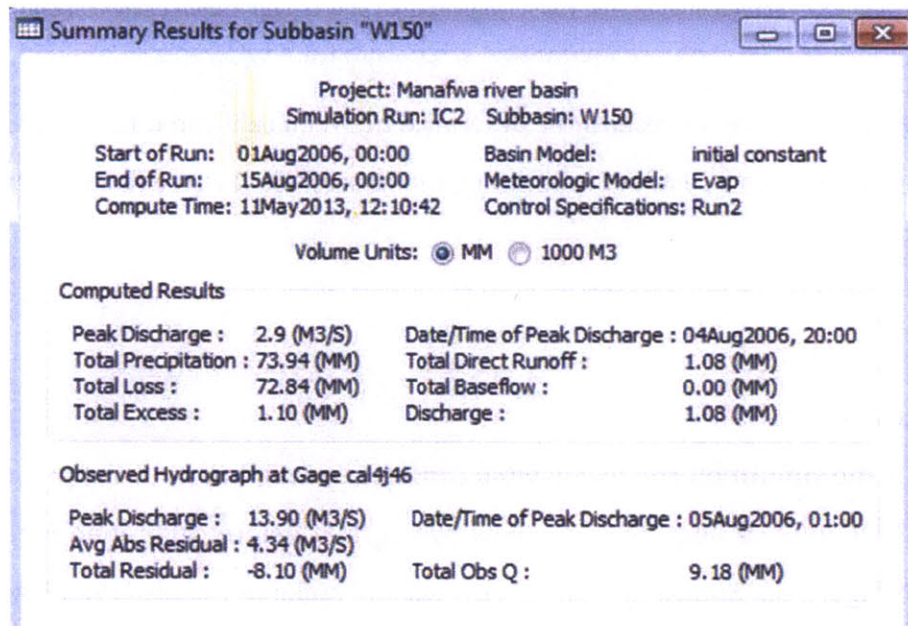


Figure 84 - Screen Shot of HEC-HMS: Summary table of w150 for RunIC2 before calibration

Before calibration, the peak discharge is as low as 2.9 cms, compared with the observed peak flow of 13.9 cms (Figure 84). The initial loss rate is too high and not enough runoff is obtained. Calibration is carried out with respect to W150 for constant loss rate and lag time. The calibrated flow hydrograph is presented in Figure 85. While the simulated peak

flow is raised to 11.3 cms (Figure 86), it is unclear why the majority of the hydrograph is below the observed flow curve. The calibrated total loss is abnormally high, resulting in a discharge flow volume 59% less than the observed flow volume (Figure 87).

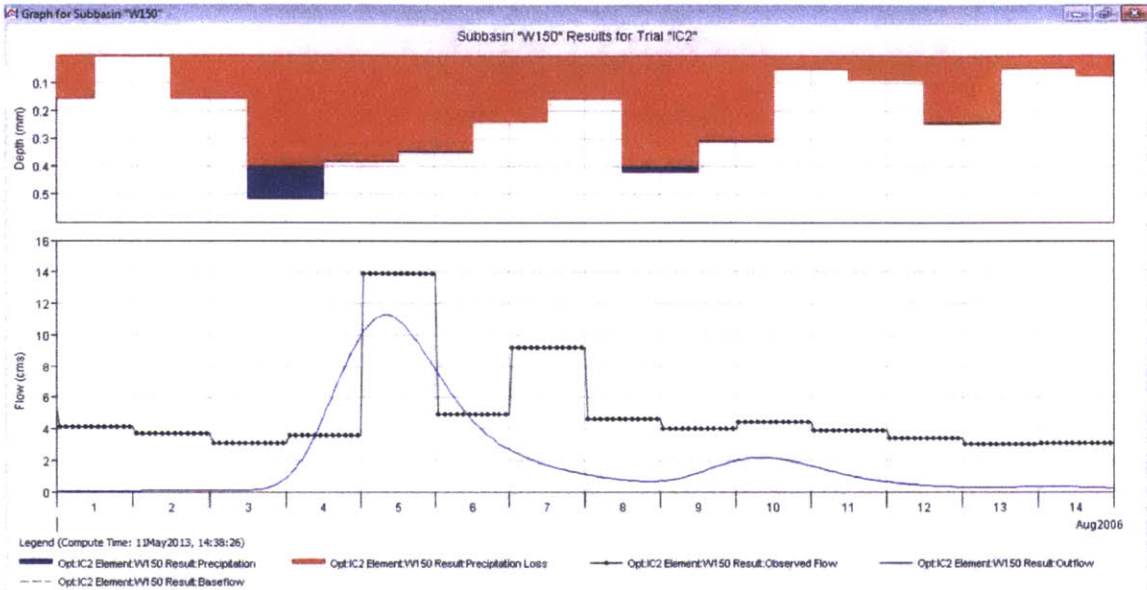


Figure 85 - Screen Shot of HEC-HMS: Flow graph of w150 for RunIC2 after calibration

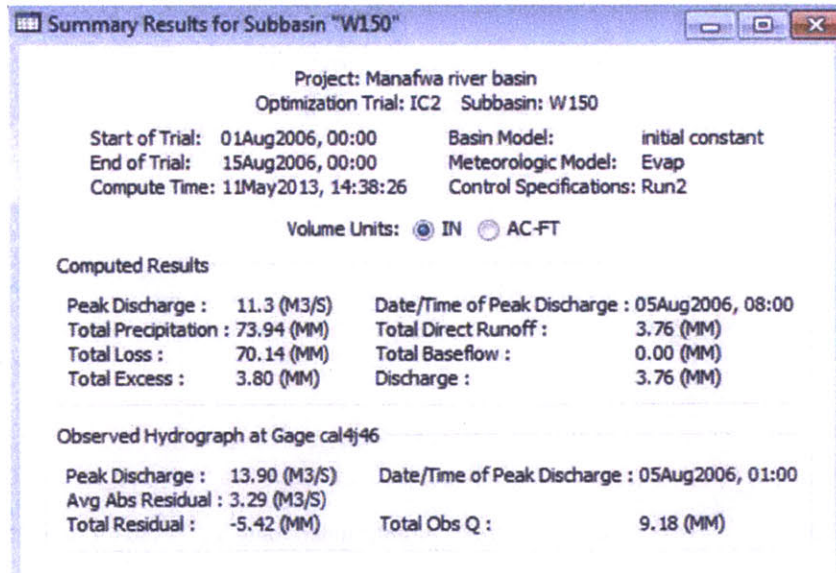


Figure 86 - Screen Shot of HEC-HMS: Summary table of w150 for RunIC2 after calibration

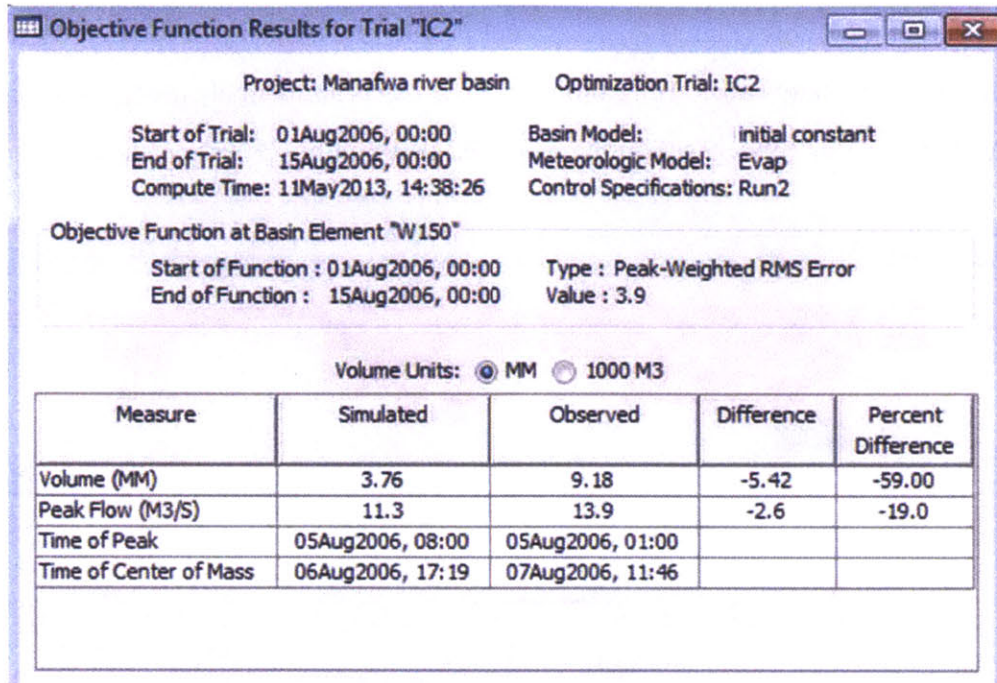


Figure 87 - Screen Shot of HEC-HMS: Optimization objective function of w150 for Run IC2

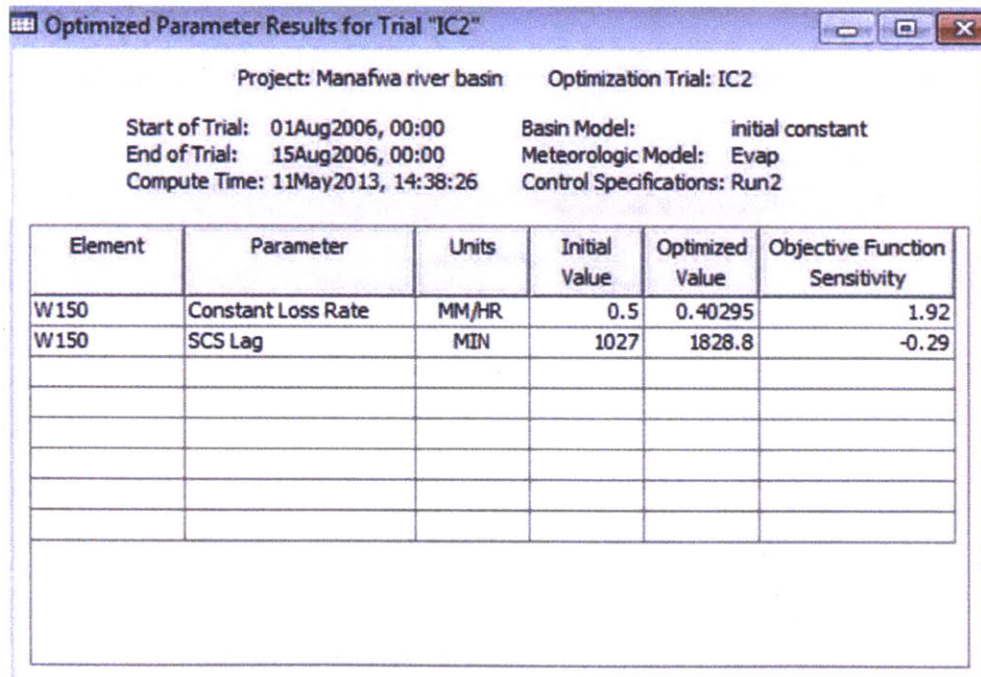


Figure 88 - Screen Shot of HEC-HMS: Optimized parameters of w150 for Run IC2

Figure 88 shows the constant loss rate is calibrated from 0.5 mm/hr to 0.40295 mm/hr.

Lag time is increased from 1027 min to 1828.8 min.

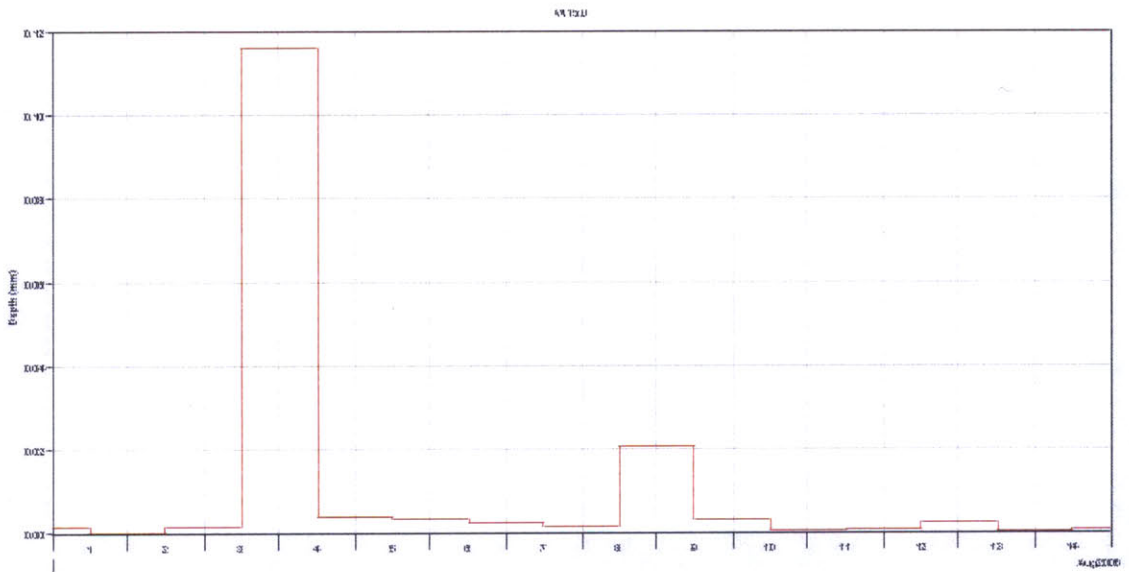


Figure 89 - Screen Shot of HEC-HMS: Excess precipitation of w150 for Run IC2 after calibration

Compared with Run CN2, the excess precipitation (Figure 89) is heavily weighted on 3 Aug 2006. The distribution of the resulting excess precipitation for Run IC2 is more realistic considering the distribution of precipitation over the simulation period. Most of the time the simulated flow rate values are below the observed flow values (Figure 90).

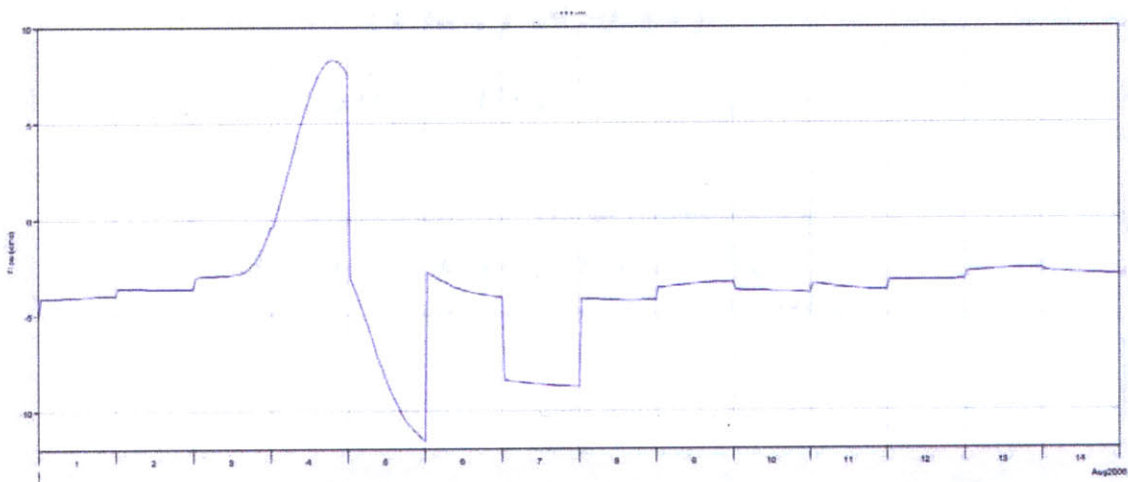


Figure 90 - Screen Shot of HEC-HMS: Flow residuals of w150 for Run IC2 after calibration

In Figure 91, the soil infiltration appears to be constant over each single day. More water

is lost to soil infiltration than that in Run CN2.

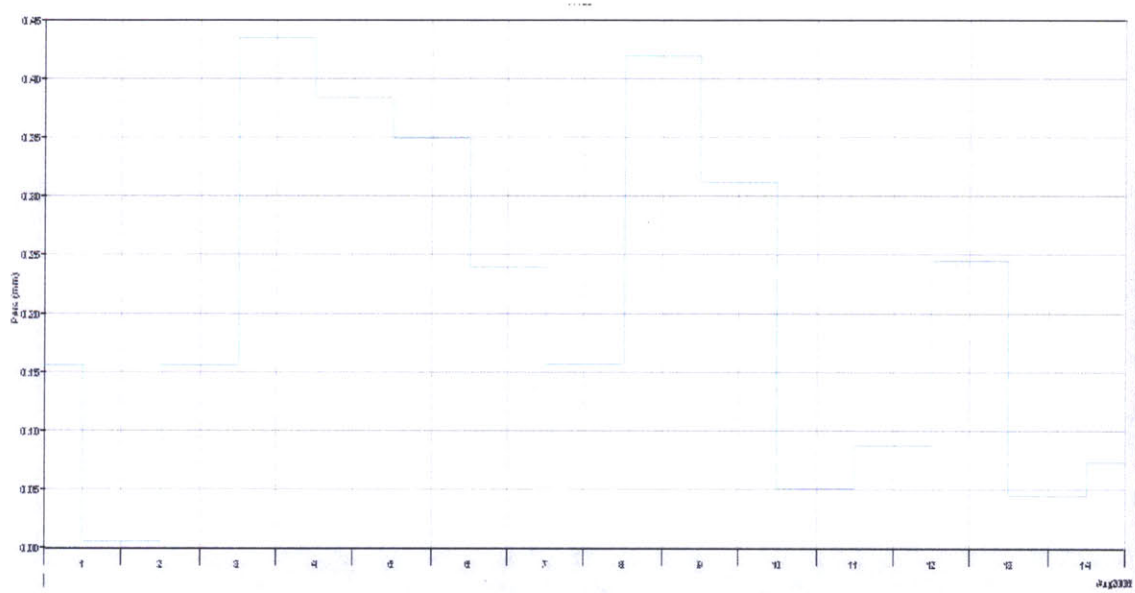


Figure 91 - Screen Shot of HEC-HMS: Soil infiltration of w150 for Run IC2 after calibration

4.5 Short term simulation Run3

4.5.1 Run CN3

Run CN3 is the simulation run using curve number loss method over the period between 17 Nov 2008 and 30 Nov 2008. The flow hydrograph before calibration for Run CN3 is presented in (Figure 92). Dramatically more runoff is calculated than the observed value. Calculated peak discharge increased dramatically to 160.2 cms (Figure 93) compared with the observed 19.8 cms.

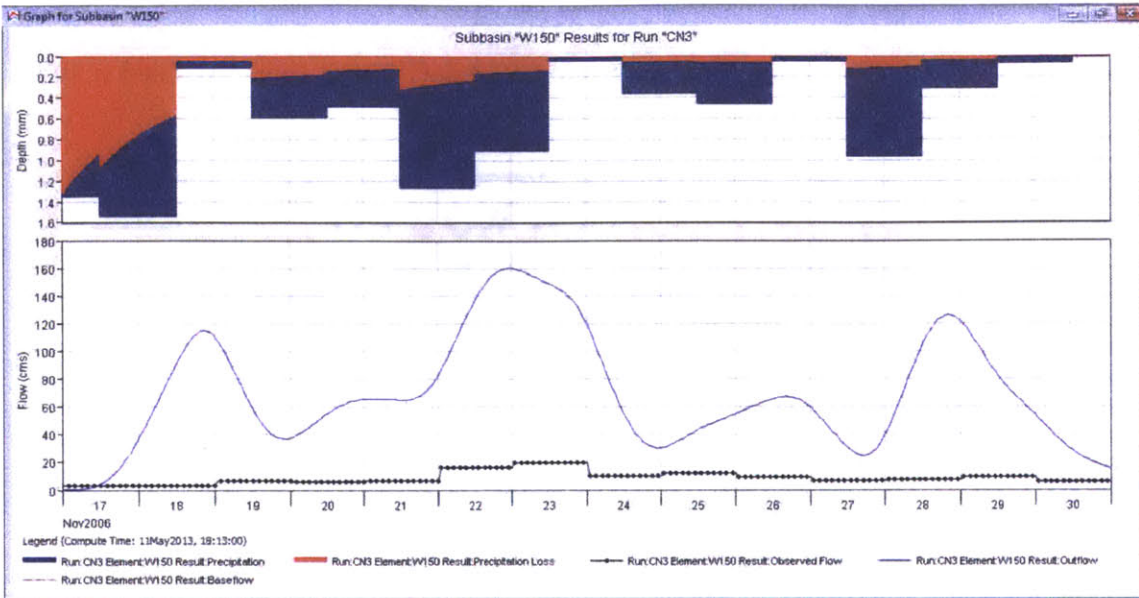


Figure 92 - Screen Shot of HEC-HMS: Flow graph of w150 for Run CN3 before calibration

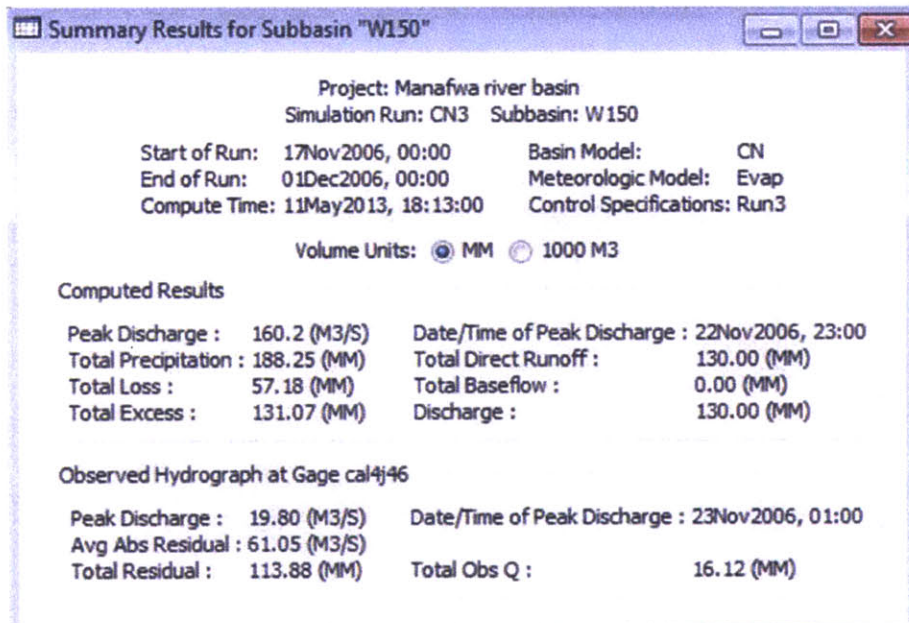


Figure 93 - Screen Shot of HEC-HMS: Summary table of w150 for Run CN3 before calibration

Calibration is carried out with respect to W150 on curve number and lag time. The calibrated flow hydrograph is presented below in Figure 94. The trend of the observed flow is decently captured by the flow hydrograph. However, the magnitude is much too high. It seems the model reaches the lower limit of the curve number (Figure 95) in

calculation after it brings the peak discharge down to 62 cms (Figure 96). The flow volume (Figure 97) is 53.79 mm after calibration, 233.66% higher than observed value.

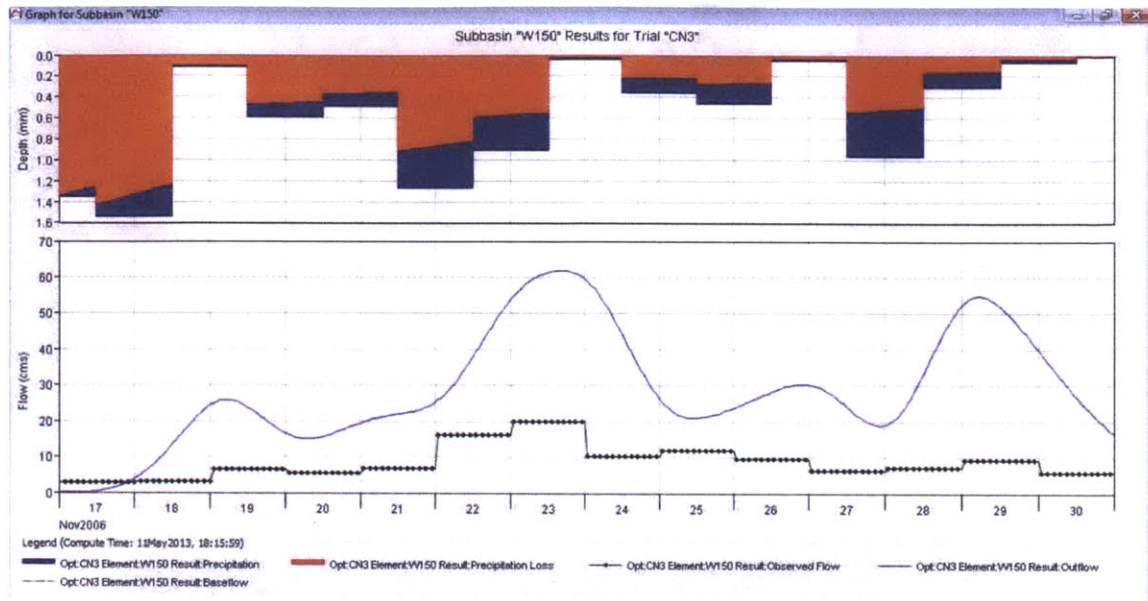


Figure 94 - Screen Shot of HEC-HMS: Flow graph of w150 for Run CN3 after calibration

Optimized Parameter Results for Trial "CN3"

Project: Manafwa river basin Optimization Trial: CN3

Start of Trial: 17Nov2006, 00:00 Basin Model: CN

End of Trial: 01Dec2006, 00:00 Meteorologic Model: Evap

Compute Time: 11May2013, 18:15:59 Control Specifications: Run3

Element	Parameter	Units	Initial Value	Optimized Value	Objective Function Sensitivity
W150	Curve Number		75.3	35.294	1.48
W150	SCS Lag	MIN	1027	1563.5	-0.23

Figure 95 - Screen Shot of HEC-HMS: Optimized parameter of w150 for Run CN3

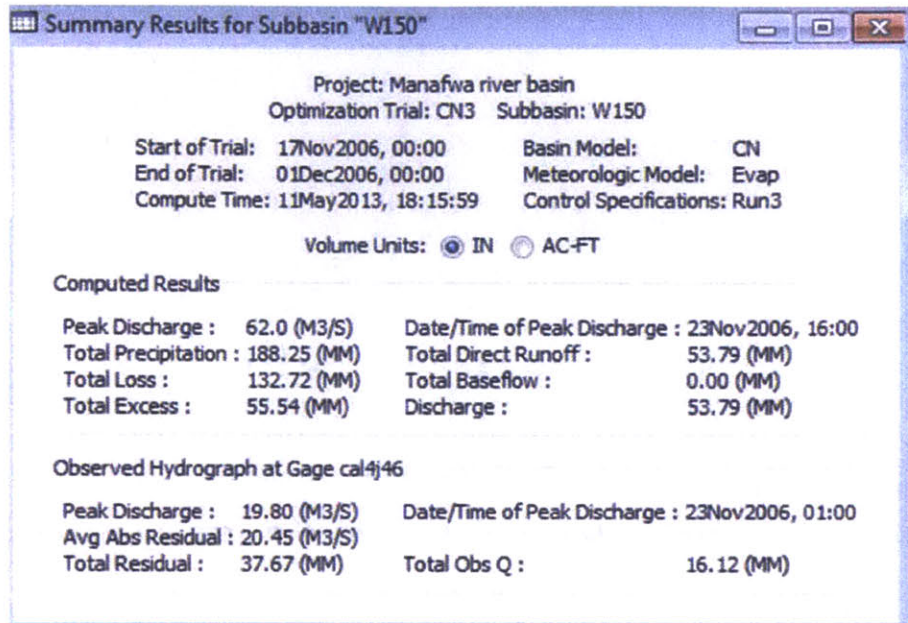


Figure 96 - Screen Shot of HEC-HMS: Summary table of w150 for Run CN3 after calibration

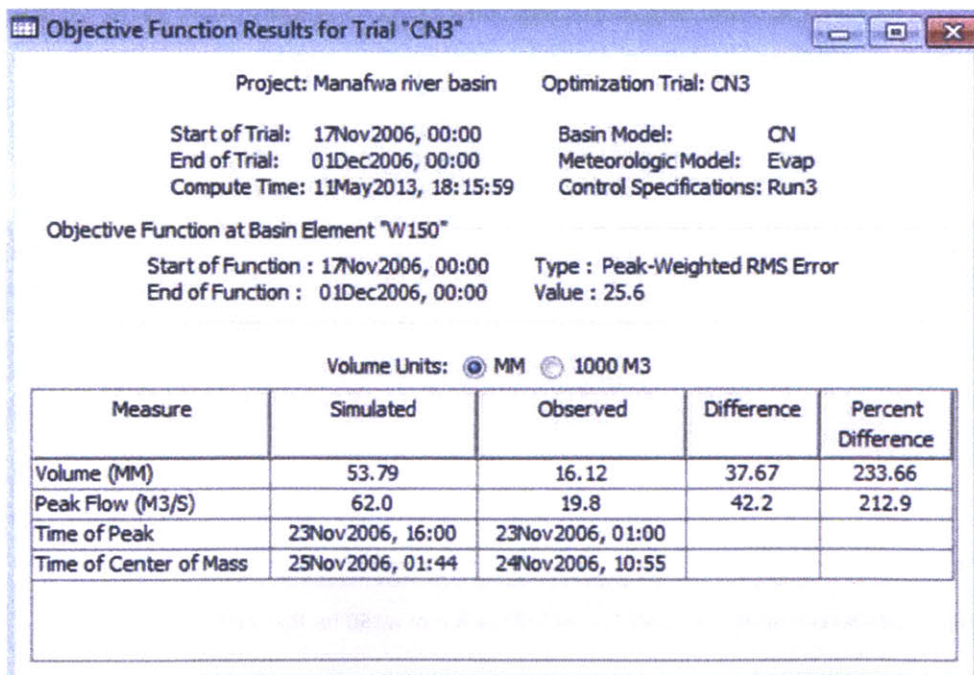


Figure 97 - Screen Shot of HEC-HMS: Optimization objective function of w150 for Run CN3

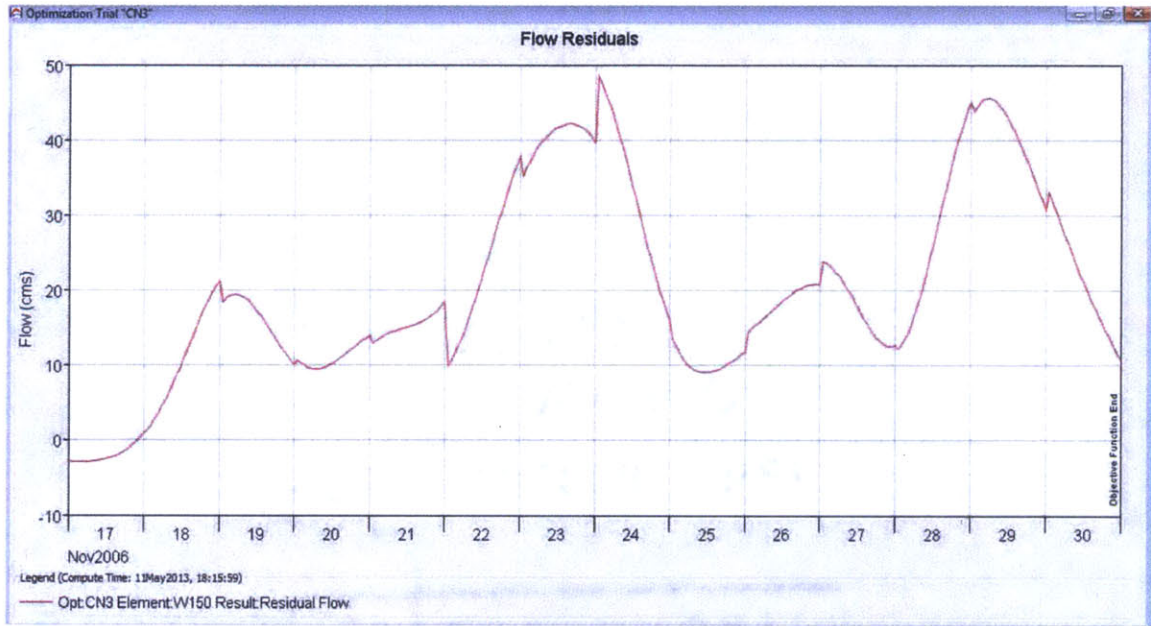


Figure 98 - Screen Shot of HEC-HMS: Flow residual of w150 for Run CN3 after calibration

Figure 98 above shows the high surplus in the calibrated result compared to the observed values over the most part of the simulation period.

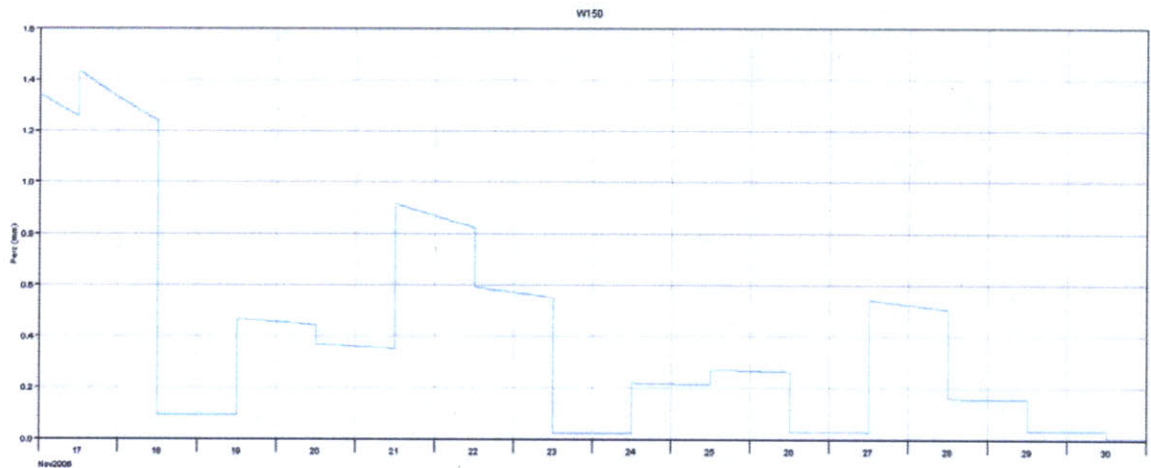


Figure 99 - Screen Shot of HEC-HMS: Soil infiltration of w150 for Run CN3 after calibration

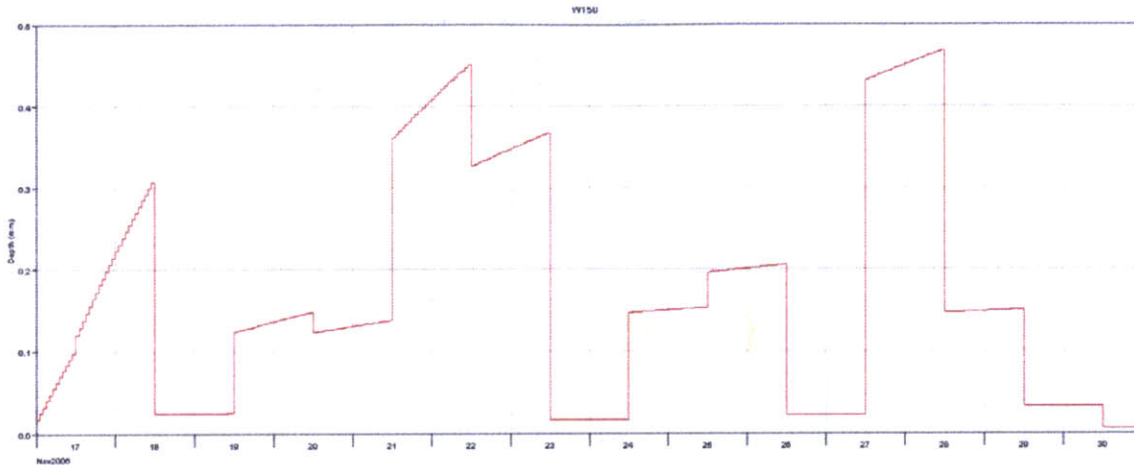


Figure 100 - Screen Shot of HEC-HMS: Excess precipitation of w150 for Run CN3 after calibration

The soil infiltration (Figure 99) is not constant over each day. The excess precipitation (Figure 100) follows the trend of soil infiltration closely.

4.5.2 Run IC3

Run IC3 is the simulation run using initial constant loss method over the period between 17 Nov 2006 and 30 Nov 2006. The results for Run IC3 are discussed below.

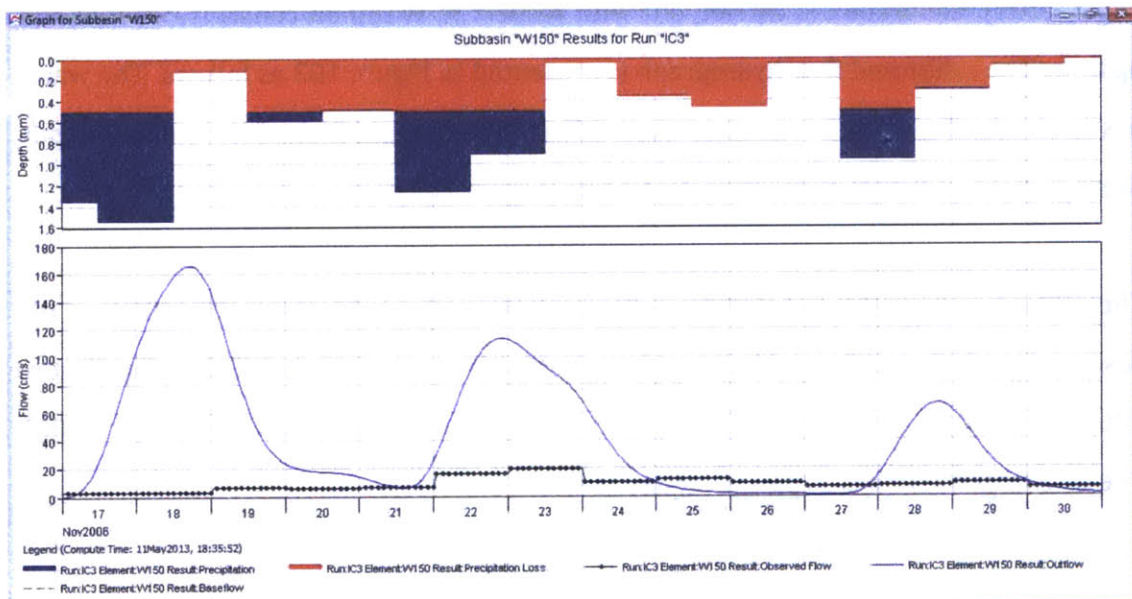


Figure 101 - Screen Shot of HEC-HMS: Flow graph of w150 for Run IC3 before calibration

As shown above in Figure 101, more runoff spikes are generated than there are in the observed flow.

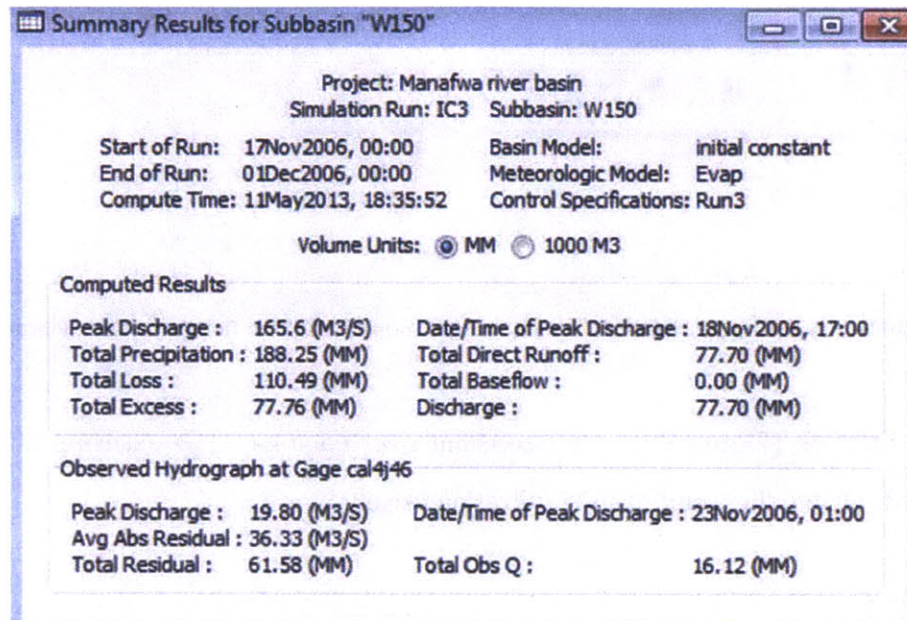


Figure 102 - Screen Shot of HEC-HMS: Summary table of w150 for Run IC3 before calibration

The peak discharge of 165.6 cms is much higher than the observed value of 19.8 cms (Figure 102). Calibration is carried out with respect to W150 on constant loss rate and lag time. The calibrated flow hydrograph is presented in Figure 103 as follows. The water loss is clearly shown to be constant over different days regardless of the rainfall depth. Average residual flow is as much as 35.42 cms (Figure 104).

The calibration is unable to bring down the peak flow value to the same magnitude as the observed peak flow. After calibrating the constant loss rate to 0.51257 mm/hr (Figure 106), the peak flow remains 720.4% higher than the observed peak flow (Figure 105). The discharge volume is 371.81% higher as well.

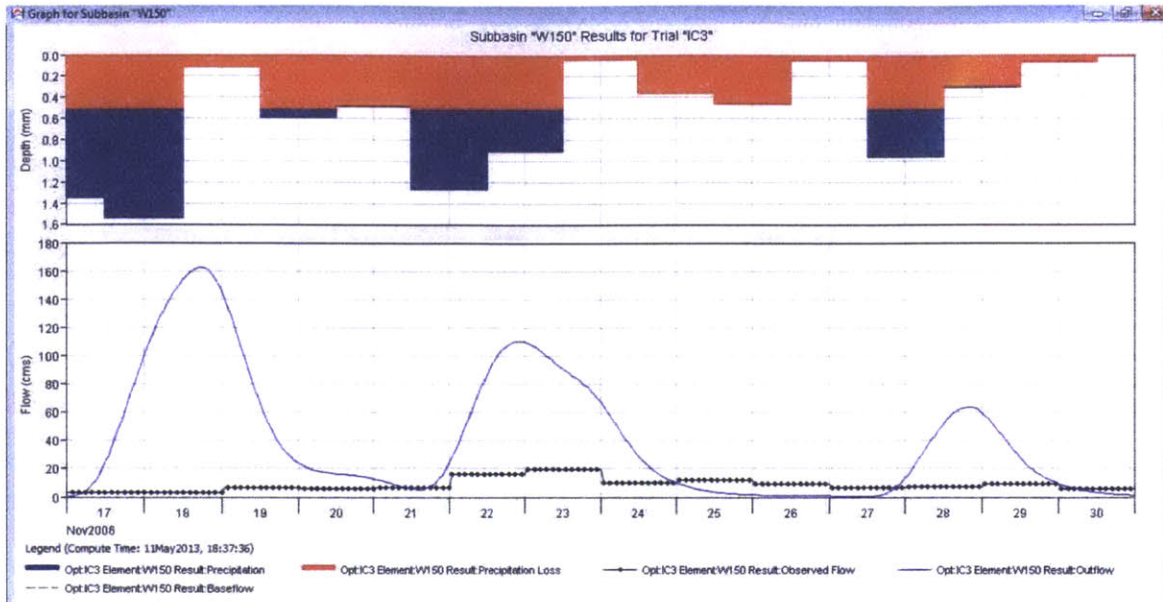


Figure 103 - Screen Shot of HEC-HMS: Flow graph of w150 for Run IC3 after calibration

Summary Results for Subbasin "W150"			
Project: Manafwa river basin			
Optimization Trial: IC3 Subbasin: W150			
Start of Trial:	17Nov2006, 00:00	Basin Model:	initial constant
End of Trial:	01Dec2006, 00:00	Meteorologic Model:	Evap
Compute Time:	11May2013, 18:37:36	Control Specifications:	Run3
Volume Units: <input checked="" type="radio"/> IN <input type="radio"/> AC-FT			
Computed Results			
Peak Discharge :	162.4 (M3/S)	Date/Time of Peak Discharge :	18Nov2006, 17:00
Total Precipitation :	188.25 (MM)	Total Direct Runoff :	76.06 (MM)
Total Loss :	112.14 (MM)	Total Baseflow :	0.00 (MM)
Total Excess :	76.12 (MM)	Discharge :	76.06 (MM)
Observed Hydrograph at Gage cal4j46			
Peak Discharge :	19.80 (M3/S)	Date/Time of Peak Discharge :	23Nov2006, 01:00
Avg Abs Residual :	35.42 (M3/S)		
Total Residual :	59.94 (MM)	Total Obs Q :	16.12 (MM)

Figure 104 - Screen Shot of HEC-HMS: Summary table of w150 for Run IC3 after calibration

Optimized Parameter Results for Trial "IC3"

Project: Manafwa river basin Optimization Trial: IC3

Start of Trial: 17Nov2006, 00:00 Basin Model: initial constant
 End of Trial: 01Dec2006, 00:00 Meteorologic Model: Evap
 Compute Time: 11May2013, 18:37:36 Control Specifications: Run3

Element	Parameter	Units	Initial Value	Optimized Value	Objective Function Sensitivity
W150	Constant Loss Rate	MM/HR	0.5	0.51257	-0.81
W150	SCS Lag	MIN	1027	1047.4	-0.21

Figure 105 - Screen Shot of HEC-HMS: Screen Shot of HEC-HMS: Optimized parameters of w150 for Run IC3

Objective Function Results for Trial "IC3"

Project: Manafwa river basin Optimization Trial: IC3

Start of Trial: 17Nov2006, 00:00 Basin Model: initial constant
 End of Trial: 01Dec2006, 00:00 Meteorologic Model: Evap
 Compute Time: 11May2013, 18:37:36 Control Specifications: Run3

Objective Function at Basin Element "W150"

Start of Function : 17Nov2006, 00:00 Type : Peak-Weighted RMS Error
 End of Function : 01Dec2006, 00:00 Value : 53.0

Volume Units: MM 1000 M3

Measure	Simulated	Observed	Difference	Percent Difference
Volume (MM)	76.06	16.12	59.94	371.81
Peak Flow (M3/S)	162.4	19.8	142.6	720.4
Time of Peak	18Nov2006, 17:00	23Nov2006, 01:00		
Time of Center of Mass	21Nov2006, 23:29	24Nov2006, 10:55		

Figure 106 - Screen Shot of HEC-HMS: Optimization objective function of w150 for Run IC3 after calibration

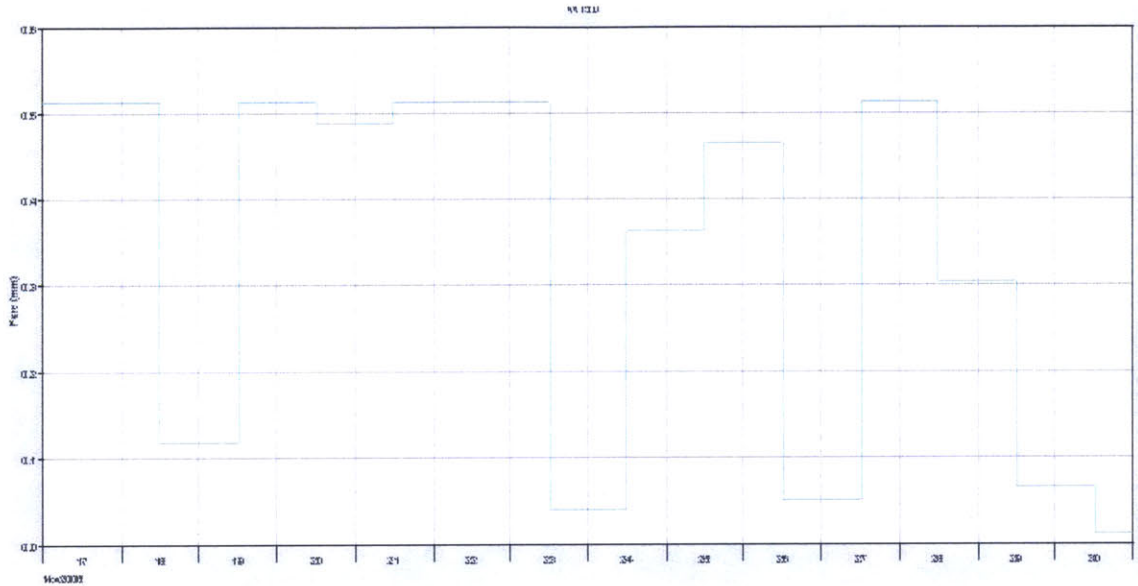


Figure 107 - Screen Shot of HEC-HMS: Soil infiltration of w150 for Run IC3 after calibration

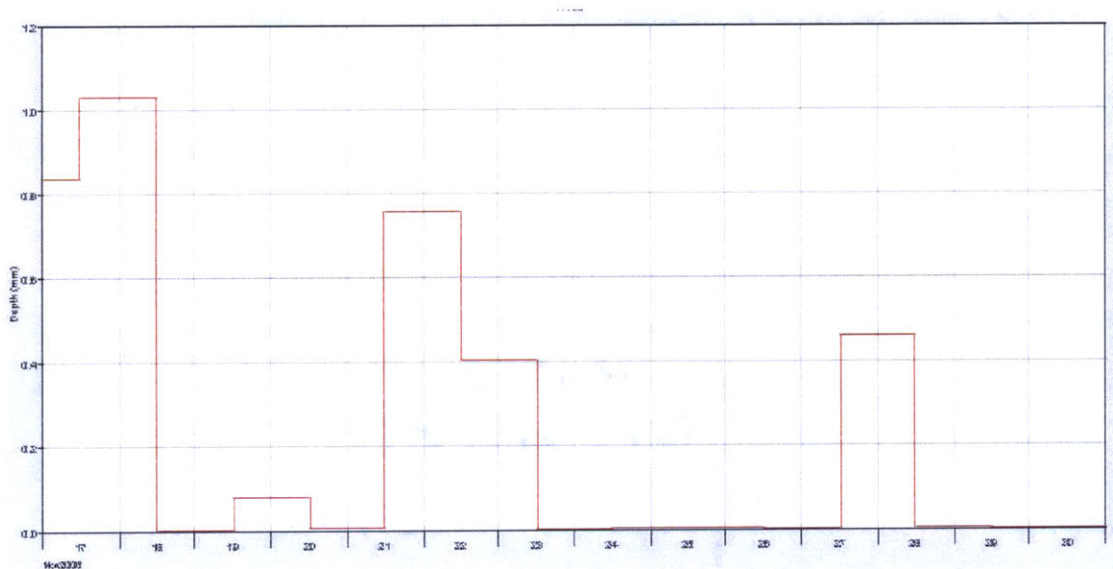


Figure 108 - Screen Shot of HEC-HMS: Excess precipitation of w150 for Run IC3 after calibration

Soil infiltration (Figure 107) shows less correlation with excess precipitation (Figure 108) compared with Run CN3. Flow residuals are largely positive over the simulation period (Figure 109).

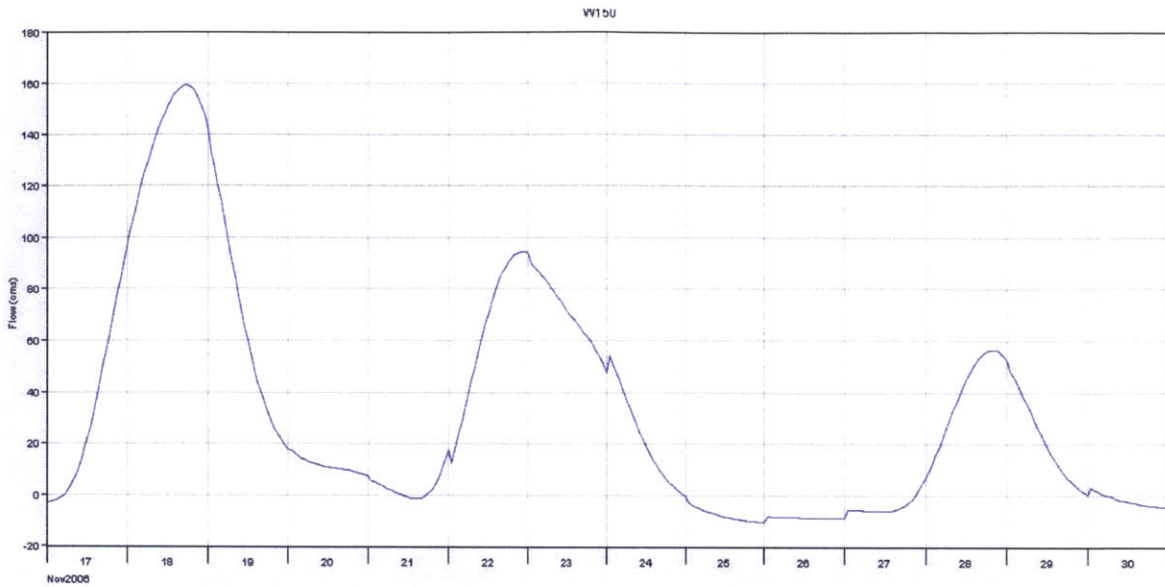


Figure 109 - Screen Shot of HEC-HMS: Flow residual of w150 for Run IC3 after calibration

4.6 Short term simulation – Run4

4.6.1 Run CN4

Run CN4 is the simulation run using curve number loss method over the period between 15 Apr 2008 and 29 Apr 2008. The results for Run CN4 are discussed below.

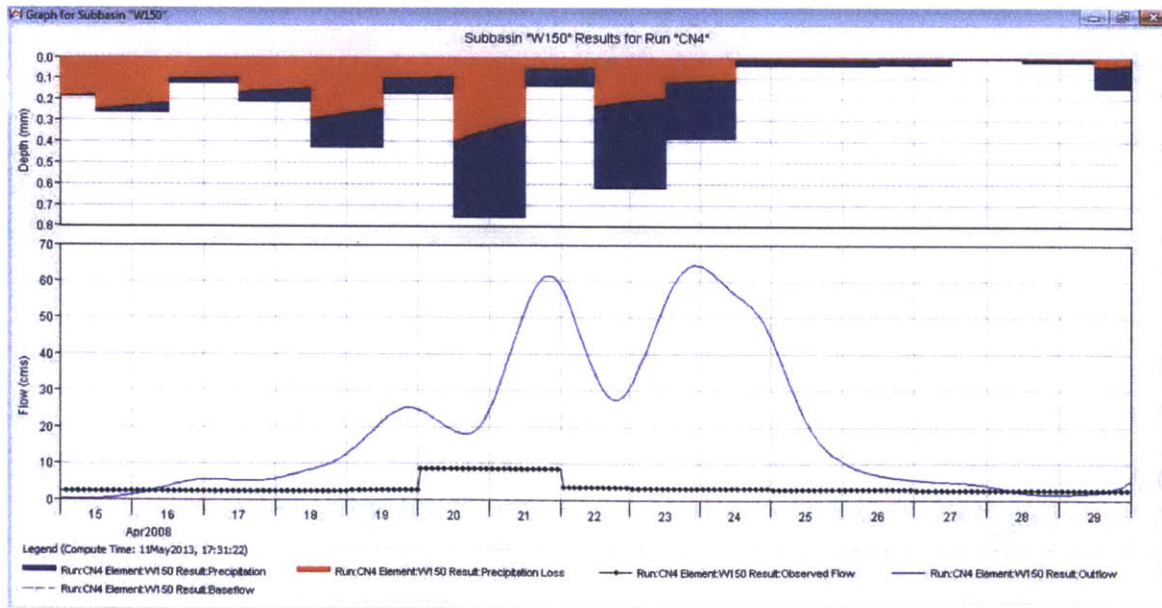


Figure 110 - Screen Shot of HEC-HMS: Flow graph of w150 for Run CN4 before calibration

As shown above in Figure 110, high abstraction is observed in the first days of the simulation. The first rainfall event leads to a calculated runoff much higher than what is observed. In the summary table in Figure 111, the peak discharge is calculated to be 64.4 cms, whereas the observed peak flow is around 8.3 cms.

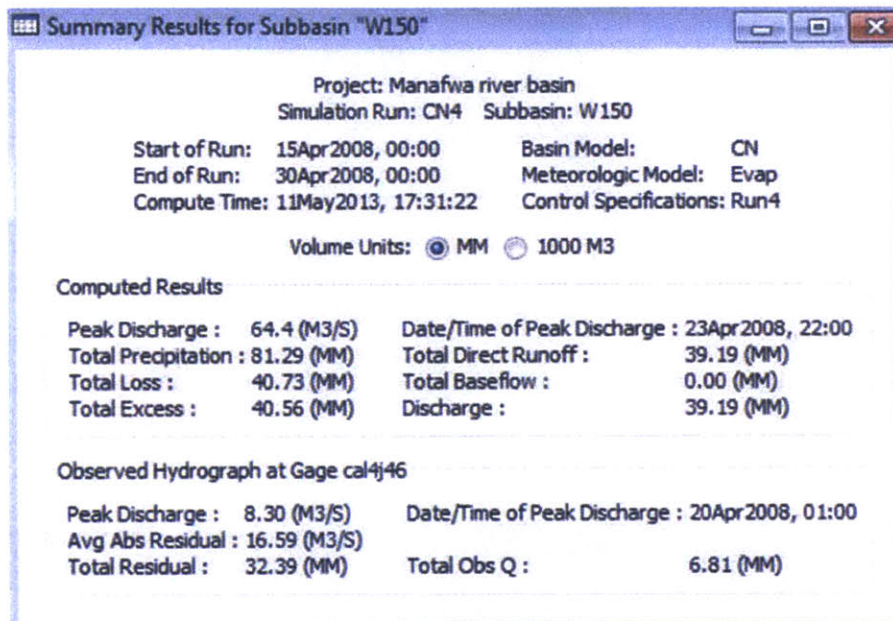


Figure 111 - Screen Shot of HEC-HMS: Summary table of w150 for Run CN4 before calibration

Calibration is carried out with respect to W150 on constant loss rate and lag time. The calibrated flow hydrograph is presented in Figure 112. The comparison between precipitation and observed flow leads again to the necessary scrutiny of the data quality. No comparable discharge is generated during the second rainfall impulse on 23 Apr 2008. There are chances that the variation is masked due to low time resolution of observed flow data. The peak discharge is brought down from 64.4 cms to 21.6 cms (Figure 113), still 160.8% higher than the observed peak flow (Figure 114) after the model calibrates the curve number from 75.3 to 35.294 (Figure 115).

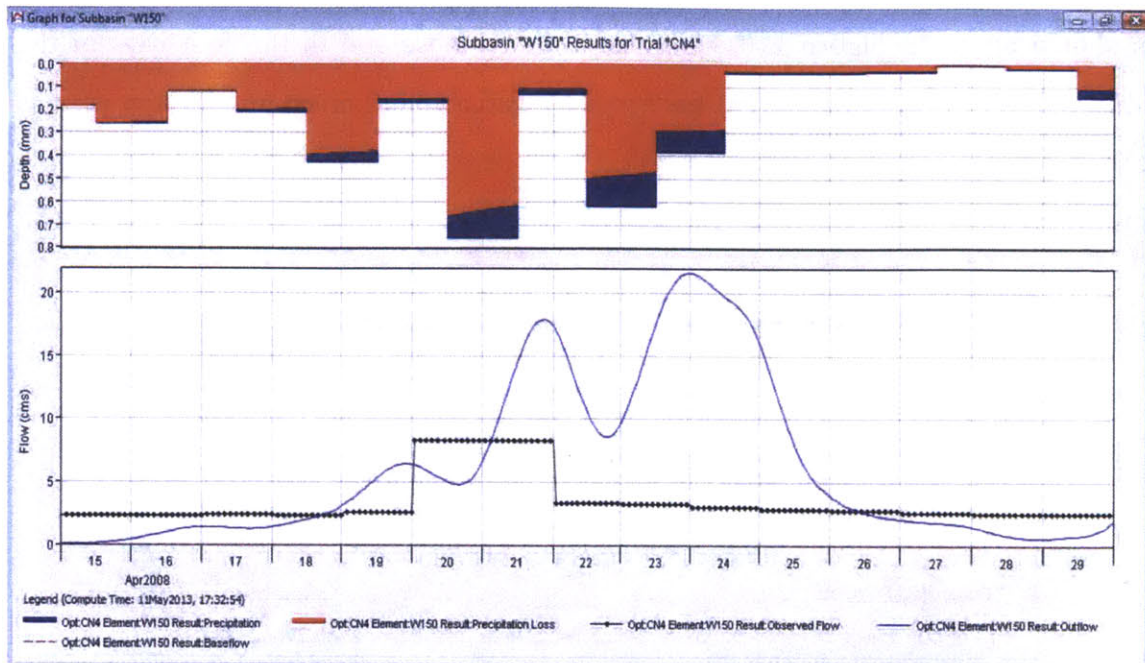


Figure 112 - Screen Shot of HEC-HMS: Flow graph of w150 for Run CN4 after calibration

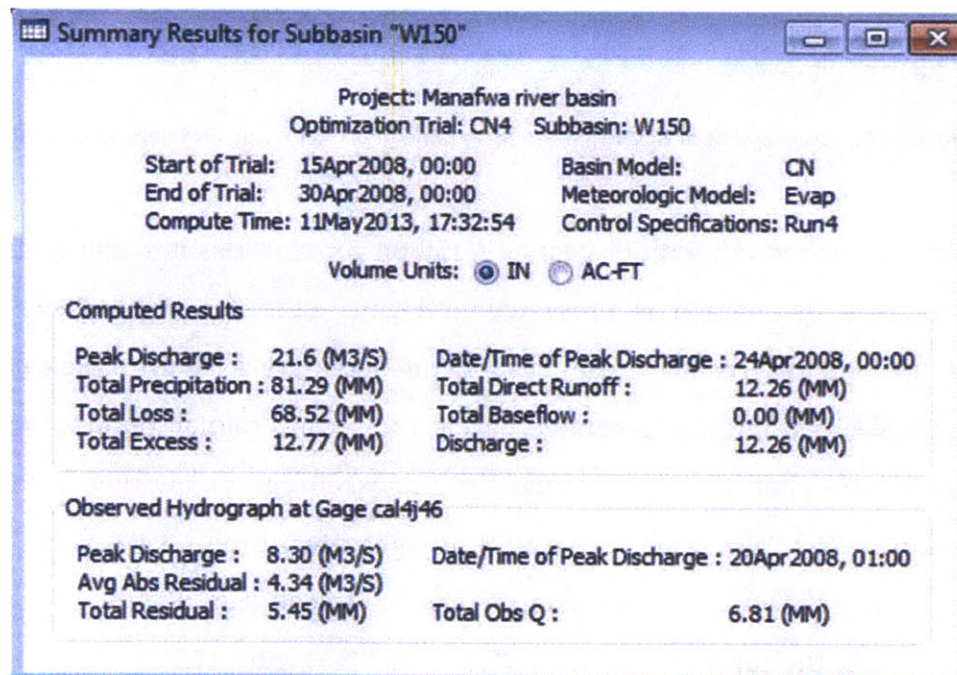


Figure 113 - Screen Shot of HEC-HMS: Summary table of w150 for Run CN4 after calibration

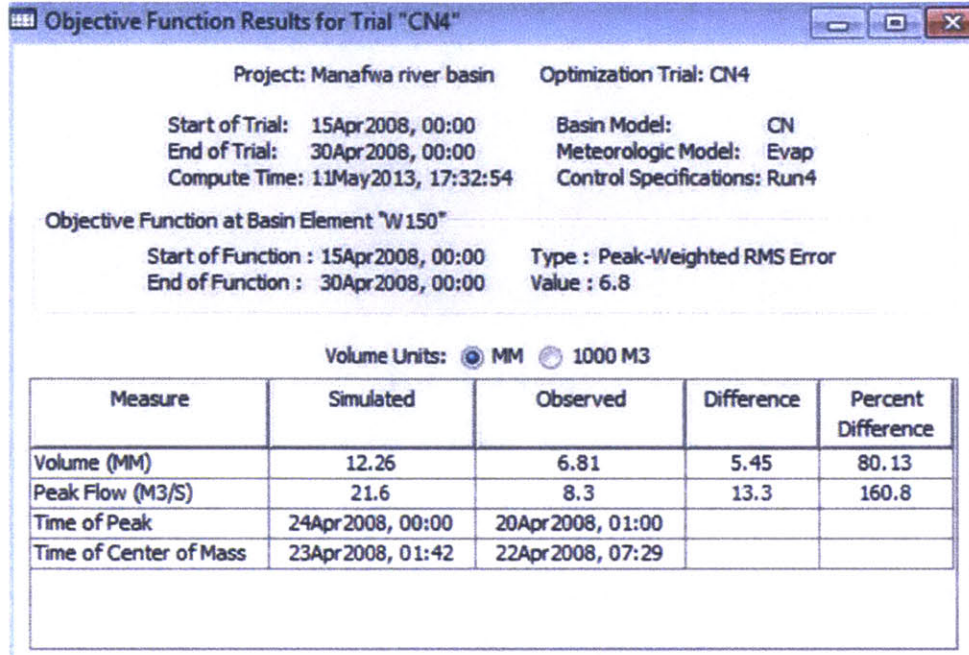


Figure 114 - Screen Shot of HEC-HMS: Objective function of w150 for Run CN4 after calibration

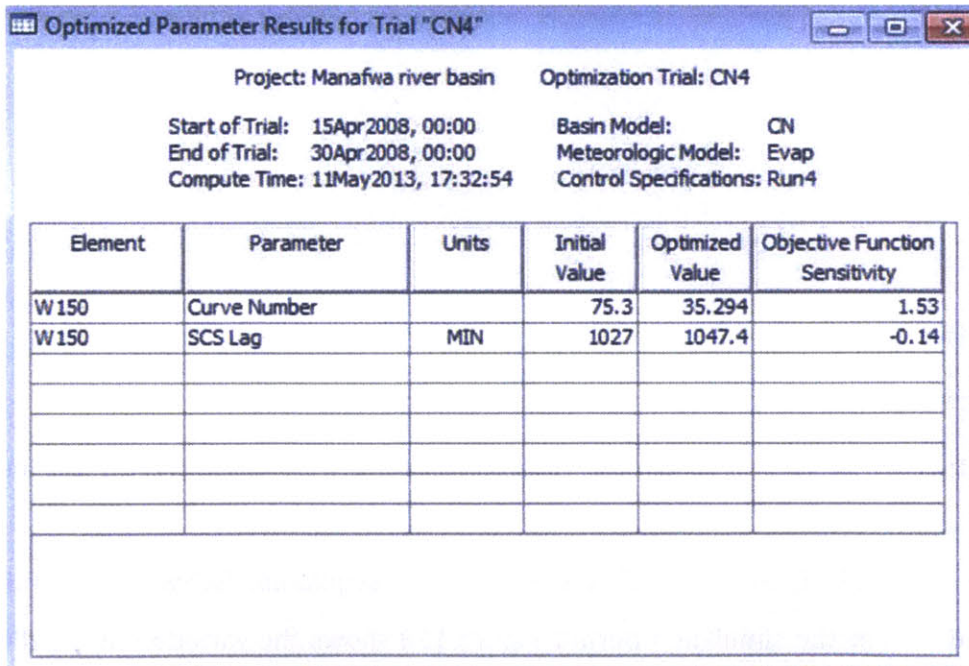


Figure 115 - Screen Shot of HEC-HMS: Optimized parameters of w150 for Run CN4

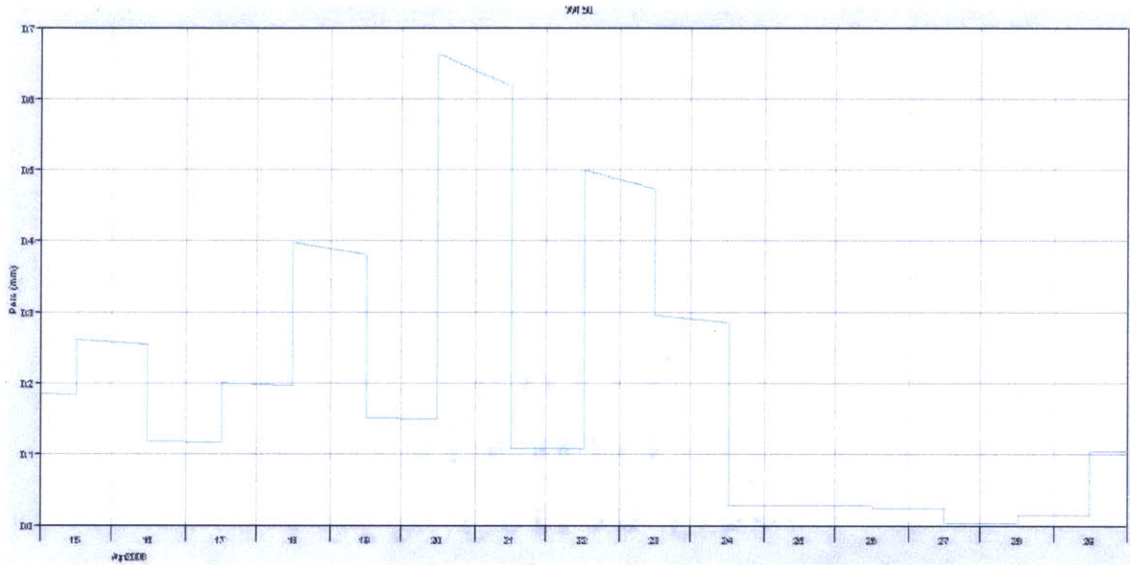


Figure 116 - Screen Shot of HEC-HMS: Soil infiltration of w150 for Run CN4 after calibration

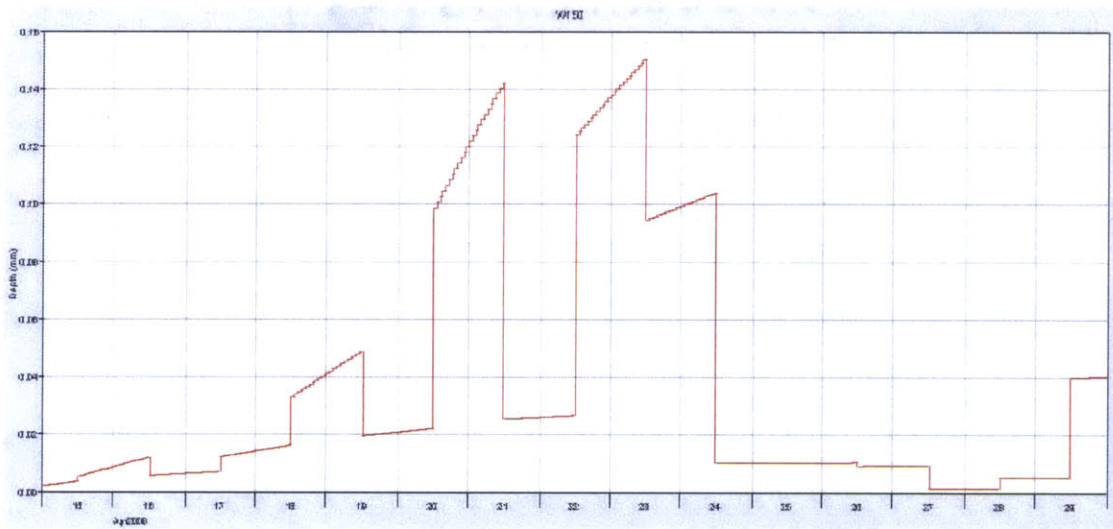


Figure 117 - Screen Shot of HEC-HMS: Excess precipitation of w150 for RunCN4 after calibration

Figure 116 and Figure 117 reflect that excess precipitation follows the trend of soil infiltration over the simulation period. Figure 118 shows the variation in the difference between the calibrated flow and the observed flow. The difference in these two values is largely positive.

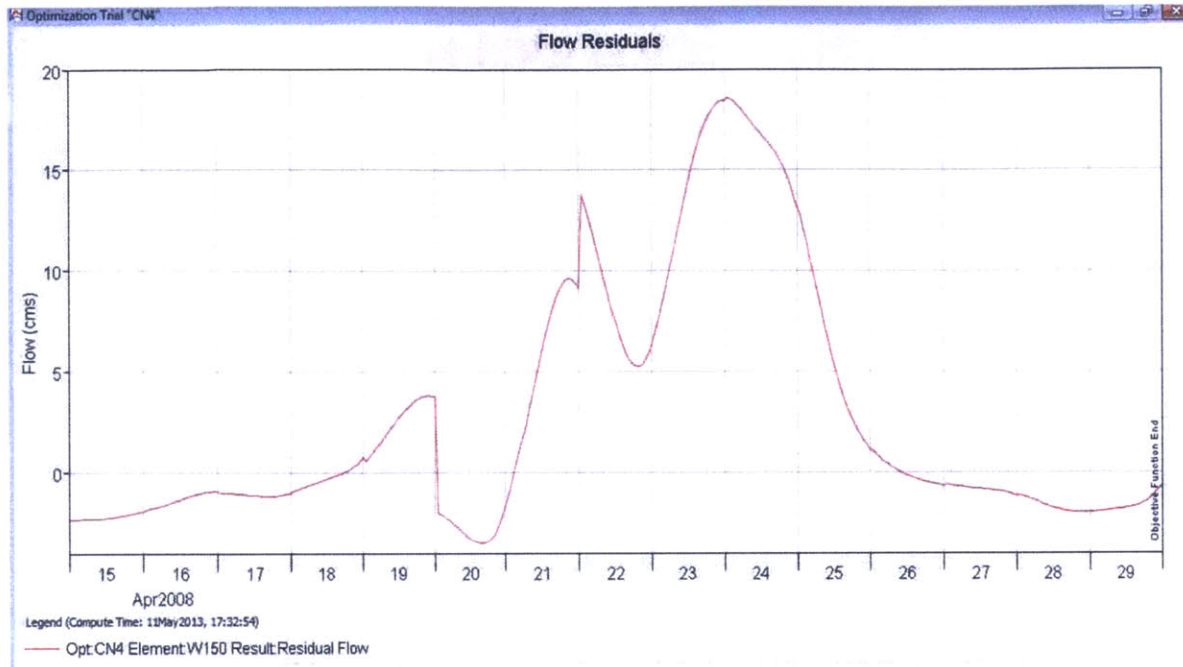


Figure 118 - Screen Shot of HEC-HMS: Flow residual of w150 for Run CN4 after calibration

4.6.2 Run IC4

Run IC4 is the simulation run using initial constant loss method over the period between 15 Apr 2008 and 29 Apr 2008. The simulated flow hydrograph for Run IC4 is shown in Figure 119 below.

An observation consistent with previous ones is that in Run IC4 the second spike of the precipitation on 07 Aug 2006 is not captured. Before calibration, the peak discharge is as high as 36.3 cms, compared with the observed peak flow of 8.3 cms (Figure 120).

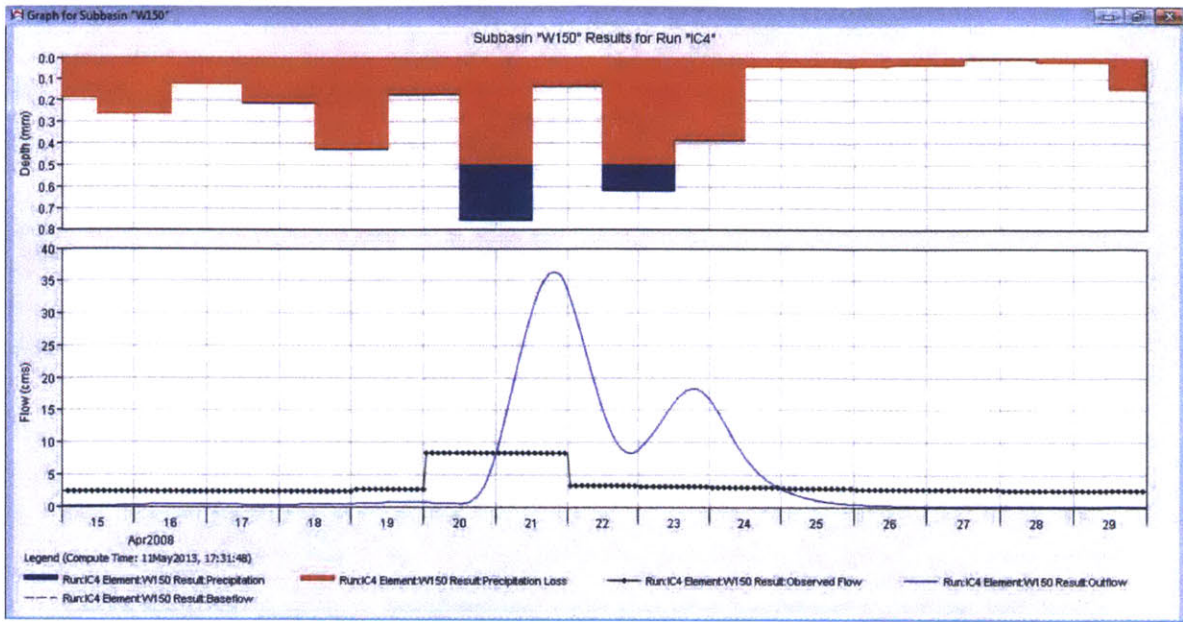


Figure 119 - Screen Shot of HEC-HMS: Flow graph of w150 for Run IC4 before calibration

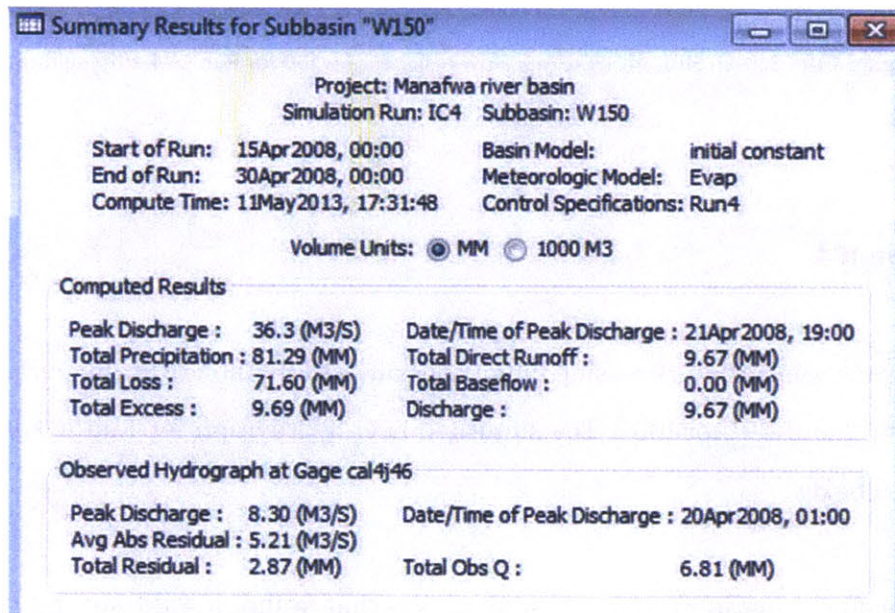


Figure 120 - Screen Shot of HEC-HMS: Summary table of w150 for Run IC4 before calibration

Calibration is carried out with respect to W150 on constant loss rate and lag time. Calibrated flow hydrograph is presented in Figure 121. While the simulated peak flow is lowered to 19.4 cms (Figure 122) the peak flow is still 134.3% higher than observed

value (Figure 123) after the constant loss rate is calibrated from 0.5 mm/hr to 0.62065 mm/hr (Figure 124). In contrast, the discharge volume is 41.58% lower than observed.

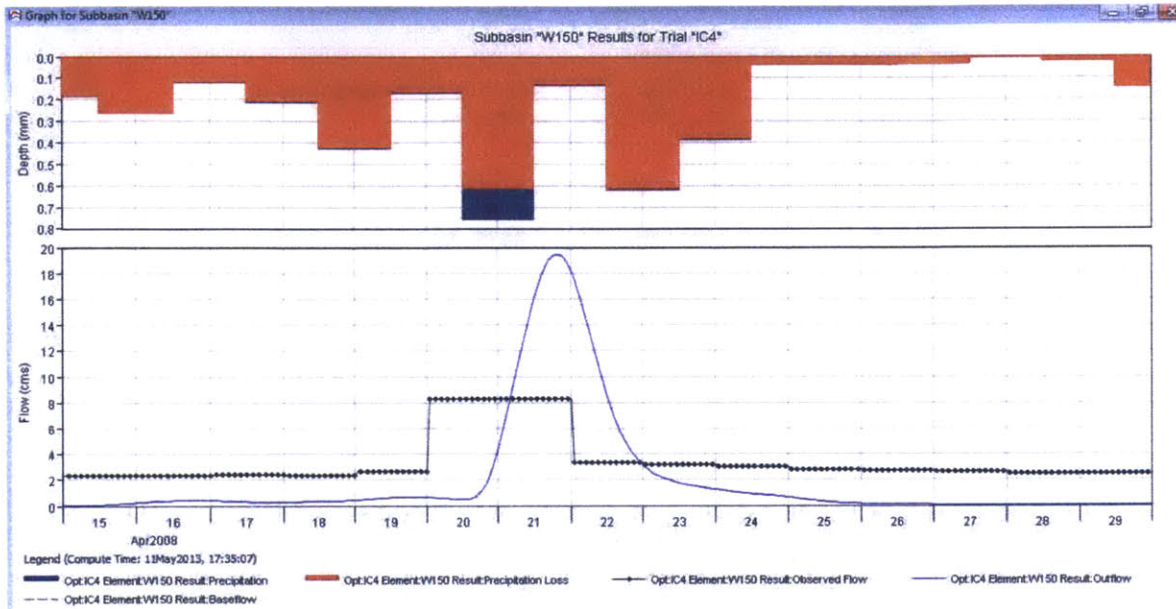


Figure 121 - Screen Shot of HEC-HMS: Flow graph of w150 for Run IC4 after calibration

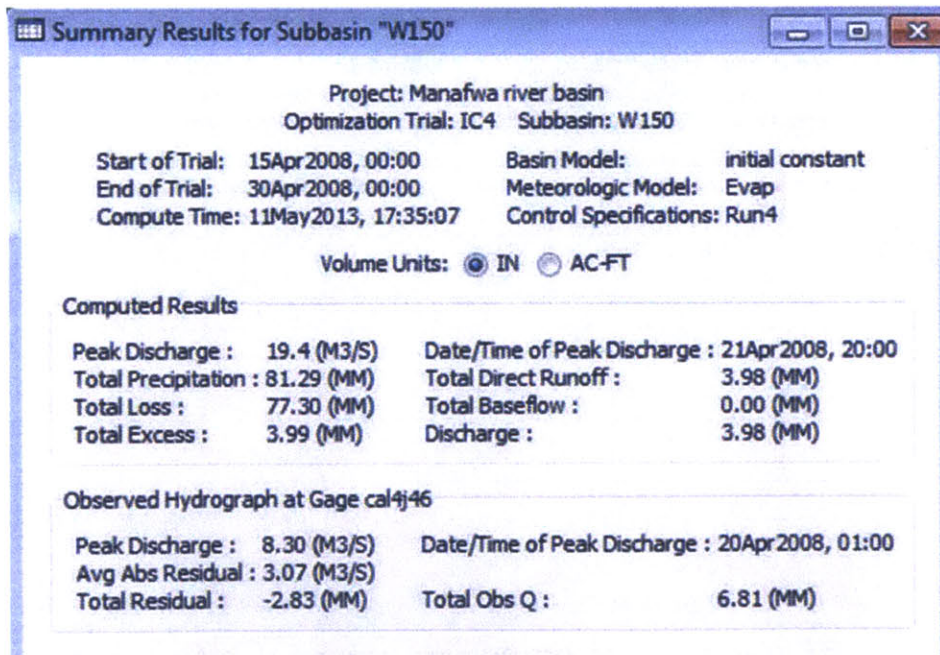


Figure 122 - Screen Shot of HEC-HMS: Summary table of w150 for Run IC3 after calibration

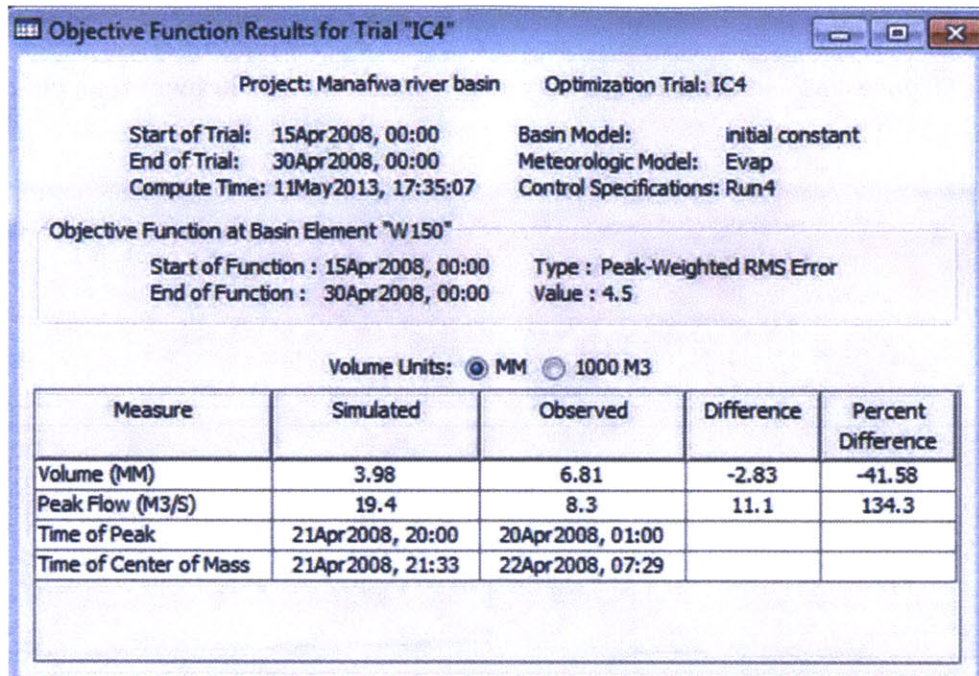


Figure 123 - Screen Shot of HEC-HMS: Objective function of w150 for Run IC3 after calibration

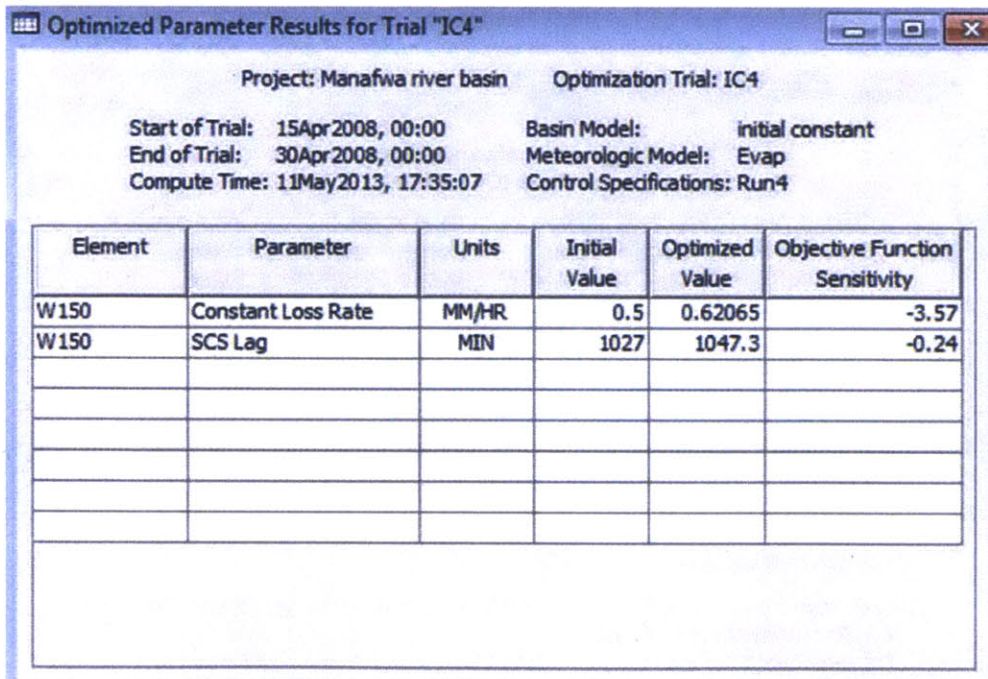


Figure 124 - Screen Shot of HEC-HMS: Optimized parameters of w150 for Run IC4

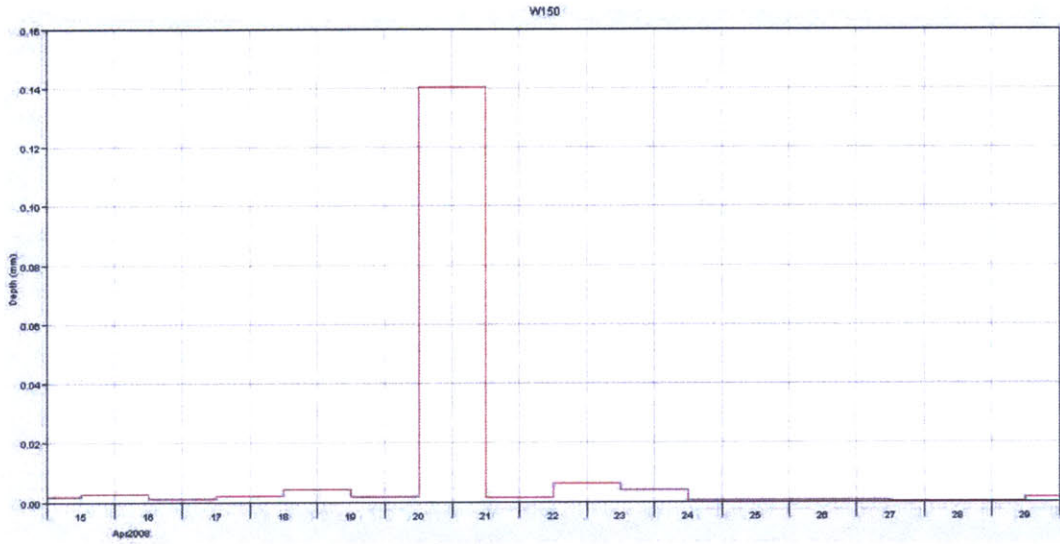


Figure 125 - Screen Shot of HEC-HMS: Excess precipitation of w150 for Run IC3 after calibration

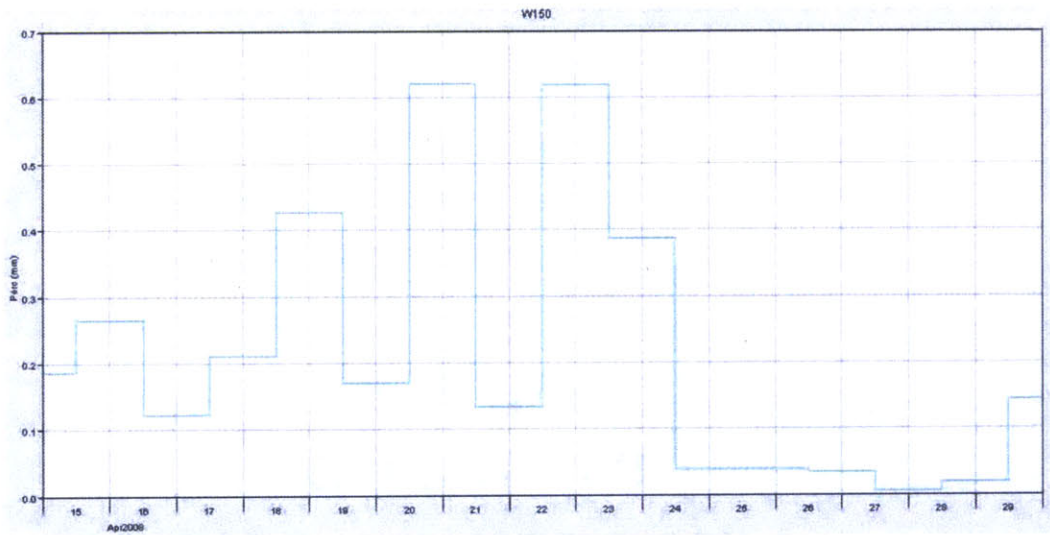


Figure 126 - Screen Shot of HEC-HMS: Soil infiltration of w150 for Run IC3 after calibration

Compared with Run CN4, the excess precipitation (Figure 126) does not mimic the trend of soil infiltration (Figure 125). The simulated flow rate values are mostly below the observed flow values (Figure 127).

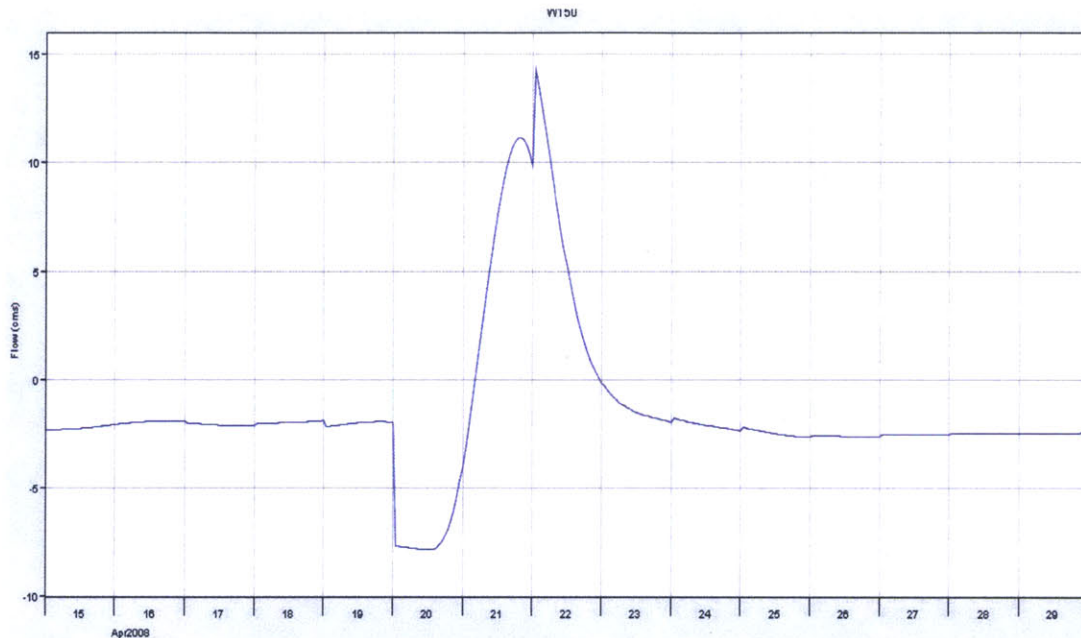


Figure 127 - Screen Shot of HEC-HMS: Flow residual of w150 for Run IC4 after calibration

4.7 Short term simulation - Run5

4.7.1 Run CN5

Run CN5 is the simulation run using curve number method over the period between 25 Jul 2007 and 6 Aug 2007. The flow hydrograph before calibration is shown in Figure 128. The variation in observed flow data is masked by the high values of the simulated flow hydrograph curve. Peak discharge is as high as 69.6 cms (Figure 129).

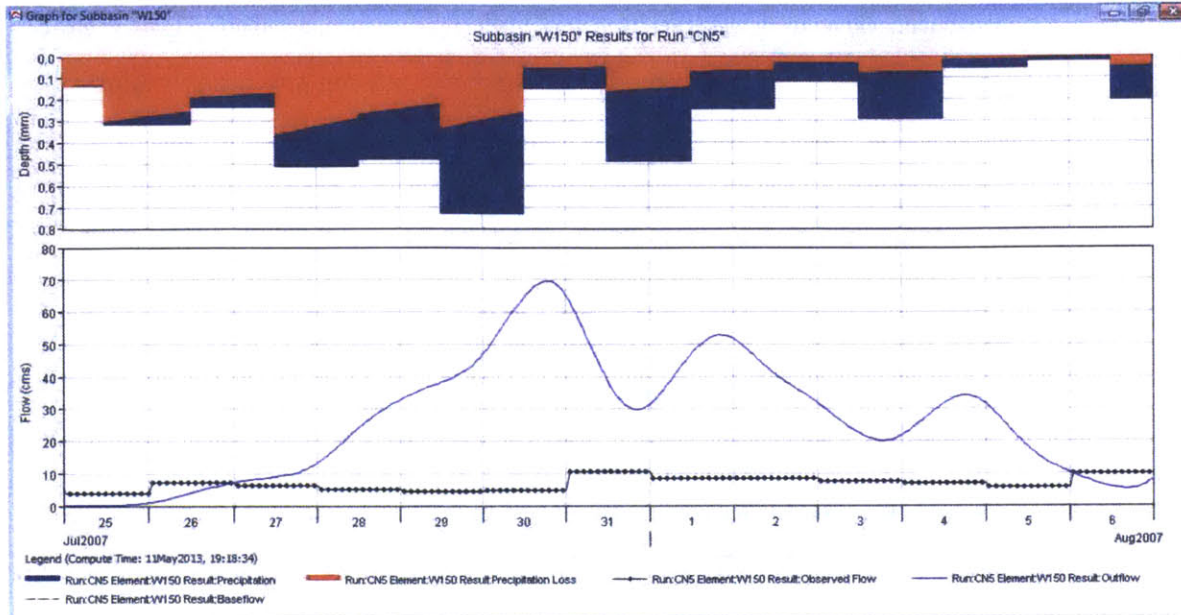


Figure 128 - Screen Shot of HEC-HMS: Flow graph of w150 for Run CN5 before calibration

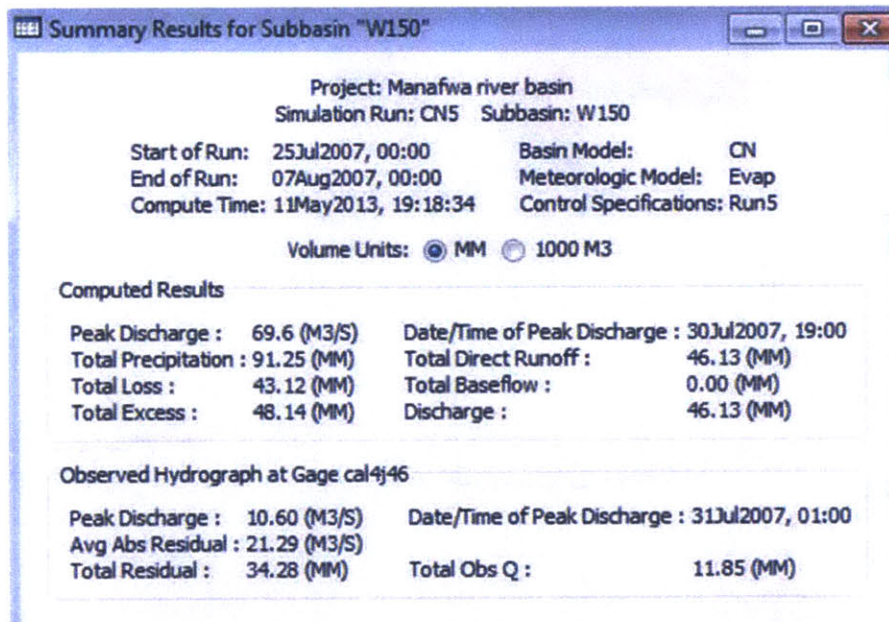


Figure 129 - Screen Shot of HEC-HMS: Summary table of w150 for Run CN5 before calibration

Calibration is carried out with respect to W150 on constant loss rate and lag time. The calibrated flow hydrograph is illustrated below in Figure 130. After calibration it is easier to notice the delay in the observed flow with respect to the precipitation around 30 Aug

2007. The simulated flow hydrograph has two spikes centered around 31 Aug 2007, whereas the observed flow has only one. It is suspected that the low time resolution of the observed flow data masked the flow rate variations in the corresponding days. The actual flow is likely to assume a shape that is similar to what is simulated after calibration.

As total loss is calibrated from 43 mm to 75 mm (Figure 131), the peak discharge drops from 69.6 cms to 21.2 cms, but is still 100% larger than the observed peak of 10.6 cms (Figure 132). The discharge volume drops from 46.13 mm to 14.91 mm as curve number is reduced from 75.3 to 35.294 (Figure 133).

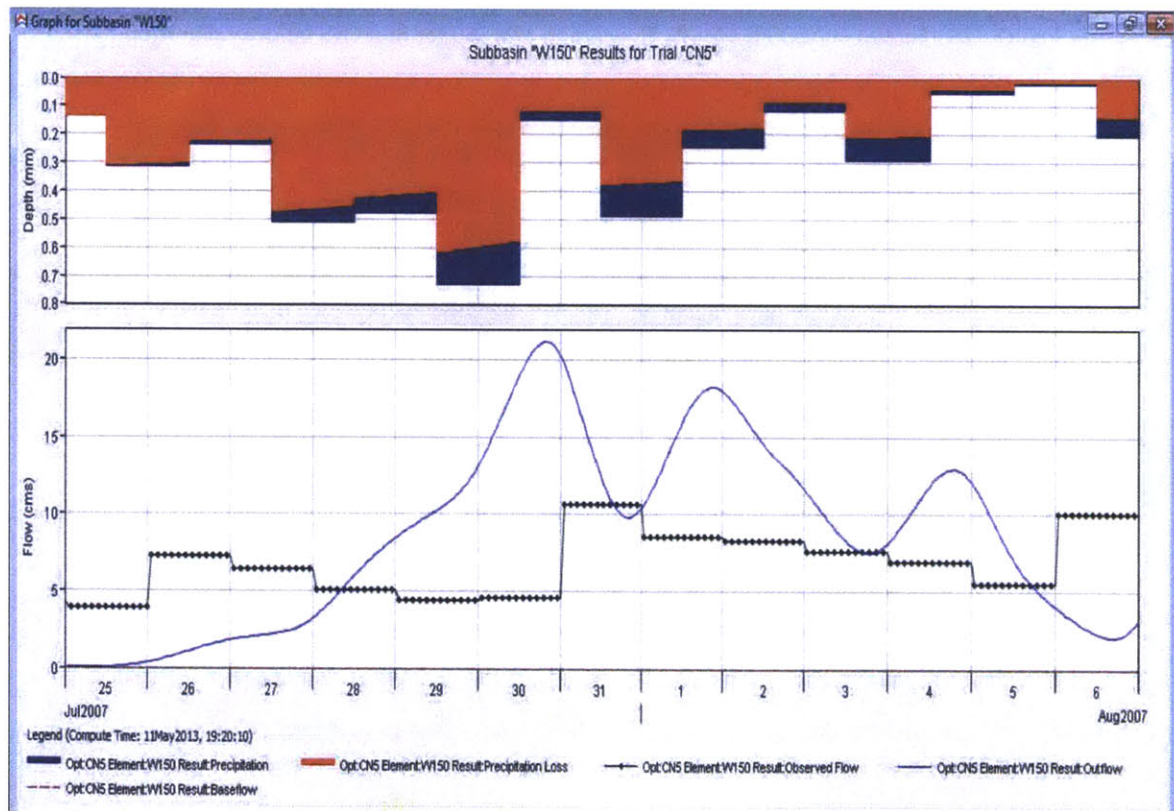


Figure 130 - Screen Shot of HEC-HMS: Flow graph of w150 for Run CN5 after calibration

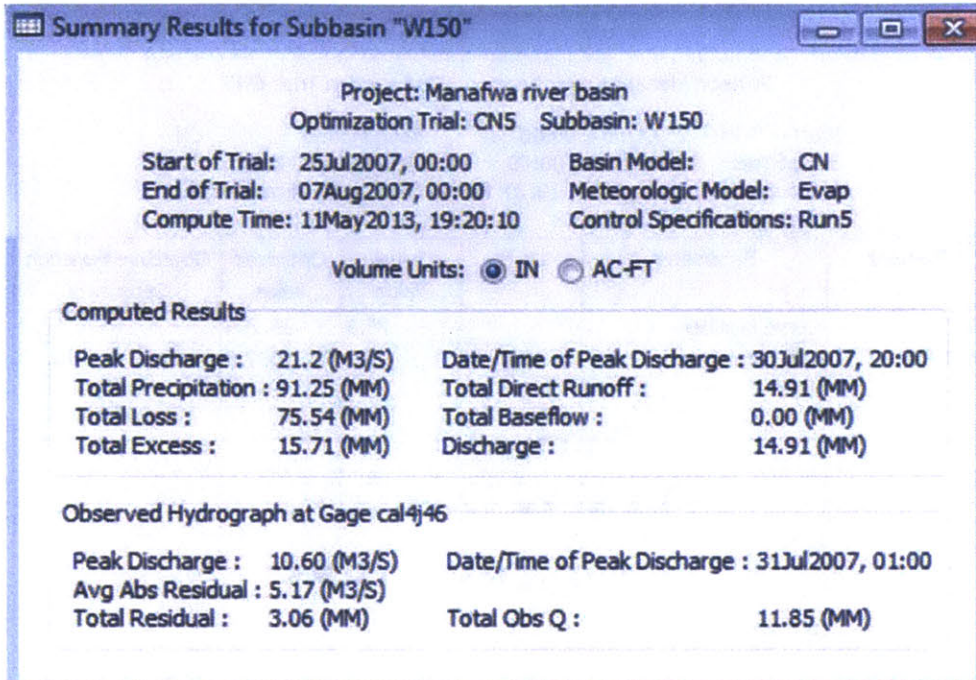


Figure 131 - Screen Shot of HEC-HMS: Summary table of w150 for Run CN5 after calibration

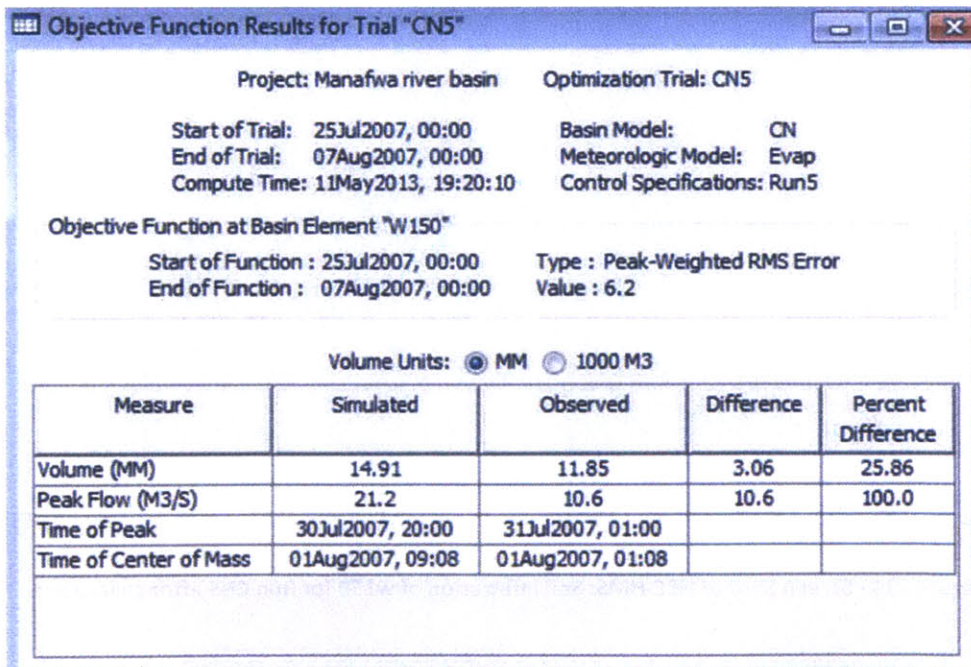


Figure 132 - Screen Shot of HEC-HMS: Objective function of w150 for Run CN5 after calibration

Optimized Parameter Results for Trial "CN5"

Project: Manafwa river basin Optimization Trial: CN5

Start of Trial: 25Jul2007, 00:00 Basin Model: CN
 End of Trial: 07Aug2007, 00:00 Meteorologic Model: Evap
 Compute Time: 11May2013, 19:20:10 Control Specifications: Run5

Element	Parameter	Units	Initial Value	Optimized Value	Objective Function Sensitivity
W150	Curve Number		75.3	35.294	1.54
W150	SCS Lag	MIN	1027	1047.0	-0.23

Figure 133 - Screen Shot of HEC-HMS: Optimized parameters of w150 for Run CN5

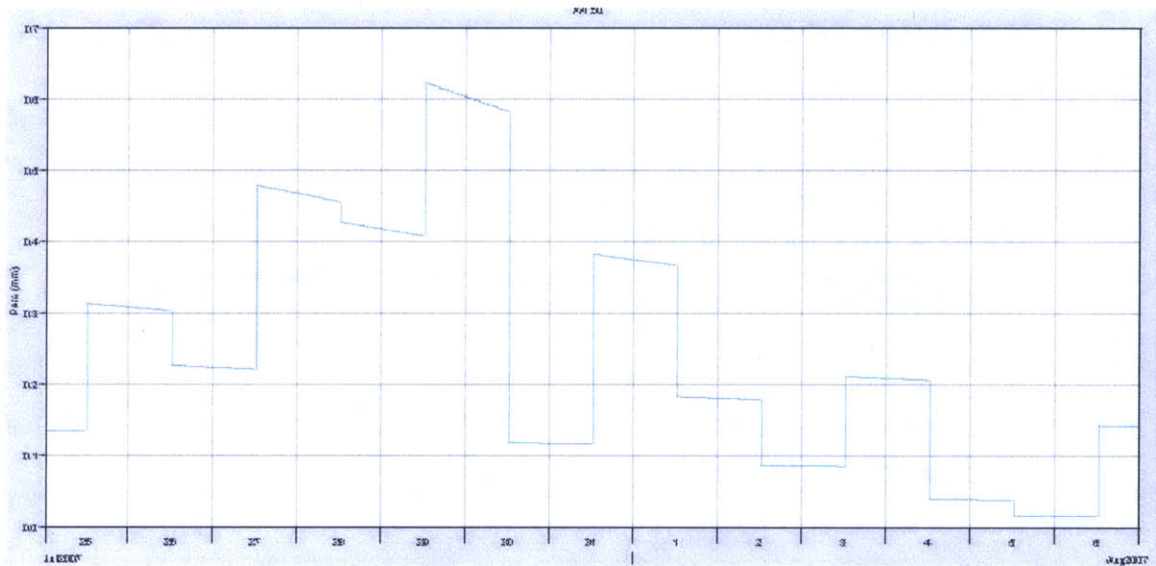


Figure 134 - Screen Shot of HEC-HMS: Soil infiltration of w150 for Run CN5 after calibration

Figure 134 shows soil infiltration of sub-basin w150 after calibration in mm. As the simulation time interval is one hour, soil infiltration is not constant through a single day.

Figure 135 shows the excess precipitation for this run after calibration.

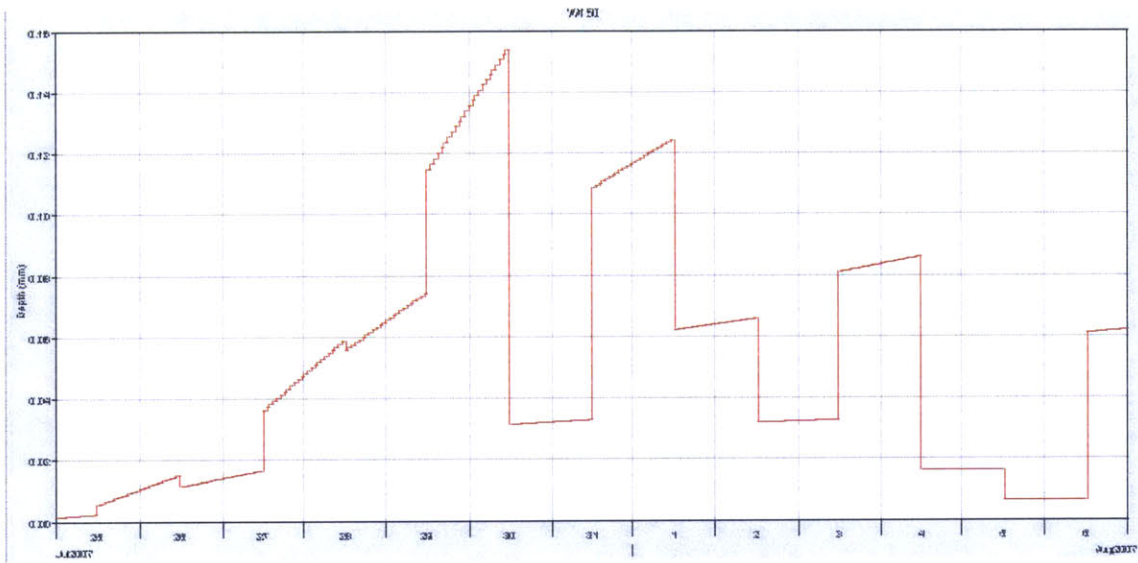


Figure 135 - Screen Shot of HEC-HMS: Excess precipitation of w150 for Run CN5 after calibration

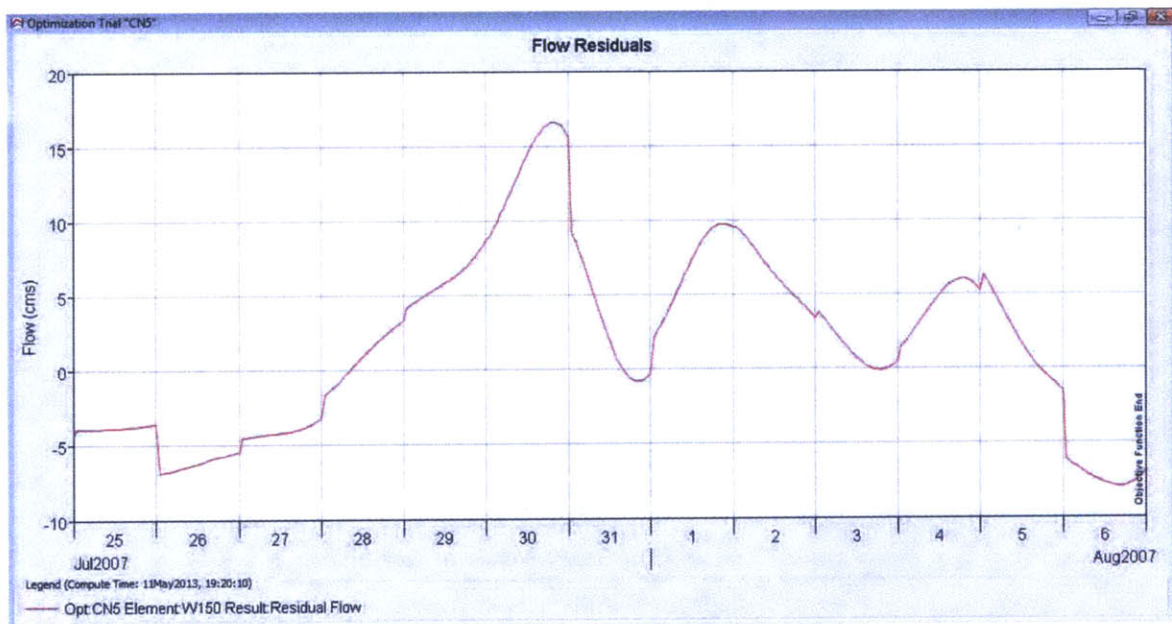


Figure 136 - Screen Shot of HEC-HMS: Flow residual of w150 for Run CN5 after calibration

Figure 136 shows that over most of the simulation time period, the simulated discharge values are higher than the observed flow values (i.e. flow residuals are greater than 0).

4.7.2 Run IC5

Run IC5 is the simulation run using initial constant loss method over the period between 25 Jul 2007 and 6 Aug 2007. The result flow hydrograph before calibration is shown below in Figure 137. The variation in observed flow data is masked by the high values of the simulated flow hydrograph curve. Peak discharge is as high as 33.2 cms compared to the observed peak flow of 10.6 cms (Figure 138).

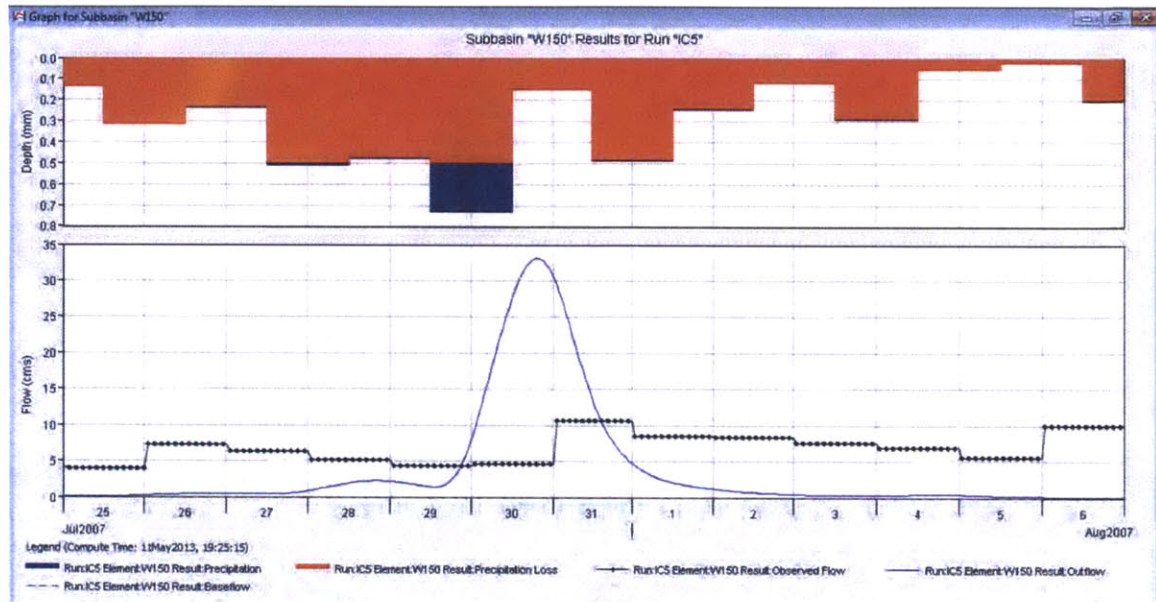


Figure 137 - Screen Shot of HEC-HMS: Flow graph of w150 for Run IC5 before calibration

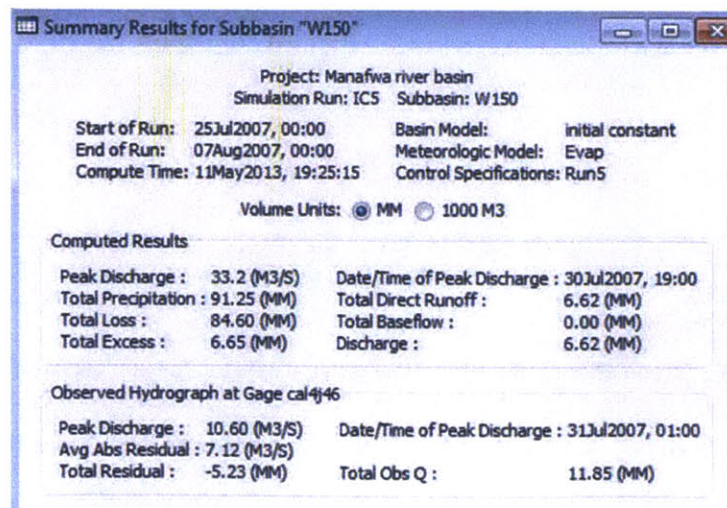


Figure 138 - Screen Shot of HEC-HMS: Summary table of w150 for Run IC5 before calibration

Calibration is carried out with respect to W150 on constant loss rate and lag time. The calibrated flow hydrograph is illustrated below in Figure 139. It is unclear why the flow rate values are calibrated to be much lower than the observed values. As total loss is calibrated from 84.6 mm (Figure 138) to 90.34 mm (Figure 140), the peak discharge drops from 33.2 cms to 1.2 cms, 88.7% lower than the observed peak flow (Figure 141). The discharge volume drops from 6.62 mm to 0.89 mm.

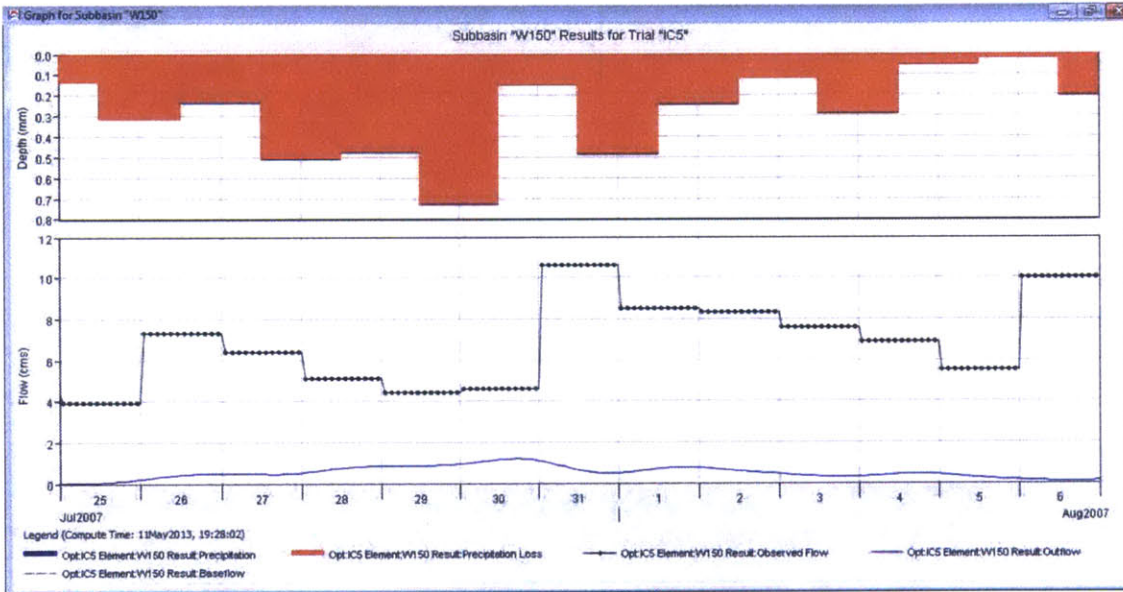


Figure 139 - Screen Shot of HEC-HMS: Flow graph of w150 for Run IC5 after calibration

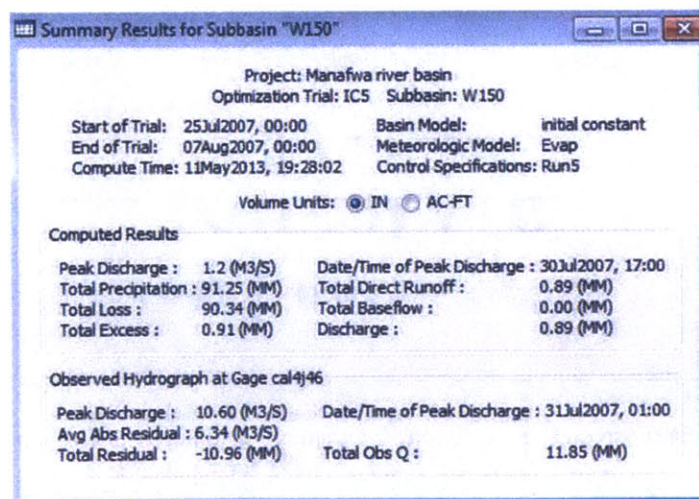


Figure 140 - Screen Shot of HEC-HMS: Summary table of w150 for Run IC5 after calibration

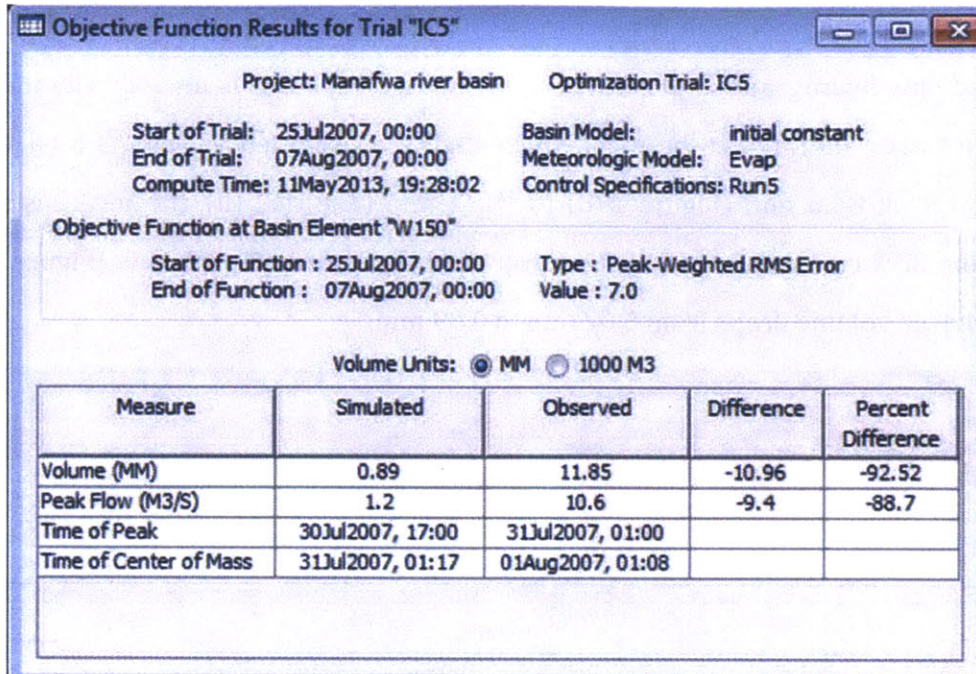


Figure 141 - Screen Shot of HEC-HMS: Objective function of w150 for Run IC5 after calibration

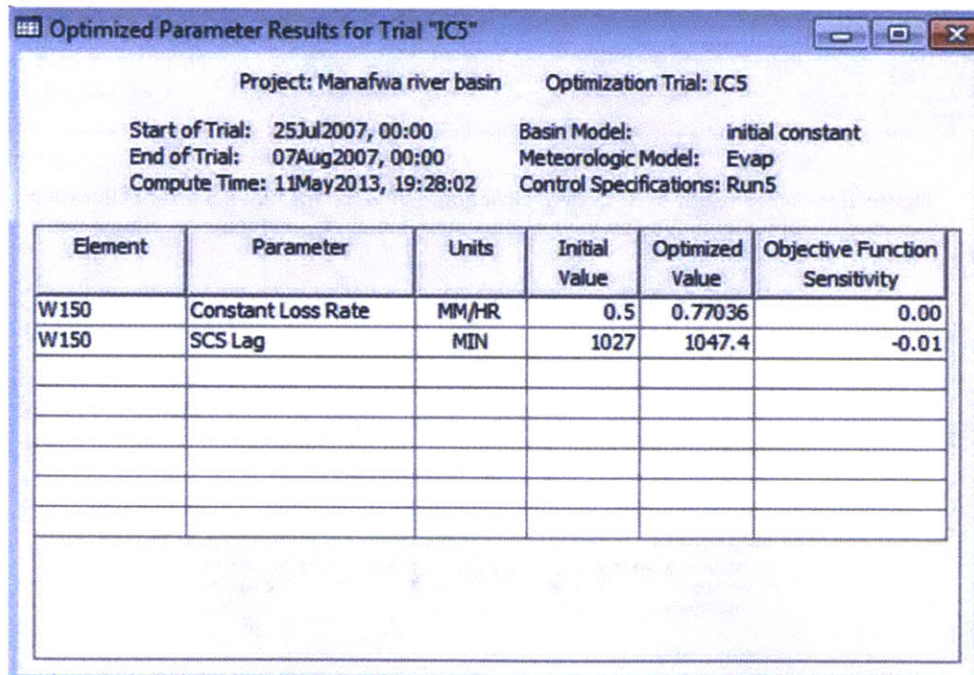


Figure 142 - Screen Shot of HEC-HMS: Optimized parameters of w150 for Run IC5

In Figure 142 above, the constant loss rate is calibrated to 0.77036 mm/hr from 0.5

mm/hr. This is the highest constant loss rate value among the five short term simulations. Flow residual curve shows, the simulated flow rate values are consistently lower than what is observed (Figure 143).

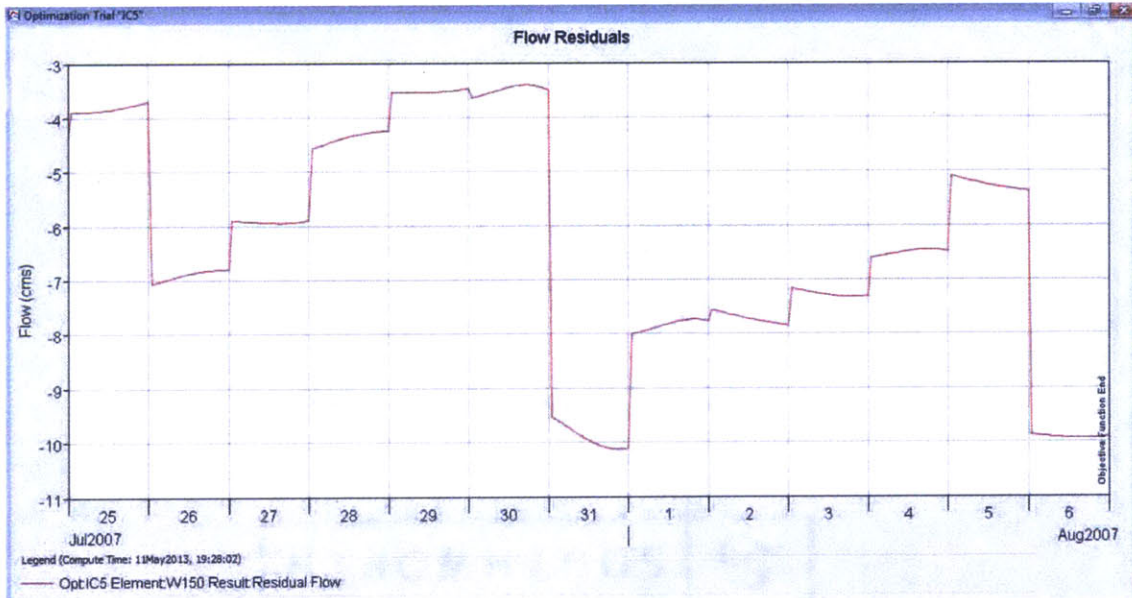


Figure 143 - Screen Shot of HEC-HMS: Flow residual of w150 for Run IC5 after calibration

Soil infiltration (Figure 144) and excess precipitation (Figure 145) resemble each other closely in their trend. Total loss for Run IC5 is greater than Run CN5.

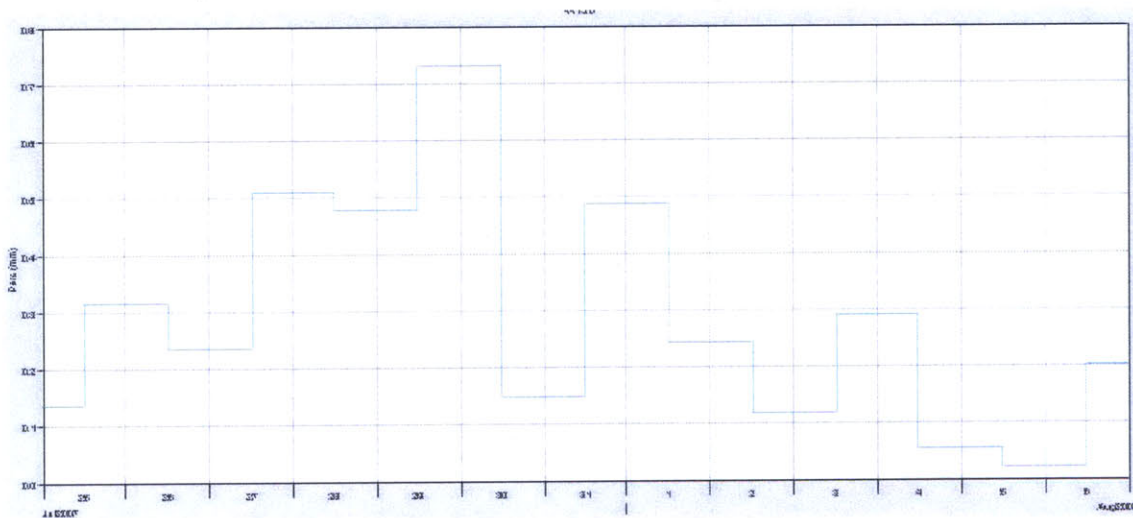


Figure 144 - Screen Shot of HEC-HMS: Soil infiltration of w150 for Run IC5 after calibration

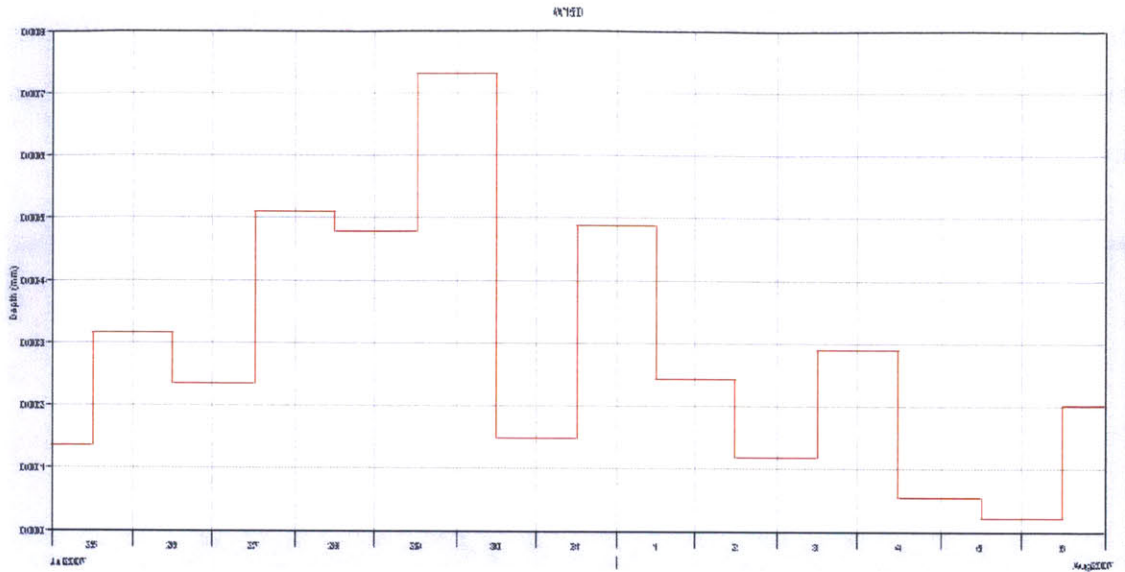


Figure 145 - Screen Shot of HEC-HMS: Excess precipitation of w150 for Run IC5 after calibration

4.8 Results Summary

Optimized values for key parameters are summarized and tabulated below.

Run	Curve Number	SCS Lag (min)
Initial	75.3	1027
CN0	35.9	1047
CN1	48.3	1047
CN2	35.5	1047
CN3	35.3	1564
CN4	35.3	1047
CN5	35.3	1047
Average	37.6	1133.2

Table 12 - Summary of optimized parameter values for Curve Number loss method

Run	constant loss rate (mm/hr)	SCS Lag (min)
Initial	0.5	1027
IC0	0.512	1047
IC1	0.498	1045
IC2	0.403	1828.
IC3	0.513	1047
IC4	0.62	1047
IC5	0.77	1047
Average	0.558	1046.7

Table 13 - Summary of optimized parameter values for Initial and Constant loss method

The curve number values after calibration are averaged to be 37.6, with only CN1 reaching above 40 (Table 12). The CN0 curve number value is higher than the rest of the simulations except for CN1. Therefore the actual average curve number for short term simulations would be slightly lower than 37.6.

In simulations with the Initial and Constant loss method, the calibrated constant loss rate averages 0.558 mm/hr with a maximum of 0.77 mm/hr and a minimum of 0.403 mm/hr (Table 13).

This comparison also indicates that the selection between the two loss method candidates has little effect on the lag time calculation in the Unit Hydrograph transform method.

4.9 Performance Evaluation

To compare the performances of the two loss methods, the difference values of the calibrated result from the observed data are generated and presented below in Table 14.

Parameter	Run 0		Run 1		Run 2	
	CN0	IC0	CN1	IC1	CN2	IC2
Water Volume Difference (%)	850.96	10.53	-2.77	-58.21	13.51	-59.00
Peak Flow Difference (%)	982.70	661.5	14.30	19.00	-4.40	-19
Objective Function Value	43.4	14.7	6.5	8.9	4.7	3.9

Parameter	Run 3		Run 4		Run 5	
	CN3	IC3	CN4	IC4	CN5	IC5
Water Volume Difference (%)	233.66	371.81	80.13	-41.58	25.86	-92.52
Peak Flow Difference (%)	212.90	720.40	160.80	134.30	100.00	-88.70
Objective Function Value	25.6	53	6.8	4.5	6.2	7

Table 14 - Summary values of objective function

Histograms are created below for better visualization.

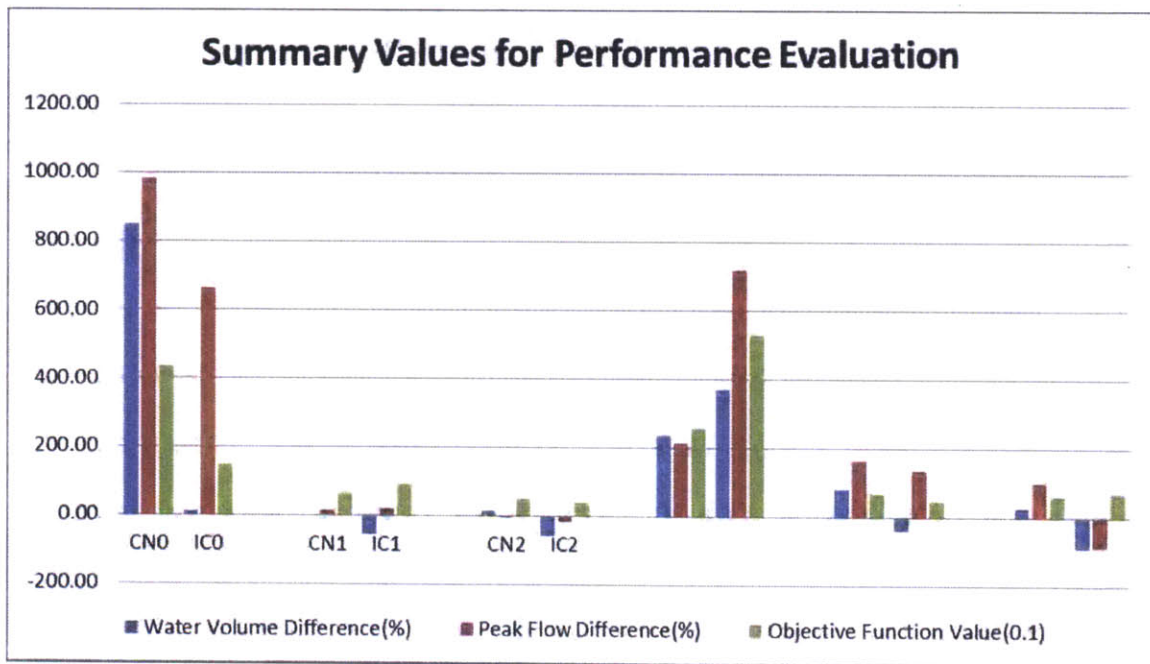


Figure 146 - Summary values histogram for performance evaluation

In Figure 146, it is observed that both of the two loss methods generated significant discrepancies in the magnitude of peak flows in long term simulation, and in some cases for the short-term simulations.

After calibration, the curve number method consistently generated peak flow and water volumes higher than observed, whereas the initial and constant loss method tends to underestimate water volume in short term simulations from what is observed. The former suggests the curve number values have been optimized to the lowest limit. That explains why no further reduction in runoff is observed. Objective function values are presented with a unit of one tenth for better visualization.

To integrate the simulation results for all five short-term simulations, average are taken over the summarized values. However, as the difference percentage values are, in some cases, below zero. A simple average is not ideal in analyzing the mean deviation. Thus root-mean-square (RMS) values are calculated and presented below (Table 15).

$$x_{rms} = \sqrt{\frac{1}{n}(x_1^2 + x_2^2 + \dots + x_n^2)}$$

Parameter	Long Term		Short Term	
	CN	IC	CN	IC
RMS of Water Volume Difference (%)	850.96	10.50	111.24	176.3
RMS of Peak Flow Difference (%)	982.70	663.80	127.60	330.33
RMS of Objective Function Value	43.4	14.8	12.68	24.38

Table 15 - Root-mean-square values for long term and short term simulations

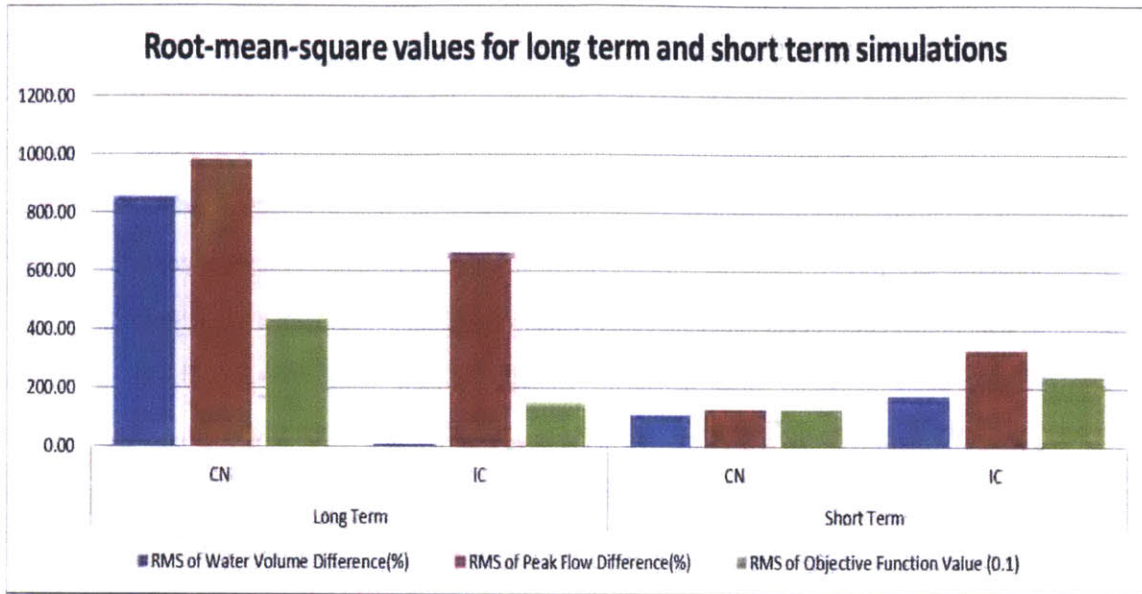


Figure 147 - Root-mean-square values histogram for long term and short term simulations

As is shown in Figure 147 above, the Initial and Constant loss method generated lower RMS values in volume percent difference, peak flow percent difference, and in objective function values, for long term simulations. On the other hand, the Curve Number loss method produced results that are on average closer to observed values in short term simulations. However, the resulting curve number values needed to achieve calibration are not very convincing in the theoretical sense. The RMS values of objective function are presented with a unit of one tenth for better visualization.

5. CONCLUSIONS AND RECOMMENDATIONS

In this work, the hydrological HEC-HMS model and the hydraulic HEC-RAS model are set up for the Manafwa River network of concern. While no HEC-RAS analysis results are presented in this work, the model is ready for preliminary simulations. Given further fine tuning, it should be able to generate flood extent visuals that are helpful in flood warning and control planning.

At the heart of the flood modeling effort is the reliability of HEC-HMS in generating accurate runoff hydrographs from the watershed. It is reinforced that loss methods and transform methods play vital roles in modeling the relationship between upstream precipitation and downstream runoff. Two widely used loss methods are investigated; their parameters are technically estimated at the start of the simulations and are auto-calibrated through the HEC-HMS optimization function.

While significant errors persist for both methods, it could be established that the Curve Number method is able to better model the precipitation-runoff processes in short term simulations. This is partly attributed to its ability to take into account precedent precipitation. In contrast, the Initial and Constant loss method tends to misrepresent successive rainfall events. However, the calibrated results with the Curve Number method relies on extremely low curve number values. The documented curve number values should be referred to and their validity be further evaluated before substantial improvements are made in water loss calculation.

Neither of the methods demonstrated reliable capability in simulating long-term rainfall-runoff processes. It is observed in corresponding simulations with the Curve Number method that soil infiltration is limited by a ceiling value. As a result, in long term simulations, the Curve Number method is likely to overestimate the runoff magnitude.

The selection between the two loss method candidates has little effect on the lag time calculation in the Unit Hydrograph transform method.

Improvements could be made to both the hydrological model and the site-specific data acquired. For instance, the values of estimated curve numbers could be validated. More understanding is needed regarding the applicability of the method to make educated assessments on discrepancies that arise from the simulations.

In this work, baseflow was not considered. Consequently, there is consistent deviation in the results at low flow rates from the observed values. While this is not of primary concern towards the main objective of predicting flood events, it actually affects the magnitude of the peak runoff that is being estimated. HEC-HMS has an array of baseflow modeling method options. Significant impacts are expected to be made on the accuracy of the resulting hydrograph once they are thoroughly considered.

The amount of conclusions that are reached could be improved with a larger quantity and higher quality of flow rate data. The equations used to transform measured flow depth to flow rate in the Manafwa River are also subject to further betterment.

REFERENCES

- HEC-1 & HEC-HMS. (1999). Retrieved from SCWA Hydrology:
<https://www.google.com/url?sa=t&rct=j&q=&esrc=s&source=web&cd=4&cad=rja&ved=0CE0QFjAD&url=http%3A%2F%2Fwww.scwa2.com%2Fdocuments%2FHydrology%2520Manual%2520for%2520Web%2520Page%2FChapter%25203.4%2520HEC-q%2520%26%2520HEC-HMS.pdf&ei=22iEUYhB58bQAe3VgfgM&us>
- Bingwa, F. (2013). *A quantitative analysis of the impact of land use changes on floods in the Manafwa River Basin, Master Thesis*. Massachusetts Institute of Technology.
- Boucher, M. (2011). *HEC-HMS Guidance for the Contra Costa County Flood Control & Water Conservation District Unit Hydrograph Method*.
- Bras, R. L. (1990). *Hydrology An Introduction to Hydrologic Science*. Addison Wesley Publishing Company.
- Cecinati, F. (2013). *Precipitation Analysis for a Flood Early Warning System in the Manafwa River Basin, Uganda, Master Degree Thesis*. Massachusetts Institute of Technology.
- Centre for Ecology & Hydrology. (n.d.). *Evaporation in Average Year*. Retrieved from Watch Water and Global Change:
<http://www.waterandclimatechange.eu/evaporation/average-monthly-1985-1999>
- Chang, C.-w. (2009). Application of SCS CN method in HEC-HMS in ShihMen Watershed - Simulation of Rainfall-Runoff Hydrologic Model. *Master Thesis, Florida State University*.
- City and County of Sacramento. (1996, 12). *Drainage Manual Volume2:Hydrology Standards Chapter 7 Basin Lag*. Retrieved from
http://www.msa2.saccounty.net/dwr/DrainageManual_Volume2/V2_Chap07.PDF
- Dagg, M., Woodhead, T., & Rijks, D. A. (1970). Evaporation in East Africa. *Bulletin of the International Association of Scientific Hydrology, XV, 1*.
- Fennessey, L. A., & Hawkins, R. H. (2001). The NRCS Curve Number, a New Look at an Old Tool. *2001 Pennsylvania Stormwater Management Symposium*. Villanova University.
- Fennessey, L., Hamlett, J., & Miller, A. (2001). The Effect of Inflection Angle and Relative Location on Runoff Curve Numbers from Zero-Order Watersheds. In *Urban Drainage Modeling* (pp. 494-506). doi: 10.1061/40583(275)47 .
- Hydrologic Engineering Center. (2000, 3). Technical Reference Manual. *Hydrologic Modeling System HEC-HMS*.
- Hydrologic Engineering Center. (2005). HEC-HMS User Manual . *Hydrologic Modeling System*.

- Loukas, A., & Quick, M. C. (1996, 2). Physically-based estimation of lag time for .
Hydrological Sciences -Journal- des Sciences Hydrologiques, 41(1).
- Merwade, V. (2012). *Hydrologic Modeling Using HEC-HMS*. Purdue University.
- NASA EOSDIS, (n.d.), *Reverb*. url:
http://reverb.echo.nasa.gov/reverb/#utf8=%E2%9C%93&spatial_map=satellite&spatial_type=rectangle
- National Resources Conservation Service. (2004, 7). *Part630 Hydrology Chapter10 Estimation of Direct Runoff from Storm Rainfall*. Retrieved from National Engineering Handbook Hydrology :
<ftp://ftp.wcc.nrcs.usda.gov/wntsc/H&H/NEHhydrology/ch10.pdf>
- Natural Resources Management and Environment Department. (n.d.). *Crop Evapotranspiration - Guidelines for Computing Crop Water Requirements*. Retrieved from FAO Coporate Document Respository:
http://www.fao.org/docrep/X0490E/x0490e0b.htm#tabulated_kc_values
- Patel, K. P. (2009). Watershed modeling using HEC-RAS, HEC-HMS, and GIS models - A case study of the Wreck Pond Brook watershed in Monmouth. *PhD Thesis, State University of New Jersey*.
- Stantec consulting Inc. (2009). *Technical Documentation for use of HEC-HMS with the Development Process Manual*.
- The Shodor Education Foundation, Inc. (1998). *Algorithm: The Mathematics of Surface Water Runoff*. Retrieved from
<http://www.shodor.org/Master/environmental/water/runoff/RunoffAlgorithm.html>
- US Army Corp of Engineers. (2008, 3). Hydraulic Reference Manual Version4.0. *HEC-RAS River Analysis System*.
- US Army Corp of Engineers. (2009, 9). User's Manual. *HEC-GeoRAS GIS Tools for Support of HEC-RAS using ArcGIS*.
- US Army Corp of Engineers. (n.d.). *HEC-HMS*. Retrieved from
<http://www.hec.usace.army.mil/software/hec-hms/>
- Walton, R. (2013, 4). *HEC-RAS for managers*. Retrieved from
https://www.google.com/url?sa=t&rct=j&q=&esrc=s&source=web&cd=5&ved=0CF1QFjAE&url=http%3A%2F%2Fdownloads.jecregistration.com%2F2011_RAS_for_Managers_11-22.ppt&ei=DUZgUYbvA4bh0wHn44DQCg&usg=AFQjCNEJMUeWX81kfiXXiScmabzO_TaKw&sig2=FTOFreD7T-mKPWRZk_DO9w&bvm

APPENDIX

Appendix A- Weighted Average Rainfall during the Year 2006 in Each Sub-basin

Date	Sub-basin (mm)										
	SB120	SB130	SB140	SB150	SB160	SB170	SB180	SB190	SB200	SB210	SB220
2006/1/1	0.41	0.36	0.36	0.82	1.63	1.72	1.20	0.75	1.37	0.73	0.68
2006/1/2	0.14	0.47	0.30	1.01	0.48	0.36	0.73	1.04	0.61	1.31	1.09
2006/1/3	0.08	0.21	0.07	0.37	0.00	0.00	0.25	0.46	0.16	0.43	0.49
2006/1/4	0.04	0.08	0.11	0.52	1.52	1.74	0.96	0.29	1.22	0.73	0.19
2006/1/5	0.27	0.25	0.08	1.30	0.00	0.00	0.29	0.54	0.19	1.54	0.58
2006/1/6	0.42	0.21	0.07	1.14	0.00	0.00	0.25	0.46	0.16	1.09	0.49
2006/1/7	0.41	0.23	0.15	1.32	0.00	0.00	0.19	0.35	0.12	1.49	0.37
2006/1/8	0.10	0.08	0.03	0.54	0.00	0.00	0.09	0.17	0.06	0.66	0.19
2006/1/9	0.09	0.00	0.00	0.43	0.00	0.00	0.00	0.00	0.00	0.51	0.00
2006/1/10	0.08	0.00	0.00	0.48	0.00	0.00	0.00	0.00	0.00	0.60	0.00
2006/1/11	0.45	0.88	0.57	1.70	1.46	1.47	1.66	1.83	1.60	2.02	1.86
2006/1/12	12.69	11.80	13.51	5.23	4.74	4.30	4.95	5.52	4.73	5.27	5.61
2006/1/13	1.90	2.00	2.83	0.37	4.69	4.70	2.78	1.12	3.42	0.56	0.87
2006/1/14	0.21	0.00	0.01	0.56	0.18	0.20	0.10	0.01	0.14	0.52	0.00
2006/1/15	0.05	0.00	0.77	0.22	13.07	14.83	7.42	0.99	9.89	0.26	0.00
2006/1/16	3.66	5.01	4.43	3.58	4.60	4.86	5.39	5.85	5.21	4.21	5.92
2006/1/17	0.00	0.42	0.16	0.32	0.42	0.47	0.72	0.94	0.64	0.48	0.97
2006/1/18	0.00	0.00	0.00	0.19	0.00	0.00	0.00	0.00	0.00	0.29	0.00
2006/1/19	0.22	0.00	0.00	0.58	0.00	0.00	0.00	0.00	0.00	0.55	0.00
2006/1/20	0.12	0.56	0.19	1.44	0.00	0.00	0.65	1.21	0.43	1.97	1.30
2006/1/21	0.47	0.00	0.00	0.85	0.00	0.00	0.00	0.00	0.00	0.58	0.00
2006/1/22	0.47	0.12	0.04	1.32	0.00	0.00	0.14	0.27	0.10	1.28	0.29
2006/1/23	0.17	0.00	0.00	0.65	0.00	0.00	0.00	0.00	0.00	0.72	0.00
2006/1/24	0.26	0.00	0.00	0.86	0.00	0.00	0.00	0.00	0.00	0.90	0.00
2006/1/25	0.32	0.00	0.00	0.68	0.00	0.00	0.00	0.00	0.00	0.55	0.00
2006/1/26	0.18	0.19	0.06	0.72	0.00	0.00	0.22	0.40	0.14	0.80	0.43
2006/1/27	0.51	0.47	0.16	1.76	0.00	0.00	0.55	1.02	0.36	1.87	1.09
2006/1/28	0.16	0.06	0.02	0.48	0.00	0.00	0.07	0.13	0.05	0.48	0.14
2006/1/29	0.09	0.00	0.00	0.32	0.00	0.00	0.00	0.00	0.00	0.35	0.00
2006/1/30	0.81	0.55	1.02	0.71	1.86	1.74	0.87	0.12	1.16	0.81	0.00
2006/1/31	0.27	0.00	0.43	0.50	0.93	0.45	0.23	0.03	0.30	0.36	0.00
2006/2/1	2.05	2.44	2.13	1.61	0.00	0.00	1.17	2.19	0.78	1.85	2.35
2006/2/2	0.22	0.24	0.08	1.55	0.00	0.00	0.28	0.53	0.19	1.99	0.57
2006/2/3	0.50	0.00	0.00	2.34	0.00	0.00	0.00	0.00	0.00	2.77	0.00

2006/2/4	0.78	0.23	0.08	1.94	0.00	0.00	0.27	0.51	0.18	1.73	0.54
2006/2/5	0.34	0.00	0.00	1.14	0.00	0.00	0.00	0.00	0.00	1.21	0.00
2006/2/6	0.58	0.57	0.19	3.17	0.00	0.00	0.67	1.25	0.45	3.89	1.34
2006/2/7	1.35	0.00	0.00	3.01	0.00	0.00	0.00	0.00	0.00	2.48	0.00
2006/2/8	0.56	0.27	0.09	2.11	0.00	0.00	0.31	0.58	0.21	2.32	0.62
2006/2/9	0.74	0.83	0.37	2.78	0.12	0.00	0.97	1.80	0.64	3.05	1.93
2006/2/10	0.54	0.00	0.00	2.84	0.00	0.00	0.00	0.00	0.00	3.45	0.00
2006/2/11	0.46	0.63	0.32	2.68	0.97	1.02	1.25	1.44	1.17	3.34	1.47
2006/2/12	0.18	0.00	0.00	0.93	0.00	0.00	0.00	0.00	0.00	1.12	0.00
2006/2/13	0.00	0.00	0.04	0.23	0.77	0.88	0.44	0.06	0.59	0.35	0.00
2006/2/14	7.46	8.10	6.69	7.98	3.73	4.09	6.80	9.15	5.90	7.82	9.51
2006/2/15	1.48	3.86	2.54	3.52	6.88	7.62	7.38	7.17	7.46	4.46	7.14
2006/2/16	0.00	0.00	0.00	0.12	0.00	0.00	0.00	0.00	0.00	0.17	0.00
2006/2/17	0.88	0.00	0.00	3.01	0.00	0.00	0.00	0.00	0.00	3.19	0.00
2006/2/18	2.05	1.43	2.13	1.78	3.64	3.62	2.05	0.70	2.58	1.73	0.49
2006/2/19	0.06	0.00	0.63	0.38	3.85	3.71	1.86	0.25	2.48	0.47	0.00
2006/2/20	11.47	10.97	12.55	6.51	13.74	14.17	10.73	7.75	11.88	6.28	7.30
2006/2/21	0.60	0.00	0.00	1.65	0.00	0.00	0.00	0.00	0.00	1.58	0.00
2006/2/22	0.88	2.59	1.19	4.22	0.43	0.00	3.02	5.63	2.01	5.01	6.03
2006/2/23	3.79	5.00	3.85	6.99	8.94	10.21	8.79	7.56	9.27	8.03	7.37
2006/2/24	11.48	13.92	14.78	5.06	17.29	18.05	14.91	12.20	15.96	5.89	11.78
2006/2/25	0.63	0.64	0.71	1.11	0.00	0.00	0.12	0.22	0.08	1.66	0.23
2006/2/26	0.76	0.69	0.48	3.62	0.51	0.21	0.91	1.51	0.68	4.29	1.60
2006/2/27	1.78	2.83	2.16	3.82	1.79	2.05	2.89	3.63	2.61	5.20	3.74
2006/2/28	10.94	14.09	12.80	15.06	20.06	19.74	19.90	20.04	19.84	15.80	20.06
2006/3/1	0.29	0.00	0.07	0.29	1.26	1.45	0.72	0.10	0.96	0.00	0.00
2006/3/2	0.49	0.62	0.57	0.37	0.12	0.12	0.34	0.54	0.27	0.49	0.57
2006/3/3	4.25	2.24	2.41	7.50	6.79	7.59	4.89	2.56	5.79	7.14	2.20
2006/3/4	1.24	0.00	0.00	3.00	0.00	0.00	0.00	0.00	0.00	2.64	0.00
2006/3/5	2.70	2.65	1.74	4.65	3.67	3.97	4.40	4.77	4.26	3.93	4.82
2006/3/6	3.07	1.87	2.34	2.70	0.00	0.00	0.00	0.00	0.00	2.72	0.00
2006/3/7	2.23	3.05	1.79	4.30	1.40	1.60	3.48	5.10	2.85	4.43	5.36
2006/3/8	24.13	21.11	30.06	13.52	64.68	64.34	39.51	17.99	47.79	10.02	14.68
2006/3/9	0.00	0.40	0.13	0.71	0.00	0.00	0.46	0.86	0.31	1.06	0.92
2006/3/10	0.53	0.00	0.04	1.00	0.05	0.00	0.00	0.00	0.00	0.71	0.00
2006/3/11	0.50	0.00	0.00	1.69	0.00	0.00	0.00	0.00	0.00	1.77	0.00
2006/3/12	0.73	0.91	0.30	3.29	0.00	0.00	1.06	1.99	0.71	3.83	2.13
2006/3/13	10.19	9.18	11.12	4.84	14.55	14.81	10.30	6.38	11.80	3.70	5.78
2006/3/14	0.44	0.18	0.06	1.27	0.00	0.00	0.21	0.40	0.14	1.26	0.43
2006/3/15	0.00	0.27	0.09	0.97	0.00	0.00	0.32	0.60	0.21	1.46	0.64
2006/3/16	0.22	0.00	0.00	1.07	0.00	0.00	0.00	0.00	0.00	1.28	0.00

2006/3/17	2.67	0.50	0.43	4.39	2.33	2.44	1.80	1.25	2.02	2.58	1.17
2006/3/18	21.39	21.56	25.79	15.54	36.70	35.08	26.97	19.95	29.67	14.81	18.87
2006/3/19	2.63	3.21	3.58	4.07	3.19	2.92	2.81	2.71	2.85	5.76	2.70
2006/3/20	0.39	1.05	0.37	1.91	0.34	0.39	1.42	2.31	1.08	2.28	2.45
2006/3/21	0.18	4.29	1.50	8.80	0.10	0.00	5.00	9.33	3.33	12.93	10.00
2006/3/22	7.77	6.91	6.47	6.30	1.75	1.81	3.94	5.78	3.23	5.34	6.06
2006/3/23	2.18	2.75	1.03	5.16	0.00	0.00	3.07	5.73	2.05	4.68	6.14
2006/3/24	31.47	31.21	33.61	15.68	6.30	4.52	11.69	17.91	9.30	16.79	18.87
2006/3/25	12.15	8.37	9.11	9.84	8.73	9.39	7.48	5.82	8.12	7.01	5.57
2006/3/26	0.87	2.25	1.09	3.37	2.82	3.22	4.00	4.68	3.74	4.09	4.79
2006/3/27	0.41	0.00	0.00	1.07	0.00	0.00	0.00	0.00	0.00	0.98	0.00
2006/3/28	0.68	0.00	0.00	1.48	0.00	0.00	0.00	0.00	0.00	1.20	0.00
2006/3/29	0.67	0.90	0.32	3.19	0.37	0.42	1.26	1.98	0.98	3.78	2.09
2006/3/30	5.76	16.90	10.41	15.80	12.22	12.65	21.86	29.84	18.79	21.34	31.07
2006/3/31	6.37	5.88	6.55	5.92	6.64	7.20	5.39	3.82	5.99	6.93	3.58
2006/4/1	1.60	1.43	2.41	4.14	8.72	7.61	5.47	3.62	6.18	3.80	3.33
2006/4/2	1.77	0.71	0.29	3.86	0.89	1.02	1.34	1.62	1.23	3.13	1.67
2006/4/3	4.39	4.68	4.63	6.10	3.17	3.03	3.76	4.39	3.51	7.38	4.49
2006/4/4	30.11	28.56	27.62	23.87	13.07	13.60	19.05	23.77	17.23	22.26	24.49
2006/4/5	4.96	5.97	5.56	6.58	6.77	7.10	6.95	6.82	7.00	7.78	6.79
2006/4/6	1.29	2.25	1.33	3.32	0.09	0.00	1.97	3.68	1.32	4.02	3.95
2006/4/7	8.94	11.44	11.49	5.98	17.05	18.16	14.89	12.06	15.98	6.87	11.63
2006/4/8	6.49	6.36	9.37	3.34	27.70	28.79	16.76	6.33	20.77	2.87	4.73
2006/4/9	1.20	1.49	1.44	0.51	0.00	0.00	0.54	1.00	0.36	0.76	1.07
2006/4/10	4.43	6.69	6.67	3.76	7.96	7.94	7.58	7.27	7.70	5.28	7.22
2006/4/11	2.49	1.10	0.37	8.67	0.00	0.00	1.29	2.41	0.86	9.28	2.58
2006/4/12	0.45	0.21	0.07	1.08	0.00	0.00	0.24	0.45	0.16	0.93	0.48
2006/4/13	4.40	5.40	3.12	9.85	1.66	1.80	5.71	9.09	4.40	10.41	9.61
2006/4/14	0.40	0.16	0.05	1.01	0.00	0.00	0.19	0.35	0.13	0.92	0.38
2006/4/15	2.76	4.23	2.59	6.49	1.15	1.32	4.18	6.66	3.22	7.72	7.04
2006/4/16	11.78	9.10	12.06	3.49	0.90	0.00	0.00	0.00	0.00	3.48	0.00
2006/4/17	9.46	9.43	9.30	10.55	9.98	9.26	10.17	10.97	9.87	9.81	11.09
2006/4/18	6.88	6.68	7.28	4.76	5.23	4.94	5.00	5.04	4.98	4.72	5.05
2006/4/19	25.99	22.61	28.60	8.68	25.27	24.66	16.99	10.34	19.55	6.63	9.32
2006/4/20	3.24	0.81	0.83	3.40	2.15	2.46	1.60	0.87	1.89	1.08	0.75
2006/4/21	16.14	14.85	16.93	10.19	15.76	14.95	13.06	11.42	13.69	8.69	11.17
2006/4/22	1.35	6.57	3.83	5.96	11.02	12.28	12.74	13.13	12.59	8.53	13.19
2006/4/23	15.07	13.68	12.95	16.94	8.63	8.39	11.23	13.69	10.28	16.18	14.07
2006/4/24	1.20	11.34	4.95	9.45	4.22	4.82	14.44	22.78	11.24	14.18	24.06
2006/4/25	6.05	5.95	5.76	6.98	4.58	4.37	5.32	6.13	5.00	7.12	6.26
2006/4/26	2.87	4.10	3.42	3.34	4.04	4.40	4.82	5.18	4.68	3.97	5.24

2006/4/27	6.01	7.16	5.47	9.04	1.41	1.38	5.40	8.89	4.06	10.00	9.43
2006/4/28	6.35	5.17	6.21	3.09	5.09	4.91	3.84	2.91	4.20	2.09	2.77
2006/4/29	0.32	0.47	0.20	2.34	0.87	0.99	1.04	1.09	1.03	3.03	1.10
2006/4/30	0.87	0.63	0.21	2.91	0.00	0.00	0.74	1.38	0.49	3.05	1.48
2006/5/1	22.19	22.10	24.82	7.75	8.13	7.73	9.23	10.53	8.73	8.98	10.73
2006/5/2	0.00	0.34	0.11	0.47	0.00	0.00	0.39	0.73	0.26	0.70	0.78
2006/5/3	10.80	8.13	9.59	12.46	11.52	11.16	8.69	6.56	9.51	12.07	6.23
2006/5/4	2.34	2.34	1.91	3.96	1.49	1.70	2.25	2.73	2.07	4.43	2.80
2006/5/5	3.63	4.23	4.33	2.68	1.40	0.71	2.36	3.80	1.81	2.95	4.02
2006/5/6	0.47	1.84	0.61	3.02	0.00	0.00	2.14	4.00	1.43	3.82	4.29
2006/5/7	0.25	2.76	1.17	4.74	3.96	4.47	5.46	6.31	5.13	6.73	6.44
2006/5/8	6.47	16.11	9.96	12.03	4.11	4.70	15.59	25.03	11.96	16.68	26.48
2006/5/9	10.02	10.05	11.12	6.33	14.32	14.54	11.53	8.92	12.53	5.65	8.52
2006/5/10	8.40	10.24	10.16	7.98	10.13	9.58	10.43	11.16	10.14	8.84	11.27
2006/5/11	4.63	12.82	9.56	7.33	10.56	10.34	15.50	19.97	13.78	10.99	20.66
2006/5/12	3.28	8.32	6.91	4.79	14.73	15.43	14.28	13.29	14.66	6.98	13.13
2006/5/13	2.91	2.62	3.63	1.54	1.40	0.48	0.77	1.01	0.67	1.75	1.05
2006/5/14	0.00	1.59	0.77	2.13	4.31	4.93	4.33	3.80	4.53	3.19	3.72
2006/5/15	1.53	1.11	0.37	7.53	0.00	0.00	1.29	2.42	0.86	8.99	2.59
2006/5/16	0.00	0.50	0.22	0.58	0.96	1.09	1.13	1.16	1.12	0.87	1.16
2006/5/17	12.50	9.63	8.61	16.82	2.18	2.49	5.76	8.60	4.67	16.56	9.03
2006/5/18	3.78	6.68	7.59	2.68	32.05	35.58	21.81	9.87	26.40	4.02	8.04
2006/5/19	14.57	8.91	9.93	11.76	2.37	2.13	3.21	4.14	2.85	8.16	4.29
2006/5/20	1.47	0.00	0.00	2.54	0.00	0.00	0.00	0.00	0.00	1.61	0.00
2006/5/21	0.61	0.17	0.21	0.42	0.00	0.00	0.00	0.00	0.00	0.00	0.00
2006/5/22	14.87	15.65	16.50	5.47	2.70	2.59	5.77	8.53	4.71	6.57	8.95
2006/5/23	0.44	1.02	1.13	1.31	8.25	8.87	5.62	2.81	6.70	1.30	2.37
2006/5/24	10.92	7.61	9.33	7.75	7.80	7.32	5.68	4.26	6.23	5.53	4.04
2006/5/25	8.40	6.38	6.91	5.86	0.85	0.56	2.02	3.28	1.53	4.75	3.48
2006/5/26	1.59	3.60	3.03	2.55	2.00	1.52	3.36	4.96	2.75	3.83	5.20
2006/5/27	6.57	6.39	5.96	5.74	0.60	0.69	2.97	4.95	2.21	5.99	5.26
2006/5/28	5.27	4.36	3.60	8.11	0.71	0.43	2.93	5.09	2.09	7.83	5.42
2006/5/29	1.12	0.00	0.10	3.15	0.85	0.89	0.44	0.06	0.59	3.05	0.00
2006/5/30	14.98	14.05	15.44	7.77	8.76	8.00	8.90	9.67	8.60	6.44	9.79
2006/5/31	0.08	0.47	0.97	2.39	6.14	6.25	3.68	1.45	4.54	3.46	1.11
2006/6/1	0.27	0.36	0.22	0.74	1.81	2.07	1.45	0.91	1.66	0.71	0.83
2006/6/2	2.45	0.00	0.00	2.64	0.00	0.00	0.00	0.00	0.00	0.29	0.00
2006/6/3	2.07	0.00	0.47	4.13	0.62	0.00	0.00	0.00	0.00	3.09	0.00
2006/6/4	18.67	14.51	16.38	9.84	3.70	3.28	4.88	6.27	4.35	7.28	6.49
2006/6/5	0.15	1.00	0.84	0.93	2.99	2.85	2.59	2.37	2.68	1.17	2.34
2006/6/6	13.21	9.90	12.41	6.17	3.33	2.85	2.37	1.95	2.53	5.36	1.89

2006/6/7	2.71	2.87	1.19	7.25	0.00	0.00	3.05	5.70	2.04	7.26	6.11
2006/6/8	0.44	0.00	0.00	0.91	0.00	0.00	0.00	0.00	0.00	0.71	0.00
2006/6/9	0.26	5.09	1.89	7.86	3.62	4.14	8.01	11.36	6.72	11.39	11.88
2006/6/10	3.10	0.79	0.98	3.35	0.00	0.00	0.00	0.00	0.00	1.76	0.00
2006/6/11	7.02	12.74	7.72	15.23	17.66	19.73	21.89	23.77	21.17	16.56	24.06
2006/6/12	43.56	37.07	43.36	26.12	45.81	47.62	34.50	23.13	38.88	22.68	21.38
2006/6/13	5.98	3.68	5.26	1.96	2.61	2.15	1.07	0.14	1.43	0.40	0.00
2006/6/14	10.75	7.52	5.71	17.20	0.00	0.00	4.69	8.76	3.13	15.79	9.39
2006/6/15	0.00	0.00	0.00	0.75	0.00	0.00	0.00	0.00	0.00	1.13	0.00
2006/6/16	8.21	9.14	6.57	11.67	0.00	0.00	6.18	11.54	4.12	11.91	12.37
2006/6/17	0.53	6.12	2.70	6.04	2.29	1.76	8.02	13.46	5.94	8.25	14.29
2006/6/18	3.51	7.23	4.90	5.69	3.85	4.06	7.82	11.07	6.57	7.24	11.58
2006/6/19	5.41	8.10	8.18	2.98	4.60	3.59	5.91	7.91	5.14	4.36	8.22
2006/6/20	3.96	3.98	2.92	4.18	0.00	0.00	2.62	4.89	1.75	3.37	5.24
2006/6/21	0.52	4.43	1.83	4.86	1.39	1.13	5.73	9.72	4.20	6.51	10.33
2006/6/22	0.13	0.02	0.03	0.28	0.00	0.00	0.00	0.00	0.00	0.25	0.00
2006/6/23	1.35	0.00	0.00	5.66	0.00	0.00	0.00	0.00	0.00	6.46	0.00
2006/6/24	3.11	0.00	0.00	5.39	0.00	0.00	0.00	0.00	0.00	3.42	0.00
2006/6/25	2.43	0.00	0.04	3.84	0.68	0.78	0.39	0.05	0.52	2.11	0.00
2006/6/26	0.34	0.76	0.25	2.43	0.00	0.00	0.89	1.65	0.59	3.14	1.77
2006/6/27	1.44	0.99	1.05	3.41	4.47	4.92	3.16	1.63	3.75	3.64	1.40
2006/6/28	3.55	0.00	0.00	5.71	0.00	0.00	0.00	0.00	0.00	3.24	0.00
2006/6/29	10.37	8.24	8.56	8.34	0.36	0.00	2.56	4.79	1.71	7.53	5.13
2006/6/30	0.25	0.00	0.65	0.83	2.38	1.88	0.94	0.13	1.25	0.87	0.00
2006/7/1	0.75	0.00	0.00	1.43	0.00	0.00	0.00	0.00	0.00	1.02	0.00
2006/7/2	0.57	0.67	0.47	0.87	0.00	0.00	0.46	0.86	0.31	0.92	0.92
2006/7/3	0.00	0.19	0.06	0.27	0.00	0.00	0.22	0.42	0.15	0.40	0.44
2006/7/4	0.11	0.00	0.00	0.22	0.00	0.00	0.00	0.00	0.00	0.17	0.00
2006/7/5	0.75	0.00	0.00	0.89	0.00	0.00	0.00	0.00	0.00	0.22	0.00
2006/7/6	2.69	0.47	1.01	2.26	0.62	0.08	0.04	0.01	0.05	0.18	0.00
2006/7/7	1.20	0.90	0.37	1.90	0.10	0.00	1.05	1.96	0.70	1.05	2.10
2006/7/8	4.38	4.06	4.72	0.92	3.28	3.75	2.56	1.53	2.96	0.89	1.37
2006/7/9	8.52	7.95	7.20	8.11	1.37	0.45	4.69	8.37	3.28	6.60	8.93
2006/7/10	5.08	5.15	5.80	1.94	2.64	2.61	2.62	2.64	2.62	2.31	2.64
2006/7/11	4.38	8.62	7.63	6.09	18.40	19.28	16.30	13.71	17.30	7.65	13.32
2006/7/12	5.91	2.91	3.64	3.22	0.00	0.00	0.00	0.00	0.00	1.06	0.00
2006/7/13	1.42	0.00	0.00	3.89	0.00	0.00	0.00	0.00	0.00	3.71	0.00
2006/7/14	0.74	0.62	1.16	1.55	3.57	3.59	1.95	0.54	2.50	2.06	0.32
2006/7/15	0.23	0.00	0.00	0.33	0.00	0.00	0.00	0.00	0.00	0.15	0.00
2006/7/16	7.21	7.34	6.52	8.02	2.32	2.65	4.87	6.79	4.13	8.74	7.09
2006/7/17	1.44	1.14	0.93	1.67	0.00	0.00	0.64	1.19	0.42	1.38	1.27

2006/7/18	7.96	12.11	10.82	11.73	13.04	13.66	14.20	14.67	14.02	15.79	14.75
2006/7/19	1.46	0.00	0.00	1.46	0.00	0.00	0.00	0.00	0.00	0.00	0.00
2006/7/20	2.81	2.20	1.34	6.46	0.14	0.00	1.94	3.62	1.29	6.42	3.88
2006/7/21	9.60	7.68	7.98	10.02	5.28	4.40	5.90	7.21	5.40	8.52	7.41
2006/7/22	7.52	7.73	8.33	8.82	16.42	17.37	12.61	8.48	14.20	9.58	7.85
2006/7/23	16.11	9.58	13.18	6.71	5.04	3.71	2.28	1.05	2.76	2.02	0.86
2006/7/24	24.28	25.50	30.03	10.69	20.49	17.69	17.13	16.63	17.32	11.82	16.56
2006/7/25	3.99	4.93	2.14	12.05	1.78	2.04	6.26	9.92	4.86	12.85	10.49
2006/7/26	0.00	0.25	0.08	2.70	0.00	0.00	0.29	0.53	0.19	4.05	0.57
2006/7/27	14.09	17.35	18.08	14.35	25.45	25.28	21.98	19.13	23.08	16.72	18.69
2006/7/28	5.77	2.78	2.47	8.68	2.56	2.20	3.12	3.91	2.81	6.21	4.04
2006/7/29	8.09	9.39	7.43	10.41	0.00	0.00	5.48	10.23	3.65	11.69	10.96
2006/7/30	3.88	4.94	4.36	6.30	13.53	15.17	11.06	7.51	12.43	7.05	6.96
2006/7/31	11.06	7.01	9.38	5.76	11.21	11.33	6.81	2.89	8.32	2.59	2.29
2006/8/1	1.34	1.43	1.01	3.75	0.98	1.12	1.61	2.04	1.45	4.54	2.11
2006/8/2	0.11	0.00	0.00	0.14	0.00	0.00	0.00	0.00	0.00	0.05	0.00
2006/8/3	2.30	0.72	1.18	3.74	4.99	5.38	2.94	0.82	3.75	3.05	0.49
2006/8/4	21.93	21.79	24.33	12.36	30.53	32.11	24.06	17.09	26.74	11.77	16.01
2006/8/5	7.94	7.29	6.25	9.20	4.95	5.38	6.88	8.19	6.38	8.35	8.39
2006/8/6	7.32	5.64	5.64	8.37	0.43	0.15	2.16	3.90	1.49	8.32	4.17
2006/8/7	4.20	3.01	3.10	5.75	3.19	2.79	3.14	3.45	3.03	4.98	3.50
2006/8/8	6.56	3.91	5.56	3.76	6.07	5.78	3.36	1.26	4.17	1.94	0.94
2006/8/9	13.15	13.08	13.88	10.07	11.39	11.41	10.91	10.47	11.08	10.48	10.41
2006/8/10	5.85	0.39	0.61	7.48	0.16	0.00	0.00	0.00	0.00	3.12	0.00
2006/8/11	0.08	0.52	0.26	1.22	1.02	1.12	1.16	1.20	1.15	1.71	1.21
2006/8/12	1.26	0.21	0.07	2.10	0.00	0.00	0.25	0.46	0.16	1.26	0.49
2006/8/13	0.54	4.41	2.00	5.88	1.67	1.47	5.67	9.31	4.27	8.33	9.87
2006/8/14	0.57	0.00	0.00	1.09	0.00	0.00	0.00	0.00	0.00	0.77	0.00
2006/8/15	1.28	0.30	0.37	1.77	0.00	0.00	0.00	0.00	0.00	1.26	0.00
2006/8/16	3.83	2.31	1.76	4.65	0.00	0.00	1.44	2.68	0.96	3.12	2.87
2006/8/17	4.83	2.92	2.48	10.33	2.23	2.08	3.06	3.91	2.73	10.34	4.04
2006/8/18	4.59	4.97	4.26	4.28	0.02	0.00	2.51	4.69	1.67	4.47	5.02
2006/8/19	0.00	0.00	0.00	0.34	0.00	0.00	0.00	0.00	0.00	0.52	0.00
2006/8/20	2.54	1.62	2.16	3.40	0.36	0.00	0.18	0.33	0.12	3.86	0.36
2006/8/21	2.85	0.00	0.42	3.41	1.05	0.61	0.30	0.04	0.41	0.83	0.00
2006/8/22	1.41	0.00	0.00	2.16	0.00	0.00	0.00	0.00	0.00	1.12	0.00
2006/8/23	0.70	0.00	0.00	1.08	0.00	0.00	0.00	0.00	0.00	0.58	0.00
2006/8/24	0.21	0.18	0.23	0.21	0.00	0.00	0.00	0.00	0.00	0.32	0.00
2006/8/25	9.38	6.71	11.94	5.05	12.52	9.03	5.01	1.52	6.35	4.50	0.99
2006/8/26	3.31	4.64	3.87	3.20	4.62	5.12	5.45	5.74	5.34	3.61	5.79
2006/8/27	0.32	0.35	0.26	1.93	0.80	0.91	0.73	0.56	0.79	2.60	0.54

2006/8/28	12.16	11.82	10.06	14.71	22.19	24.65	20.42	16.76	21.83	12.37	16.19
2006/8/29	7.27	9.34	8.11	4.84	0.16	0.00	4.69	8.75	3.13	5.66	9.38
2006/8/30	1.65	4.69	2.13	7.43	0.00	0.00	4.75	8.88	3.17	9.76	9.51
2006/8/31	2.45	0.89	0.70	4.03	0.80	0.91	1.04	1.15	1.00	3.05	1.17
2006/9/1	5.57	3.57	3.50	5.68	3.24	3.37	3.41	3.44	3.40	3.83	3.44
2006/9/2	11.06	10.92	10.51	7.23	3.45	3.68	6.28	8.53	5.41	6.70	8.88
2006/9/3	0.82	0.00	0.00	1.51	0.00	0.00	0.00	0.00	0.00	1.05	0.00
2006/9/4	0.00	0.00	0.00	0.17	0.00	0.00	0.00	0.00	0.00	0.26	0.00
2006/9/5	0.00	0.00	0.00	0.31	0.00	0.00	0.00	0.00	0.00	0.46	0.00
2006/9/6	2.28	0.00	0.00	5.37	0.00	0.00	0.00	0.00	0.00	4.64	0.00
2006/9/7	2.91	2.41	2.07	14.74	0.18	0.00	1.38	2.58	0.92	19.89	2.77
2006/9/8	17.16	28.58	21.15	23.73	9.82	9.93	25.22	38.47	20.12	29.50	40.51
2006/9/9	0.00	1.75	0.70	3.17	1.15	1.23	2.66	3.90	2.18	4.76	4.09
2006/9/10	9.05	6.29	7.86	1.95	0.00	0.00	0.00	0.00	0.00	0.35	0.00
2006/9/11	1.15	3.24	1.35	8.64	4.69	5.33	6.45	7.41	6.08	11.25	7.56
2006/9/12	7.46	3.62	4.72	8.71	0.26	0.00	0.00	0.00	0.00	8.22	0.00
2006/9/13	1.62	7.24	4.31	7.08	2.31	1.47	7.85	13.37	5.72	10.19	14.22
2006/9/14	2.41	1.18	0.96	5.29	6.81	7.79	5.02	2.62	5.94	4.68	2.25
2006/9/15	0.00	5.17	1.72	6.05	0.00	0.00	6.03	11.26	4.02	9.08	12.07
2006/9/16	0.34	1.12	0.37	1.36	0.00	0.00	1.30	2.43	0.87	1.52	2.61
2006/9/17	14.28	8.04	9.43	10.05	5.47	5.46	4.53	3.73	4.84	5.03	3.60
2006/9/18	13.03	7.78	8.04	12.28	3.52	3.43	4.56	5.54	4.19	8.22	5.69
2006/9/19	2.22	2.21	1.95	2.37	1.29	1.47	1.86	2.20	1.73	2.41	2.25
2006/9/20	14.50	18.96	18.07	9.18	10.09	9.20	14.30	18.72	12.60	10.65	19.40
2006/9/21	39.35	29.33	35.72	14.41	10.83	9.14	9.07	9.02	9.09	7.16	9.01
2006/9/22	1.63	7.48	5.39	6.31	16.98	17.35	16.51	15.78	16.79	8.35	15.67
2006/9/23	6.76	7.54	8.62	4.06	3.16	2.08	3.49	4.70	3.02	5.47	4.89
2006/9/24	9.07	7.89	15.00	2.21	30.45	27.59	15.05	4.18	19.23	1.64	2.51
2006/9/25	0.21	3.76	1.25	4.11	0.00	0.00	4.39	8.20	2.93	5.84	8.78
2006/9/26	0.35	2.19	1.24	1.47	3.50	3.92	4.17	4.38	4.09	2.20	4.41
2006/9/27	0.29	2.36	0.83	3.12	0.86	0.98	3.24	5.20	2.49	4.26	5.50
2006/9/28	4.39	4.95	6.24	2.89	15.78	16.74	10.41	4.93	12.52	3.35	4.09
2006/9/29	0.86	0.72	0.24	1.73	0.00	0.00	0.84	1.56	0.56	1.31	1.67
2006/9/30	3.40	4.07	4.76	3.67	14.43	15.08	10.07	5.72	11.74	3.74	5.05
2006/10/1	6.46	10.70	11.37	7.26	26.33	27.11	20.27	14.35	22.55	9.84	13.44
2006/10/2	0.54	0.27	0.09	0.75	0.00	0.00	0.31	0.58	0.21	0.31	0.63
2006/10/3	0.00	1.33	0.44	2.79	0.00	0.00	1.55	2.89	1.03	4.18	3.09
2006/10/4	10.71	0.00	0.00	12.81	0.00	0.00	0.00	0.00	0.00	3.14	0.00
2006/10/5	2.06	5.62	1.96	11.16	1.58	1.80	7.45	12.35	5.57	13.65	13.11
2006/10/6	0.64	0.49	0.26	2.10	1.86	2.13	1.63	1.21	1.80	2.19	1.14
2006/10/7	2.27	3.93	2.80	3.76	2.12	2.42	4.05	5.45	3.50	4.86	5.67

2006/10/8	2.93	1.37	1.60	5.31	0.00	0.00	0.15	0.27	0.10	5.74	0.29
2006/10/9	7.54	11.11	11.99	5.32	22.43	23.24	17.47	12.48	19.40	7.32	11.71
2006/10/10	1.77	3.11	1.77	6.75	0.00	0.00	2.69	5.02	1.79	8.87	5.37
2006/10/11	0.00	0.00	0.07	1.09	1.32	1.51	0.75	0.10	1.00	1.64	0.00
2006/10/12	0.51	0.00	0.00	1.33	0.00	0.00	0.00	0.00	0.00	1.23	0.00
2006/10/13	1.67	1.29	1.07	2.37	0.00	0.00	0.70	1.31	0.47	2.28	1.40
2006/10/14	0.44	0.00	0.00	0.44	0.00	0.00	0.00	0.00	0.00	0.00	0.00
2006/10/15	0.51	0.38	0.13	2.04	0.00	0.00	0.44	0.82	0.29	2.29	0.88
2006/10/16	0.18	0.00	0.00	0.45	0.00	0.00	0.00	0.00	0.00	0.41	0.00
2006/10/17	0.59	1.94	0.72	4.59	0.44	0.43	2.48	4.25	1.79	5.99	4.53
2006/10/18	0.04	0.35	0.16	0.70	0.83	0.95	0.88	0.82	0.90	0.99	0.81
2006/10/19	4.88	6.16	5.33	4.07	1.66	1.64	4.17	6.36	3.32	4.54	6.70
2006/10/20	1.23	2.18	0.73	6.21	0.00	0.00	2.54	4.74	1.69	7.47	5.08
2006/10/21	8.32	6.93	9.27	4.85	9.58	8.18	6.15	4.39	6.83	3.82	4.12
2006/10/22	13.79	12.78	12.89	13.83	10.30	10.12	11.00	11.77	10.71	13.49	11.89
2006/10/23	28.75	22.33	26.88	21.90	34.06	35.06	24.25	14.88	27.85	18.73	13.44
2006/10/24	10.76	8.92	8.14	10.58	2.95	2.78	5.88	8.57	4.85	8.59	8.98
2006/10/25	0.23	0.52	0.26	0.63	1.55	1.77	1.49	1.25	1.58	0.61	1.21
2006/10/26	3.24	1.92	2.37	3.69	0.40	0.00	0.42	0.79	0.28	3.39	0.85
2006/10/27	4.64	8.29	5.11	9.55	9.19	10.34	12.63	14.60	11.87	10.69	14.91
2006/10/28	18.90	19.83	24.09	6.68	28.90	28.38	20.74	14.12	23.29	6.55	13.11
2006/10/29	48.57	46.40	45.61	33.59	24.43	25.70	32.06	37.58	29.94	29.90	38.43
2006/10/30	9.54	8.43	9.09	5.85	3.66	2.95	4.55	5.93	4.01	4.61	6.15
2006/10/31	28.77	21.77	23.42	19.65	7.88	7.23	10.39	13.13	9.34	14.26	13.55
2006/11/1	1.83	3.42	2.62	3.00	2.29	2.31	3.67	4.84	3.22	3.98	5.02
2006/11/2	0.00	1.47	0.49	2.02	0.00	0.00	1.71	3.19	1.14	3.04	3.42
2006/11/3	0.00	0.00	0.00	0.43	0.00	0.00	0.00	0.00	0.00	0.64	0.00
2006/11/4	0.17	6.80	2.84	7.31	10.50	12.00	13.93	15.60	13.29	10.70	15.86
2006/11/5	3.12	0.97	1.32	2.78	2.05	2.34	1.17	0.16	1.56	1.19	0.00
2006/11/6	0.39	0.00	0.67	0.39	0.88	0.00	0.00	0.00	0.00	0.00	0.00
2006/11/7	0.00	0.99	0.33	1.40	0.00	0.00	1.15	2.15	0.77	2.10	2.31
2006/11/8	0.00	1.18	0.66	0.92	4.89	5.59	4.18	2.95	4.65	1.38	2.76
2006/11/9	0.00	0.00	0.05	0.41	0.85	0.97	0.48	0.06	0.65	0.62	0.00
2006/11/10	0.16	0.00	0.00	0.16	0.01	0.00	0.00	0.00	0.00	0.00	0.00
2006/11/11	9.04	9.44	10.47	3.97	4.09	3.97	4.52	4.99	4.33	5.12	5.07
2006/11/12	0.57	5.84	2.31	5.12	6.67	7.62	10.63	13.23	9.63	6.82	13.63
2006/11/13	1.99	1.55	1.53	1.11	0.04	0.00	0.56	1.04	0.37	0.56	1.11
2006/11/14	1.20	0.86	1.26	0.20	0.25	0.00	0.00	0.00	0.00	0.00	0.00
2006/11/15	5.38	5.34	8.28	0.56	10.85	9.69	5.69	2.22	7.02	0.84	1.69
2006/11/16	0.80	2.03	0.95	4.73	5.03	5.75	5.24	4.80	5.41	5.90	4.74
2006/11/17	56.32	49.11	51.81	32.26	13.27	11.50	21.75	30.64	18.33	25.86	32.00

2006/11/18	39.16	33.93	35.41	36.89	34.42	33.72	32.59	31.62	32.97	32.37	31.47
2006/11/19	2.13	1.44	2.94	2.82	19.27	21.37	11.08	2.16	14.51	2.97	0.78
2006/11/20	10.18	15.53	13.45	14.09	11.43	11.37	15.39	18.86	14.05	18.49	19.40
2006/11/21	3.12	2.60	1.32	11.71	3.40	3.62	4.72	5.66	4.35	13.07	5.81
2006/11/22	17.72	28.93	22.85	30.39	51.26	55.22	50.76	46.89	52.24	34.90	46.30
2006/11/23	19.38	19.88	19.09	21.91	8.12	6.97	13.20	18.61	11.13	24.01	19.44
2006/11/24	0.15	0.74	0.25	0.94	0.00	0.00	0.86	1.61	0.58	1.20	1.73
2006/11/25	4.48	7.94	7.95	8.72	8.37	7.09	8.59	9.89	8.09	12.70	10.09
2006/11/26	6.15	9.86	6.08	11.17	9.13	9.87	13.96	17.50	12.60	11.25	18.04
2006/11/27	0.43	0.00	0.00	1.22	0.00	0.00	0.00	0.00	0.00	1.19	0.00
2006/11/28	16.94	6.00	7.81	23.24	37.45	41.62	23.94	8.62	29.84	15.24	6.26
2006/11/29	8.03	3.28	4.57	7.31	7.41	7.31	4.48	2.03	5.42	3.41	1.65
2006/11/30	1.11	0.62	0.21	1.59	0.00	0.00	0.72	1.35	0.48	0.72	1.44
2006/12/1	3.06	2.40	3.27	0.26	0.35	0.00	0.00	0.00	0.00	0.00	0.00
2006/12/2	0.00	0.00	0.26	0.34	1.94	1.96	0.98	0.13	1.31	0.52	0.00
2006/12/3	0.39	0.39	0.13	0.69	0.00	0.00	0.45	0.84	0.30	0.45	0.90
2006/12/4	0.00	6.07	2.02	5.40	0.00	0.00	7.08	13.21	4.72	8.09	14.15
2006/12/5	2.86	2.44	3.52	0.20	5.69	6.17	3.13	0.49	4.14	0.21	0.09
2006/12/6	4.41	4.37	4.79	2.95	10.92	12.48	7.84	3.82	9.39	3.05	3.20
2006/12/7	2.55	1.59	2.19	2.10	1.69	1.76	0.88	0.12	1.17	2.11	0.00
2006/12/8	0.52	0.00	0.00	1.10	0.00	0.00	0.00	0.00	0.00	0.88	0.00
2006/12/9	0.43	0.00	0.00	0.75	0.00	0.00	0.00	0.00	0.00	0.49	0.00
2006/12/10	0.33	0.00	0.00	0.46	0.00	0.00	0.00	0.00	0.00	0.20	0.00
2006/12/11	0.46	0.00	0.00	1.23	0.00	0.00	0.00	0.00	0.00	1.16	0.00
2006/12/12	1.32	0.47	0.59	1.62	0.00	0.00	0.00	0.00	0.00	1.28	0.00
2006/12/13	25.42	18.44	21.91	15.71	11.08	9.76	9.39	9.08	9.51	10.93	9.03
2006/12/14	3.63	4.45	3.28	6.46	3.02	3.35	4.88	6.20	4.37	7.24	6.41
2006/12/15	0.00	1.14	0.72	0.88	6.36	7.27	4.96	2.96	5.73	1.32	2.65
2006/12/16	0.33	0.00	2.48	0.90	8.33	6.24	3.12	0.42	4.16	0.87	0.00
2006/12/17	0.51	0.00	0.00	0.67	0.00	0.00	0.00	0.00	0.00	0.24	0.00
2006/12/18	0.23	6.48	2.35	5.51	3.60	4.12	9.61	14.38	7.78	7.93	15.11
2006/12/19	0.00	0.41	0.18	0.32	0.84	0.96	0.96	0.96	0.96	0.48	0.96
2006/12/20	0.00	0.45	0.22	1.38	1.28	1.46	1.25	1.08	1.32	2.07	1.05
2006/12/21	0.31	0.61	0.72	0.78	9.52	10.89	6.16	2.06	7.73	0.71	1.43
2006/12/22	0.00	1.47	0.49	3.34	0.00	0.00	1.72	3.21	1.15	5.01	3.44
2006/12/23	7.29	6.56	7.40	3.73	1.20	0.56	2.01	3.27	1.53	3.53	3.47
2006/12/24	0.97	0.00	0.00	2.73	0.00	0.00	0.00	0.00	0.00	2.64	0.00
2006/12/25	0.22	2.07	0.93	2.77	4.44	5.08	4.96	4.85	5.00	3.83	4.83
2006/12/26	0.24	1.41	0.47	3.07	0.00	0.00	1.65	3.07	1.10	4.24	3.29
2006/12/27	2.74	1.21	0.93	4.91	1.68	1.92	1.82	1.73	1.86	4.10	1.72
2006/12/28	20.96	19.20	18.81	16.75	9.60	8.89	13.36	17.23	11.87	13.92	17.82

2006/12/29	6.32	5.12	4.65	12.00	11.96	12.71	10.16	7.94	11.01	11.77	7.60
2006/12/30	0.00	0.00	0.00	0.53	0.00	0.00	0.00	0.00	0.00	0.80	0.00
2006/12/31	0.00	0.00	0.00	0.00	0.00	0.00	0.00	0.00	0.00	0.00	0.00

Appendix B - Basin “n” overbank reference roughness values for developed and undeveloped channelization

Basin Land Use	Percent Impervious	Channelization Description	
		Developed Pipe/Channel	Undeveloped Natural
Highways, Parking	95	0.030	0.067
Commercial, Offices	90	0.031	0.070
Intensive Industrial	85	0.032	0.071
Apartments, High Density Res.	80	0.033	0.072
Mobil Home Park	75	0.034	0.073
Condominiums, Med. Density Res.	70	0.035	0.074
Residential 8-10 du/acre (20-25 du/ha), Ext Industrial	60	0.037	0.076
Residential 6-8 du/acre (15-20 du/ha), Low Density Res., School	50	0.040	0.080
Residential 4-6 du/acre (10-15 du/ha)	40	0.042	0.084
Residential 3-4 du/acre (7.5-10 du/ha)	30	0.046	0.088
Residential 2-3 du/acre (5-7.5 du/ha)	25	0.050	0.090
Residential 1-2 du/acre (2.5-5 du/ha)	20	0.053	0.093
Residential .5-1 du/acre (1-2.5 du/ha)	15	0.056	0.096
Residential .2-.5 du/acre (0.5-1 du/ha), Ag Res.	10	0.060	0.100
Residential <.2 du/acre (0.5 du/ha), Recreation	5	0.065	0.110
Open Space, Grassland, Ag	2	0.070	0.115
Open Space, Woodland, Natural	1	0.075	0.120
Dense Oak, Shrubs, Vines	1	0.080	0.150
Shaded values are normally not used.			

*du = dwelling units